The role of DNA gyrase in illegitimate recombination

Natassja Grethe Bush

John Innes Centre

Department of Biological Chemistry

September 2017

This thesis is submitted in partial fulfilment of the requirements of the degree of

Doctor Philosophy at the University of East Anglia

This work was supported by the Biotechnology and Biological Sciences Research Council

(grant number BB/J014524/1)

Statement

The work submitted within this thesis is entirely my own, except where due reference has been paid, and has not been submitted to this or any other university as part of any degree.

Dedication

This thesis is dedicated to my Grandmother, Lillian Bannerman, who was a strong and independent woman, to the very end.

‘Two roads diverged in a wood, and I–/ I took the one less traveled by, / And that has made all the difference.’ - Robert Frost

Abstract

DNA, due to its double-helical structure, is subject to changes in topology due to the nature of transcription and replication. To overcome this, cells have processes and enzymes that ameliorate these changes. One such group of enzymes are the DNA topoisomerases, which are responsible for the maintenance of DNA topology. Despite this important role, these enzymes participate in illegitimate recombination (IR), which is genetic recombination between regions of DNA that share little or no homology. This can result in chromosomal rearrangements and is often a consequence of DNA-damaging agents. A consequence of topoisomerase-induced IR is thought to be therapy-related acute myeloid leukaemia (tAML). Analogously, there is evidence that exposure to sublethal concentrations of ciprofloxacin, a topoisomerase inhibitor, can cause resistance to non-quinolone antibiotics. This may work by a similar mechanism as that proposed for t-AML. This project centres around the examination of DNA gyrase-mediated IR focussing on the proposed subunit-exchange model. Using Blue-Native PAGE, I set up an assay to examine subunit exchange in topoisomerases. I have also characterised previously identified gyrase hyper-recombination mutations, known to increase the frequency of IR. Furthermore, I have investigated quinolone-induced antibiotic resistance and what the mechanism is. Here, I show that DNA gyrase can undergo subunit exchange, and that this seems to occur within higher-order oligomers of the enzyme, which have not been investigated before. Biochemical characterisation of the hyper-recombination mutations shows that they impair DNA gyrase activity which, *in vivo*, may have downstream consequences that may lead to IR. Using an *in vivo* assay where *E. coli* is treated with subinhibitory levels of quinolones, I have seen resistance to other non-quinolone antibiotics. This is not seen when other antibiotics, including other topoisomerase inhibitors, are tested. Whole genome sequencing has revealed point mutations that explain the resistances seen, however other larger chromosomal modifications have been observed as well.

Acknowledgements

First and foremost, I would like to thank my supervisor and mentor Prof. Anthony Maxwell for all of his support, guidance and for having faith in me. Especially after I broke my elbow where he also became my chauffeur, allowing me to continue working.

I would like to thank the members of my supervisory board. To Dr. Richard Bowater and Prof. Graham Moore for their advice and support and their time. Also to Dr. Rachel Stovold, Dr. Sarah Kaye, Dr. Cedric Charrier, and Dr. Nicola Ooi, all previously of Redx Anti-Infectives, who all served on my supervisory board.

I would also like to thank Prof. Justin Benesch and Mr Bernardo Clavijo for their collaborations and contributions to this thesis. I would also like to thank my summer student, Shannon McKie for her contribution to this thesis.

Special thanks to the BBSRC Doctoral Training Programme and Redx Anti-Infectives who funded this studentship.

Thanks to the Maxwell lab members, both past and present, for their discussions and support. Especially Dr. Thomas Germe for his advice, the many discussions and the use of his amazing GyrB protein. Thanks to Lesley Mitchenall as well for discussions and support.

If it takes a village to raise a child, I believe it takes a department to support a PhD student. So, many thanks to all the members, both past and present, of the Biological Chemistry Department at JIC for their support, advice and suggestions. Especially Dr. Dave Lawson for his help with structural aspects of my project, Claire Stevenson for her support, and Sarah Tolland and Jenna Conway for being fonts of knowledge and administrative support. Thank as well to the Media Preparation and Lab Support teams at JIC, especially Dr. Gill Ashby.

I would also like to thank the Topoisomerase community that I have met and had many discussions with at various conferences. Your suggestions and discussions were often inspirational.

I would like to thank my fellow PhD students for being amazing colleagues and 'brothers-in-arms'. Especially, I would like to thank Dr. Katarzyna Ignasiak for her support and advice and for being an amazing friend. A very special thank you to Jenny Walton, who has shared every up and down on this journey with me and has been on the same wavelength as me during this PhD. Your support has been invaluable and I know you will be a life-long friend.

I would also like to thank Sam Hicks for her support and friendship and for being a sounding board when I needed one.

I would like to thank my extended family and friends who have been so supportive and tried to sound interested when I have bored them to death with the details of my project. Especially my grandparents, who wrote down my project title to tell all their friends.

I would like to thank my sister for her constant love and encouragement. To my parents, I cannot begin to thank you enough. You have been in my corner from the beginning and have supported me in all of my decisions, even if you weren't entirely convinced they were the right ones. Your love and encouragement has been unending and thank you for always being interested in my work.

Finally, to my husband Skye. Thank you so much for always believing in me and for all of the big and small things that you do for me every day. Your support has been the bed rock on which this PhD thesis was built.

Table of Contents

List of Figures

List of Tables

Chapter 1: General Introduction

During the cell cycle, DNA can be subject to a number of topological and structural changes. However, the integrity of DNA structure and sequence is vital to all cells. Large amounts of DNA damage and accumulations of mutations can cause apoptosis. However, changes to DNA sequence through homologous recombination can result in an important increase in genetic variation, whilst non-homologous recombination can provide important mutations that help organisms survive in hostile environments. During replication and transcription, the maintenance of sequence fidelity is important and cells have a number of repair systems to ensure this, as well as having processes in place to fix damaged DNA. In this introduction, the topological challenges involved with replication and transcription and how the cell ameliorates these challenges through the use of DNA topoisomerases will be described, as well as the problems that can arise when things go wrong, including the consequences of targeting these enzymes in antibiotic chemotherapy.

1.1 Topology of chromosomes

DNA compaction is essential for chromosomal DNA to fit inside the cell. It involves structural proteins and changes in DNA topology, in both prokaryotes and eukaryotes, to achieve this. The structural proteins involved include histones (eukaryotes), HU protein (prokaryotes) and SMC proteins (both) to help arrange the DNA into topological domains (Cobbe & Heck, 2000, Sherratt, 2003, Luijsterburg *et al.*, 2008, Vos *et al.*, 2011).

DNA, due to its double-helix structure, is subject to topological changes during processes such as replication and transcription, which require the two strands of the double helix to be separated (Watson & Crick, 1953a, Watson & Crick, 1953b). The DNA helix is considered to have topological properties due to the length and high frictional energy of chromosomes, the fact that plasmids and many chromosomes are circular, and that chromosomes are often anchored by biological membranes or other chromosomal scaffolds (Bates & Maxwell, 2005, Deweese *et*

al., 2009, Espeli & Marians, 2004). In addition to the fact that the linkages formed in DNA cannot change unless there is breakage and reunion (Bates & Maxwell, 2005, Lindsley, 2001). DNA topological conformations include supercoils, knots and catenanes (Bates & Maxwell, 2005, Lindsley, 2001, Seol & Neuman, 2016). Supercoiled DNA is a structural consequence of the two strands of DNA wrapped around each other in the double helix, which is then coiled upon itself. It can be found in two forms: plectonemic supercoils and solenoidal (toroidal) supercoils (Lindsley, 2001). DNA supercoiling is best described in terms of twist, writhe and linking number. Linking number (Lk) is a topological property applied to closed circular DNA (or constrained DNA) and it is defined as the number of times two DNA strands are wrapped around each other (Bates & Maxwell, 2005). It is the sum of the twist and writhe, which are the two geometric properties of DNA. Twist (Tw) is the number of helical turns in a molecule of DNA while writhe (Wr) is the number of superhelical turns (Bates & Maxwell, 2005). Supercoiled DNA is defined in the change in Lk (ΔLk) from a relaxed state (Lk = 0). Negatively-supercoiled DNA (underwound) is defined as a reduction in Lk (ΔLk < 0) and is accommodated by a reduction in Tw and the formation of negative (right-handed) Wr. Whilst positively supercoiled DNA (overwound) is defined as an increase in Lk (ΔLk > 0) which results in an increase in Tw and positive (left-handed) Wr (Bates & Maxwell, 2005, Seol & Neuman, 2016). Negatively-supercoiled DNA primarily forms plectonemes whilst toroidal supercoils, which are not normally found in free DNA, tend to be a result of packaging of DNA around structural DNA-binding proteins (Bates & Maxwell, 2005, Lindsley, 2001, Seol & Neuman, 2016). The DNA crossings in knots and catenanes are generally described in terms of nodes. In knots, the rotation direction defines whether the node is positive or negative, where as in catenanes this may be arbitrary depending on the similarity of the circles and the degree to which they can be orientated by DNA sequence (Bates & Maxwell, 2005).

Plectonemic supercoiling can compact the *E. coli* bacterial chromosome, which is about 4.6 Mb long, by three orders of magnitude to fit inside the cell (Boles *et al.*, 1990, Blattner *et al.*,

1997, Holmes & Cozzarelli, 2000, Sherratt, 2003). This leaves most of the chromosome unconstrained by proteins (Holmes & Cozzarelli, 2000, Sherratt, 2003). However, the *E. coli* chromosome has been shown to be further organised into approximately 400 topological domains that are structurally maintained with the help of the SMC proteins (Deng *et al.*, 2005, Postow *et al.*, 2004). Despite the level of compaction, the structured nature of the chromosome, as well as the fact that the *E. coli* chromosome has a single replication origin, replication and segregation can be achieved in 20 min (Postow *et al.*, 2004). As a result of the physical properties of the negatively-supercoiled DNA and the high level of spatial organisation within the chromosome, processes such as replication and transcription result in a number of topological challenges that have to be overcome for continued survival.

1.2 Topological changes during replication and transcription

Negative supercoiling has been shown to be important in bacteria (Holmes & Cozzarelli, 2000), though, it has been shown to be more important in *E. coli* than in some others (such as in *Salmonella* sp.) (Higgins, 2016). Due to its physical properties, negative supercoiling allows for the denaturation of the DNA duplex on the initiation of replication at the origin (Holmes & Cozzarelli, 2000, Seol & Neuman, 2016). Moreover, negative supercoiling has been shown to be essential for replication to proceed (Funnell *et al.*, 1986, Schvartzman & Stasiak, 2004). During replication, the binding of the replication machinery to single-stranded DNA requires the unwinding and separation of the DNA duplex. Replication initiation begins with the binding and subsequent oligomerisation of DnaA (Cunningham & Berger, 2005). This causes unwinding of the DNA duplex at *oriC*, followed by the recruitment of the helicase loader DnaC and the replicative helicase DnaB, in complex, onto single-stranded DNA (Duderstadt *et al.*, 2014, Sherratt, 2003, Cunningham & Berger, 2005). Replication elongation begins with the concomitant dissociation of DnaC and recruitment of DnaG, the replication primase, which in complex with DnaB synthesises RNA primers. DNA polymerase III is then loaded onto the primed DNA with the help of the β-clamp and the clamp loader (Duderstadt *et al.*, 2014, Katayama *et*

al., 1998, Graham *et al.*, 2017). These events and replication fork progression causes positive supercoils to build up ahead of the fork (Postow *et al.*, 2001, Schvartzman & Stasiak, 2004) (Figure 1.1). These positive supercoils need to be resolved as a build-up will cause a large amount of torsional stress (Seol & Neuman, 2016) that can stall replication. This stalling can cause replication fork regression (Postow *et al.*, 2001) or double-stranded DNA breaks (Michel *et al.*, 2004). To relieve the torsional stress, the replication fork may rotate causing the development of precatenanes behind the fork (Figure 1.1) (Peter *et al.*, 1998, Postow *et al.*, 2001, Sogo *et al.*, 1999, Cebrián *et al.*, 2015). These precatenanes can become tangled and knotted if left unresolved, leading to incomplete segregation at the end of replication. The conversion of positive supercoils into precatenanes by replication fork rotation is more likely towards the end of replication, where there is no longer space for the removal of positive supercoils ahead of the replication fork (Postow *et al.*, 2001, Cebrián *et al.*, 2015). Further to this, as replication forks converge towards the end of replication, the interwound (pre-catenated) DNA is then converted to catenated DNA which, if left, will stop chromosome segregation (Figure 1.1) (Schvartzman & Stasiak, 2004). At the termination of replication, occasionally a hemicatenane may form. This is a topological linkage where the two newly replicated DNA circles are still linked by a duplex of the parental strands (Figure 1.1) (Laurie *et al.*, 1998, Vos *et al.*, 2011). Alternatively, the positive supercoils ahead of the replication fork at the termination of replication may be resolved into Holliday Junctions that will need to be disentangled before segregation (Sherratt, 2003). Despite the topological stress that is associated with positive supercoils, the chromosomes of thermophiles have been shown to be positively supercoiled. This is most likely due to the higher melting point of positive supercoiling and thus greater stability at high temperatures (Forterre, 2002, Forterre *et al.*, 1985, Kikuchi & Asai, 1984).

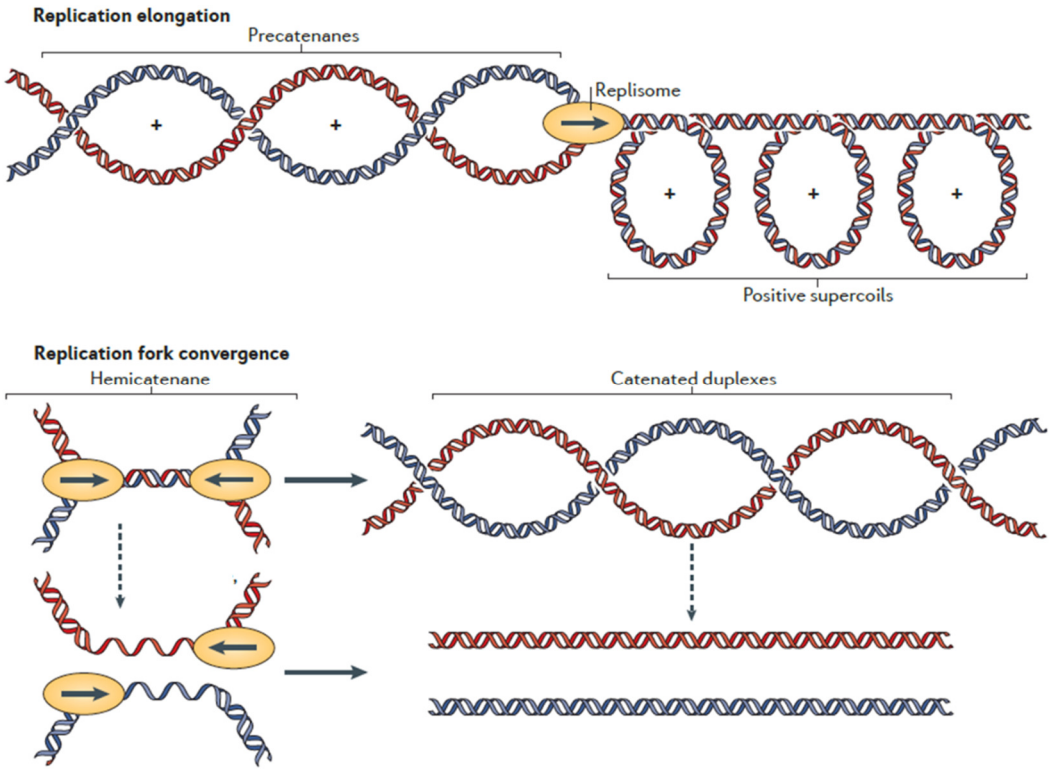

Figure 1.1: Various topological products that form during replication. As the replisome moves along the DNA, it can cause a build-up of positive supercoils ahead of the fork and precatenanes behind, which if left unresolved can cause replication fork collapse or stalling and knotting of sister duplexes, which may cause missegregation, respectively. At fork convergence, hemicatenanes can be formed which can be resolved into catenanes, both of which, if left, can cause missegregation. Figure adapted from (Vos *et al.*, 2011) with permission.

DNA topology and the control of negative supercoiling has also been demonstrated to be important during transcription. In a similar way to replication, positive supercoils can build up ahead of RNA polymerase whilst negative supercoils can build up behind it (Figure 1.2). If left unresolved these can impede transcription (Dorman & Dorman, 2016, Lilley *et al.*, 1996, Liu & Wang, 1987, Seol & Neuman, 2016). The degree of superhelical density of promoters has also been shown to influence gene expression. Additionally, the topological changes caused during transcription can locally affect the expression of other genes upstream or downstream (Dorman & Dorman, 2016, Lilley *et al.*, 1996).

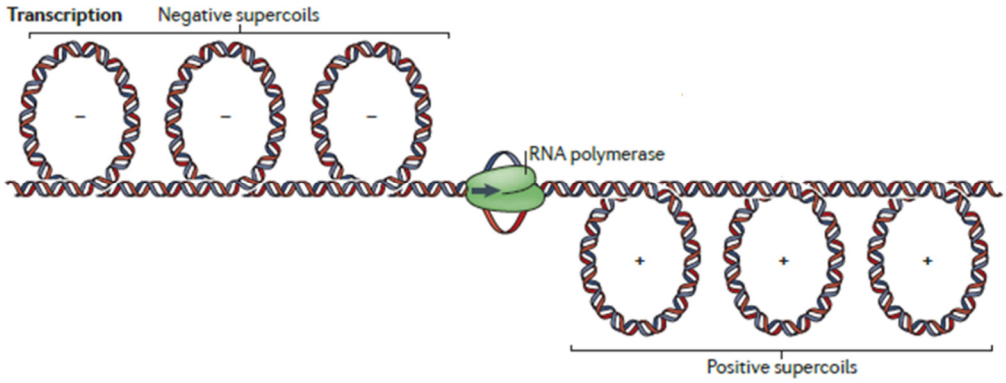

Figure 1.2: Topological problems arising during transcription. During transcription, as RNA polymerase unwinds the DNA, increased negative supercoils can form behind and positive supercoils can form ahead of the transcribed region. If left unresolved, this will result in stalling of RNA polymerase or failure of transcription. Figure adapted from (Vos *et al.*, 2011) with permission.

There is an added level of complication in bacteria and particularly in fast-growing species. Here replication and transcription are happening at the same time and collisions between the replication machinery and RNA polymerase occur frequently (McGlynn *et al.*, 2012). These can be head-on collisions or co-directional where the replication machinery catches up with RNA polymerase which moves at a much slower rate (McGlynn *et al.*, 2012, Hamperl & Cimprich, 2016, Mangiameli *et al.*, 2017). Head-on collisions have been shown to be the more devastating on fork progression. This can be either due to direct clashing of RNA polymerase with the replicative helicases or due to a build-up of positive supercoils between the converging processes (McGlynn *et al.*, 2012, Hamperl & Cimprich, 2016). Therefore, the highly-transcribed genes in fast replicating bacteria, such as *E. coli*, have been demonstrated to be orientated such that co-directional collisions are more likely. However, this does not completely solve the problem with highly-transcribed genes consistently causing replication blockages (McGlynn *et al.*, 2012, Hamperl & Cimprich, 2016).

In terms of recombination, negative supercoiling has also been demonstrated to be important. This is most often seen with bacteriophage chromosomes, which need to be negatively supercoiled for integrase-type site-specific recombination to occur (Mizuuchi *et al.*,

1978a, Nash, 1990). Another type of site-specific recombination involving resolvases (such as transposons), termed transposition site-specific recombination, can result in various knotted and catenated products. These products need to be resolved for continued survival of the cell (Bates & Maxwell, 2005).

Overall, the maintenance of DNA topology is crucial for survival. Negative supercoiling needs to be maintained at approximately 20% of the normal mean value for continued growth in *E. coli* (Drlica, 1992, Deng *et al.*, 2005). Loss of supercoiling can result in problems with chromosomal segregation (Hiraga *et al.*, 1989, Holmes & Cozzarelli, 2000, Sawitzke & Austin, 2000) and issues with gene expression and replication (Deng *et al.*, 2005, Zechiedrich *et al.*, 1997). While increased DNA supercoiling can cause unwanted DNA structures that can affect transcription or cause stalling of replication forks (Deng *et al.*, 2005, Higgins & Vologodskii, 2015). Like many other processes in biology, the interconversion of the various topological forms of DNA is maintained enzymatically. This maintenance of DNA topology is mediated by a group of diverse enzymes called DNA topoisomerases.

1.3 DNA Topoisomerases

Topoisomerases are enzymes that catalyse the interconversion of different topological forms of DNA (Bates & Maxwell, 2005). They are found ubiquitously and are essential to all cells. Topoisomerases work by cleaving either one or both strands of DNA. They then allow one strand to rotate around the other (controlled rotation) or pass the uncleaved strand through the cleaved strand (strand passage) before resealing the DNA backbone. In fact, topoisomerases are classified by the type of cleavage they make with DNA (i.e. single-stranded or double-stranded breaks). Type I topoisomerases catalyse reactions by cleaving one strand of the DNA backbone whilst type II topoisomerases cleave both strands. During topoisomerase-catalysed reactions, the cleavage is transient and is formed by the creation of a phosphodiester bond between the

catalytic tyrosine in the topoisomerase active site and the DNA backbone. These breaks in the DNA alter the linking number; type I topoisomerases alter the linking number by one per reaction cycle whilst type II topoisomerases alter the linking number by two. The respective reactions that each type of topoisomerase catalyses is depicted in Figure 1.3 and Figure 1.4 (Champoux, 1981, Deweese *et al.*, 2009, Liu *et al.*, 1980, Schoeffler & Berger, 2008, Sissi & Palumbo, 2010, Vos *et al.*, 2011). Type I topoisomerases typically catalyse ATP-independent reactions whilst type II topoisomerases require ATP for their catalytic cycles. Furthermore, many topoisomerases require a divalent metal ion cofactor for catalysis (Champoux, 1981, Schoeffler & Berger, 2008).

Type I topoisomerases can be further subdivided into types IA, IB and IC whilst the type II enzymes are divided into types IIA and type IIB. These subdivisions are based on differences in mechanism, structure and evolution (Schoeffler & Berger, 2008, Vos *et al.*, 2011). The specific types of reactions that the different topoisomerases have been shown to catalyse *in vitro* are indicated in Table 1.1.

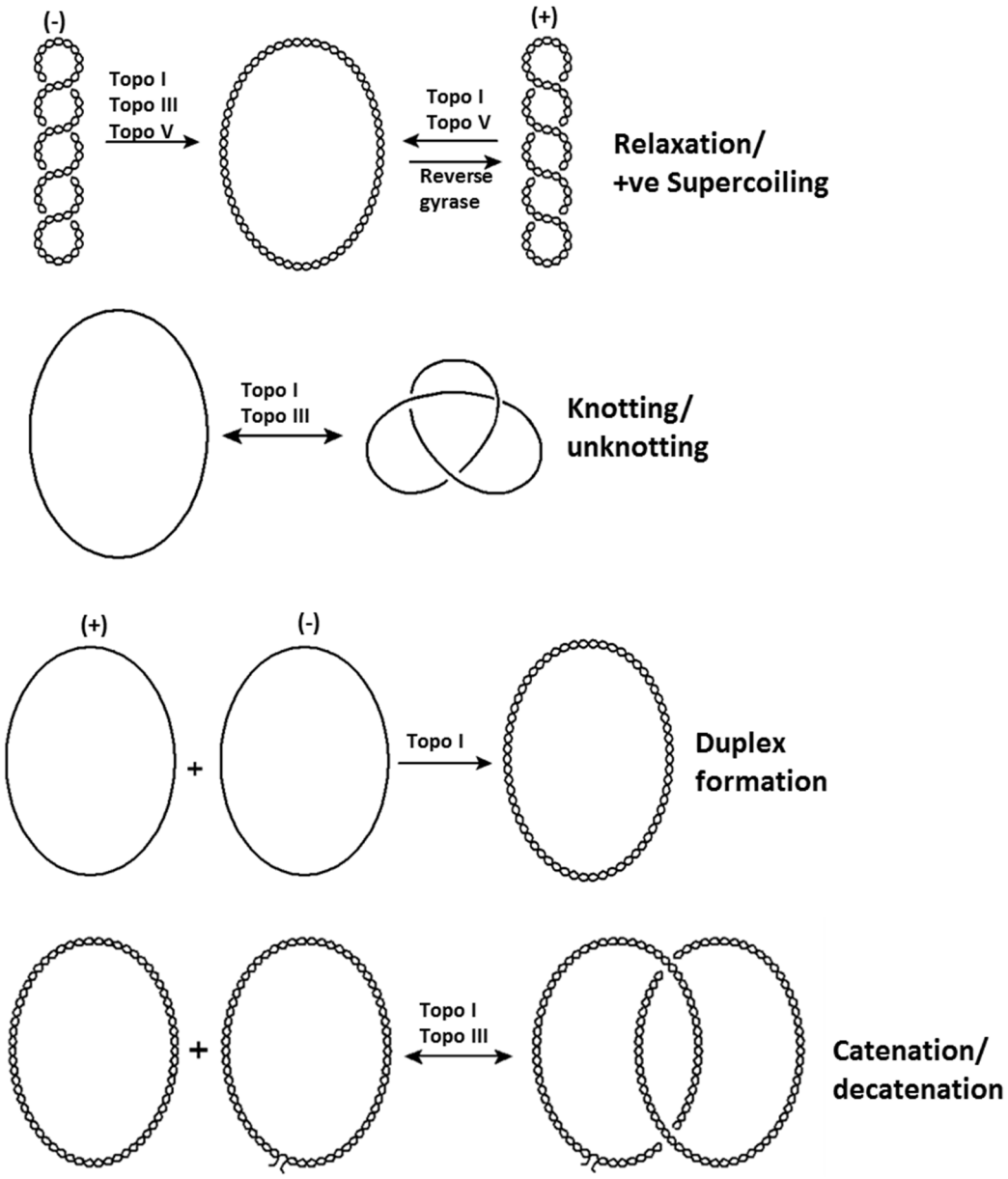

Figure 1.3: Reactions performed by type I topoisomerases. Examples of specific type I topoisomerases that catalyse the indicated reactions are given above the arrows. It is important to note that in the decatenation/catenation reaction, the non-nicked plasmid may be supercoiled before decatenation/catenation occurs; for illustrative purposes it has been drawn as relaxed. Figure taken from EcoSal Plus (Bush *et al.*, 2015) with permission.

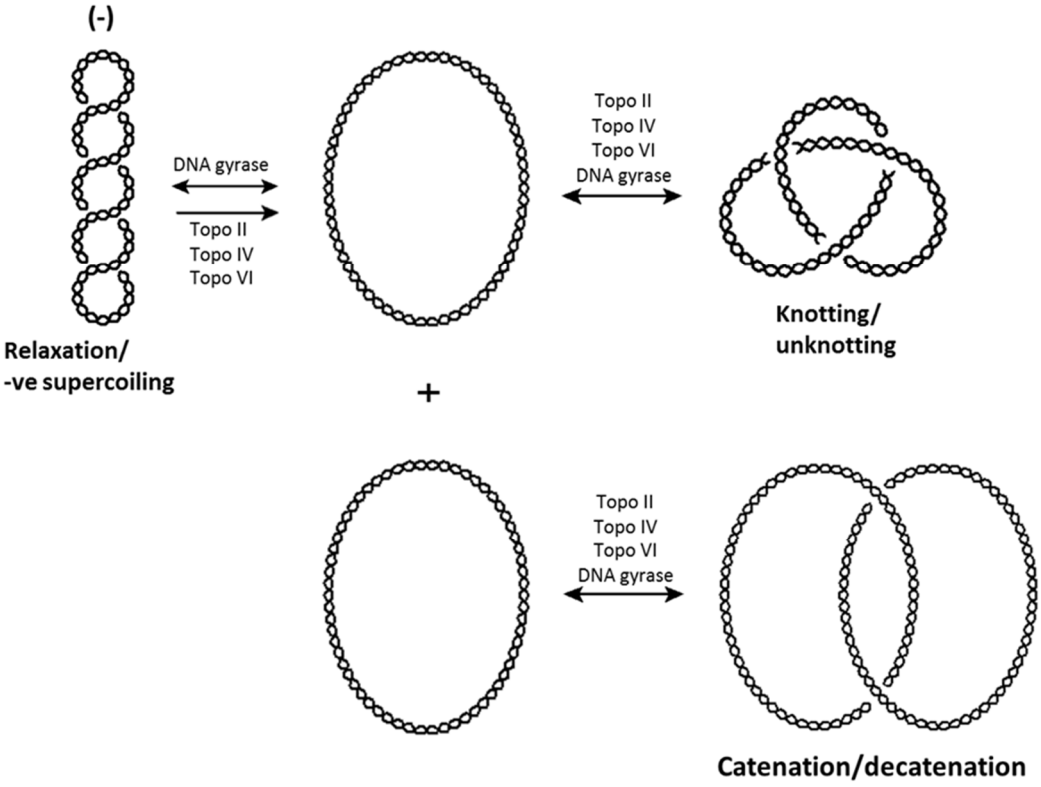

Figure 1.4: Reactions performed by type II topoisomerases. Examples of specific type II topoisomerases that catalyse the indicated reactions are given above the arrows. It is important to note that in the decatenation/catenation reaction, the plasmids may be supercoiled before decatenation/catenation occurs; for illustrative purposes they have been drawn as relaxed. Although only relaxation of negative supercoils is indicated, type II topoisomerases can relax positively supercoiled DNA as well. Figure from EcoSal Plus (Bush *et al.*, 2015) with permission.

Table 1.1: Properties of various DNA topoisomerases. Taken from EcoSal Plus (Bush *et al.*, 2015) with permission

Topoisomerase	Type	Enzyme structure	No. of DNA strands cleaved	5´ or 3´ bond formed	Proposed mechanism	ATP-dependent	Mg(II) dependent	Activities: Catenation/ decatenation	Knotting/ unknotting	Relaxation -ve	Relaxation +ve	Supercoiling -ve	Supercoiling +ve
Topo I Bacterial	IA	Monomer	1	5´	Strand passage	No	Yes	Yes[b]	Yes[b]	Yes	No	No	No
Eukaryotic	IB	Monomer	1	3´	Controlled rotation	No	No	Yes[b]	Yes[b]	Yes	Yes	No	No
Topo II	IIA	Homodimer	2	5´	Strand passage	Yes	Yes	Yes	Yes	Yes	Yes	No	No
Topo III	IA	Monomer	1	5´	Strand passage	No	Yes	Yes[b]	Yes	Yes	No	No	No
Topo IV	IIA	Heterotetramer	2	5´	Strand passage	Yes	Yes	Yes	Yes	Yes	Yes	No	No
Topo V	IB/IC[a]	Monomer	1	3´	Controlled rotation	No	No	Unknown	Unknown	Yes	Yes	No	No
Topo VI	IIB	Heterotetramer	2	5´	Strand passage	Yes	Yes	Yes	Unknown	Yes	Yes	No	No
Topo VIII	IIB	Homodimer?	2	5´	Strand passage	Yes	Yes?	Yes	Unknown	Yes	Yes	No	No
DNA gyrase	IIA	Heterotetramer	2	5´	Strand passage	Yes	Yes	Yes[c]	Yes	Yes	Yes	Yes	No
Reverse gyrase	IA	Monomer	1	5´	Strand passage	Yes	Yes	No	No	Yes	No	No	Yes

Notes:

[a] Topo V was originally described as type IB but has been proposed to form a new class (IC)

-ve indicates negatively-supercoiled DNA; +ve indicates positively supercoiled DNA

[b] Possible only if one substrate is nicked or single-stranded

[c] Decatenation by *E. coli* DNA gyrase is weak

? – presumed

Type I topoisomerases

Type I topoisomerases are historically named with odd numbers. There are currently four known type I topoisomerases: topo I, topo III, topo V and reverse gyrase. The respective domain diagrams for these type I topoisomerases are shown in Figure 1.5. A brief appraisal of the type I topoisomerases follows (for a more extensive review, see (Schoeffler & Berger, 2008, Capranico *et al.*, 2017)).

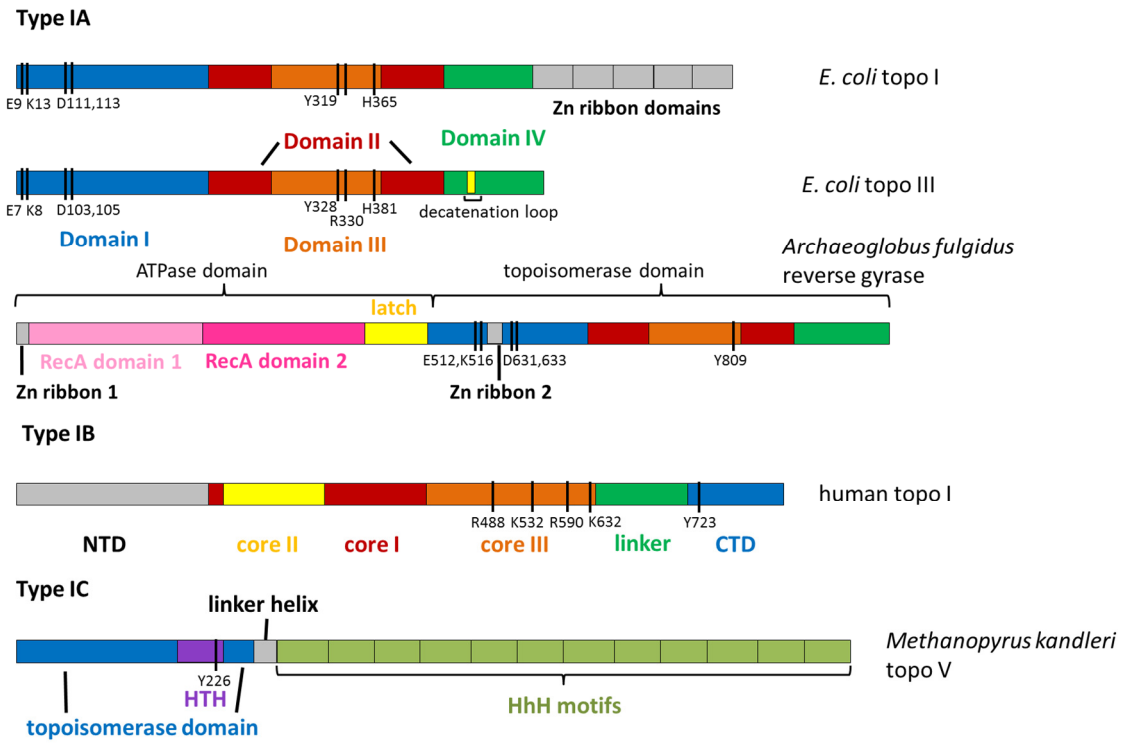

Figure 1.5: Primary domain structures of type I topoisomerases. Black bars indicate catalytic residues. Y is the catalytic tyrosine which forms the covalent bond with the phosphodiester backbone of the cleaved single-strand of DNA (319 in *E. coli* topo I, 328 in *E. coli* topo III, 809 in *A. fulgidus* reverse gyrase, 723 in human topo I and 226 in *M. kandleri* topo V) (for full description of all catalytic residues see reference (Schoeffler & Berger, 2008)). Type IB: NTD is N-terminal domain; CTD is C-terminal domain. Type IC: HTH is helix-turn-helix; HhH is helix-hairpin-helix. Figure taken from EcoSal Plus (Bush *et al.*, 2015) with permission.

Topo I was the first DNA topoisomerase to be discovered and was initially called ω protein (Wang, 1971, Wang, 2009). It is found in prokaryotes and eukaryotes; however, the bacterial and eukaryotic enzymes show mechanistic and structural differences (Table1.1) (Champoux & Dulbecco, 1972, Wang, 1971). Eukaryotic topo I is a type IB topoisomerase which is capable of relaxing both negative and positive supercoils by a controlled rotation mechanism (Stewart *et al.*, 1998). In contrast, bacterial topo I is a type IA topoisomerase which only relaxes negative supercoils and this is by strand passage (Lima *et al.*, 1994, Schoeffler & Berger, 2008). Both enzymes can catenate or decatenate DNA provided that one of the DNA strands is nicked (Tse & Wang, 1980). Topo I is non-essential in bacteria, except in species where it is the only type I topoisomerase such as in the *Mycobacterium* species. However, in topo I-inactivated strains, cold sensitivity and compensatory mutations in the DNA gyrase genes *gyrA* and *gyrB* can be found (Dinardo *et al.*, 1982, Pruss *et al.*, 1982, Richardson *et al.*, 1984, Stupina & Wang, 2005). Although topo I is non-essential in many bacteria, it can cause double-stranded DNA breaks that lead to induction of the SOS response (Cheng *et al.*, 2005).

Topo III is a type IA topoisomerase that relaxes and decatenates DNA but has also been shown to catenate and decatenate RNA (Digate & Marians, 1989, Digate & Marians, 1992). Topo III has been identified in prokaryotes, eukaryotes and archaea and is well-conserved across evolutionary lineages (Schoeffler & Berger, 2008). It shares considerable homology to prokaryotic topo I (Digate & Marians, 1989) and like topo I is non-essential (Digate & Marians, 1989); except in a topoisomerase IV temperature-sensitive background, where it is lethal (Lopez *et al.*, 2005). Although topo III is capable of relaxation, it is thought that its primary function in the cell is the resolution of precatenanes, chromosome segregation as well as the resolution of some recombination intermediates (Digate & Marians, 1989, Lopez *et al.*, 2005, Oakley & Hickson, 2002, Perez-Cheeks *et al.*, 2012, Valenti *et al.*, 2012). This may point to the reason behind the lethality of *topB* (topo III) deletions in a topoisomerase IV-depleted background. With

regard to recombination, RecQ helicases are often linked to topo III in the resolution of stalled and converging replication forks (Suski & Marians, 2008).

Topo V is the only member of the type IC topoisomerases which has, to date, only been found in the archaeal genus *Methanopyrus* sp. (Slesarev *et al.*, 1993). It was previously identified and classed as a type IB topoisomerase but has recently been reclassified based on structural and biochemical analyses (Rajan *et al.*, 2010, Slesarev *et al.*, 1993, Taneja *et al.*, 2006). Topo V has been shown to relax both positively- and negatively-supercoiled DNA by controlled rotation (Taneja *et al.*, 2007). It has recently been shown to participate in DNA repair as it was demonstrated to have AP lyase (apurinic/apyrimidinic) and deoxyribose-5-phosphate (dRP) lyase activities (Belova *et al.*, 2002, Rajan *et al.*, 2016, Taneja *et al.*, 2006).

Reverse gyrase is an unusual type IA topoisomerase as it is capable of introducing positive supercoils into DNA in an ATP-dependent reaction. It is also able to relax negatively-supercoiled DNA in an ATP-independent manner (Forterre *et al.*, 1985, Shibata *et al.*, 1987). The crystal structure has revealed a C-terminal that resembles a type IA topoisomerase but the N-terminal resembles a helicase (Confalonieri *et al.*, 1993, Rodríguez, 2002, Rudolph *et al.*, 2013). Concurrently, if you delete the C-terminal domain, the enzyme has been shown to transiently unwind DNA (Ganguly *et al.*, 2013). Additionally, the full-length enzyme has been shown to unwind DNA and it is thought that this capability directs strand passage in a positive supercoiling direction (Ganguly *et al.*, 2013, Rodríguez, 2002). Reverse gyrase is found in thermophilic and hyperthermophilic archaea, and eubacteria (Forterre, 2002, Forterre *et al.*, 1985, Shibata *et al.*, 1987).

Type II topoisomerases

Type II topoisomerases are found in eukaryotes, prokaryotes and in archaea. They are typically named with even numbers and there are four currently characterised. These are topo II, topo IV, topo VI, topo VIII and DNA gyrase (Table 1.1). Their respective domain diagrams are shown in Figure 1.7 (excluding topo VIII). All type II topoisomerases operate through the same

basic mechanism, however, the process in DNA gyrase has been best characterised. The basic mechanism of relaxation is outlined below Figure 1.6).

A gate (G) segment of DNA is bound and bent across the enzyme at the interface between the DNA-binding domain and the ATPase domain. The binding of ATP to the ATPase region results in the capture of a transport (T) segment. Hydrolysis of ATP to ADP triggers cleavage of the double-stranded G-segment DNA, with a 4-bp stagger between the cuts in the two strands. This is followed by the T-segment passing through the gap in the G-segment and into the cavity formed by the two C-terminal domains. Following strand passage, the two ATPase domains rotate around each other ensuring the unidirectional movement of the T-segment. The G-segment is religated, and the T-segment passes out of the enzyme through the bottom gate. The release of the ADP molecules allows the enzyme to return to its original conformation (Bates *et al.*, 2011, Schmidt *et al.*, 2012). The exact timing of and sequence of ATP hydrolysis is yet to be fully determined. Variations to this mechanism will be discussed with reference to the respective enzyme.

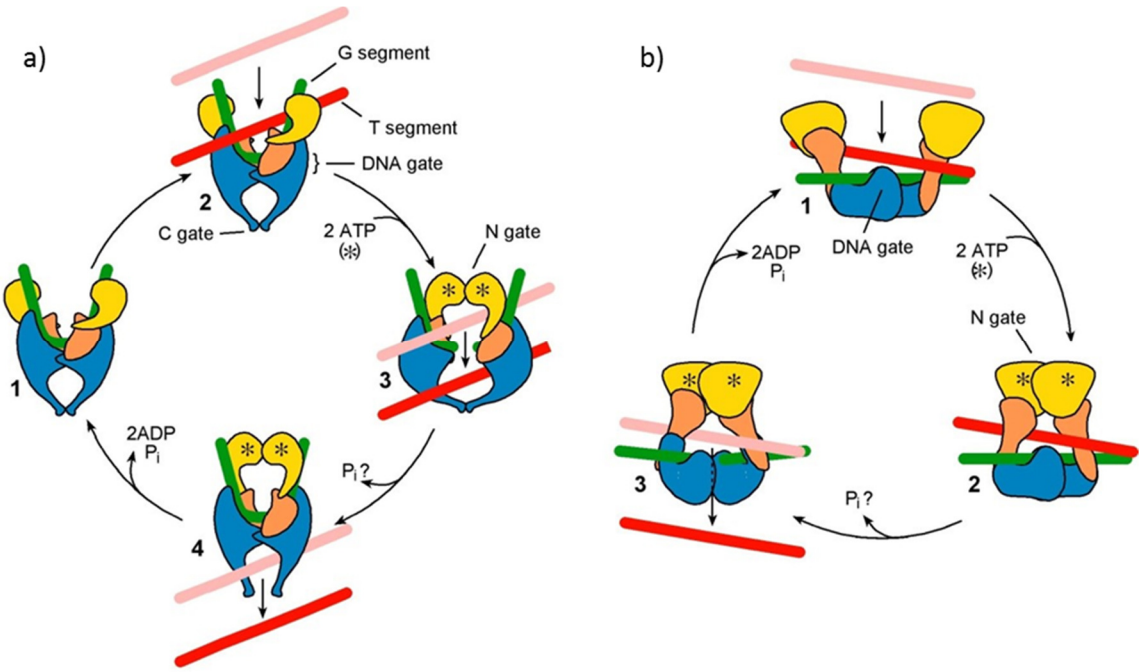

Figure 1.6: Structure and mechanism of type II topoisomerases. Type IIA topoisomerase mechanism. Domains of the protein are indicated in colour. Yellow indicates the GHKL domain, orange the TOPRIM domain and blue the cleavage-religation domain. The T-segment (red/pink) is transported through the enzyme-stabilised double-stranded break in the G-segment (green). b) Type IIB (topo VI) mechanism (note lack of C (exit)-gate). Figure adapted from (Bates *et al.*, 2011).

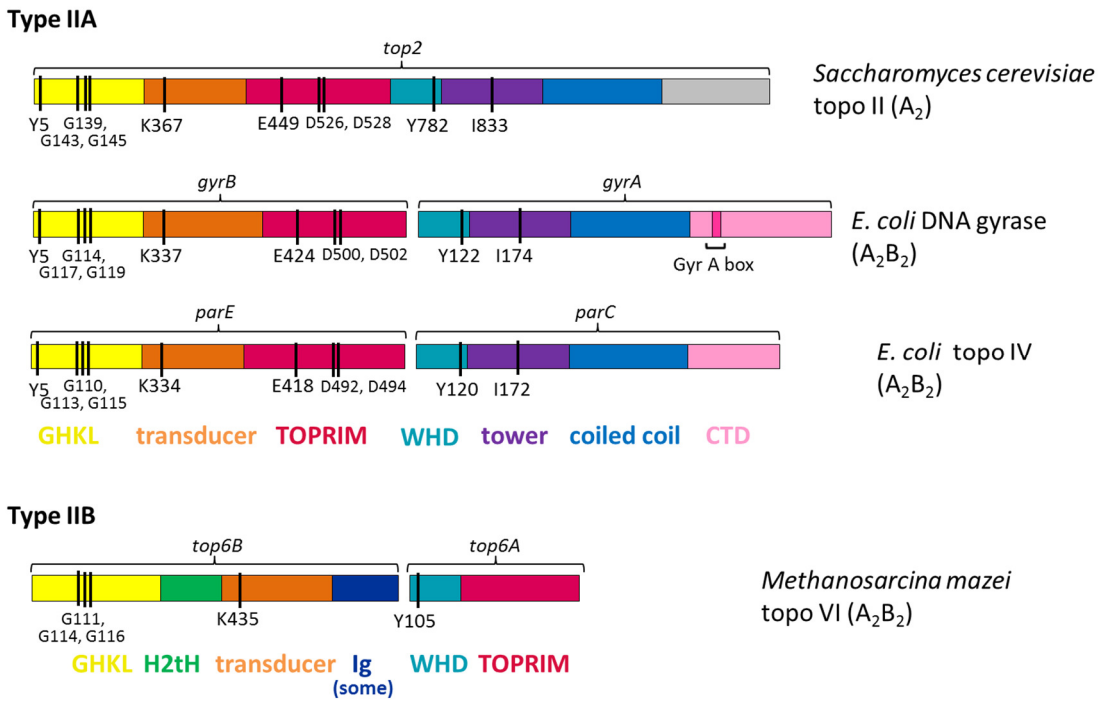

Figure 1.7: Primary domain structures of type II topoisomerases. Black bars indicate catalytic residues. Y is the catalytic tyrosine which forms the covalent bond with the phosphodiester backbone of the cleaved strand of DNA (782 in *S. cerevisiae* topo II, 122 *in E. coli* DNA gyrase, 120 in *E. coli* topo IV, and 105 in *M. mazei* topo VI) (for full description of all catalytic residues see reference (Schoeffler & Berger, 2008)). GHKL is the ATPase domain, TOPRIM stands for topoisomerase/primase domain, WHD is winged-helix domain, CTD is C-terminal domain, H2tH is helix-helix-turn helix domain, and Ig is an immunoglobulin type fold (not seen in all species). Figure taken from EcoSal Plus (Bush *et al.*, 2015) with permission.

Topo VI

Topo VI is an archaeal type IIB topoisomerase that is found in all known archaea (Bergerat *et al.*, 1997, Bergerat *et al.*, 1994), however, it has also recently been found in plants (Hartung & Puchta, 2000) and in the apicomplexan parasite Plasmodium sp. (Aravind *et al.*, 2003). In *Arabidopsis thaliana* it has been shown to be involved in endoreduplication (Hartung *et al.*, 2002, Sugimoto-Shirasu *et al.*, 2002) whilst in *Plasmodium* sp. it is thought to play a role in schizogeny (Aravind *et al.*, 2003). Topo VI is able to decatenate DNA and relax both positive and negative supercoils, and it acts as an A_2B_2 heterotetramer (Bergerat *et al.*, 1997). Apart from three motifs in the ATPase domain and the topoisomerase-primase (TOPRIM) fold, topo VI shows little sequence homology to type IIA topoisomerases (Aravind *et al.*, 1998, Bergerat *et al.*,

1997). A number of structures from topo VI have been resolved including the topo VIA subunit (topo VIA) from *Methanococcus jannaschii*, the topo VIB from *Sulfolobus shibatae* in a variety of conformations involving a range of nucleotides, and the full structure of topo VI from *Methanosarcina mazei* (Corbett *et al.*, 2007, Corbett & Berger, 2003, Corbett & Berger, 2005, Nichols *et al.*, 1999). One major difference ascertained from these structures is the lack of a post-strand passage cavity, it has only two protein gates rather than three, which is unlike type IIA topoisomerases (Figure 1.6) (Corbett *et al.*, 2007, Nichols *et al.*, 1999). Another difference is the double-stranded breaks made by topo VI have a 2-bp stagger in contrast to the 4-bp stagger created by the type IIA topoisomerases (Buhler *et al.*, 2001). As yet, topo VI has not been investigated in topoisomerase-mediated illegitimate recombination, however, the topo VIA protein has been identified as an orthologue of the meiotic recombination protein SpoII (Bergerat *et al.*, 1997). More recently, in mice and *A. thaliana* a topo VIB-like protein has been identified as an associate protein of SpoII and demonstrated to be involved in initiating double-strand breaks during meiosis (Robert *et al.*, 2016a, Vrielynck *et al.*, 2016, Robert *et al.*, 2016b).

Topo VIII

A second type IIB topoisomerase, topo VIII has recently been discovered *in silico* (Gadelle *et al.*, 2014). It has been found in a number of bacterial genomes, two bacterial plasmids and an archaeal plasmid and is thought to have originated from a conjugative plasmid or some other mobile genetic element (Gadelle *et al.*, 2014). Unlike the other type IIB topoisomerases, the A and B subunits are fused and topo VIII is proposed to be a homodimer. It has been demonstrated to have both relaxation and decatenation activities, much like topo VI, although much weaker and the protein was far less stable (Gadelle *et al.*, 2014).

Topo II

Topo II is a type IIA topoisomerase that can relax both positively and negatively-supercoiled DNA in an ATP- dependent manner. It can also catenate and decatenate DNA (Table 1.1) and has been found in all eukaryotes (Baldi *et al.*, 1980, Bauer *et al.*, 2012, Hsieh & Brutlag, 1980, Liu *et*

al., 1980). Topo II is also involved in the condensation, structural preservation and segregation of daughter chromosomes following DNA replication (Bauer *et al.*, 2012, DiNardo *et al.*, 1984). Higher eukaryotes generally contain two isoforms, termed topo IIα and topo IIβ (Drake *et al.*, 1989a), which appear to be expressed at different times in the cell cycle and in different cell types (Capranico *et al.*, 1992, Gonzalez *et al.*, 2011). The two isoforms share 72% homology in protein sequence with the greatest divergence at the N-terminal domain (NTD) and C-terminal domain (CTD) (Bollimpelli *et al.*, 2017). Topo IIα is found in proliferating cell types, and expression peaks during the G2 and M phases of the cell cycle. Topo IIβ is found in all cell types, and its expression is constant throughout the cell cycle (Turley *et al.*, 1997). Topo IIα also participates in chromosome condensation during apoptosis (Durrieu *et al.*, 2000) and topo IIβ has also been shown to participate in cell differentiation and tissue development (Vávrová & Šimůnek, 2012). When topo IIα is deleted it results in embryonic death whilst a topo IIβ knock-out results in death shortly after birth (Akimitsu *et al.*, 2003, Yang *et al.*, 2000). Topo II in yeast is also indicated to be cell cycle regulated (Clarke *et al.*, 2006, DiNardo *et al.*, 1984, Furniss *et al.*, 2013, Uemura *et al.*, 1987). More recently, it has been demonstrated that double-stranded breaks induced by topo IIβ may be vital for transcriptional activation of some genes (Calderwood, 2016).

Topo II shares many structural and mechanistic similarities with DNA gyrase and topo IV. The NTD of topo II aligns with the DNA gyrase subunit GyrB and the topo IV subunit ParE whilst the CTD aligns with GyrA and ParC (Figure 1.7). It is thought that topo II may have evolved following the fusion of the genes encoding the A and B subunits of gyrase (Lynn *et al.*, 1986). Topo II does, however, differ significantly from topo IV and DNA gyrase at the C terminus. In DNA gyrase and topo IV, this domain is important mechanistically. Whereas in topo II it has been determined to have a regulatory role and includes nuclear localisation signals (Watt & Hickson, 1994, Meczes *et al.*, 2008, Nitiss, 2009a). The structure of residues 1-1177 (fully active construct) of *S. cerevisiae* topo II complexed with ADPNP (5'-adenylyl β,γ-imidodiphosphate, a non-

hydrolysable ATP analogue) and DNA has been determined by X-ray crystallography (Figure 1.8) (Schmidt *et al.*, 2012). It shows a homodimer with the NTDs in a domain-swapping conformation (the subunits wrapped around one another). A previous crystal structure of a 92 kDa fragment of the enzyme complexed with a nicked DNA oligonucleotide denoted a 150° bend in the DNA (Dong & Berger, 2007). These structural data, as well as data collected from the other type II topoisomerases, have provided information of a possible mechanism. Topo II (despite the enzyme having three protein interfaces) is thought to operate using the "two-gate" mechanism, as described above (Berger *et al.*, 1996, Roca *et al.*, 1996).

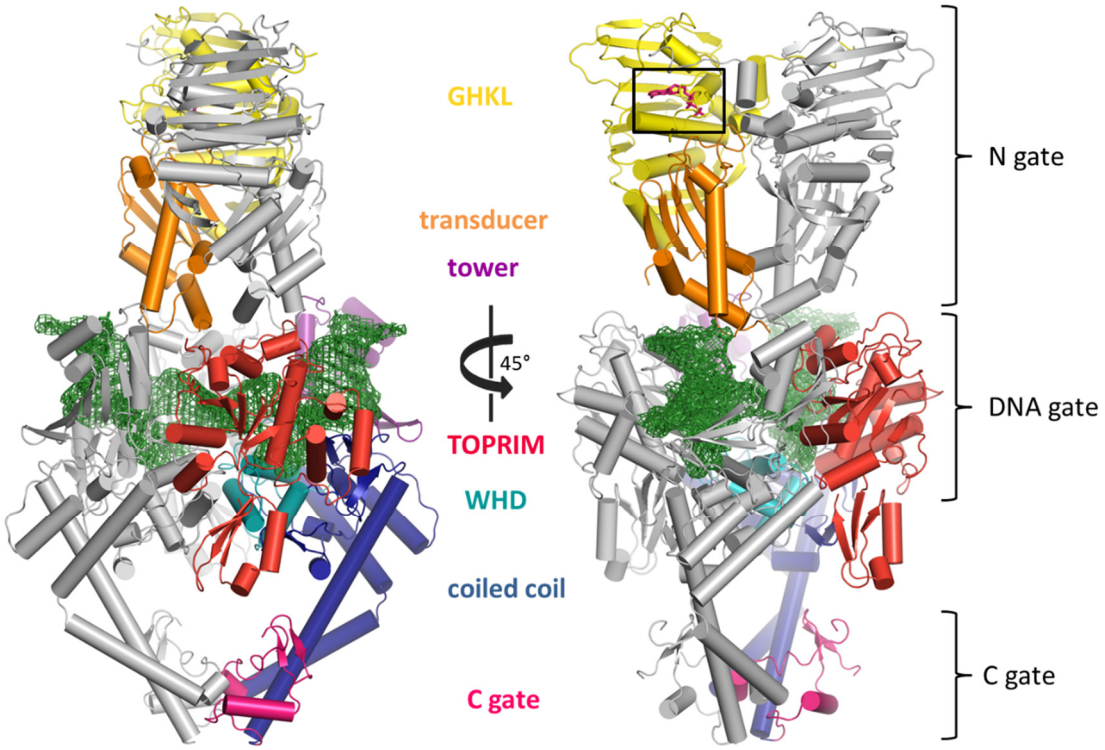

Figure 1.8: Structure of truncated (amino acids 1-1177) *S. cerevisiae* topo II bound to DNA and ADPNP. One monomer is shaded grey the other coloured by functional region (see domain diagram Figure 1.7). WHD is winged-helix domain; TOPRIM is topoisomerase-primase domain. Black box indicates position of ADPNP and green indicates DNA. Figure taken from EcoSal Plus (Bush *et al.*, 2015) with permission.

Topo IV

Topo IV (Figure 1.9) is a type IIA topoisomerase that uses ATP hydrolysis (Peng & Marians, 1993) to decatenate replication products (Levine *et al.*, 1998), relax positive and negative (although less efficiently) supercoils (Crisona *et al.*, 2000), and knot and unknot DNA (Table 1.1) (Deibler *et al.*, 2001). Topo IV consists of two subunits, encoded by the *parC* and *parE* genes (Madhusudan & Nagaraja, 1996, Peng & Marians, 1993, Springer & Schmid, 1993). The *E. coli* ParC and the ParE subunits (84 kDa and 70 kDa respectively) are homologous to GyrA and GyrB (from DNA gyrase) both in sequence and in structure. However, there are some differences between the two enzymes, the principal being that topo IV is not capable of DNA supercoiling (Peng & Marians, 1995). Furthermore, although gyrase and topo IV share sequence similarities they have quite distinct cellular roles. Topo IV is the predominant enzyme responsible for decatenation and unknotting, whereas gyrase is responsible for supercoiling (Deibler *et al.*, 2001, Ullsperger & Cozzarelli, 1996, Zechiedrich & Cozzarelli, 1995, Zechiedrich *et al.*, 1997). Topo IV also plays a major role in chromosome segregation after DNA replication with the help of motor proteins and cytoskeletal components (Adams *et al.*, 1992). In particular, topo IV has been shown to interact with the SMC complex MukBEF in *E. coli*. It has been shown that MukBEF associates with topo IV at the origin of replication (Nicolas *et al.*, 2014) and along with MatP and XerD/C ensures successful and timely decatenation at the replication termination site (Nolivos *et al.*, 2016, El Sayyed *et al.*, 2016). Furthermore, the interaction between MukB and topo IV has been shown to be important for DNA condensation with topo IV stabilising MukB on the DNA which increased the level of DNA compaction (Kumar *et al.*, 2017).

A number of structures of various full length and truncated forms of the ParE and ParC subunits have been solved (Bellon *et al.*, 2004, Corbett *et al.*, 2005, Hsieh *et al.*, 2004, Laponogov *et al.*, 2013, Laponogov *et al.*, 2007). These structures have highlighted the differences and similarities between gyrase and topo IV and have also provided useful mechanistic insights. One particular difference they have highlighted is between the ParC and GyrA CTD. ParC CTD has been shown to be a broken five-bladed β-pinwheel (Figure 1.9D) (Corbett *et al.*, 2005, Hsieh *et*

al., 2004) whereas GyrA CTD forms a six-bladed β-pinwheel (Corbett *et al.*, 2004) (Figure 1.8C4). Additionally, the ParC CTD is anchored to the NTD, which would limit the movement of the domain (Corbett *et al.*, 2005). In contrast, the GyrA CTD domain is connected to the NTD by a flexible linker, allowing movement (Corbett *et al.*, 2005, Costenaro *et al.*, 2005). These differences mean that topo IV cannot wrap DNA in the same way as DNA gyrase, providing an explanation for the inability of topo IV to negatively supercoil DNA (Kampranis & Maxwell, 1998a). This is also confirmed by the fact that when the GyrA CTD is deleted it is converted into a topo IV-like enzyme (Kampranis & Maxwell, 1996). It has been proposed that the ParC CTD is important for substrate specificity as topo IV shows chiral discrimination between positively and negatively-supercoiled DNA (Corbett *et al.*, 2005, Neuman *et al.*, 2009, Stone *et al.*, 2003). It has also been recently demonstrated to be able to discriminate between left-handed and right-handed nodes in catenanes and knots that allow for the resolution of these topological forms without causing relaxation (Rawdon *et al.*, 2016).

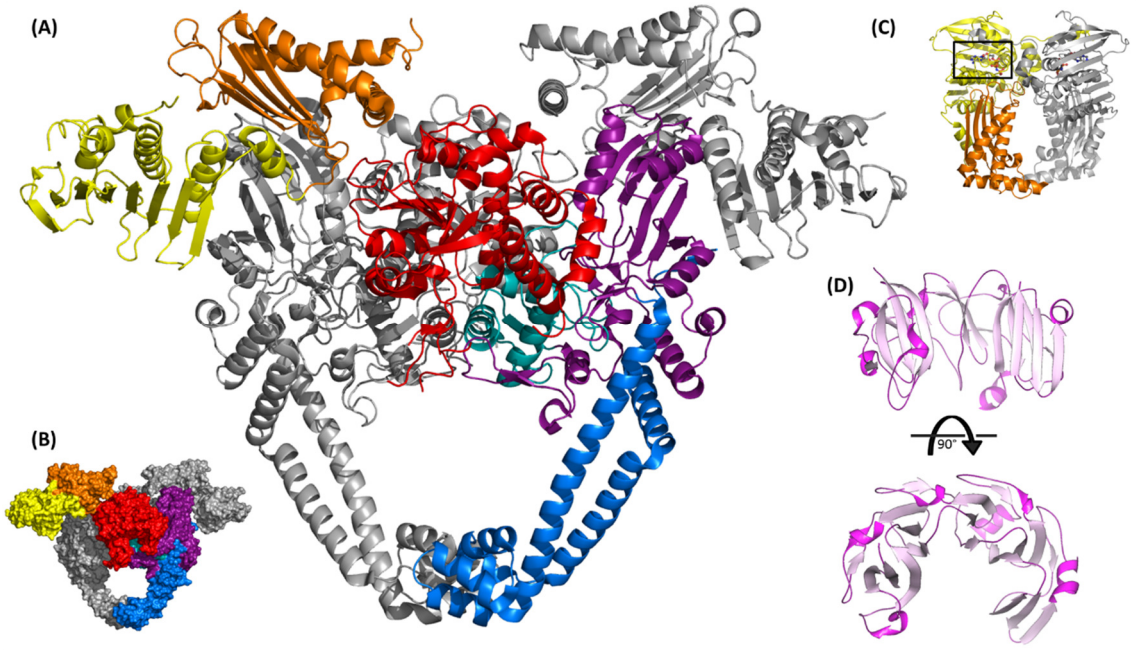

Figure 1.9: Structures of topoisomerase IV. (A) is the structure of the ParE- ParC55 fusion construct (Laponogov *et al.*, 2013) (PDB: 4I3H). Yellow indicates the GHKL domain; orange the transducer domain; teal is the winged-helix domain (WHD); purple is the tower domain; and blue shows the coiled-coil domain (see Figure 1.7 for domain structure). (B) is the space-filled model of (A). (C) is the ParE 43 kDa N-terminal fragment complexed with ADPNP (black box) (PDB: 1S16) (Bellon *et al.*, 2004). It is proposed that the open conformation of ParE as seen in (A) is the conformation pre-ATP binding whereas the conformation seen in (C) is the post-ATP binding conformation. (D) is the ParC C-terminal domain in two orientations (PDB: 1ZVT) (Corbett *et al.*, 2005). Figure from EcoSal Plus (Bush *et al.*, 2015) with permission.

DNA gyrase

DNA gyrase (Figure 1.10) is a type IIA topoisomerase that is unique in its ability to introduce negative supercoils in the presence of ATP into covalently-closed double-stranded DNA (Gellert *et al.*, 1976a). Gyrase also uses ATP hydrolysis to relax positively supercoiled DNA in a reaction equivalent to the introduction of negative supercoils, even though this process is energetically favourable (Gellert *et al.*, 1976b, Sugino *et al.*, 1978, Brown & Cozzarelli, 1979). It has been demonstrated to be capable of decatenation and unknotting reactions in the presence of ATP as well (although not shown, it is also presumably capable of the converse reactions) (Kreuzer &

Cozzarelli, 1980, Liu *et al.*, 1980, Marians, 1987, Mizuuchi *et al.*, 1980). Furthermore, DNA gyrase can relax negatively-supercoiled DNA in an ATP-independent reaction (Gellert *et al.*, 1979, Higgins *et al.*, 1978). DNA gyrase is responsible for all processes in bacteria that require negative supercoiling, including chromosome compaction, origin firing and recombination. It is also responsible for the resolution of unwanted positive supercoils ahead of replication forks or ahead of RNA polymerase during transcription (Dorman & Dorman, 2016, Nollmann *et al.*, 2007a, Seol & Neuman, 2016, Wang, 2002). DNA gyrase works together with bacterial Topo I to maintain the levels of supercoiling in the cell (Drlica, 1992). In fact, the genome-wide recruitment of *Mycobacterium tuberculosis* DNA gyrase and topo I have recently been demonstrated to be closely coupled to transcription, with DNA gyrase shown to be recruited ahead of RNA polymerase and topo I behind it (Ahmed *et al.*, 2017).

DNA gyrases are ubiquitous in bacteria but have additionally been discovered in plants (Cho *et al.*, 2004, Wall *et al.*, 2004) and in apicomplexan parasites (Carucci *et al.*, 1998, Dar *et al.*, 2007, Lin *et al.*, 2015). However, they do not appear to be present in other eukaryotes. This, along with the fact that DNA gyrase is an essential bacterial enzyme, has made it a successful target for several antibacterial agents. *E. coli* DNA gyrase is made up of two 97 kDa GyrA subunits and two 90 kDa GyrB subunits encoded by the *gyrA* and *gyrB* genes, respectively, and organised as an A_2B_2 heterotetramer (Adachi *et al.*, 1987, Klevan & Wang, 1980, Sugino *et al.*, 1980, Swanberg & Wang, 1987). Transcription of the *gyrA* and *gyrB* genes themselves is controlled by the level of supercoiling in an autoregulatory feedback system (Menzel & Gellert, 1983, Snoep *et al.*, 2002, Dorman & Dorman, 2016).

The GyrA and GyrB subunits can each be split into two principal domains (Kampranis & Maxwell, 1998a, Reece & Maxwell, 1989). *E. coli* GyrB comprises a 43 kDa NTD and a 47 kDa CTD. The former is responsible for ATP binding and hydrolysis whilst the latter interacts with GyrA and DNA (Chatterji *et al.*, 2000, Noble & Maxwell, 2002, Schoeffler *et al.*, 2010, Wigley *et al.*, 1991). The 47 kDa domain of GyrB may be further subdivided into two subdomains, the

TOPRIM domain and the tail (Costenaro *et al.*, 2007, Fu *et al.*, 2009). GyrA consists of a 59 kDa NTD responsible for DNA breakage (Horowitz & Wang, 1987) and a 35 kDa CTD that wraps DNA (Corbett *et al.*, 2004). The 59 kDa domain can be further divided into the tower/shoulder, winged-helix, and coiled-coil domains in line with other type IIA topoisomerases (Berger *et al.*, 1996, Dong & Berger, 2007, Morais Cabral *et al.*, 1997, Schoeffler & Berger, 2008). The structures of all of the gyrase domains have been resolved (Corbett *et al.*, 2004, Fu *et al.*, 2009, Hsieh *et al.*, 2010, Morais Cabral *et al.*, 1997, Piton *et al.*, 2010, Ruthenburg *et al.*, 2005, Schoeffler *et al.*, 2010, Tretter & Berger, 2012b, Wigley *et al.*, 1991), but only individually in the form of truncated and fusion constructs. Thus, no full-length, high-resolution gyrase structure exists. There are, however, low-resolution structures of the whole protein obtained through small-angle X-ray scattering (SAXS) (Baker *et al.*, 2011, Costenaro *et al.*, 2005, Costenaro *et al.*, 2007), supramolecular mass spectrometry and 3D cryo-electron microscopy (cryo-EM) (Papillon *et al.*, 2013).

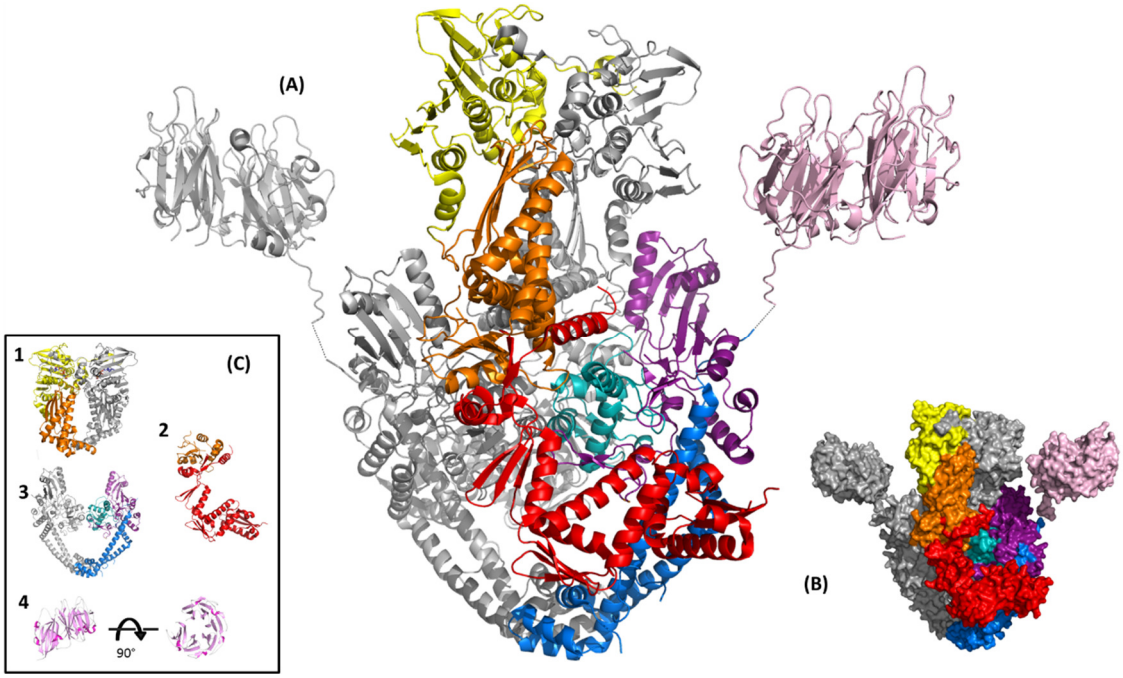

Figure 1.10: Structures of DNA gyrase. (A) is a model of the full-length structure of DNA gyrase. Yellow indicates the GHKL domain; orange the transducer domain; teal is the winged-helix domain (WHD); purple is the tower domain; blue shows the coiled-coil domain and pink indicates the CTD (see Figure 4 for domain structure). The full-length protein structure was modelled on the ATPase 43 kDa fragment (PDB: 1EI1); a B-A fusion construct (PDB: 3NUH) (Schoeffler *et al.*, 2010) and the GyrA 35 kDa C-terminal domain (PDB: 3L6V). (B) is the space-filled model of (A). Panel (C) shows the four principal domains of gyrase. (C1) is the *E. coli* GyrB 43 kDa fragment complexed with ADPNP; (C2) is the *E. coli* GyrB TOPRIM domain; (C3) is the *E. coli* GyrA 59 kDa subunit; and (C4) is the *E. coli* GyrA C-terminal domain in two orientations (PDB: 1ZI0). Figure taken from EcoSal Plus (Bush *et al.*, 2015) with permission.

With the wealth of biochemical and structural data available on DNA gyrase, it is not surprising that its mechanism is the best described of all the type II topoisomerases. Furthermore, single-molecule experiments have served to verify these data and further extend our knowledge (Koster *et al.*, 2010, Neuman, 2010, Nollmann *et al.*, 2007a, Gubaev *et al.*, 2009, Gubaev & Klostermeier, 2011, Gubaev & Klostermeier, 2014, Lanz & Klostermeier, 2011, Rudolph & Klostermeier, 2013, Basu *et al.*, 2016). The proposed mechanism of negative supercoiling by gyrase (Figure 1.11) is outlined below.

Negative supercoiling occurs via a two-gate mechanism (see above, Figure 1.6) (Mizuuchi *et al.*, 1980). The G-segment, binds across the top dimer interface of the GyrA NTDs (Gellert *et al.*, 1976b, Morais Cabral *et al.*, 1997). The bound G-segment is bent at an angle of approximately 70° (Papillon *et al.*, 2013). Binding induces an upward movement of the GyrA CTDs, resulting in an adjacent section of the DNA becoming wrapped around the CTDs (Heddle *et al.*, 2004, Lanz & Klostermeier, 2011, Basu *et al.*, 2016). This wrapping positions the T-segment across the G-segment at an angle of approximately 60° and it also provides gyrase with its unique ability to supercoil DNA (Heddle *et al.*, 2004, Papillon *et al.*, 2013, Ruthenburg *et al.*, 2005). A conserved region on the CTD, termed the GyrA box, is proposed to orientate the T-segment in a positive node that favours DNA supercoiling (Kramlinger & Hiasa, 2006). The total length of DNA bound by gyrase is estimated to be between 120 and 150 bp (Fisher *et al.*, 1981, Kirkegaard & Wang, 1981, Morrison & Cozzarelli, 1981). DNA wrapping and the presentation of the T-segment has been demonstrated to occur in the absence of ATP, however, ATP (or ADPNP) is crucial for strand passage to occur (Sugino & Cozzarelli, 1980, Bates *et al.*, 1996, Kampranis *et al.*, 1999a, Basu *et al.*, 2012). Following DNA binding and wrapping, ATP is bound to the NTDs of the two GyrB subunits, causing dimerisation and the closure of the clamp. This closure traps the T-segment in the complex (Basu *et al.*, 2012, Kampranis *et al.*, 1999a, Basu *et al.*, 2016). In *E. coli* supercoiling is thought to be influenced by a small acidic tail on the GyrA CTD which has been shown to couple ATP binding to DNA binding (Tretter & Berger, 2012a, Lanz *et al.*, 2014).

The bound G-segment forms phosphotyrosine bonds with the active-site tyrosines, generating a double-strand break (DSB) with 4-bp overhangs (Horowitz & Wang, 1987, Morrison & Cozzarelli, 1981). Cleavage of the DNA strand requires two Mg^{2+} ions bound within the TOPRIM fold of GyrB (Noble & Maxwell, 2002). The top dimer interface (winged-helix domains) with the cleaved G-segment are pulled apart allowing the T-segment to pass through into the cavity formed by the GyrA NTDs (Morais Cabral *et al.*, 1997). The G-segment is religated, and the T-segment is released through the bottom gate of the GyrA NTDs. It has been proposed that the

unidirectional movement of the T-segment into the GyrA cavity may be driven by the closing and swivelling observed in the GyrB subunits (Gubaev & Klostermeier, 2011, Papillon *et al.*, 2013). ATP hydrolysis allows the resetting of the enzyme (Sugino *et al.*, 1978, Kampranis *et al.*, 1999a), however, to date the mechanism that drives ATP hydrolysis is uncertain (Williams & Maxwell, 1999a, Bates & Maxwell, 2007, Bates *et al.*, 1996). Despite this, the rate-limiting step of DNA supercoiling by DNA gyrase, like other type IIA topoisomerase, is proposed to be the rate of ADP and phosphate release (Baird *et al.*, 2001). An alternative mechanism of negative supercoiling has recently been proposed by Gubaev *et al.* who have suggested that negative supercoiling by DNA gyrase occurs through a nick-closing mechanism and controlled rotation (Gubaev *et al.*, 2016). This works by the T-segment being constrained by the GyrB subunit on the GyrA subunit after ATP binding, cleavage of one strand of the double-stranded DNA, followed by loss of the DNA wrap around the CTD thus rotation within the DNA saddle, followed by resealing. This results in a change in the linking number by -2 (Gubaev *et al.*, 2016). Although this mechanism has been suggested, the widely-held view is that DNA supercoiling proceeds by the strand-passage mechanism outlined above and shown in Figure 1.11.

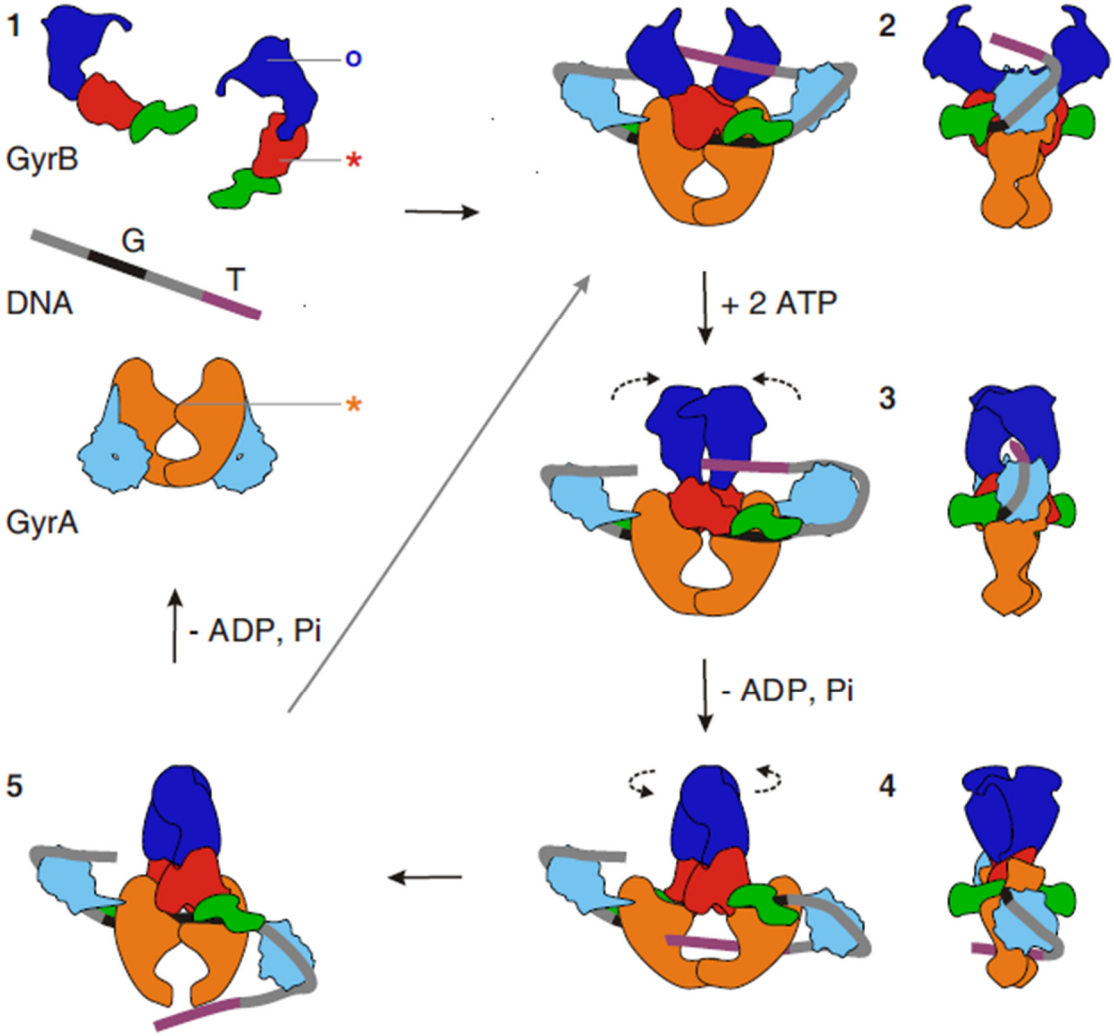

Figure 1.11: Model for negative supercoiling by DNA gyrase. The domains are coloured as follows: GyrB43 - dark blue; GyrB TOPRIM - red; GyrB tail - green; GyrA59 - orange; GyrA C-terminal domain - light blue. The G and T DNA segments are coloured black and purple, respectively. 1) shows the subunits and DNA in their proposed free states in solution. Stars indicate the active-site residues for DNA cleavage and the circle indicates the ATP-binding pocket. 2) The G-segment binds across GyrA, at the dimer interface and the GyrA C-terminal domain wraps the DNA to present the T-segment in a positive cross over. 3) ATP is bound, which closes the GyrB clamp capturing the T-segment, and the G-segment is transiently cleaved. 4) Hydrolysis of one ATP molecule allows GyrB to rotate, the DNA gate to widen, and the transport of the T-segment through the cleaved G-segment. 5) The T-segment exits through the C-gate, and the G-segment is religated. The hydrolysis of the remaining ATP molecule resets the enzyme. The right panel shows the side view for 2 – 4. Figure taken from Cell (Costenaro *et al.*, 2007) with permission.

The topoisomerases are a diverse class of enzymes both structurally and mechanistically, and given their essentiality, many of them are key targets for chemotherapy. In particular, gyrase and topo IV are well-validated targets for antibiotics.

1.4 Antibiotic resistance

Antibiotics are small molecules that selectively act against bacteria, either by killing them (bactericidal) or stopping them from growing (bacteriostatic). These molecules can be natural or synthetic in origin and are formed by a number of different chemical classes that target a number of different molecular processes. Antibiotic classes include: quinolones, β-lactams, sulphonamides, aminoglycosides, tetracyclines, amphenicols, lipopeptides, macrolides, oxazolidinones, glycopeptides, streptogramins, ansamycins, and lincosamides (Aminov, 2017). All of these classes broadly affect one or more of five main pathways or targets, including cell wall synthesis, protein synthesis, DNA replication or transcription, folate synthesis or membrane disruption (Figure 1.12) (Walsh & Wencewicz, 2016).

Disrupting these targets leads to a number of cellular responses by the bacteria in order to ameliorate the damage done. These include, upregulation of the SOS response, DNA damage repair, and upregulation of stress-response pathways including those that manage reactive oxygen species.

The SOS response is a bacterial stress-response pathway that involves about 40 genes, all regulated by RecA and LexA (in most bacteria) (Janion, 2008, Baharoglu & Mazel, 2014, Kreuzer, 2013). It has been found to be upregulated in response to lethal and sublethal doses of a number of antibiotics, including quinolones, β-lactams, trimethoprim and aminoglycosides (aminoglycosides have been shown not to induce SOS in *E. coli*) (Baharoglu & Mazel, 2014, Cirz *et al.*, 2007, Cirz *et al.*, 2006, Miller *et al.*, 2004). SOS induction is often caused by the

accumulation of single-stranded DNA (ssDNA) either from collapsed replication forks, or from resolution of double-stranded breaks (DSBs) caused by stalled replication forks or stalled RNA polymerase. This causes the recruitment of a number of DNA repair proteins or error-prone polymerases (Baharoglu & Mazel, 2014, Kreuzer, 2013). The SOS response can result in increased homologous recombination, mutagenesis and pathogenesis responses in bacteria (Baharoglu & Mazel, 2014, Kreuzer, 2013). It has also been demonstrated to play a role in various cell checkpoints and the rise in persistence (Dörr *et al.*, 2009, Kreuzer, 2013).

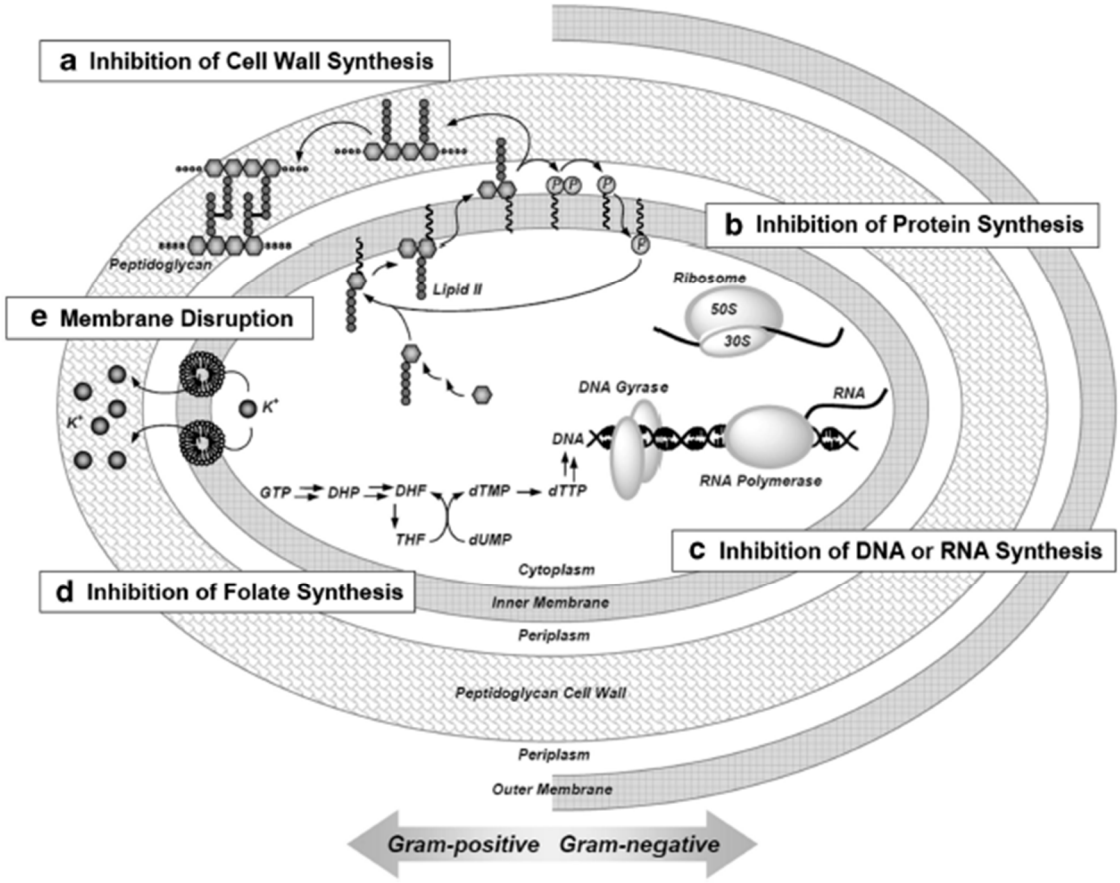

Figure 1.12: The five major clinically validated targets or pathways. Figure taken from The Journal of Antibiotics (Walsh & Wencewicz, 2014) with permission

DNA repair proteins involved in DSB repair include various endonucleases and the RecBCD helicase (Dillingham & Kowalczykowski, 2008, Yeeles & Dillingham, 2010). These proteins are part of bacterial metabolism and are involved in the resolution of naturally occurring DSBs in

DNA. They are closely associated with other homologous recombination proteins and have been demonstrated to load RecA onto ssDNA (Dillingham & Kowalczykowski, 2008, Yeeles & Dillingham, 2010). Furthermore, they are usually the first response to exogenous sources of DSB and have been linked with non-SOS response recombination pathways in response to quinolones (Lopez & Blazquez, 2009, Lopez *et al.*, 2007). Additionally, RecBCD has been shown to convert topo I- and DNA gyrase-DNA complexes into DSBs in preparation for induction of SOS response (Sutherland & Tse-Dinh, 2010).

Other stress-response pathways include upregulation of those that ameliorate oxidative stress and general stress-response pathways. The role of oxidative stress in bacterial cell death (or programmed cell death) is controversial. A number of studies have suggested that the lethality and increased mutagenesis by antibiotics, and in particular that of β-lactams, aminoglycosides and quinolones, is due to an increase in ROS (reactive oxygen species) (Kohanski *et al.*, 2010, Kottur & Nair, 2016, Zhao & Drlica, 2014, Zhao *et al.*, 2015). Many of these studies have shown that there is a reduction in cell death when pathways that are involved in protection against ROS are perturbed; or they have used chemical probes to show an increase in various oxygen species. In response to these suggestions, other studies have disputed the role of ROS in the lethality of antibiotics (Fang, 2013, Imlay, 2015, Keren *et al.*, 2013, Liu & Imlay, 2013). These papers have argued that antibiotics are still lethal under anaerobic conditions where ROS are not formed, and that some of the dyes used to detect oxidation are readily transformed by antibiotics in the absence of oxygen. Furthermore, there have been few targets identified that increase susceptibility to antibiotics that are involved in scavenging ROS or involved in their formation (Tamae *et al.*, 2008). Moreover, in catalase and peroxidase deficient *E. coli* no increase in susceptibility to ampicillin and kanamycin was observed and only modest increases in susceptibility norfloxacin was seen (Imlay, 2015). There are significant differences in the methods and procedures used in these studies which may be contributing to the

inconsistencies and differing results (Fang, 2013) and it seems as though the debate is set to continue.

General stress-response factor RpoS has been shown to upregulate error-prone polymerase in response to DSBs and cell wall stress, such as with treatment with β-lactams (Gutierrez *et al.*, 2013, Koskiniemi *et al.*, 2010, Rosenberg *et al.*, 2012). It has been shown to work closely with the SOS response and protects cells from ROS damage (Baharoglu & Mazel, 2014).

Ultimately, the bacterial response to antibiotics seems to be varied and complex and the relative stress and repair pathways in different bacterial species have been shown to respond in slightly different ways. For example, ROS formation has been shown in *Vibrio cholerea* whereas not in *E. coli* (Baharoglu *et al.*, 2013) and there are also subtle differences in the SOS response pathway between bacterial species (Baharoglu & Mazel, 2014, Kreuzer, 2013).

Since their introduction in the 1940's, antibiotics have changed global medicine and been central to the reduction of the lethality of bacterial infections. However, resistance to antibiotics is rising and with it deaths as a result of drug-resistant infections (Figure 1.13) (Bush *et al.*, 2011, Gelband *et al.*, 2015, O'Neill, 2016). Coupled to this is the paucity of new classes of chemical compounds being discovered to tackle this problem and fewer pharmaceutical companies investing in the search for novel antibiotics (Figure 1.14) (Brown & Wright, 2016, Lewis, 2012, Walsh, 2003, Walsh & Wencewicz, 2016, Walsh & Wencewicz, 2014). Bacteria have been shown to be exposed to antibiotics in a number of environments, not just in a clinical or veterinary setting, but also in external and natural ecosystems (Andersson & Hughes, 2014). This constant barrage of chemical warfare is increasingly adding to the resistance problems and the effects of sublethal exposure to these antibiotics is progressively being shown to have far reaching consequences (see Chapter 6).

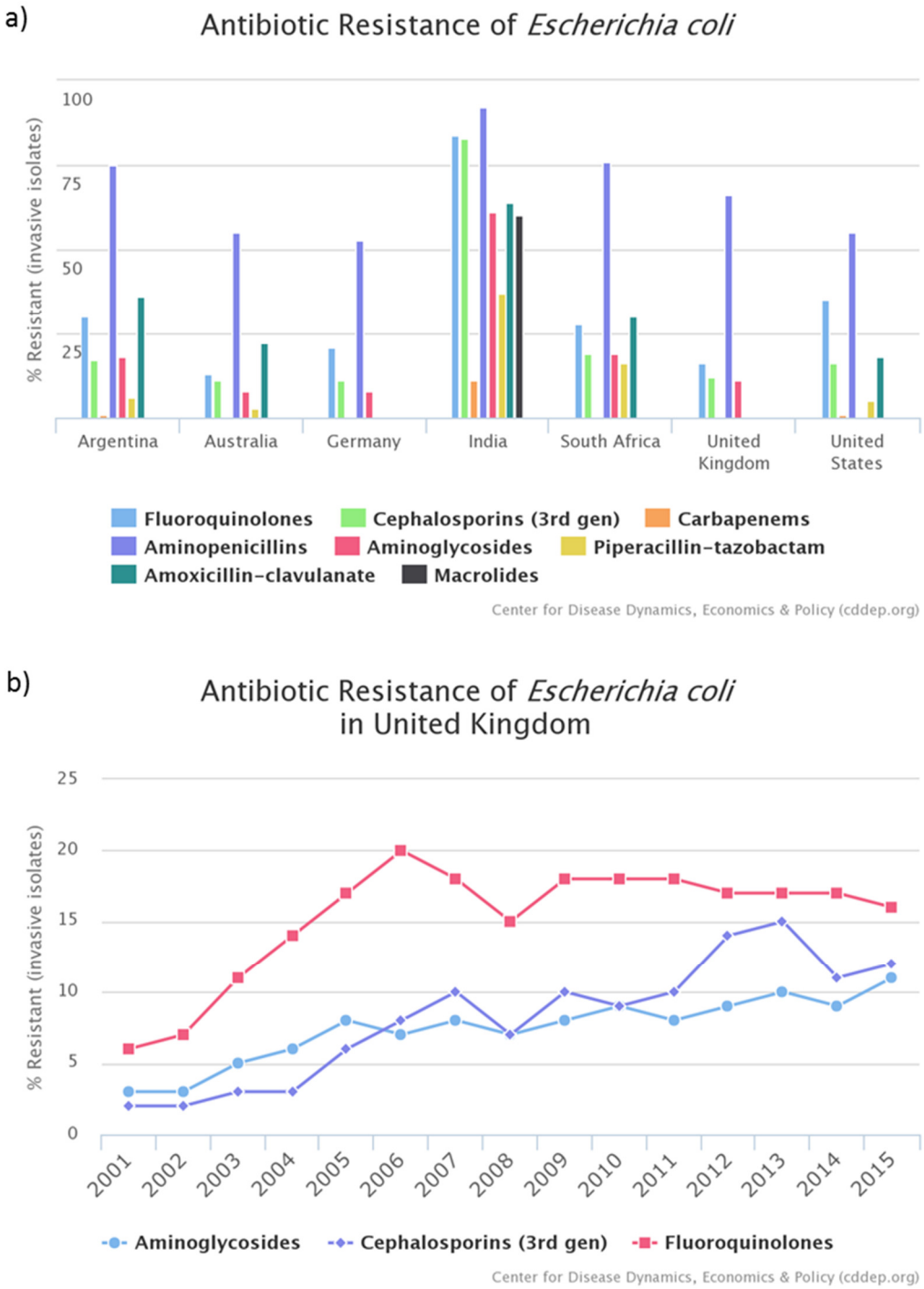

Figure 1.13: Rise in antibiotic resistance. a) Bar graphs showing % resistant *E. coli* isolates in various countries. Data collected between 2011 and 2015. Aminoglycoside (pink), Aminopenicillin (dark blue), Carbapenem (orange), Fluoroquinolones (light blue), Cephalosporin (green), Amoxicillin-clavulanate (turquoise), Piperacillin-tazobactams (yellow) and Macrolides (black). b) Shows the rise in resistant *E. coli* isolates in the United Kingdom to the Aminoglycosides (light blue), Cephalosporins (dark blue) and the Fluoroquinolones (pink). Isolates were collected from blood and cerebrospinal fluid from inpatients of all ages. Figure was collated from http://resistancemap.cddep.org/resmap/resistance.

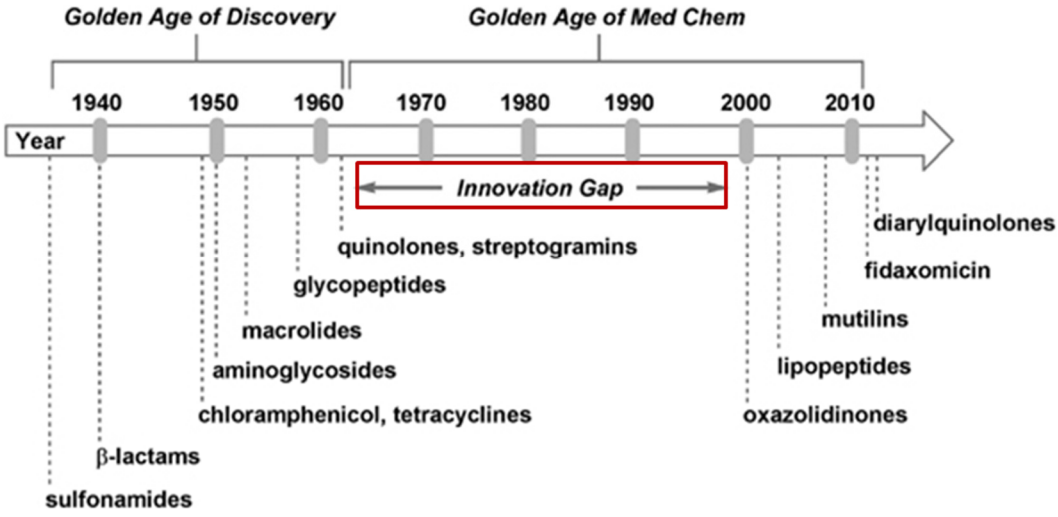

Figure 1.14: Timeline showing the "Golden Age" of antibiotic discovery and medicinal chemistry. The red Box highlights the innovation gap where no new structural classes of antibiotics were introduced. Figure adapted from (Walsh & Wencewicz, 2014) with permission.

In general, resistance mechanisms are varied and are often as a result of the SOS- and stress-response mechanisms described above and can be classed as molecular or genetic. The molecular mechanisms include modifications that reduce the uptake of the antibiotic such as in the alteration of the physical structures of porins or a reduction in the number of porins (Gram-negative species organisms), the upregulation of efflux pumps, the acquisition or upregulation of enzymes that degrade or inactivate antibiotics, and modifications of the target of the antibiotic such that the activity is unaffected but the antibiotic is no longer effective (Walsh & Wencewicz, 2016). The genetic mechanisms involve the acquisition of resistance cassettes which are usually embedded within biosynthetic clusters. This occurs through transformation, transduction and conjugation. Another genetic mechanism is through mutation, which can result in modifications that can cause some of the molecular mechanisms of resistance, such as alterations in target proteins, or upregulation of quiescent resistance genes (Walsh & Wencewicz, 2016).

Ultimately, better understanding of the resistance mechanisms and the target themselves will give us novel ways of tackling antibiotic-resistant infections. The DNA topoisomerases are one such group that are both well-validated targets for antibiotics and are linked with the development of resistance.

1.5 DNA topoisomerase inhibitors

As mentioned above, topoisomerases are clinically-relevant targets for antibacterials and other chemotherapeutic agents. DNA gyrase and topo IV are ideal targets for antibiotics as they are not found in humans (Collin *et al.*, 2011). Furthermore, inhibitors of human topo I and both isoforms of topo II are currently used in cancer-related chemotherapy regimens (Jain *et al.*, 2017).

Bacterial topo I, although not an established target for antibacterials, is a prospective new target with a number of studies investigating potential compounds and the viability of topo I as a target (Bansal *et al.*, 2012, Cheng *et al.*, 2007, Cheng *et al.*, 2005, Tse-Dinh, 2009). This is particularly true in *M. tuberculosis* where topo I is essential (Godbole *et al.*, 2015). Human topo I is the target of camptothecin, which is an anti-tumour alkaloid that functions by stabilising the cleavage complex (Hsiang *et al.*, 1985, Pommier *et al.*, 1998).

Inhibitors of topo VI are not currently clinically-relevant and not many have been described. However, there is evidence that radicicol, a topo VI and HSP90 inhibitor, also inhibits human topo II. Conversely, a number of topo II inhibitors also inhibit topo VI (Gadelle *et al.*, 2006). Furthermore, as this enzyme has been found in apicomplexan parasites (a group that contains a number of human pathogens) and in some plants, it would be an ideal target for drugs such as antimalarials or herbicides.

Inhibitors of type IIA topoisomerases generally consist of two types of inhibitors: those that interfere with the catalytic cycle of the enzyme, or those that stabilise the cleavage complex (the covalent phosphotyrosine bond formed between the enzyme and DNA at the DSB). Although,

many known inhibitors will be mentioned, only those with relevance to this thesis will be expanded on.

Competitive inhibitors of DNA topoisomerases

Catalytic inhibitors are those that block DNA binding or compete with ATP binding. These include inhibitors such as the aminocoumarins, simocyclinones, cyclothialidines and the bisdioxopiperazines. Aminocoumarins and cyclothialidines bind partially in the ATP pocket and are thus competitive inhibitors of ATP hydrolysis (Gellert *et al.*, 1976b, Lewis *et al.*, 1996, Mizuuchi *et al.*, 1978b), whilst the bisdioxopiperazines are non-competitive inhibitors of ATPase activity (Nitiss, 2009b). Simocyclinones are known to prevent DNA binding (Edwards *et al.*, 2009, Edwards *et al.*, 2011, Flatman *et al.*, 2005).

Aminocoumarin antibiotics (Figure 1.15) that target DNA gyrase were discovered as *Streptomyces* natural products in the 1950s and include novobiocin, clorobiocin and coumermycin A_1 (Heide, 2009, Maxwell & Lawson, 2003). They bind to the ATPase (NTD) domain of GyrB and block the binding of ATP (Lewis *et al.*, 1996, Wigley *et al.*, 1991). Although the aminocoumarins do not resemble ATP, it was demonstrated that the novobiose sugar of the aminocoumarins overlaps the adenine-binding site in the ATPase pocket, thereby preventing the binding of ATP. Novobiocin also forms a hydrogen bond with R163 in GyrB which has been shown to prevent dimerisation of the GyrB NTDs (Ali *et al.*, 1993, Lewis *et al.*, 1996).

Aminocoumarins have been demonstrated to be very effective inhibitors of gyrase and topo IV (Kampranis *et al.*, 1999b). However, they have not had a high degree of success as clinical antibiotics with safety concerns having led to discontinuation of the use of these drugs (Mayer & Janin, 2014). Toxicity issues associated with these drugs may be due to the fact that they bind to the ATPase domain of GyrB/ParE, which is part of the GHKL ATPase/kinase superfamily (Dutta & Inouye, 2000). This means that secondary eukaryotic targets are likely, which was further demonstrated by Burlison *et al.* who reconfigured novobiocin to target a mammalian heat shock

protein (Hsp90) (Burlison *et al.*, 2006). Furthermore, the aminocoumarins suffer from solubility issues, making it difficult to develop them as drugs.

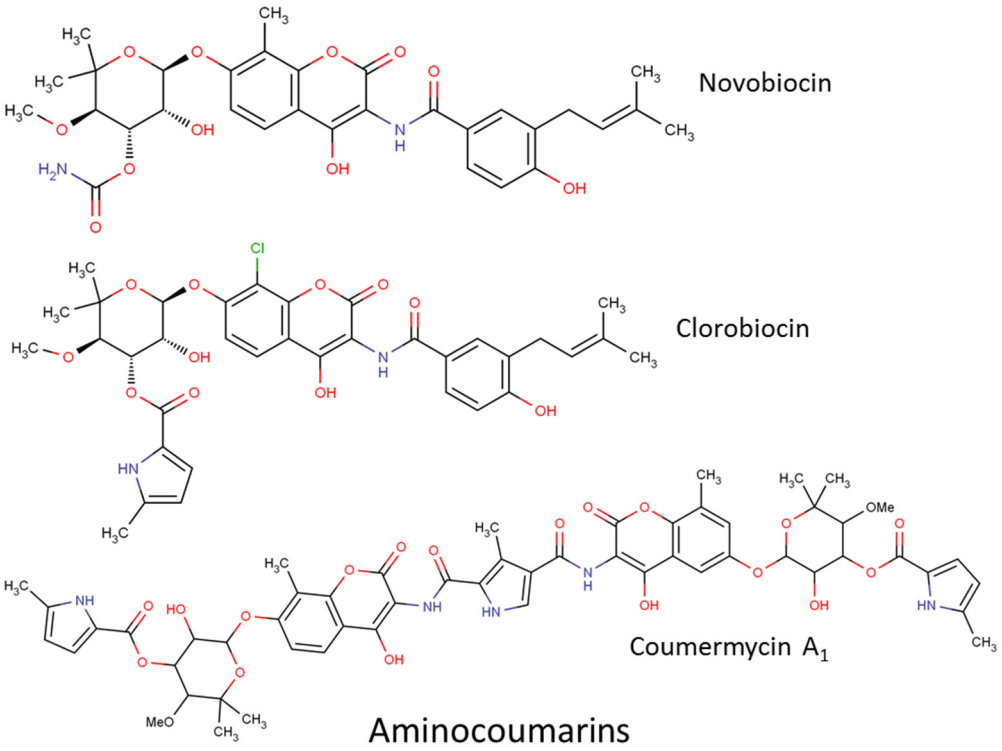

Figure 1.15: Chemical structures of various aminocoumarin topoisomerase inhibitors.

Topoisomerase poisons

Topoisomerase poisons are inhibitors that bind to type II topoisomerases and stabilise the cleavage complex. These include some of the most potent and clinically important inhibitors of topoisomerases. Inhibitors of the bacterial enzymes, DNA gyrase and topo IV, include the quinolones (Collin *et al.*, 2011, Drlica & Malik, 2003), microcin B17 (Herrero *et al.*, 1986, Vizan *et al.*, 1991), CcdB (Miki *et al.*, 1984a, Miki *et al.*, 1992, Miki *et al.*, 1984b) and albicidins (Birch & Patil, 1985). Topo II inhibitors include the anthracyclines (e.g. doxorubicin) (Binaschi *et al.*, 1997), and epipodophyllotoxins (e.g. teniposide and etoposide) (Baldwin & Osheroff, 2005, Hande, 1998), as well as mAMSA (Marshall *et al.*, 1983), and merbarone (Drake *et al.*, 1989b).

Quinolones

The quinolones (Figure 1.16) are arguably the most successful class of topoisomerase inhibitors to date. They are synthetic antimicrobials with the initial compound, nalidixic acid, being discovered as a by-product of chloroquine synthesis in 1962 (Lesher *et al.*, 1962, Bisacchi, 2015). Nalidixic acid was released for clinical use in the late 1960's for the treatment of uncomplicated urinary tract infections (UTI's) (Correia *et al.*, 2017). By the 1970's several other quinolones, including oxolinic acid had been introduced to the clinic and these, along with nalidixic acid (although, technically, nalidixic acid is a 1,8 naphthyridone and not a true quinolone (Lesher *et al.*, 1962, Bisacchi, 2015)), are the first-generation quinolones (Aldred *et al.*, 2014b, Collin *et al.*, 2011). The second-generation quinolones included a fluorine on the C6 position, which led them to be called the fluoroquinolones, and a piperazine or methyl-piperazine ring at C7 (Aldred *et al.*, 2014b, Emmerson & Jones, 2003). The second-generation fluoroquinolones had better pharmacodynamic and pharmacokinetic properties, including broader spectrum activity, and better bioavailability. They were also less toxic and were less susceptible to single point mutations that led to high levels of resistance seen against the first-generation quinolones (Emmerson & Jones, 2003, Correia *et al.*, 2017). This class began with norfloxacin, however it was ciprofloxacin (CFX) that was the first quinolone that showed activity outside the urinary tract (Aldred *et al.*, 2014b, Correia *et al.*, 2017, Emmerson & Jones, 2003). CFX remains one of the most clinically important antibiotics to date, with the World Health Organisation classing it (amongst other fluoroquinolones) as a critically important antibiotic (WHO, 2017). The success of CFX led to a medicinal chemistry effort that produced a wide range of newer generation fluoroquinolones (third and fourth generations) that have even broader spectra of activity, greater efficacy and less resistance, including moxifloxacin, gatifloxacin and levofloxacin (Figure 1.16) (Aldred *et al.*, 2014b, Collin *et al.*, 2011, Emmerson & Jones, 2003). There is now potentially a fifth generation of quinolones in delafloxacin, which is a weak acid due to the loss of the strong base at C7, and it is chlorinated at C8 (Candel & Peñuelas, 2017).

Despite their success, some promising fluoroquinolones, such as trovafloxacin and grepafloxacin, have had to be removed from the clinic due to safety concerns (Emmerson & Jones, 2003). However, many have remained in clinic and are used in the treatment of UTI's, pyelonephritis, gastroenteritis, sexually transmitted diseases such as Gonorrhoea, tuberculosis (moxifloxacin) (Gillespie, 2016), prostatitis, nosocomial infections, community acquired pneumonia, and skin and soft tissues infections (Oliphant & Green, 2002, Aldred *et al.*, 2014b). Delafloxacin has also been demonstrated to be effective against quinolone- and methicillin-resistant *Staphylococcus aureus* (Chan *et al.*, 2014, Candel & Peñuelas, 2017).

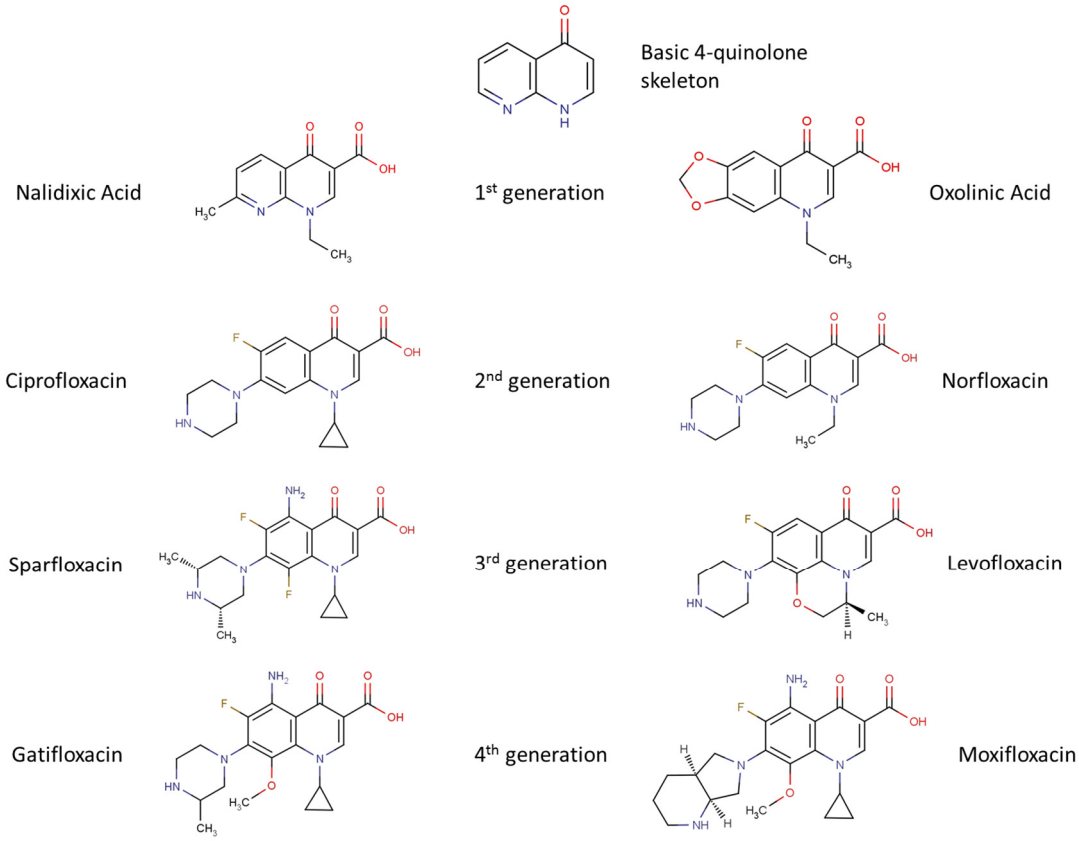

Figure 1.16: Chemical structures of a selection of quinolones. Quinolones are divided into generations based on their antibacterial spectrum. The first generation (e.g. nalidixic acid and oxolinic acid) are examples of older acidic (narrow spectrum) quinolones whereas the higher generations (e.g. ciprofloxacin, levofloxacin and gatifloxacin) are examples of the amphoteric fluoroquinolones (expanded-spectrum compounds). Figure taken from EcoSal Plus (Bush *et al.*, 2015) with permission

The quinolones inhibit DNA supercoiling and relaxation by binding to both gyrase and DNA and stabilising the gyrase-DNA cleavage complex (Gellert *et al.*, 1977, Sugino *et al.*, 1977). This is also true for topo IV which has also been shown to be a target for quinolones, and the primary target in a number of Gram-positive species. However, this is often dependent on the specific quinolone, and some quinolones have been shown to target both enzymes equally (Aldred *et al.*, 2014b, Ferrero *et al.*, 1994, Khodursky *et al.*, 1995, Redgrave *et al.*, 2014, Correia *et al.*, 2017). The quinolones have been shown to have interactions with both subunits of the enzyme (GyrA and GyrB for gyrase, and ParC and ParE for topo IV). Binding has been shown to be mediated by a Mg^{2+} ion via a "water-metal ion bridge" along with S83 and D87 in GyrA (amino acids in *E. coli* numbering) and the 3-carboxyl end of the quinolone. Interactions between position 466 in GyrB and the C7 ring of the quinolone are also important for binding of the compound (Aldred *et al.*, 2014a, Aldred *et al.*, 2013, Mustaev *et al.*, 2014, Hooper & Jacoby, 2015). The resulting quinolone-enzyme-DNA complex is the cause of the inhibition of DNA synthesis by quinolones which leads to the hindrance of cell growth (Hiasa *et al.*, 1996, Wentzell & Maxwell, 2000, Willmott *et al.*, 1994).

DNA replication has been demonstrated to be promptly stalled when DNA gyrase is targeted with quinolone drugs which was suggested to be due to the collision of replication forks with quinolone-enzyme-DNA complexes (Snyder & Drlica, 1979). For example, norfloxacin has been shown to cause stalled replication forks *in vivo*; some of these were reversible and did not lead to cell death but others were not reversed and were lethal (Pohlhaus & Kreuzer, 2005). This stalling of replication is the likely cause of the bacteriostatic action of quinolones (Drlica *et al.*, 2008), however, the lethality is due to DNA breaks and chromosome fragmentation which induces the SOS response and leads to cell death (Drlica *et al.*, 2008, Malik *et al.*, 2006, Aldred *et al.*, 2014b, Redgrave *et al.*, 2014). Induction of the SOS regulon caused by quinolone-induced DSBs has been shown to be mediated by RecBC (Lewin *et al.*, 1989, McDaniel *et al.*, 1978, McPartland *et al.*, 1980). The action of killing by quinolones appears to be dependent on the

chemical structure of the specific quinolone in question. The difference in chemical structure results in three pathways of quinolone killing: one that is dependent on aerobic growth and continued protein synthesis, one that is dependent only on continued protein synthesis and the third that can occur independently of aerobic growth or protein synthesis (Malik *et al.*, 2007, Malik *et al.*, 2006). Although the mode of action of quinolones in inhibiting DNA gyrase or topo IV is relatively straightforward, the lethality of quinolones to cells appears not to be. This is also evident by the minimum inhibitory concentrations (MIC) of quinolones being an order to two orders of magnitude lower (*in vivo*) than their IC50's (*in vitro*) (Domagala *et al.*, 1986, Gellert *et al.*, 1977). This can be explained by the triggering the downstream processes that lead to cell death in response to a small amount of DNA damage.

Bacterial resistance to quinolones is increasingly being reported. Mechanisms include upregulation of efflux pumps, a reduced ability to uptake the drug, plasmid-mediated resistance, or actual mutations in the DNA gyrase or topo IV genes (Figure 1.17) (Redgrave *et al.*, 2014, Hooper & Jacoby, 2015).

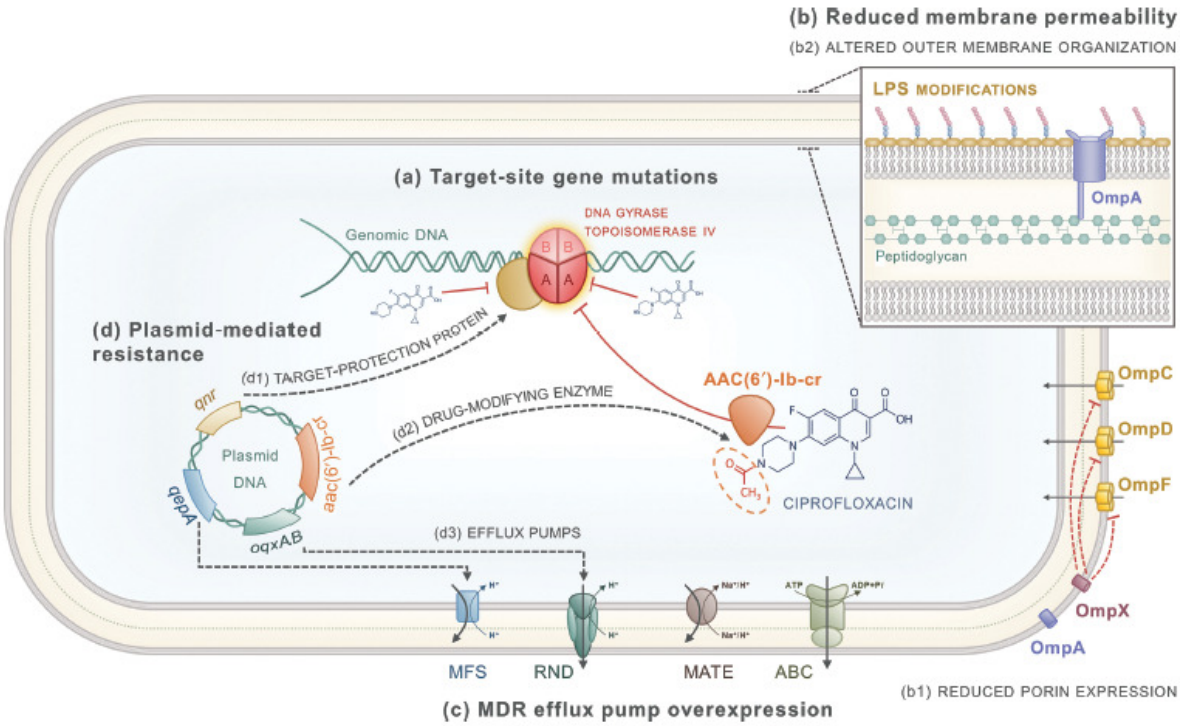

Figure 1.17: Known quinolone-resistance mechanisms. Including a) point mutations in the GyrA/GyrB or ParE/ParC proteins of DNA gyrase and topo IV respectively; b) alterations of porins or the cell membrane that reduce the uptake of the quinolone; c) overexpression of efflux pumps; or d) plasmid-based resistance mechanisms. Figure taken from the Journal of Medical Microbiology (Correia *et al.*, 2017) with permission.

The mutations in gyrase that confer resistance to quinolones are often found in a region termed the quinolone resistance-determining region (QRDR) which is between amino acids 67 and 106 of GyrA (*E. coli* numbering) or 63 and 102 in ParC (Yoshida *et al.*, 1990). There is also a QRDR found in GyrB between amino acids 426 and 447 (*E. coli* numbering), with the two most common mutations found to be D426N and L447E (Avalos *et al.*, 2015, Gensberg *et al.*, 1995, Wohlkonig *et al.*, 2010, Yoshida *et al.*, 1991). However, the most prevalent quinolone resistance mutations are found in GyrA. These mutations cluster at the dimer interface, near the active-site tyrosines (Morais Cabral *et al.*, 1997). Due to their specific interactions with the quinolone through the water-metal ion bridge, the residues most commonly mutated in ciprofloxacin-resistant strains are the serine and aspartic acid/glutamic acid on helix IV in GyrA/ParC (Aldred

et al., 2014b, Correia *et al.*, 2017, Hooper & Jacoby, 2015, Redgrave *et al.*, 2014). Resistance-conferring mutations outside the traditional QRDR have also been identified. For example, an A51V mutation results in a six-fold increase in ciprofloxacin resistance (Friedman & Court, 2001).

Plasmid-mediated quinolone resistance have been found in some clinical strains (Hooper & Jacoby, 2015). This has been shown to be due to the expression of pentapeptide-repeat proteins which mimic DNA and bind gyrase and inhibit its activity. These include the Qnr's (QnrA, QnrB and QnrS), MfpA and McbG (Aldred *et al.*, 2014b, Correia *et al.*, 2017, Hooper & Jacoby, 2015, Redgrave *et al.*, 2014). Other plasmid-based resistance mechanisms include the efflux pumps OqxAB, QepA1, and QepA2, and aac(6')-Ib-cr which is a variant of an aminoglycoside transferase which alters the structure of some quinolones, making them less effective (Aldred *et al.*, 2014b, Correia *et al.*, 2017, Hooper & Jacoby, 2015, Redgrave *et al.*, 2014).

Other chromosomal mutations that have been identified that confer quinolone resistance include those involved with uptake of the drug, upregulation of efflux pumps and in the regulons that control the expression of these. In Gram-negative bacteria, modifications of the bacterial membrane either structurally by the reduction of the number of porins (via OmpA and OmpX) in the cell membrane, or through the alteration of the porins themselves have been reported (Bolla *et al.*, 2011, Correia *et al.*, 2017, Fernández & Hancock, 2012). Additionally, overexpression of various efflux pumps (also found in Gram-positive species) can lead to increased resistance (Aldred *et al.*, 2014b, Correia *et al.*, 2017, Hooper & Jacoby, 2015, Redgrave *et al.*, 2014). The overexpression of efflux pumps in *E. coli* is often linked to mutations in MarRA, SoxRS and Rob regulons, which are involved in the regulation of these efflux pumps, as well as many other pathways in the cell (Aldred *et al.*, 2014b, Correia *et al.*, 2017, Hooper & Jacoby, 2015, Redgrave *et al.*, 2014).

Ultimately, the quinolones, despite being extremely successful antibiotics are coming under increasing pressure due to the rise in resistance. This resistance is multifactorial and

complicated. Likewise, the mode of action of the quinolones themselves appears to complex including the way cells respond to being challenged by them.

One complexity associated with the quinolones, and other cleavage-stabilising compounds (such as those that target human topo II), is that they have been demonstrated to increase the frequency of topoisomerase-mediated illegitimate recombination.

1.6 Topoisomerase-mediated illegitimate recombination

Illegitimate recombination (IR) has been defined and is used here as recombination between DNA sequences that share little to no homology (Franklin, 1971, Weisberg & Adhya, 1977). It is distinct from general recombination as it is independent of general recombination pathways. IR can result in genomic rearrangements such as deletions, duplications, insertions, and translocations (Weisberg & Adhya, 1977). It is often a result of DNA damage, such as during UV irradiation (Weisberg & Adhya, 1977) and seems to occur during the repair of DSBs.

In bacteriophage, IR is observed during generalised and specialised transduction (Franklin, 1971). Transduction is defined as the transfer of bacterial DNA from one bacterial chromosome to another by bacteriophage (Franklin, 1971). Generalised transduction occurs when bacteriophage P1 and P22 phage package fragments of the bacterial chromosome instead of their own chromosomes (Ikeda & Tomizawa, 1965). Specialised transduction occurs when part of the bacterial chromosome is excised with part of the phage genome, this is then packaged into infective particles (Franklin, 1971).

IR has been reported in viruses, prokaryotes and eukaryotes and has been suggested to be the major influence in the evolution of genomes (van Rijk & Bloemendal, 2003). In particular, it has been demonstrated to play a role in plant genome size variation (Michael, 2014), as well as in the size of LRR (Leucine-Rich Repeat) genes which are important in plant resistance to pathogens (Wicker *et al.*, 2007). It has been implicated in chromosomal rearrangements that

has led to the divergence in the control of gene regulation in maize (Wicker *et al.*, 2007). Furthermore, IR has been demonstrated to have facilitated the evolution of *Pseudomonas aeruginosa* as a human pathogen (Rau *et al.*, 2012) as well as shaped bacterial evolution and plasticity in general (Darmon & Leach, 2014). It has also been demonstrated to play a role in exon shuffling that results in novel genes (Long, 2001, van Rijk & Bloemendal, 2003). Topoisomerases have been indicated to play a role in IR, although the mechanism is not known.

Topo I-mediated IR

Although not the main focus of this thesis, topo I has been implicated in IR (Kim & Jinks-Robertson, 2017). Topo I from vaccinia virus has been shown to facilitate excisive recombination of λ prophage that is integrase-independent (Shuman, 1991). Topo I has also been shown to mediate strand transfer in HeLa cells (Halligan *et al.*, 1982) and participate in the non-homologous excision of SV40 from eukaryotic chromosomes (Bullock *et al.*, 1985). Furthermore, topo I mediates integration of woodchuck hepatitis virus into cellular DNA in an IR reaction (Wang & Rogler, 1991). In spite of all of this, camptothecin, a human topo I cleavage-stabilising inhibitor, which induces DSBs, does not increase the frequency of non-homologous recombination *in vivo* (Aratani *et al.*, 1996).

DNA gyrase-mediated IR

DNA gyrase was the first of the type II topoisomerases implicated in IR. Kobayashi and Ikeda (1977) developed an *in vitro* assay to study IR using a bacteriophage λ-based packaging assay developed by Hohn and Hohn (1974) (see Chapter 3). They found that when oxolinic acid was added to the *in vitro* assay, they saw a 13-fold increase in ampicillin-resistant transductants (Ikeda *et al.*, 1980). This increase was abolished when the assay was run in the presence of both oxolinic acid and coumermycin A_1, but was restored when the same assay was performed with packaging mixtures made from coumermycin resistant lysogens. The stimulation of recombination was also reduced when the assay was run in the presence of oxolinic acid but the packaging mixture was prepared from nalidixic acid-resistant (*nal*^{r}) lysogens (Ikeda *et al.*, 1980).

This indicated that the recombination induced by oxolinic acid was mediated by DNA gyrase. Furthermore, when the recombination step was separated from the packaging step in the assay, addition of exogenous gyrase showed a 50-fold increase in IR when compared to the reaction where no gyrase was added. This was increased a further 40-fold in the presence of both gyrase and oxolinic acid. Interestingly, it was shown that gyrase was unable to induce IR in the absence of cell extracts implying that some extra factor was needed (Ikeda & Shiozaki, 1984). Gyrase-mediated IR has been determined to be independent of viral *int* and *red* functions, and of the *E. coli* homologous recombination (RecABCF) functions (Ikeda *et al.*, 1980). When the structures of these recombination events were analysed, it was found that some were insertions of the ampicillin-resistance gene from pBR322 into λ whilst others were translocations (Ikeda *et al.*, 1982). Moreover, these events could occur at multiple sites in either of the DNA molecules (Naito *et al.*, 1984). While most studies implicate gyrase in insertions and translocations, it has also been shown to participate in deletion events between direct repeats (Saing *et al.*, 1988, Miura-Masuda & Ikeda, 1990). The recombination junctions at insertions and translocations have no sequence homology (Ikeda *et al.*, 1982, Naito *et al.*, 1984), although, in some later studies, some regions of short homology (<10 bp) were found (Kumagai & Ikeda, 1991, Shanado *et al.*, 1998, Shimizu *et al.*, 1995, Shimizu *et al.*, 1997). *In vivo* studies have also implicated gyrase in IR. Gyrase has been demonstrated to increase the frequency of λ*bio* transducing phage through oxolinic acid-induced abnormal excision of the prophage (Tomono *et al.*, 1989, Kumagai & Ikeda, 1991, Shimizu *et al.*, 1995). It appears that gyrase-mediated IR can be short-homology dependent (SHDIR) or short-homology independent (SHIIR). SHDIR is thought to occur more frequently *in vivo* in both chromosomal and plasmid DNA (Kumagai & Ikeda, 1991, Shimizu *et al.*, 1997, Saing *et al.*, 1988) whereas SHIIR seems to be linked with drug-induced IR (Naito *et al.*, 1984, Miura-Masuda & Ikeda, 1990, Ikeda *et al.*, 1982, Shanado *et al.*, 1998). Gyrase-mediated IR has also been shown to occur at preferred gyrase cleavage sites, however, a preferred cleavage site is not necessary for gyrase-mediated IR to occur (Ikeda *et al.*, 1984). Temperature-sensitive mutations in gyrase have been identified that confer a hyper-IR phenotype. These

mutations are in the breakage-reunion domain of the GyrA subunit and include a double mutant (I203V/I205V) in the α18 helix, and two single mutations in the α10′ helix (L488P, L492P) (see Chapter 4). These mutations are thought to result in religation defects in GyrA similar to that seen in quinolone-stabilised cleavage (Ashizawa *et al.*, 1999). There is also some evidence for topoisomerase-mediated IR to be linked primarily with DNA replication (primarily shown in gyrase) (Ikeda & Shiozaki, 1984). *E. coli* HU protein, which is a DNA-binding protein that has been linked to the preservation of supercoiling in chromosomal and plasmid DNA, has been shown to supress gyrase-mediated IR and the SOS response (Shanado *et al.*, 1998).

Ikeda *et al.* (1982) have proposed a subunit-exchange model to explain gyrase-mediated IR based on the increase in IR during drug-stabilised cleavage (see Chapter 5). As for the deletions between direct repeats, Ikeda (1994) suggests that during DNA cleavage, the ends are processed by exonucleases resulting in DNA deletion upon religation.

Topo II-mediated IR

Like DNA gyrase, topo II has been shown to mediate IR. Bae *et al.* (1988) were the first to demonstrate this with calf thymus topo II. They found that calf thymus topo II-mediated IR was similar to gyrase-mediated IR except that this enzyme is capable of IR in the absence of any crude cell extracts. This suggests that unlike gyrase, topo II does not need any other factors for the reaction to occur. They suggested the subunit-exchange model as a possible mechanism of action.

In a separate study, using a shuttle vector carrying three bacterial markers, amp^r and kan^r (two resistance genes), and *galK*, the topo II inhibitor teniposide (VM26) was shown to increase the frequency of deletion formation. This was done by growing the vector for a number of generations in monkey COS1 cells treated with or without teniposide (an epipodophyllotoxin), before purifying the vectors and transforming them into *E. coli* cells and scoring the number of

amp^{s} and *galK* $^{-}$ double mutants among the *kan*^{r} cells (Bae *et al.*, 1991). Further to this, Han *et al.* (1993) found that teniposide-induced deletion/duplication junctions strongly correlated with teniposide-induced topo II cleavage sites. However, they indicated that none of their mutants were likely to have been due to a subunit-exchange model (Han *et al.*, 1993). Topo II has also been observed to induce the integration of SV40 (simian virus 40) into cellular DNA in an IR reaction in the presence of teniposide (Bodley *et al.*, 1993). In concurrence with other studies, the recombination sites were associated with preferred teniposide-induced topo II cleavage sites. The topo II inhibitors etoposide, teniposide and ICRF-193 were also revealed to stimulate IR *in vivo* by 3–5-fold by integration of an exogenous *aprt* gene into adenine phosphoribosyltransferase-deficient (APRT^{-}) CHO (Chinese hamster ovary) cells (Aratani *et al.*, 1996). Etoposide has also been demonstrated to increase IR in yeast cells through deletions on chromosome III (Asami *et al.*, 2002). Although, in a different study, the primary repair pathway for etoposide-induced DSBs in yeast was shown to be through single-strand invasion, a homologous recombination repair pathway, and only to a lesser extent through IR (Sabourin *et al.*, 2003).

Cancer chemotherapy regimens that include the human topo II inhibitors such as etoposide and doxorubicin, have been implicated in the occurrence of therapy-related acute myeloid leukaemia (t-AML) (linked to the chromosomal translocations in band 11q23) (Pendleton *et al.*, 2014, Cowell & Austin, 2012). The topo II inhibitors mitoxantrone and epirubicin are also associated with t(15;17) rearrangements (translocations between the *PML* gene and the retinoic receptor α (*RARA*) gene causing promyelocytic leukaemia) (Pendleton *et al.*, 2014). Furthermore, childhood leukaemias such as infant AML and acute lymphoid leukaemia, which are linked to the mixed lineage leukaemia gene translocations, have been associated with maternal consumption of genistein (a topo II poison found in soy products) (Azarova *et al.*, 2010). Furthermore, analysis of chromosomal breaks in an infant AML revealed potential topo II binding sites at the break points (Negrini *et al.*, 1993) further implicating topo II in this kind of

IR. Alongside these, topo IIβ has been implicated in the fusion of two genes that lead to poor prognosis in prostate cancer (Ashour *et al.*, 2015) and although not directly linked to topoisomerases, a number of other gene fusions and translocations are associated with various cancers and often, when connected with the gene fusions, poor prognosis (Mani & Chinnaiyan, 2010, Mitelman *et al.*, 2007). The role of human topo II in these genomic rearrangements is not yet fully elucidated, however, evidence is currently pointing to non-homologous end joining and homologous recombination, rather than through direct subunit exchange of the topo II homodimers (Ashour *et al.*, 2015, Elguero *et al.*, 2012). Alternatively, it has also been suggested that a number of different DNA repair and recombination pathways may be involved (Rocha *et al.*, 2016).

Other topoisomerases and IR

The only other type II topoisomerase that has been shown to participate in IR is that of bacteriophage T4. Bacteriophage T4 topoisomerase-mediated IR is very similar to that mediated by gyrase. It was shown to be stimulated by oxolinic acid in the *in vitro* assay and it also needed crude cell extracts (that is, some other unknown factor) for the reaction to occur. Similarly, a subunit-exchange model has been suggested (Ikeda, 1986a).

1.7 Summary and aims

DNA topology in all types of cells is under constant flux due to many exogenous and endogenous processes. These changes in topology can be deleterious and thus there are a number of important pathways and enzymes that maintain DNA topology to ensure fidelity in DNA sequence and structure. These include the DNA topoisomerases and other DNA repair proteins. DNA topoisomerases are the targets for a number of chemotherapeutic agents, such as antibiotics. One class of antibiotics, the quinolones, have been extremely successful antibiotics, however more recently there has been growing problems with resistance against

them. Due to this, understanding the mechanisms behind this has become increasingly important. The quinolones have been implicated in topoisomerase-mediated IR, which is a type of illegitimate recombination, which may play a role in this rise in resistance.

The initial aims of my PhD were to determine the molecular details of the role that topoisomerases play in IR. In particular, investigating the subunit-exchange model, as well as identifying the other proteins/factors that may be involved in the process. When the initial experiments that involved confirming and repeating the published work on topo-mediated IR (Chapter 3) were unsuccessful, more focus was laid on investigating the subunit-exchange model and elucidation of whether this is possible with topoisomerases (Chapter 5). Two other lines of enquiry were also pursued. These were the purification and characterisation of three mutations in GyrA that were shown to have a hyper-recombination phenotype *in vivo* (Chapter 4) and how treatment with sublethal concentrations of quinolones are involved in the acquisition of resistance (Chapter 6). The hypothesis is that DNA topoisomerases are directly involved with the acquisition of resistance to quinolones and other antibiotics through their involvement in IR by subunit exchange.

Chapter 2: General Methods

2.1 Bacterial and phage strains

Table 2.1 shows the genotypes of the various *Escherichia coli* and bacteriophage λ strains used in this work. The source of these strains is indicated in the right-hand column.

Table 2.1: *E. coli* and bacteriophage λ strains used in this work.

Strain		Genotype	Source
E. coli	α-Select Gold	F$^-$ *deoR endA*1 *recA*1 *relA*1 *gyrA*96 *hsdR*17(rk$^-$, mk$^+$) supE44 *thi*-1 *phoA* Δ(*lacZYA-arg*F)*U*169 Φ80*lacZ*ΔM15λ$^-$	Purchased from Bioline
	BH2688	F$^-$ *λ[Eam*4 *b*2 *red*3 *imm*434 *cIts Sam*7*] recA*3 *IN(rrnD-rrnE)*1 *rpsL*200	(Hohn, 1979) Obtained from DSMZ (#5451) and ATCC (#35131).
	BHB2690	F$^-$ *λ*[*Dam*4 *b*2 *red*3 *imm*434 *cIts Sam*7] *recA*3 *IN(rrnD-rrnE)*1 *rpsL*200	(Hohn, 1979) Obtained from DSMZ (#5452).
	BL21(DE3)	B strain F$^-$ *ompT gal dcm lon hsdS$_B$*($r_B^-m_B^-$) λ(DE3 [*lacI lacUV*5-*T7p07 ind*1 *Sam7 nin*5]) [*malB*$^+$]$_{K\text{-}12}$(λ^S)	(Studier & Moffatt, 1986) Purchased from New England Biolabs® (NEB®)
	BW25113	F$^-$ Δ*(araB–D)*567 Δ*(rhaD–B)*568 Δ*lacZ*4787(::*rrnB*-3) *hsdR*514 *rph*-1	(Baba *et al.*, 2006, Datsenko & Wanner, 2000, Grenier *et al.*, 2014) Gift from Peter McGlynn, University of York
	C600	F$^-$ [*e*14$^-$ (*McrA*) or *e*14$^+$ (*McrA*$^+$)] *thr*-1 *leuB*6 *thi*-1 *lacY*1 *glnV*44 *rfbD*1 *fhuA*21	(Appleyard, 1954) Lab strain
	DH5α	F$^-$ Φ80*lac*ZΔM15 Δ(*lac*ZYA-*arg*F) U169 *rec*A1 *end*A1 *hsd*R17 (rK$^-$, mK$^+$) *pho*A *sup*E44 λ$^-$ *thi*-1 *gyr*A96 *rel*A1	(Taylor *et al.*, 1993) Lab strain

	LE392MP	F⁻ *e*14⁻ (*McrA*⁻) Δ(*mcrC-mrr*) (*TetR*) *hsdR*514 *supE*44 *supF*58 *lacY*1 or Δ(*lacIZY*)6 *galK*2 *galT*22 *metB*1 *trpR*55 λ⁻	Host strain supplied with Epicentre® MaxPlax™ packaging extracts
	MA156	F⁻ Δ(*cod-lacI*)265, λ⁻, *IN*(*rrnD-rrnE*)1, *rpsL*200, Δ*hfl*-150, *zjf*-599*::Tn*10	Obtained from CGSC (#6881). Cited in (Young & Davis, 1983)
	MG1655	F⁻ λ⁻ *ilvG*⁻ *rfb*-50 *rph*-1	(Blattner *et al.*, 1997, Guyer *et al.*, 1981) Used both a lab strain and a strain obtained from CGSC (#6300)
	MLS83L	MG1655 *gyrA* S83L	(Parks, 2004) Lab strain
	MM293	F⁻ *glnX*44 λ⁻ *endA*1 *thiE*1 *hsdR*19	(Meselson & Yuan, 1968) Obtained from CGSC (#6337)
	NEB® 5α	F⁻ *fhuA*2 Δ*(argF-lacZ)U*169 *phoA glnV*44 Φ80 Δ(*lacZ*)*M*15 *gyrA*96 *recA*1 *relA*1 *endA*1 *thi*-1 *hsdR*17	Purchased from NEB®
	NGB345	MG1655 *gyrA* I203VS204RI205V	This work
	NM759	W3110 *recA*56, Δ(*mcrA*) *e14*, Δ(*mrr-hsd-mcr*), (λ*imm*434, *clts*, *b*2, *red*3, *Dam*15, *Sam*7)/λ	Packaging extract lysogen supplied with Epicentre® MaxPlax™ packaging extracts
	Y-Mel	F⁻ *tyrT*58 *mel*-1	(Ikeda *et al.*, 1980, Kobayashi & Ikeda, 1977, Rickenberg & Lester, 1955) Obtained from CGSC (#5032)
Bacteriophage λ	Temperature-sensitive strain	λ *cI*857 *Sam*7	(Goldberg & Howe, 1969) Purchased as 'Lambda DNA' from Sigma-Aldrich®

	Spectinomycin -resistant strain	λ *lom*::*aadA*	(Fogg *et al.*, 2010) Gift from Heather Allison via Andy Bates at the University of Liverpool

CGSC is the Coli Genetic Stock Centre at Yale University; ATCC is the American Type Culture Collection; DSMZ is the Leibniz Institute DSMZ - German Collection of Microorganisms and Cell Cultures GmbH.

2.2 Plasmids and DNA substrates

Various plasmids and DNA substrates were used in this work (Table 2.2). Some were used *in vitro* as substrates for the various assays that were run and others were used *in vivo*, either as expression vectors or in recombineering. For the various maps see Appendix I.

Table 2.2: Plasmids and other DNA substrates used in this work.

Plasmid or Substrate	Features	Use	Source
Cam Fragment	1869 bp, Cam-resistance cassette, Mu SGS, pBR322 SGS	Linear substrate for non-λ IR assay	This work – synthesised by ThermoFisher using Gene strings application
MiniCircle	1814 bp, Cam-resistance cassette, Mu SGS, pBR322 SGS, AttR site	Circular substrate for non-λ IR assay	This work – Synthesised by Twister Biotech
pACYC177	Kan resistance cassette, Amp-resistance cassette, p15A origin	PCR substrate for Kan^R linear fragment for non-λ IR assay	(Chang & Cohen, 1978)
pBR322*	High-copy number derivative of pBR322. Amp resistance, ColE1 origin	Plasmid substrate for λ and non-λ IR assay, as well as DNA substrate for topoisomerase biochemical assays	(Boros *et al.*, 1984) This is a variant of the pBR322 in the refence as it has a deletion that inactivates the Tetracycline resistance gene.
pGDV1	*Bacillus subtilis* plasmid – cannot replicate in *E. coli*. Cam-resistance cassette	Plasmid substrate for non-λ IR assay	(Sarkar *et al.*, 1997, Bron, 1990) Obtained from BGSC (#1E60)
pIR	Derivative of pUC19 with pSC101 origin,	Plasmid substrate for non-λ IR assay –	This work – synthesised by

	Cam-resistance cassette, Mu SGS, pBR322 SGS	designed to have ColE1 origin cut out	ThermoFisher's GeneArt plasmid construction service
pKD46	pSC101 origin, Amp-resistance cassette, λ Red genes: *exo*, *beta*, *gam* with P_{araB} inducible promoter	ssOligo Recombineering plasmid, overexpresses λ recombination genes	(Datsenko & Wanner, 2000) – obtained in *E. coli* MG1655 from CGSC, Yale University
pPH3	Amp-resistance cassette, *E. coli gyrA* gene with P_{tac} promoter, pBR322 origin	*E. coli* GyrA over expression plasmid	(Hallett *et al.*, 1990, Maxwell & Howells, 1999)
pUC19	pMB1 origin, Amp-resistance cassette, MCS, *lacZα* gene from *E. coli*	Plasmid substrate for non-λ IR assay – used for Blue-white colony screening	(Yansich-Perron *et al.*, 1985)
pI203V/I205V	Amp-resistance cassette, *E. coli gyrAG*607*G*609*G*613 gene with P_{tac} promoter, pBR322 origin	*E. coli* GyrA over expression plasmid with I203V/I205V hyper-recombination mutations	This work
pL488P	Amp-resistance cassette, *E. coli gyrAC*1463 gene with P_{tac} promoter, pBR322 origin	*E. coli* GyrA over expression plasmid with L488P hyper-recombination mutations	This work
pL492P	Amp-resistance cassette, *E. coli gyrAC*1475*G*1476 gene with P_{tac} promoter, pBR322 origin	*E. coli* GyrA over expression plasmid with L492P hyper-recombination mutations	This work

Amp – Ampicillin, BGSC – Bacillus Genetic Stock Centre, Cam – is chloramphenicol, Kan – Kanamycin, MCS – multiple cloning site, SGS – strong-gyrase binding site

DNA concentrations were measured using UV/Vis spectroscopy either using a NanoDrop or using a TrayCell (Hellma®Analytics) using a 1 mm path length.

2.3 Primers and PCR

Primers were synthesised by Sigma-Aldrich using their Standard DNA Oligo form. Oligos were ordered at 0.025 µmole scale with a desalting purification step.

Table 2.3: Primers and Oligo's used in this work.

Assay	Primer	Sequence (5´ - 3´)	Notes
Non-λ	Kan100 F	TGTGTCTCAAAATCTCTGATGTT	900bp product with Kan resistance cassette from pACYC177
	Kan100 R	TTAGAAAAACTCATCGAGCATC	
	Kan200 F	TGCTTTGCCACGGAACGGTCTGC	1200bp product with Kan resistance cassette from pACYC177
	Kan200 R	ATCCAGCCAGAAAGTGAGGGAGCCACG	
	Kan400 F	TTCGTAAGCCATTTCCGCTCGCCGCAG	1200bp product with Kan resistance cassette from pACYC177
	Kan400 R	ACATCACCTTCCTCCACCTTCATCCTCAGC	
	CamFragF	GTCAGATTTCGTGATGCTTGTCAGG	Primers for the amplification of the ~1800 bp Cam Frag DNA substrate
	CamFragR	ATCATGCAGCTGGTTGGTCAGGTTC	
	pUC19AmpF	CGTCAATACGGGATAATACCGC	Primers from within the Ampicillin-resistance gene of pUC19 – used for primer walking by Eurofins
	pUC19AmpR	TAAATCTGGAGCCGGTGAGC	
Hyper-recombination mutants - SDM	I203VF	GTATATTGATGATGAAGACGTGAG	Primers designed with PrimerX[a] online Protein-based primer design tool
	I203VR	CATTGAAGGGCTGATG CATCAGCCCTTCAATGCTCACGTCTTCATCAT CAATATAC	
	I205VF	GATGAAGACATCAGCGTTGAAGGGCTGATG G	
	I205VR	CCATCAGCCCTTCAACGCTGATGTCTTCATC	
	L488PF	CTGGATCAGATCGCGGAACCGTTGCGTATTC TTGGTAGCG	Primers designed with PrimerX[a] online Protein-based primer design tool
	L488PR	CGACCTAGTCTAGCGCCTTGGCAACGCATAA GAACCATCG	

	L492PF	GAACTGTTGCGTATTCCGGGTAGCGCCGATCGTC	Primers designed with PrimerX[a] online Protein-based primer design tool
	L492PR	GACGATCGGCGCTACCCGGAATACGCAACAGTTC	
	TGM33	TGCATAATTCGTGTCGCTCAAGG	Sequencing primers that cover the entire *gyrA* gene in pPH3. Designed by Thomas Germe (JIC)
	TGM34	AAATCTGCCCGTGTCGTTGG	
	TGM35	TCGTCGCGGTATTGAAGAAGC	
	TGM36	TGGTTGCTAATCCGTGGCAG	
	TGM37	TGCCGCACGTATTAAAGAAGAAGAC	
	TGM38	AATGCTGTTCTCCGCTGAAGG	
Hyper-recombination mutants - ssOligo recombineering	I203V/I205V	G*A*T*T*GCCGCCGTCGGGAAGTCCGGCCCCGGGATGTGTTCCATCAGCCCTTCcaccctcacGTCTTCATCATCAATATACGCCAGACAACC	ssOligo designed with the help of MODEST[b]
	I203V/I205V wt	CGGGATGTGTTCCATCAGCCCTTCAAT	Colony PCR primers designed by MODEST[b]
	I203V/I205V mut	GTTCCATCAGCCCTTCCACCCTCAC	
	I203V/I205V R500	CCGTCGCGTACTTTACGCCATGAAC	
	I203V/I205V F	CGGTACGGTAAGCTTCTTCAATAC	Primers upstream and downstream from mutation
	I203V/I205V R	GACGTCATGCCAACCAAAATTC	
	L488P	C*T*G*T*TCACGAACCAGCTCCAGCTCTTCACGGATCACTTCCATCAGACGATCGGCGCTTCCCAGGATGCGGAGcgGTTCCGCGATCTGATC	ssOligo designed with the help of MODEST[b]
	L488P wt	CGATCGGCGCTACCAAGAATACGCAAC	Colony PCR primers designed by MODEST[b]
	L488P mut	CGATCGGCGCTTCCCAGGATGCGGAGC	
	L488P R400	GTCGTACTATTTTCGAACTGCGTAAAGCTCGC	
	L492P	T*C*C*A*GCTCTTCACGGATCACTTCCATCAGACGATCCGCACTTCCcgGTATACGCAACAGTTCCGCGATCTGATCCAGCAGCTCTTTGTAT	ssOligo designed with the help of MODEST[b]
	L492P wt	CCATCAGACGATCGGCGCTACCA	Colony PCR primers designed by MODEST[b]
	L492P mut	CCATCAGACGATCCGCACTTCCC	
	L492P R600	GTATGCGCATCGTGATTGAAGTGAAACGC	

a - http://www.bioinformatics.org/primerx/index.htm, b – MODEST online tool (Bonde *et al.*, 2014)
*indicates Phosphorothioate linkages

PCR reactions were run with 0.5 µM of each primer, 1 ng of template, 1 U of DNA polymerase, 200 µM dNTP's (equimolar deoxynucleotide triphosphates, dGTP, dCTP, dATP and dTTP), 1 x PCR buffer and nuclease free water to the required volume. This is unless otherwise stated and specifics are outlined in individual Chapters. PCR reactions were incubated in an Eppendorf Mastercycler® nexus thermocycler.

2.4 Gel electrophoresis

Agarose gels

Agarose (1% w/v) gels were made in TAE buffer (40 mM Tris-Base, 20 mM Acetic Acid, 1 mM Disodium EDTA). Gels were run between 80 – 100 V for between 1 and 3 h, unless otherwise indicated. Gels were then stained in a 1 µg/mL Ethidium Bromide (EtBr) bath for 10 min before destaining for a further 10 min in TAE buffer. Gels were then visualised on a Syngene G:BOX Gel Doc system.

Blue-Native polyacrylamide gel electrophoresis (BN-PAGE)

Proteins (normally between 0.1 µg and 2 µg) were added, along with relevant other factors, such as ATP, DNA and or antibiotics, native-PAGE sample buffer (2.5 µL of a 4 × solution) and ultrapure water (to a final volume of 10 µL) to a 10 or 15 well NativePAGE™ Novex® 4 – 16% gradient Bis-Tris Gel (Life Technologies). Gels were placed in a XCell SureLock™ Mini-Cell Electrophoresis System in the cold room (~7°C). The upper buffer chamber was filled with cold 1 × Cathode buffer and the lower chamber filled with cold 1 × Anode buffer. The gels were run at 150 V, restricted to 8 mA (max 10 mA for 2 gels) for 60 min, after which the voltage was increased to 250 V, restricted to 2 mA per gel for a further 2 h. The gels were either stained with InstantBlue Coomassie (Expedeon) stain or transferred for Western Blotting. Gel pictures were taken using a Syngene G:BOX Gel Doc system.

Sodium dodecyl sulphate polyacrylamide gel electrophoresis (SDS PAGE)

Either purchased 12% Run Blue SDS PAGE (Expedeon) or homemade 12.5% SDS PAGE gels were run. The Run Blue SDS PAGE gels were run in the buffer supplied with the gels (TEO-tricine running buffer). The 12.5% SDS PAGE gels (0.75 mm thickness) were prepared as in Table 2.4 and run in SDS PAGE running buffer. Initially gels were run at 120 V for 15 min, then at 180 V for 1 h. The gels were either stained with InstantBlue Coomassie (Expedeon) stain and gel pictures were taken using a Syngene G:BOX Gel Doc system.

Table 2.4: SDS PAGE gel components.

	12.5% Resolving gel	3.75% Stacking gel
30% Polyacrylamide (Severn Biotech Ltd, acrylamide:bisacrylamide 37.5:1)	2.5 mL	0.75 mL
Resolving Buffer (377 mM Tris.HCl pH 8.8, 0.1% SDS final concentration)	2.0 mL	-
Stack Buffer (130 mM Tris.HCl pH 6.8, 0.1% SDS final concentration)	-	2.25 mL
TEMED (N,N,N´,N´-tetramethylethylenediamine) (Sigma)	10 µL	10 µL
10% Ammonium Persulphate (Sigma)	100 µL	50 µL
Ultrapure H_2O	1.5 mL	3.0 mL

2.5 Media, buffers and antibiotics

LB

Luria-Bertani broth (also known as Lysogeny Broth) (LB) was made using either a premade Formedium LB powder, or using Oxoid™ Tryptone power, Oxoid™ Yeast Extract and NaCl (Sigma). The composition of the broth either way is 10% tryptone, 5% yeast extract and 10% NaCl. This was made in Milli-Q® (Merck-Millipore) Ultrapure H_2O and sterilised by autoclaving at 121°C for 15 min at 15 psi.

λB

Lambda Broth (λB) was made using 10 % Oxoid™ Tryptone and 5% NaCl (sigma). Again, in Milli-Q® Ultrapure H_2O and sterilised by autoclaving at 121°C for 15 min at 15 psi.

NZM

NZM broth was made using 10% Oxoid™ Tryptone, 5% NaCl, and 2% $MgSO_4$ in Milli-Q® Ultrapure H_2O and sterilised by autoclaving at 121°C for 15 min at 15 psi.

SOC

Super Optimal Broth with Catabolite repression (SOC) was made using a premixed Formedium powder. The composition of the broth is 2% tryptone, 0.5% yeast extract, 10 mM NaCl, 2.5 mM KCl, 10 mM $MgCl_2$, 10 mM $MgSO_4$ and 20 mM glucose. All but the $MgCl_2$, $MgSO_4$ and glucose were suspended in Milli-Q® Ultrapure H_2O and sterilised by autoclaving at 121°C for 15 min at 15 psi. The other components were mixed together and filter sterilised (0.2 µm filter) before being added to the autoclaved components.

Antibiotics

Antibiotic stocks were made as per Table 2.5. Where applicable they were filtered through a 0.2 µm filter to ensure sterility before freezing in aliquots to avoid freeze thawing.

Table 2.5: Antibiotics, their stock solutions and solvents used in this work.

Antibiotic	Solvent	Stock Concentration (mg/mL)
Ampicillin	Ultrapure H_2O	100
Chloramphenicol	70% Ethanol	30
Ciprofloxacin	Ultrapure H_2O	10
Coumermycin A_1	DMSO*	10
Kanamycin	Ultrapure H_2O	50
Moxifloxacin	0.1 N NaOH	10
Norfloxacin	Ultrapure H_2O	10
Oxolinic Acid	0.1 N NaOH	10
Sparfloxacin	70% Ethanol	10
Spectinomycin	Ultrapure H_2O	100
Streptomycin	Ultrapure H_2O	100
Tetracycline	70% Ethanol	15
Triclosan	70% Ethanol	15
RedX05931	DMSO*	5

* was not filter sterilised.

TGED buffer

This is the standard buffer used in purification of *E. coli* GyrA protein - 50 mM Tris.HCl (pH 7.5), 1 mM EDTA, 2 mM DTT and 10 % (v/v) glycerol in Milli-Q® Ultrapure H_2O.

Supercoiling assay buffer (ScAB)

ScAB is the standard assay buffer used in the topoisomerase biochemical assays that require ATP – 35 mM Tris.HCl, 24 mM KCl, 4 mM $MgCl_2$, 2 mM DTT, 1.8 mM spermidine, 1 mM ATP, 6.5% (w/v) glycerol and 0.1 mg/ml albumin in Milli-Q® Ultrapure H_2O.

Enzyme buffer (EB)

EB is the storage buffer for GyrA and GyrB proteins – 50 mM Tris.HCl (pH 7.5), 100 mM KCl, 2 mM DTT, 1 mM EDTA, and 10% (w/v) glycerol in Milli-Q® Ultrapure H_2O.

Assay stop buffer (STEB)

STEB is the standard stop buffer for enzymatic assays and for gel loading. It is made as a 2 × solution and used at 1 × - 40% (w/v) sucrose, 0.1 M Tris.HCl (pH 8.0), 0.1 M EDTA, and 0.5µg/mL bromophenol blue in Milli-Q® Ultrapure H_2O.

Sample application buffer (SAB)

SAB is the standard SDS buffer SDS PAGE gel loading. It is made as a 5 × solution and used at 1 × - 62.5 mM Tris.HCl (pH 6.8), 2% SDS, 10% glycerol, 5% β-mercaptoethanol and 0.001% Bromophenol Blue in Milli-Q® Ultrapure H_2O.

Native PAGE sample buffer

Native-PAGE sample buffer is used as a gel loading buffer for BN-PAGE gels. It is made as a 4 × solution and used at 1 × (pH 7.2) - 50 mM Bis-Tris, 6 N HCl, 50 mM NaCl, 10% (w/v) glycerol, and 0.001% Ponceau S in Milli-Q® Ultrapure H_2O.

Cathode buffer

This was the cathode buffer used in the BN-PAGE protocol – 50 mM Tricine, 15 mM Bis-Tris and 0.002% Coomassie G250 in Milli-Q® Ultrapure H_2O. The pH was adjusted to 7.0 with HCl.

Anode buffer

This was the anode buffer used in the BN-PAGE protocol – 50 mM Bis-Tris (pH 7.0) in Milli-Q® Ultrapure H_2O.

SDS PAGE running buffer

This was the running buffer used with the SDS-Tris Glycine PAGE gels – 25 mM Tris.HCl (pH 6.8), 192 mM glycine and 0.1% SDS in Milli-Q® Ultrapure H_2O.

2.6 Electroporation and transformation

Electroporation

Two microlitres (approximately 100 ng) of a DNA sample was added to 25 µL of electrocompetent *E. coli* cells (either purchased (see Table 2.1 or homemade by centrifuging through a glycerol/mannitol cushion (Warren, 2011) – unless otherwise stated). This was then transferred to precooled 1 cm electroporation cuvettes and electroporated at 1.7 kV with time constants between 4.5 and 5.5. After electroporation 975 µL of warm SOC was added to the samples and these were incubated at 37°C for 1 h with shaking. The samples were then centrifuged at 3000 g for 5 min and resuspended in 450 µL of LB before plating on 1.2% LB agar plates with appropriate antibiotics at suitable dilutions.

Transformation

Plasmid DNA (>100 ng) was incubated with 50 µL of chemically-competent *E. coli* cells on ice for 20 min before heat shocking at 42°C for 42 s. These were then returned to ice for 2 min

before 950 µL of prewarmed SOC was added. The samples were incubated at 37°C for 1 h with shaking before plating on 1.2% LB agar plates with appropriate antibiotics at suitable dilutions.

2.7 Overexpression and purification of GyrA

The pPH3 overexpression plasmid was transformed into the expression host *E. coli* BL21 (DE3). A single colony was inoculated into 5 mL LB with 100 µg/mL ampicillin and incubated overnight at 37°C with shaking (unless otherwise stated). The following day all 5 mL of the overnight culture was inoculated into 500 mL of LB which was incubated at 30°C with shaking at 220 rpm until an OD_{600} of about 0.6 was reached. Isopropyl β-D-1-thiogalactopyranoside (IPTG) was added to 0.5 mM and the cultures were returned to the shaking incubator for a further 4 h or overnight. The cultures were centrifuged in 1 L pots in the SLC-4000 rotor at 7000 rpm for 10 min. The pellet was resuspended in TGED and flash frozen in liq N_2 before storing at -80°C.

After incubation with IPTG, protein expression was identified using SDS PAGE. Samples were prepared by boiling 100 µL of the culture with 20 µL of 5 × SAB for five minutes. These were run on a 12.5% polyacrylamide resolving gel with a 4% polyacrylamide stacking gel initially at 135 V for 20 min then 180 V for 60 min, partially submerged in an SDS running buffer.

The resuspended pellet was defrosted on ice and the cells lysed using either a Cell Disrupter (Constant Systems). The cell debris was removed by centrifugation at 18500 rpm for 30 min using a SS34 rotor in a RC 6+ Sorvall Centrifuge. Only the supernatant was retained and purified with an ÄKTA Pure FPLC system (GE healthcare). Firstly, the supernatant was applied to a HiLoad Q-Sepharose High Performance ion exchange column (GE Healthcare) and the protein eluted using a NaCl gradient (0 – 1 M NaCl in TGED). Fractions were collected and identified using SDS PAGE. The fractions that were identified as having the GyrA protein were pooled and $(NH_4)_2SO_4$ was added to 1 M. This was applied to a Phenyl-Superose column HR 5/5 (Pharmacia) and the protein eluted using a reverse $(NH_4)_2SO_4$ gradient (1 M - 0 in TGED). Fractions were collected and identified using SDS PAGE. Again, the fractions that were identified as having the GyrA protein

were pooled before dialysing overnight in SnakeSkin™ dialysis tubing (ThermoFisher) at 4°C in TGED. The dialysed fractions were applied to a MonoQ column (Pharmacia 10/10) using the same ÄKTA FPLC protocol, however the desired fractions were dialysed overnight in TGED with 100 mM KCl.

Protein concentrations were determined using a calorimetric Bradford assay. Briefly 1 – 10 µL of the protein (or made up to 10 µL in EB) was added to 90 µL of ultrapure H_2O. This was added to 900 µL of Bradford reagent in a cuvette with a 1cm path length, briefly mixed and incubated at room temperature for 5 min. This was analysed at a 595 nm wavelength in a spectrophotometer against a pre-programmed standard curve.

2.8 Supercoiling reactions

The general supercoiling reactions were set up as follows. The relevant GyrA protein, GyrB (made by Thomas Germe, JIC), 0.5 µg relaxed pBR322* DNA, EB, 5 × ScAB, and Milli-Q® water to a final volume of 30µL (unless otherwise stated). GyrA and GyrB were mixed in equimolar concentrations and then diluted (see individual assays for specific concentrations). The pBR322* DNA, and supercoiling assay buffer were all supplied by Inspiralis Ltd. The supercoiling reaction was incubated at 37°C for 30 minutes. After incubation 30µL of 2 × STEB and 30µL chloroform-isoamyl alcohol (24:1) were added and briefly vortexed before centrifuging at 13000 rpm for 1 min. Samples were analysed by agarose gel electrophoresis at 80 V for 3 h or 16 V overnight.

Chapter 3: Topoisomerase-Mediated Illegitimate Recombination

3.1 Introduction

Bacteriophage λ (λ) is a temperate phage that infects *E. coli* (Hershey & Dove, 1971). It is a double-stranded DNA virus (Figure 3.1) that is encapsidated in an icosahedral head attached to a tubular tail (Kellenberger & Edgar, 1971). λ infects the bacterium by adsorbing to the host cell and injecting its DNA into the host. Once inside the host, the phage genome circularises and the phage can then multiply either by entering the lytic or the lysogenic phase of its life cycle (Figure 3.2) (Hershey & Dove, 1971).

The lytic cycle (also known as the productive or active phase) commences upon expression of the *cro* gene and *N* gene. The *cro* gene product negatively regulates the repressor gene *cI* whilst the *N* gene product provides positive regulation of the genes involved in replication, recombination and the *Q* gene. The *Q* gene product regulates the genes involved in capsid development and packaging of the DNA (Echols, 1971). The λ chromosome undergoes rolling circle replication resulting in concatemeric DNA that is packaged from *cos* end to *cos* end (Feiss & Becker, 1983) (Figure 3.1). Maturation of the head protein occurs upon packaging of the DNA (Hohn & Hohn, 1974). The newly packaged and assembled λ are released from the bacterium by lysis (Wilson, 1982).

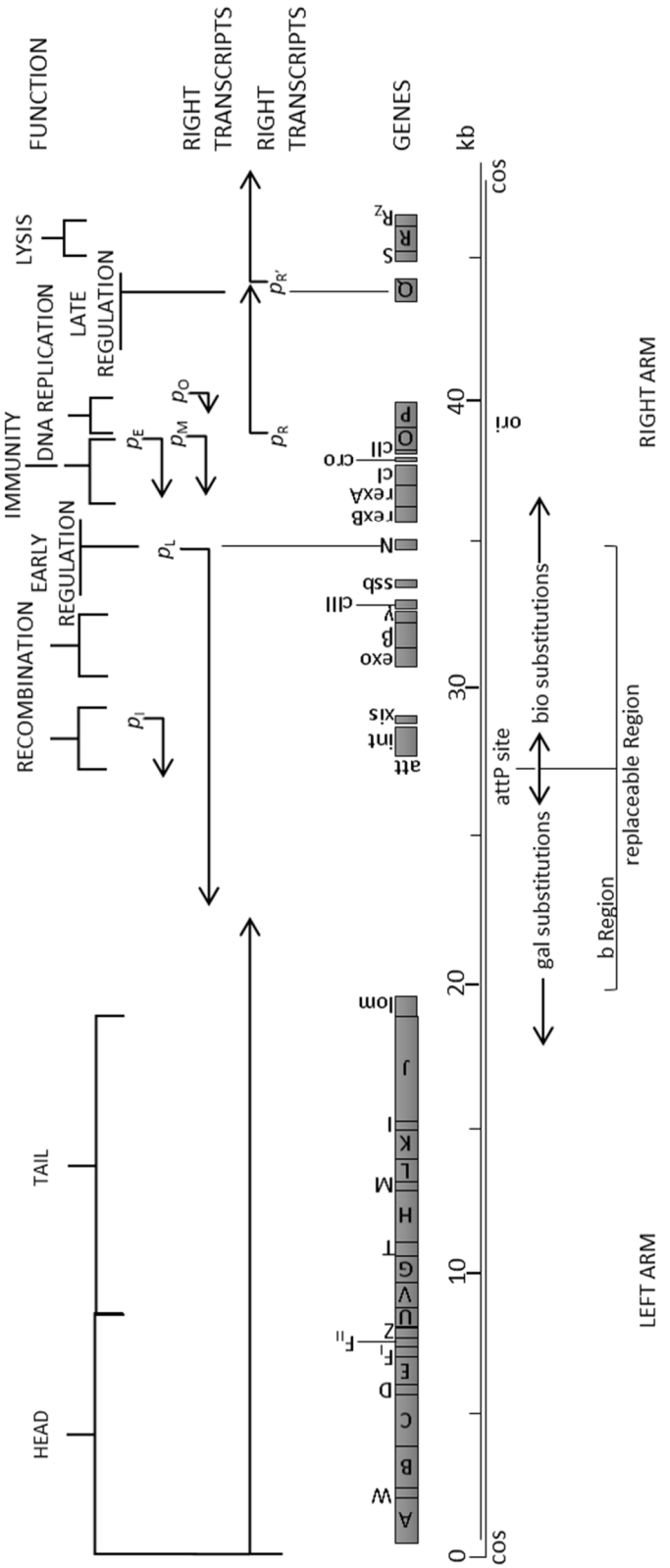

Figure 3.1: Bacteriophage λ DNA map. A drawing of the molecular map of λ beginning and ending with the cos ends (cos – shown as overhangs). The scale is in kb. Gene functions and clusters are given above the brackets (in line with FUNCTION). Known promoters are shown with single-headed arrows (head denotes the direction of transcription; length is the extent

of the transcript) and indicated by *p* with the subscript indicating the point of origin: p_I – *int* promoter; p_E – cI promoter (Establishment); p_M – cI promoter (Maintenance); p_L – major leftward promoter; p_R – major rightward promoter; p_O – *oop* promoter; $p_{R'}$ – late promoter. Areas of known deletion or substitution are indicated below the scale with gal substitutions denoting the position of the area of recombination during excision giving rise to gal transducing phage, likewise with bio giving rise to bio transducing phage. attP is the attachment site where the phage integrates into the bacterial chromosome and ori is the phage replication origin. Figure adapted from (Daniels *et al.*, 1983).

Lysogeny is a passive way for λ to multiply as it replicates as part of the bacterial chromosome (Hershey & Dove, 1971, Arber, 1983). The initial stages of infection are the same as in the lytic phase however the switch between lysis and lysogeny relies on the production of the repressor cI, cII and cIII proteins. The *cro* gene product competes with cI for occupation of the operator and each represses each other's synthesis (Gussin *et al.*, 1983) with cII stimulating the expression of cI (Friedman & Gottesman, 1983). Once the "decision" to enter lysogeny is taken, the circularised and supercoiled λ chromosome integrates into the bacterial chromosome. This is mediated by the *int* gene and the recombination generally occurs between the *att*B site on the *E. coli* chromosome and the *att*P site on the phage chromosome (Arber, 1983). The infected *E. coli* bacterium is now referred to as a lysogen and the λ is now referred to as a prophage. In this lysogenic form enough cI is produced to maintain the prophage and alongside the production of cII and cIII will stop superinfection with another λ phage leading to the establishment of immunity (Kaiser, 1957, Eisen & Ptashne, 1971). The λ genome will passively replicate this way until some switch (such as induction of the SOS response) induces the lytic cycle, where upon the cI repressor is cleaved and the expression of the *xis* gene, which excises the phage genome from the bacterial genome to begin the lytic cycle (Echols, 1986).

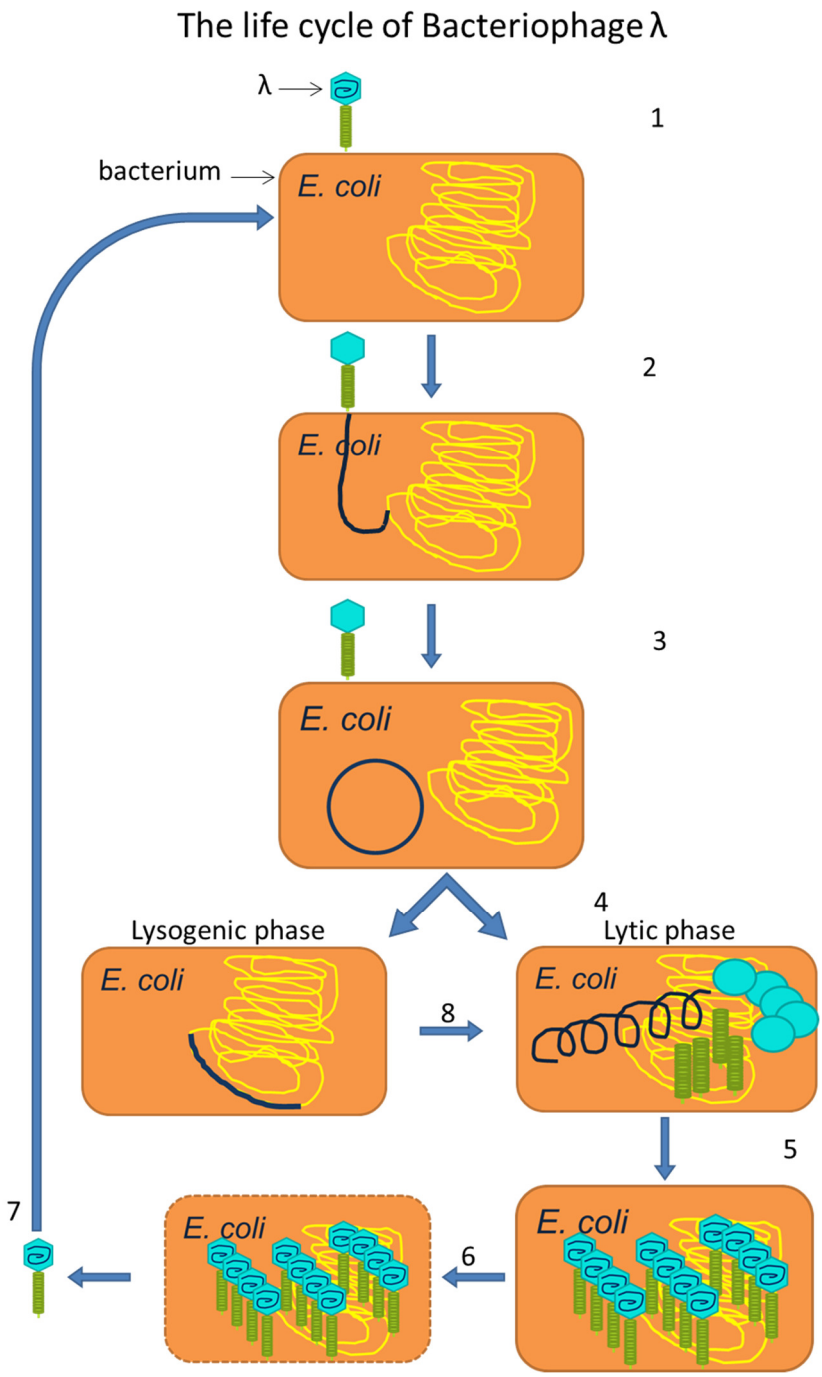

Figure 3.2: Diagram of the life cycle of Bacteriophage λ. 1 – the phage (λ) adsorbs to a bacterium (*E. coli*) and 2 – injects its DNA into the cell. 3 – the DNA circularises and is supercoiled by DNA gyrase. 4 – it then either integrates into the bacterial chromosome (enters the Lysogenic phase) or it begins to replicate its genome by rolling circle replication and assembling the proteins necessary for making the capsid (Lytic phase). 5 – the concatemeric DNA (result of rolling circle replication) is packaged into the phage head capsid and the whole infective phage is assembled. 6 – the bacterial cell is lysed and 7 – the infective phage is released to start the cycle again. 8 – upon induction (such as during SOS response) the phage chromosome excises from the bacterial genome and begins the Lytic phase (steps 5 – 7).

As outlined in the Introduction (Chapter 1), IR is defined as recombination between DNA sequences that share little to no homology (Franklin, 1971, Weisberg & Adhya, 1977). It is distinct from general recombination as it is independent of general recombination functions. In bacteriophage, IR is observed during generalised and specialised transduction (Franklin, 1971). Transduction is defined as the transfer of bacterial DNA from one bacterial chromosome to another by phage (Franklin, 1971). Generalised transduction occurs when P1 and P22 phage package fragments of the bacterial chromosome instead of their own chromosomes (Ikeda & Tomizawa, 1965). Specialised transduction occurs when part of the bacterial chromosome is excised with the phage genome and packaged along with part of the phage genome (e.g. *gal* or *bio* specialised transducing phage) (Franklin, 1971).

DNA gyrase was the first of the type II topoisomerases implicated in topoisomerase-mediated-IR. Kobayashi and Ikeda (1977) developed an *in vitro* assay to study IR using a bacteriophage λ-based packaging assay (Figure 3.3) which was established by Hohn and Hohn (1974). This assay involved the incubation of two induced *E. coli* lysogens which have a large amount of endogenous concatenated λ DNA with a plasmid containing an antibiotic-resistance gene. These lysogens had amber mutations in either the *D* and F_I genes or the *E* gene (λ *cIts*857 *S*am7 *D*am15 $F_I$am96B and λ *cIts*857 *S*am7 *E*am4). Amber mutations are part of a set of specific nonsense mutations that can be overcome by growing in a suppressor host, such as *supF* or *supE* (Brenner *et al.*, 1965, Brenner & Stretton, 1964, Casali, 2003).

The first of the two lysogens acts as an acceptor lysate whilst the latter acts as a donor lysate in a complementation reaction. The *D* gene mutant results in an acceptor that is defective in DNA packaging, and the F_I mutant stops the creation of non-infectious particles by interfering with the head-tail attachment protein (the wild-type F_I protein with the D mutant may yield complete particles lacking DNA) (Hohn & Hohn, 1974, Kellenberger & Edgar, 1971). The *E* mutant does not produce head particles (Kellenberger & Edgar, 1971) whilst the *S* mutant, seen in both

lysogens, stops lysis (Wilson, 1982). The *S* gene encodes a holin, which is a protein that provides a small hole in the inner membrane for the passage of small molecules, and the *R* gene encodes endolysin that lyses the cells and frees the newly-made phage (Wilson, 1982, White *et al.*, 2010). Packaging of the λ DNA into the head is only efficient if the DNA length is 78% – 105% of the whole λ chromosome (~50 kb); meaning that neither the plasmid alone, nor the full-length plasmid and the λ DNA together, can be packaged efficiently (Feiss & Becker, 1983, Feiss *et al.*, 1977).

Once the reaction containing the packaging mixture and plasmid was complete, the newly packaged phage were released and used to infect an appropriate host. This was then plated onto media, with or without the respective antibiotic. The frequency of IR was calculated by the number of antibiotic-resistant transductants over the number of plaque forming units (Kobayashi & Ikeda, 1977).

Although DNA gyrase and other topoisomerases have been shown to mediate IR (discussed in Chapter 1 – Introduction), the exact molecular mechanism behind this has not been investigated. In order to evaluate topoisomerase-mediated IR, I attempted to repeat the λ-based experiments done previously as well as develop a non-λ *in vitro* assay.

3.2 Specific materials and methods

λ – based assay

This assay (Figure 3.3) was run in various ways in an attempt to repeat the work done previously. The basic outline is described below but more discussion on the variations is in the Results and Discussion section.

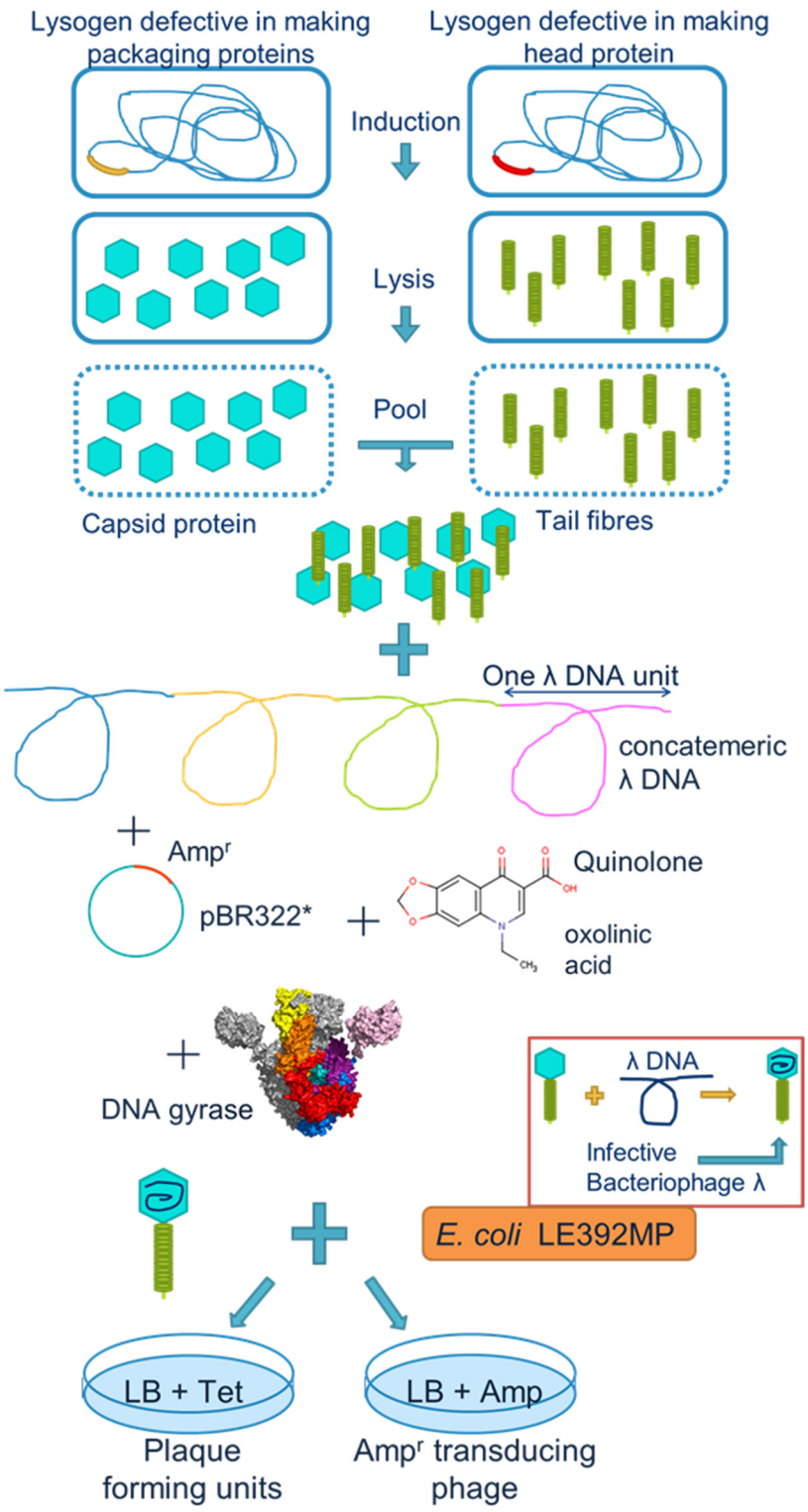

Figure 3.3: Diagram of the *in vitro* λ – based assay. Packaging extracts were prepared from two lysogens, one that cannot make the proteins required for packaging DNA (yellow lysogen) and the other the cannot make the capsid heads (red lysogen). These are mixed together along with concatemeric λ DNA and pBR322* as well as oxolinic acid. *E. coli* LE392MP is then infected by the newly packaged phage and assayed for the number of plaque forming units and for the number of ampicillin-resistant transducing phage.

Transfection

λ *cI*857 *Sam*7 DNA (Sigma) was transfected into *E. coli* C600 (Table 2.1) using the protocol outlined in Davis *et al.* (Davis *et al.*, 1980). Briefly, an overnight culture of C600 was diluted 1/100 in LB (see Chapter 2) and incubated at 37°C until an OD_{600} of 0.6-0.7 was reached. Thymidine was added to 12 µg/mL at an OD_{600} of 0.3. Cells were sedimented at 5000 rpm at 4°C and resuspended in 50 mL ice-cold CT media (50 mM $CaCl_2$ and 50 µg/mL thymidine). The resuspended cells were incubated on ice for 5 min before centrifuging again at 5000 rpm at 4°C before resuspending the sedimented cells in 5 mL ice-cold CT media. Two hundred microlitres of the resuspended cells was incubated with 100 µL of λ *cI*857 *S*am7 DNA (100 ng maximum) in 100 mM Tris. HCl pH 7.2 and 50 µg/mL thymidine for 60 min on ice before heat shocking at 45°C for 2 min and plating on room temperature plates with 2.5 mL LB-0.7% agar (soft agar). These were incubated, inverted, overnight at 42°C.

Preparation of phage stocks: confluent lysis and plate lysis with scraping

Freshly poured 9 cm LB agar plates were overlayed with 3 mL of soft agar with 200 µL of an *E. coli* strain, alone if it was a lysogen, or with 100 µL of a phage stock. These were incubated without inversion at either 37°C or 42°C (42°C for temperature-sensitive λ *cI*857 *Sam*7).

Confluent Lysis – 5 mL of cold SM buffer (100 mM NaCl, 10 mM $MgSO_4$, 50 mM Tris.HCl pH 7.5) was added to the plate and incubated at 4°C on a shaking platform for 3 h. The SM buffer was pipetted off the plate and into a chloroform-resistant tube. One millilitre of fresh SM was added to the plate, gently swirled and left for 15 min, tilted for the SM to drain into one area. This was pipetted into the same chloroform-resistant tube. One hundred microlitres of chloroform was added to the harvested SM buffer and briefly vortexed before centrifuging at 4000 g at 4°C for 10 min. The supernatant was placed in a fresh chloroform-resistant tube and a drop of chloroform was added. This was titered and stored at 4°C.

Plate Lysis with scraping – 5 mL of cold SM buffer was added to the plate and the top soft agar was gently scraped into a sterile chloroform-resistant centrifuge tube. Two millilitres of SM

was added to the scraped plate and gently swirled to collect any remaining top agar before adding it to the rest of the soft agar in the centrifuge tube. One hundred microlitres of chloroform was added to the tube and the agar suspension was incubated at 4°C with gentle agitation for 15 min. This was then centrifuged at 4000 g at 4°C for 10 min. The supernatant was placed in a fresh chloroform-resistant tube and a drop of chloroform was added. This was titered and stored at 4°C.

Titering

Phage stocks or newly packaged phage were serially diluted from 10^{-2} to 10^{-9} in phage dilution buffer (10 mM Tris.HCl pH 8.3, 100 mM NaCl, 10 mM $MgCl_2$). One hundred microlitres of the dilution was added to 100 µL of plating bacteria (grown in 50 mL LB with 10 mM $MgSO_4$, and 0.2% maltose, to an OD_{600} between 0.8 and 1.0) and incubated at 30°C for 15 min before adding to 3 mL soft agar (at 48°C) and overlaying onto prewarmed 9 cm LB 1.2% agar plates. These were inverted and incubated overnight at 42°C. Plates with between 30 and 300 plaques were counted and the titer calculated by multiplying the number of plaques with the dilution factor and 1000 (to convert µL to mL) and dividing this number by the volume of phage plated (µL). This will yield a titer in PFU/mL. Alternatively, 200 µL of plating bacteria was added to the soft agar and overlayed onto LB 1.2% agar plates and left to set before 5 µL of each dilution was spotted onto the plate. These were incubated inverted at 42°C overnight. The titer is calculated as above in spots that have between 3 and 30 plaques visible in them. The plating bacteria used was *E. coli* LE392MP (Table 2.1) unless otherwise stated. Where LE392MP was used, all media was supplemented with 15 µg/mL tetracycline.

Packaging extracts

Either MaxPlax™ (epicentre®) commercially available lambda packaging extracts were used as per manufacturer's instructions, or packaging extracts were prepared as described below.

The packaging extracts were made from two *E. coli* lysogens, BHB2688 and BH2690 (Table 2.1) using the method outlined in Sambrook *et al.* (1989). Briefly, the lysogens' temperature-

sensitive phenotype was confirmed by streaking onto two LB 1.2% agar plates and incubating one at 30°C and the other at 42°C. If there was little to no growth on the 42°C plate when compared to the 30°C plate, then the packaging extracts were made from a colony picked and grown in an overnight culture from each 30°C plate. The overnight cultures were diluted to an OD_{600} of 0.1 in 500 mL NZM media. The cultures were grown to an OD_{600} of 0.3 at which point they were induced by swirling in a 45°C water bath for 15 min. The induced cultures were then incubated at 39°C with shaking for 3 h before they were centrifuged at 4000 g for 10 min at 4°C. From here one lysogen was prepared by lysis, the other by sonication.

For the BHB2688 lysogen which acts as the packaging protein donor, the pellet was retained and resuspended in a total of 3 mL of an ice-cold sucrose solution (10% sucrose in 50 mM Tris.HCl pH 8.0). The suspension was divided into chilled microfuge tubes (0.5 mL each) and 25 µL of ice-cold Lysozyme solution (2 mg/mL lysozyme in 10 mM Tris.HCl pH 8.0) was added to each, gently mixed and flash frozen in liq N_2. The tubes were then thawed on ice before 25 µL of packaging buffer (6 mM Tris.HCl pH 8.0, 50 mM spermidine, 50 mM putrescine, 20 mM $MgCl_2$, 30 mM ATP and 30 mM β-mercaptoethanol) was added to each tube and briefly mixed. The contents of all the tubes was then combined into one tube and centrifuged at 45 000 g for 1 h at 4°C. This was then dispensed into 10 µL aliquots, flash frozen in liq N_2 and stored at -80°C.

For the BHB2690 lysogen the pelleted cells were resuspended in 3.6 mL sonication buffer (20 mM Tris. HCl pH 8.0, 1 mM EDTA and 5 mM β-mercaptoethanol). The suspension was then sonicated using a microtip probe at maximum amplitude in short bursts, 10 s on, 20 s off, until the solution cleared and was less viscous. This was then centrifuged at 12 000 g for 10 min at 4°C. The supernatant was added to an equal volume of ice-cold sonication buffer and a sixth of the volume (500 µL) of packaging buffer. The solution was gently mixed and dispensed into microfuge tubes in 15 µL aliquots before flash freezing in liq N_2 and storing -80°C.

For the packaging assay, one tube of each prepared packaging extract was thawed on ice and mixed together with up to 1 µg of concatemeric λ DNA. This was incubated at 30°C for 1 – 3 h and the titer measured as described above.

Packaging extracts of BHB2688 and BH2690 were also prepared as per Kobayashi and Ikeda (1977). Briefly, the lysogens were grown to an OD_{600} of 0.2, induced at 42°C for 15 min then incubated for a further hour at 37°C. Four hundred millilitres of each culture was cooled on ice and centrifuged at 5000 g for 5 min. The pellets were resuspended together in 10 mL 40 mM Tris.HCl pH 8.0 and 10 mM $MgCl_2$. This was then centrifuged again and resuspended in 700 µL of 40 mM Tris.HCl pH 8.0, and 10 mM $MgCl_2$ and 175 µL of a solution of 50% DMSO, 50 mM spermidine, and 7.5 mM ATP. Twenty five microlitre aliquots were dispensed into microfuge tubes and flash frozen in liq N_2.

Concatemeric DNA

Bacteriophage λ was prepared by confluent lysis. Once clarified the lysates were treated with RNAse and DNAse in 10 mM $CaCl_2$ for 1 h at 37°C before stopping the reaction with 10 mM EDTA. The phage were then precipitated by adding PEG8000 (10% w/v) and incubated for 1 h at 4°C with constant but gentle stirring. The precipitated phage were then pelleted by centrifuging at 10 000 g for 10 min and the pellet was resuspended in 500 µL of 10 mM Tris.HCl pH 8.0. An equal volume of phenol-chloroform-isoamyl alcohol (25:24:1 v/v/v) was added, gently mixed then centrifuged at 10 000 g for 10 min. The upper phase was pipetted off, being careful not take-up any of the white precipitate, and added to an equal volume of phenol-chloroform-isoamyl alcohol. This was repeated 5 times, or until no further white precipitate was visible at the interface between the upper phase and lower phase. After the final phenol extraction, an equal volume of chloroform was added, briefly mixed and centrifuged at 10 000 g for 1 min. The upper phase was retained and ethanol (EtOH) precipitation of the DNA was performed. Twice the volume of ice-cold 95% EtOH was added to the upper phase with 0.3 M NaOAc (sodium acetate) pH 5.2 and incubated at -80°C for 10 min. This was then centrifuged at 2500 g for 1 min

at 4°C. The pellet was washed gently with ice-cold 70% (v/v) EtOH before pelleting again at 1000 g for 30 s at 4°C. The pellet was left to dry before resuspending in 10 mM Tris.HCl pH 8.0. The newly extracted λ DNA (200 – 500 µg) was incubated in TEK buffer (10 mM Tris.HCl pH 8.0, 50 mM KCl, and 1 mM EDTA) at 65°C for 10 min then at 45°C for a further 2 h. Formation of concatemers was confirmed by HindIII digestion and gel electrophoresis (General Methods - Chapter 2).

In vitro recombination assay

The IR assay was set up in variety of ways but the general protocol was as follows (Figure 3.3). Concatemeric λ DNA (λ *cI*857 *S*am7) (1 µg) was incubated with 25 µL packaging extracts, with and without 1 µg relaxed pBR322* (Table 2.2), 50 µg/mL oxolinic acid (OA) or DNA gyrase (25 ng). This was incubated for 1.5 h at 30°C before a further 25 µL of the packaging extract was added and incubated for 1.5 h at 30°C. After the incubation, 500 µL of phage dilution buffer and 25 µL chloroform was added followed by very gentle vortexing. This solution was then titered to assay the number of PFU/mL whilst 100 µL was added undiluted to 100 µL of the plating bacteria (LE392MP unless otherwise stated; prepared as described above). This was incubated at 30°C for 15 min to 1 h before all 200 µL was plated onto 9 cm LB 1.2% agar supplemented with 20 µg/mL ampicillin and incubated at 30°C overnight looking for ampicillin-resistant colonies (ampicillin-resistant transducing phage).

In vivo recombination assay

This was designed as a simpler *in vivo* version of the *in vitro* λ-based assay (Figure 3.4). The plasmid pBR322* was transformed into *E. coli* LE392MP. This transformant was grown in λB supplemented with 2 mM $MgSO_4$, 0.2% (w/v) maltose, 10 µg/mL Tet and 100 µg/mL Amp overnight at 37°C. This overnight culture was inoculated into 50 mL λB supplemented with 2 mM $MgSO_4$, 0.2% (w/v) maltose, 10 µg/mL Tet and 100 µg/mL Amp and incubated until an OD_{600} of 0.4 was reached where 2 mL was removed and centrifuged at 3000 rpm for 15 min. The pellet was resuspended in 4.4 mL of λ *cI*857 *S*am7 (0.6×10^9 PFU/mL, approximately a MOI of 5) and

incubated initially at 30°C for 15 min then for a further hour at 30°C with gentle shaking. This (200 µL) was plated onto λB 1.2% agar plates with 100 µg/mL Amp. Twenty colonies were selected and streaked onto two separate plates, λB 1.2% agar plates with 100 µg/mL Amp and 10 µg/mL Tet, one was incubated overnight at 30°C and the other was incubated overnight at 42°C. Lysogens were assumed to be colonies that were Amp resistant and temperature-sensitive. The newly-made *E. coli* LE392MP (pBR322*)(λ *cI*857 *S*am7) lysogen was grown overnight in LB with 10 µg/mL Tet and 100 µg/mL Amp at 30°C. One hundred microlitres of this overnight culture was inoculated into 10 mL LB with 20 µg/mL Amp with either no oxolinic acid (OA), 0.01 µg/mL OA, 0.1 µg/mL OA, 1 µg/mL OA or 10 µg/mL OA. These were incubated at 30°C with shaking for 2 h. The 1 µg/mL OA and 10 µg/mL OA samples were incubated overnight. After incubation, the samples were induced at 45°C for 15 min before a further 1 h incubation was performed at 38°C with gentle shaking. One hundred microlitres of chloroform was added to the cultures, gently vortexed and then centrifuged at 4000 g for 10 min. The supernatant was then titered and assayed for ampicillin transducing phage with an untransformed *E. coli* LE392MP.

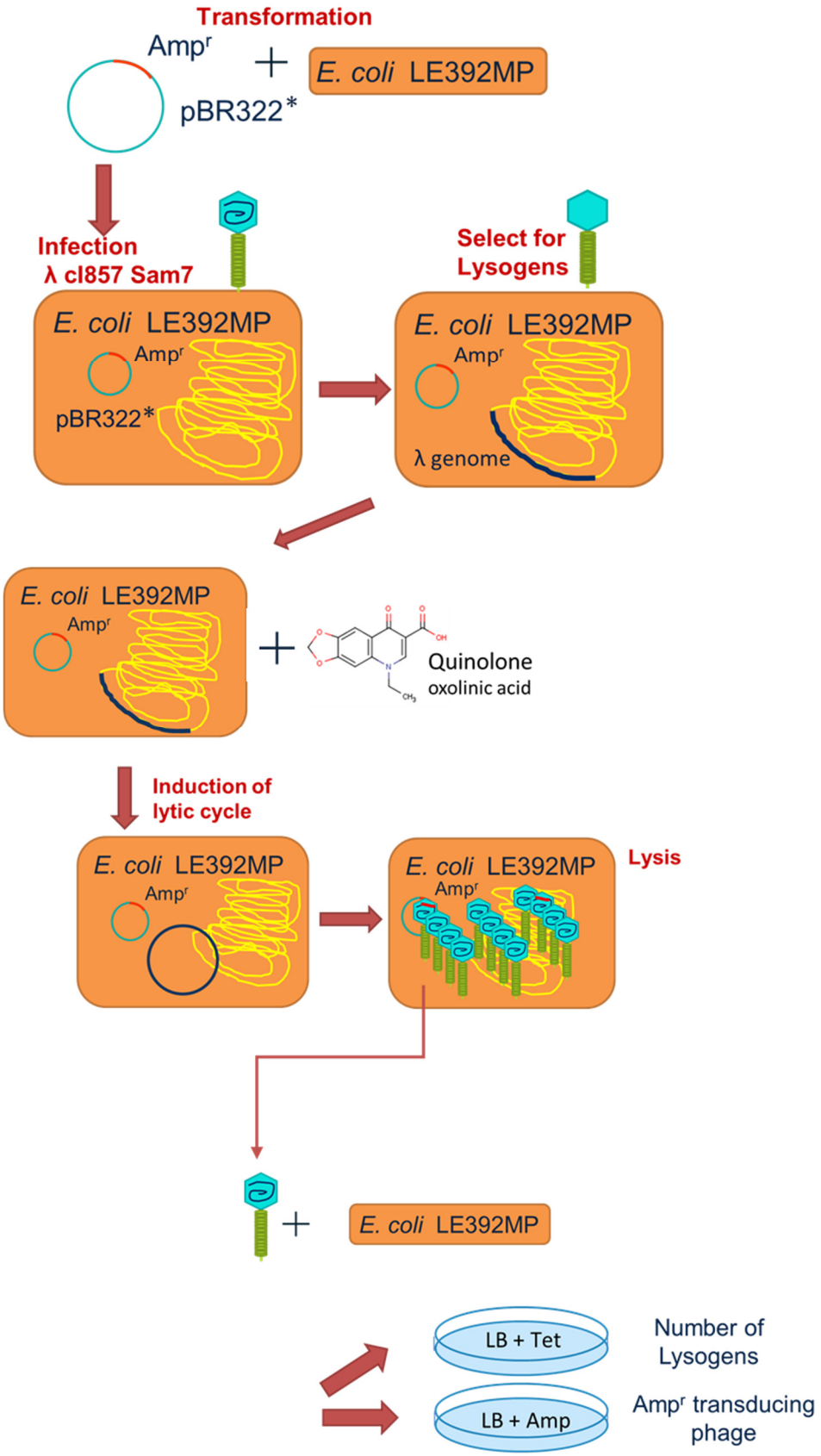

Figure 3.4: Diagram of the *in vivo* λ – based assay. Amp^R indicates ampicillin resistance (red line). The yellow line is the bacterial chromosome, and the navy line is the phage chromosome.

Non-λ assay

This assay was originally developed by Richard Bowater (UEA) and then updated by myself (Figure 3.5). It works on a similar basis to the λ-based assay in that it involves the transfer of an antibiotic-resistance gene from one DNA molecule to another. Although, the assay was also run where the disruption of the *lacZ* gene in pUC19 was selected for (Figure 3.5b). The basic premise is a supercoiling reaction (as described in the General Methods) where relaxed pBR322* (or pUC19) is incubated in supercoiling assay buffer with another piece of DNA carrying a kanamycin or a chloramphenicol resistance cassette (see Table 2.2 and Appendix I for all substrates used), with up to 250 ng of DNA gyrase, 50 μg/mL OA and cell extracts. Post-incubation the samples were either cleaned-up and electroporated (see General Methods) into electrocompetent *E. coli* NEB® 5-alpha (see Table 2.1) or transformed (see General Methods) into chemically-competent α-Select Gold Efficiency *E. coli* (Bioline). These were plated onto LB 1.1% agar plates supplemented with 100 μg/mL ampicillin (Amp) or 50 μg/mL kanamycin (Kan) or 35 μg/mL chloramphenicol (Cam) (or both Amp and Kan, or both Amp and Cam). Any resistant colonies were cultured and the plasmids extracted using Qiagen Miniprep kits. These plasmids were then characterised using restriction digests or by PCR with primers (Table 2.3) designed from the origin or from within the resistance cassettes of the starting substrates (see General Methods).

DNA substrates

Relaxed pBR322* was purchased from Inspiralis Ltd. The linear Kan substrate was made by PCR (General Methods) from pACYC177 (Table 2.2 and Appendix I) using primers (Table 2.3) that included 100 bp, 200 bp or 400 bp flanking the kanamycin cassette (total length of 900 bp, 1200 bp or 1500 bp). I designed a linear substrate with the Cam-resistance cassette flanked by 200 bp from pACYC184 (Table 2.2 and Appendix I) modified to include the strong-gyrase binding site (SGS) from pBR322 and the Mu SGS and to reduce secondary structure. This linear substrate was constructed by ThermoFisher using their GeneArt Strings Linear DNA fragments application. I also had a MiniCircle fabricated by Twister Biotech (Table 2.2 and Appendix I), that was a circular version of the linear Cam and I designed and had fabricated (ThermoFisher GeneArt) a plasmid

with the pSC101 origin of replication and a Cam-resistance cassette substrate (Table 2.2 and Appendix I). pGDV1 (Table 2.2 and Appendix I) is a *Bacillus subtilis* plasmid that cannot replicate in *E. coli*. It carries a Cam-resistance cassette and it was purchased from the Bacillus Genetic Stock Centre (Ohio State University).

Cell extracts

Cell extracts of NEB® 5-α cells or *E. coli* MM293 (Table 2.1) were grown in 10 mL LB with 0.05 µg/mL OA at 37°C overnight. The cells were harvested by centrifugation and the pellet was resuspended in 100 µL 50 mM Tris. HCl pH 8.0. To this 10 µL of 10 mg/mL lysozyme was added, briefly mixed and subjected to two freeze thaw cycles where the samples were frozen in liq N_2 then slowly thawed on ice. After the second round of freeze-thawing, the lysates were either stored at -80 °C or they were clarified by centrifuging at 16 000 g for 30 min at 4°C. The supernatant was divided into 10 µL aliquots and flash frozen in liq N_2 and kept at -80°C until required.

Restriction digests

Restriction enzymes ApaLI, AgeI, HindIII and NcoI were purchased from Roche or NEB® and were used as follows: 1 U of the enzyme was incubated with 100 ng of DNA at 37°C for 30 min to 1 h. The products of the digestion were then analysed using agarose gel electrophoresis.

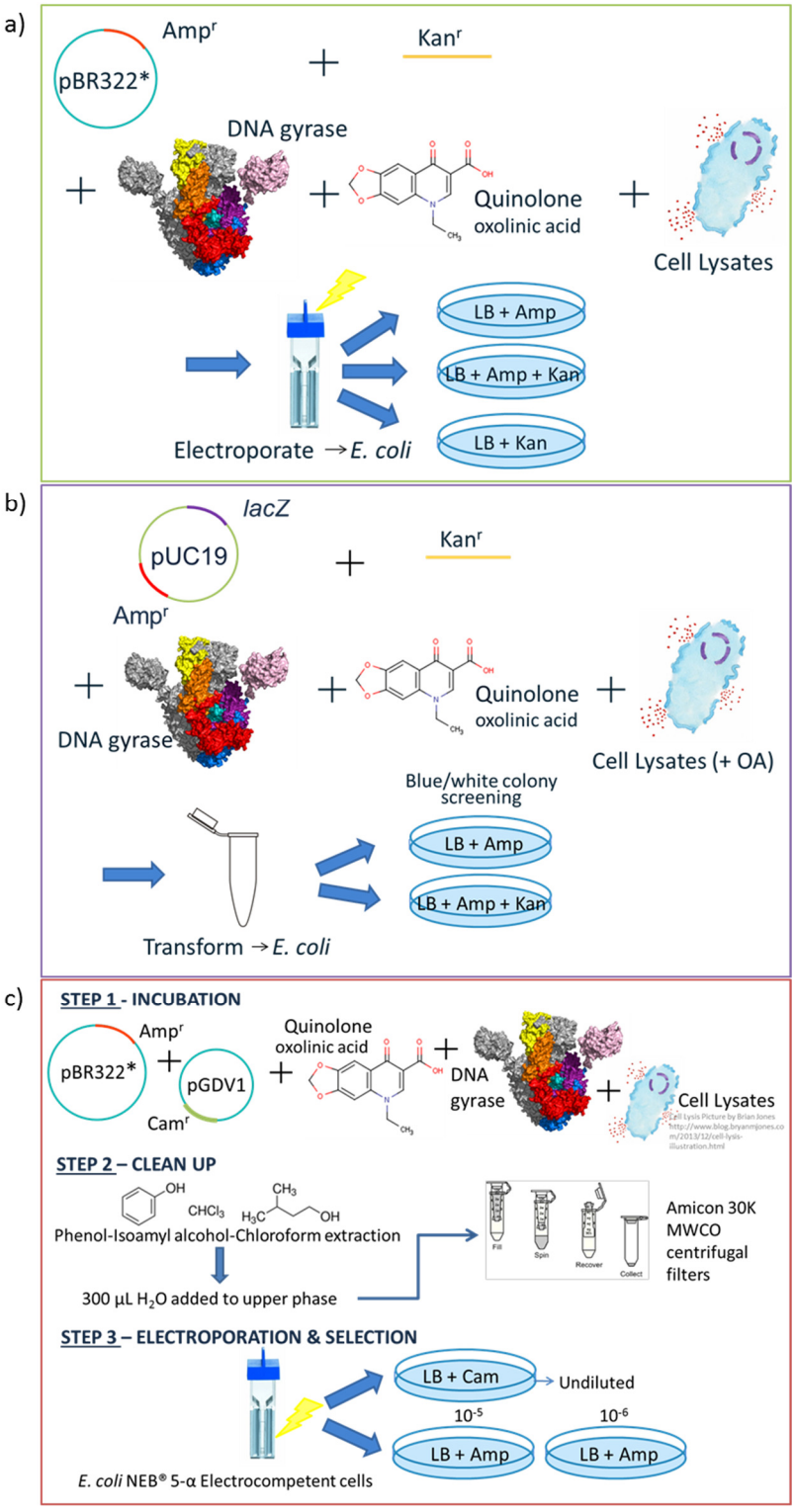

Figure 3.5: Diagram of various ways the non-λ assay was performed. a) Diagram of non-λ assay with pBR322* and the linear fragment containing the kanamycin resistance cassette. b) Diagram of non-λ assay with pUC19 and the linear fragment containing the kanamycin resistance cassette. c) Diagram of non-λ assay with pBR322* and the pGDV1 *B. subtilis* plasmid containing the chloramphenicol resistance cassette. Cell lysate image is used with permission from Brian Jones (http://www.blog.bryanmjones.com/2013/12/cell-lysis-illustration.html).

3.3 Results and discussion

λ-based assays

I tried to detect IR following a number of variations of the procedure outlined in Figure 3.3. These included using different packaging extracts, both commercially available and made by myself. I tried different λ-phage and various *E. coli* hosts, including high frequency lysogeny hosts and phage with different selectable markers. Despite these attempts and the fact that IR has been demonstrated in repeated publications of this assay (Kobayashi & Ikeda, 1977, Ikeda *et al.*, 1980, Ikeda *et al.*, 1982, Ikeda *et al.*, 1984, Naito *et al.*, 1984, Ikeda & Shiozaki, 1984), I have not been able to replicate the transfer of the Amp resistance to λ mediated by DNA gyrase. To date, I have seen one temperature-sensitive Amp-resistant transducing phage (Figure 3.6) which was found after incubation of the packaging extracts with λ *cI857 Sam7* DNA and relaxed pBR322* in the presence of ATP, however no exogenous DNA gyrase or OA was added to this assay. From Figure 3.6, the transductant is temperature sensitive (no growth on the 42°C plate) and it is resistant to Amp (likely to have come from pBR322*) and Tet (from the host LE392MP). The cause of this is not known and I have also not been able to repeat this result. The transduction of resistance by phage is not uncommon and other groups have shown recombination between pBR322 and λ-phage *in vivo* (Pogue-Geile *et al.*, 1980).

There are quite a few possible reasons why I have not been able to reproduce the work done previously. I will deal with these individually below, explaining how I tried to address these challenges.

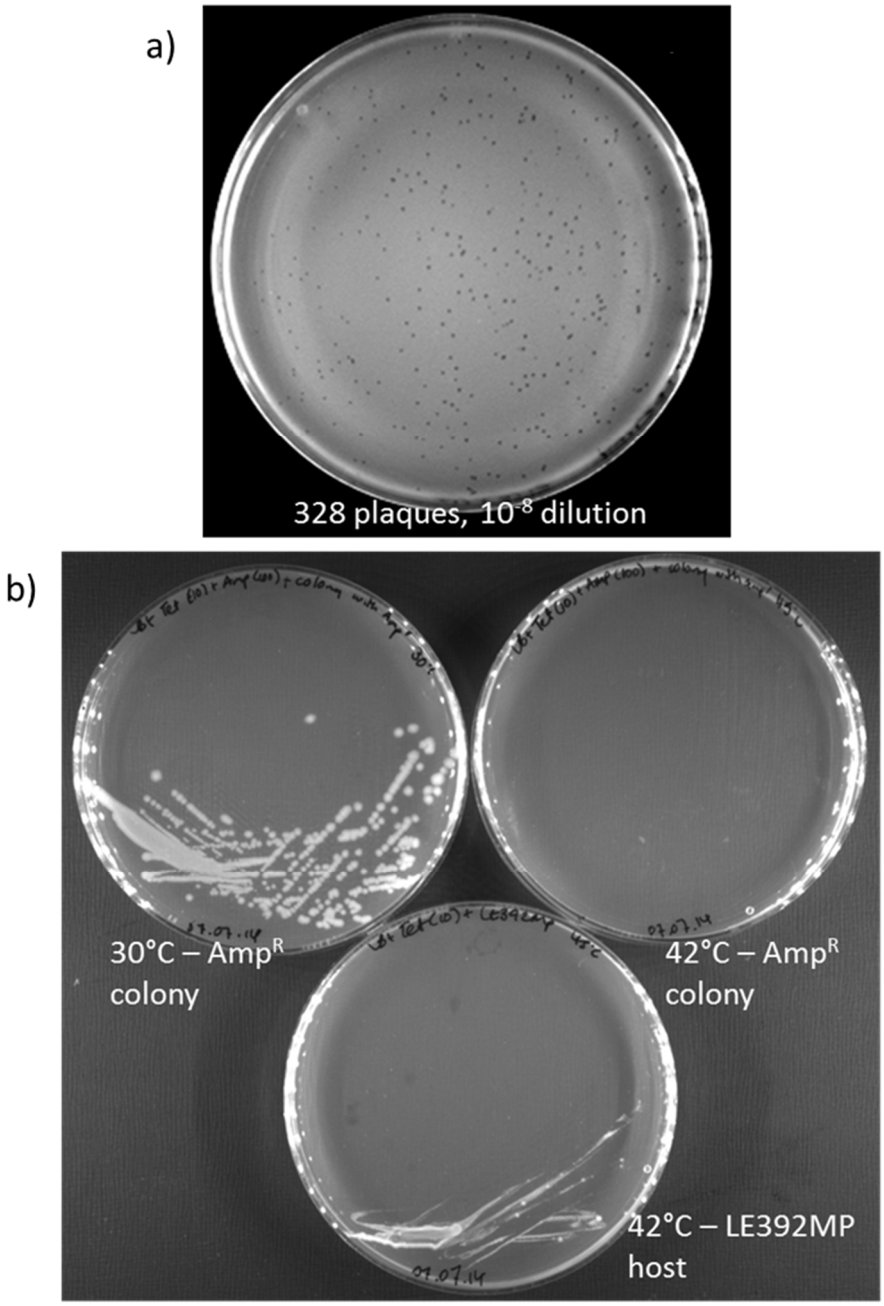

Figure 3.6: LB agar plates showing temperature-sensitive ampicillin transductants. a) Plate showing plaques from the assay containing the plasmid pBR322*, λ *cI*857 *S*am7 DNA and packaging extracts at a 10^{-8} dilution. b) shows the isolated ampicillin-resistant colony that was grown overnight in LB with tetracycline and ampicillin then restreaked on two plates, one was incubated at 30°C (top left) and the other at 42°C (top right). The bottom plate shows the host streaked on LB and tetracycline and incubated at 42°C. This shows that this is an ampicillin-resistant transductant of λ *cI*857 *S*am7 as it is resistant to tetracycline (from the LE392MP host), ampicillin (likely from the pBR322*) and is temperature-sensitive (from the phage).

Substrates, packaging extracts, and hosts.

To start with it was difficult to find the original *E. coli* host (Y-Mel – Table 2.1), λ strain (*E. coli* 594 lysogen) and packaging extracts from the initial publications (Kobayashi & Ikeda, 1977, Ikeda *et al.*, 1980, Ikeda *et al.*, 1982, Ikeda *et al.*, 1984, Naito *et al.*, 1984, Ikeda & Shiozaki, 1984). Thus, I tried to obtains hosts and strains for packaging extracts that were not too dissimilar from the original work. I did manage to find extracts used in other IR publications and tried those.

The first assay where the Amp transductants induced by the addition of OA were identified used packaging extracts made from *E. coli* lysogens 594 (λ *cI*857 *D*am15 $F_I$am19B *S*am7) and 594 (λ *cI*857 *E*am4 *S*am7) (Ikeda *et al.*, 1980, Ikeda *et al.*, 1982). These extracts work in the same way as the ones I used (BHB2688 and BHB2690) except the λ prophages were able to excise from the genomes upon induction, thus the concatemeric DNA was endogenous to the packaging extracts. In some of the later publications (Ikeda *et al.*, 1984, Naito *et al.*, 1984, Ikeda & Shiozaki, 1984), the lysogens were switched to similar lysogens carrying the *b*2 mutation which causes the prophage to be defective in excision (Gottesman & Yarmolinsky, 1968), meaning that there would be very little endogenous concatemeric DNA present in the packing extracts. In these cases, exogenous λ *cI*857 *S*am7 DNA that had been annealed to make concatemers was added to the assay along with the pBR322*. I was unfortunately unable to acquire these lysogens to make packaging extracts. I did not think this would be a problem as in later publications (Ikeda, 1986a, Ikeda, 1986b, Bae *et al.*, 1988, Saing *et al.*, 1988, Tomono *et al.*, 1989, Chiba *et al.*, 1989, Bae *et al.*, 1991, Kumagai & Ikeda, 1991, Shimizu *et al.*, 1995, Shimizu *et al.*, 1997, Shanado *et al.*, 1998, Ashizawa *et al.*, 1999) the BHB2688 and BHB2690 packaging extracts were used. Although, these assays were slightly different from the original assays (the formation of Spi^- phage instead of the formation of Amp transductants was used as a measure of IR - see Chapter 4) (Ikeda *et al.*, 1980, Ikeda *et al.*, 1982, Ikeda *et al.*, 1984, Naito *et al.*, 1984, Ikeda & Shiozaki, 1984), I thought that these packaging extracts should work. To try and make packaging extracts that more closely resembled the original protocol that identified the DNA gyrase-mediated IR (Ikeda *et al.*, 1980), I also used a helper phage to excise the prophages from the BHB2688

lysogens, however, this did not make a difference. The commercial MaxPlax™ packaging extracts use the BHB2688 lysogen and another lysogen NM759 (see Table 2.1) and seem to be prepared in a similar way to the Sambrook packaging extracts (Sambrook *et al.*, 1989).

I attempted to prepare packaging extracts following the protocol outlined in Kobayashi and Ikeda (1977), as all reported packaging extracts used in the DNA gyrase-mediated IR papers cited this method. These packaging extracts didn't yield plaques, however, on subsequent inspection of my protocol, I had not grown the lysogens sufficiently prior to induction due to a miscalculation on my part (the paper called for 1.5×10^8 cells, and I was using 3×10^7 cells). This factor of 5 difference in cell number, combined with my lack of experience with this protocol could explain why this protocol did not work in my hands. The importance of working with these extracts is that they are made with high percentages of DMSO. There is some suspicion that the topoisomerase-mediated IR may be an artefact of the assay and may be a result of the DMSO. DMSO has been shown to affect the efficiency of type II topoisomerases *in vitro* (Alison Howells (Inspiralis) and Thomas Germe (JIC) Personal Communication and personal observation) although the mechanism behind this is not known.

In order to remove the packaging extracts from the equation, I designed the λ-based *in vivo* assay. This involved transforming *E. coli* LE392MP with pBR322* and then infecting it with λ *cI*857 *S*am7 and selecting for lysogens (Figure 3.7). This lysogen carrying the pBR322* plasmid was then exposed to various amounts of OA, before the prophage was induced. The newly-made phage were separated from the bacterial lysates by centrifugation and used to infect an untransformed host. Ampicillin-resistant transducing phage were selected for but a number of false positives were obtained. The false positives were clustered in patches, seemingly where I had added the cultures for plating (Figure 3.8). None of the isolated colonies regrew on Amp. Upon discussion with other members in the lab, it was suggested that these were due to carryover of the beta lactamase produced by the pBR322* plasmid. This was confirmed when the strange Amp-resistant colonies disappeared when the phage were purified from the lysates

through a glycerol step gradient before infection. Ultimately, this assay requires further optimisation as no Amp-transducing phage were isolated. However, this also implied that the packaging extracts were not necessarily the primary problem.

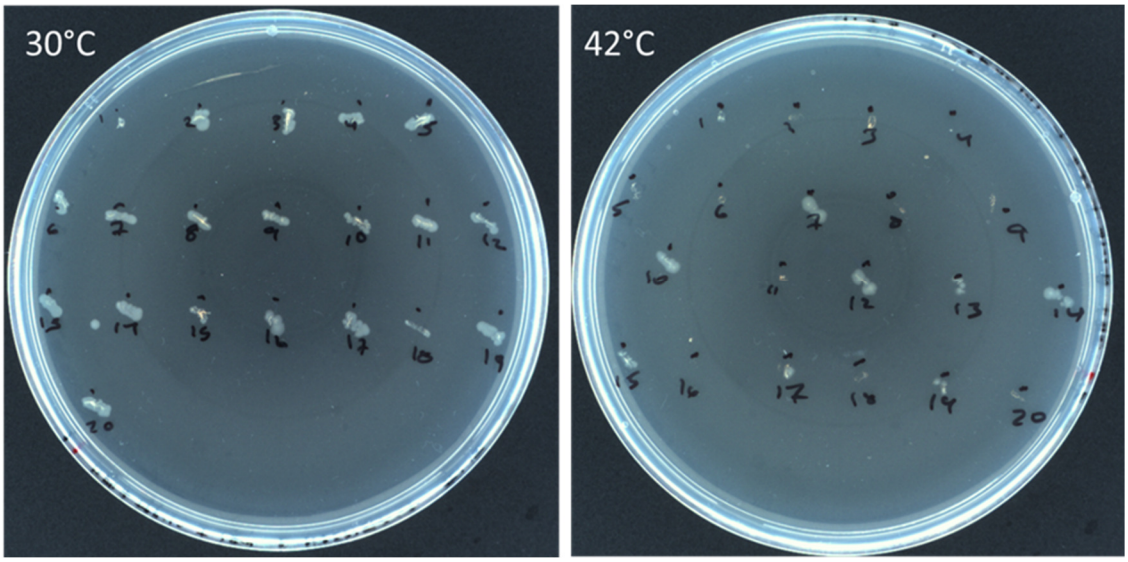

Figure 3.7: λ *cI*857 *S*am7 lysogens of LE392MP (pBR322*). An overnight culture of LE392MP (pBR322) was grown in λB supplemented with 10 mM $MgSO_4$, 0.2% maltose (w/v) and 100 µg/mL ampicillin. One hundred microlitres of this culture was mixed with λ cI857 Sam7 with a multiplicity of about 5. This was incubated for 15 min at 30°C then incubated with gentle shaking for a further hour at 30°C. Dilutions were then plated on λB (see General Methods) 1.2% agar with 100 µg/mL ampicillin at 30°C overnight. Twenty colonies were selected and each streaked on two λB 1.2% agar with 10 µg/mL tetracycline and 100 µg/mL ampicillin. One was incubated at 30°C and the other at 42°C. Colonies were selected based on those that grew at 30°C but not 42°C. Colony 5 was taken forward.

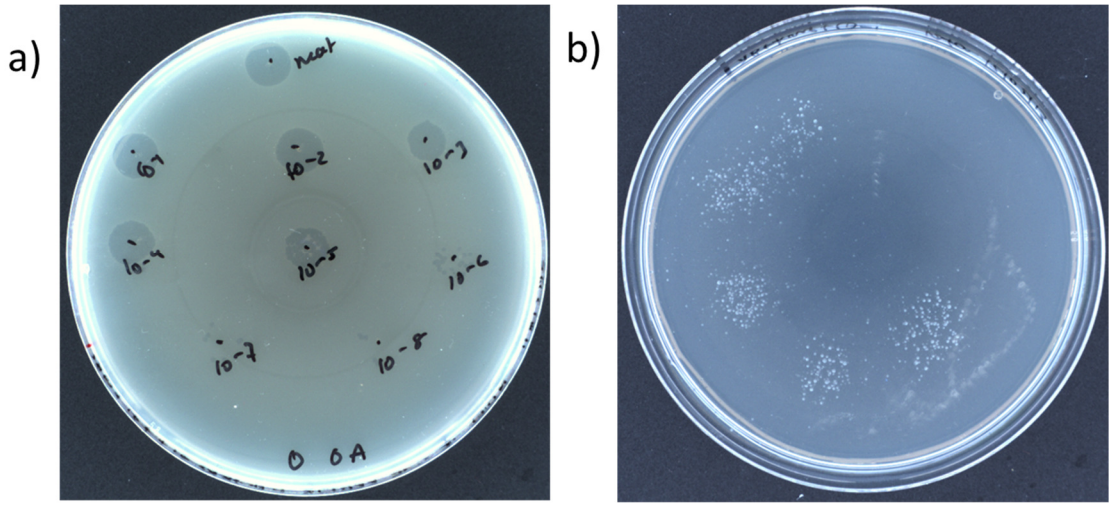

Figure 3.8: Ampicillin-resistant colonies from λ-based *in vivo* assay. a) spot titer and b) ampicillin-resistant colonies from no oxolinic acid (OA) sample from λ-based *in vivo* assay. LE392MP (λ *cI*857 *S*am7)(pBR322*) was incubated at 30°C with various concentrations of OA (including a no OA control) before induction at 42°C for 15 min. After induction, the cultures were incubated for 1 h at 38°C. One hundred microlitres of chloroform was added and briefly vortexed. The lysates were clarified by centrifugation at 10 000 g for 10 min and the supernatants were retained. a) 200 µL LE392MP, grown to OD_{600} of 1.0 in λB with 10 µg/mL tetracycline, 10 mM $MgSO_4$ and 0.2% (w/v) maltose, was added to molten λB 0.7% agar and poured over λB 1.2% agar + 10 µg/mL tetracycline and left to set. The clarified lysates were serially diluted (10^{-1} – 10^{-8}) and 5 µL of each dilution (plus an undiluted sample) was spotted onto the set plate and left to dry for 30 min. These were then incubated overnight at 42°C. The plate shown is the one from the no added OA control. The 10^{-6} spot contains 21 plaques. b) 100 µL of an overnight culture of LE392MP, grown in λB with 10 µg/mL tetracycline, 10 mM $MgSO_4$ and 0.2% (w/v) maltose, was added to 100 µL of phage lysate (MOI of between 2-3) and incubated for 15 min at 30°C. λB was added to 1 mL and the culture was incubated for a further hour at 30°C with shaking at 110 rpm. This was then diluted 1 in 10 and plated on λB 1.2% agar with 100 µg/mL ampicillin. The plate shown is the no added oxolinic acid control. The ampicillin-resistant colonies can be seen arranged in 5 groups.

I eventually found the *E. coli* Y-Mel strain from the Coli Genetic Stock Centre (CGSC) at Yale University, however, when I infected it with λ *cI*857 *S*am7, I didn't get any plaques. Unfortunately, I ran out of time to follow this up.

Another potential pitfall was the λ strain. The λ *cI*857 *S*am7 DNA was purchased from Sigma and is primarily sold to make DNA ladders. Thus, I am not sure that this strain is completely to type and is capable of all the expected phenotypes of the genotype. However, I am able to package the DNA which implies that it is the correct length, and the cos ends are intact. The packaged phage are able to form plaques on the appropriate host (*supF*), which suggests that the packaging proteins, capsid proteins and all proteins necessary for the lytic phase are functional. Furthermore, I have been able to identify lysogens that are temperature-sensitive and, upon induction, produce infective phage (from the *in vivo* assay) (Figures 3.7 and 3.8). This suggests that all the genes necessary for lysogeny and induction of prophage are functional. However, to address this separately, I also began setting up the assay to use the spectinomycin-resistant λ *lom::aadA* (Fogg *et al.*, 2010) (a gift from Heather Allison and Andy Bates at the University of Liverpool) (see Table 2.1), but I ran out of time to use it in the assays.

Concatemeric DNA

From discussions with Maggie Smith at York University, it seemed that concatemeric DNA was an important step in the assay. I had thought I was using concatemeric λ *cI*857 *S*am7 DNA as there was a large amount of DNA remaining in the well of the gel after electrophoresis (Figure 3.9a) however, when I switched to using the λ *lom::aadA* strain, I checked if I was making concatemers by digesting the newly annealed DNA with the restriction enzyme HindIII. If concatemeric DNA was being made, the band at about 4 Kb would be lost due to the annealing of the cos ends (Figure 3.9c). However, as seen in Figure 3.9b, there is no difference between the bands pre- and post- annealing and the banding pattern reflects that of the predicted banding pattern for the non-catemeric sample (left-hand side of Figure 3.9c). Unfortunately, I ran out of time to fully investigate this problem.

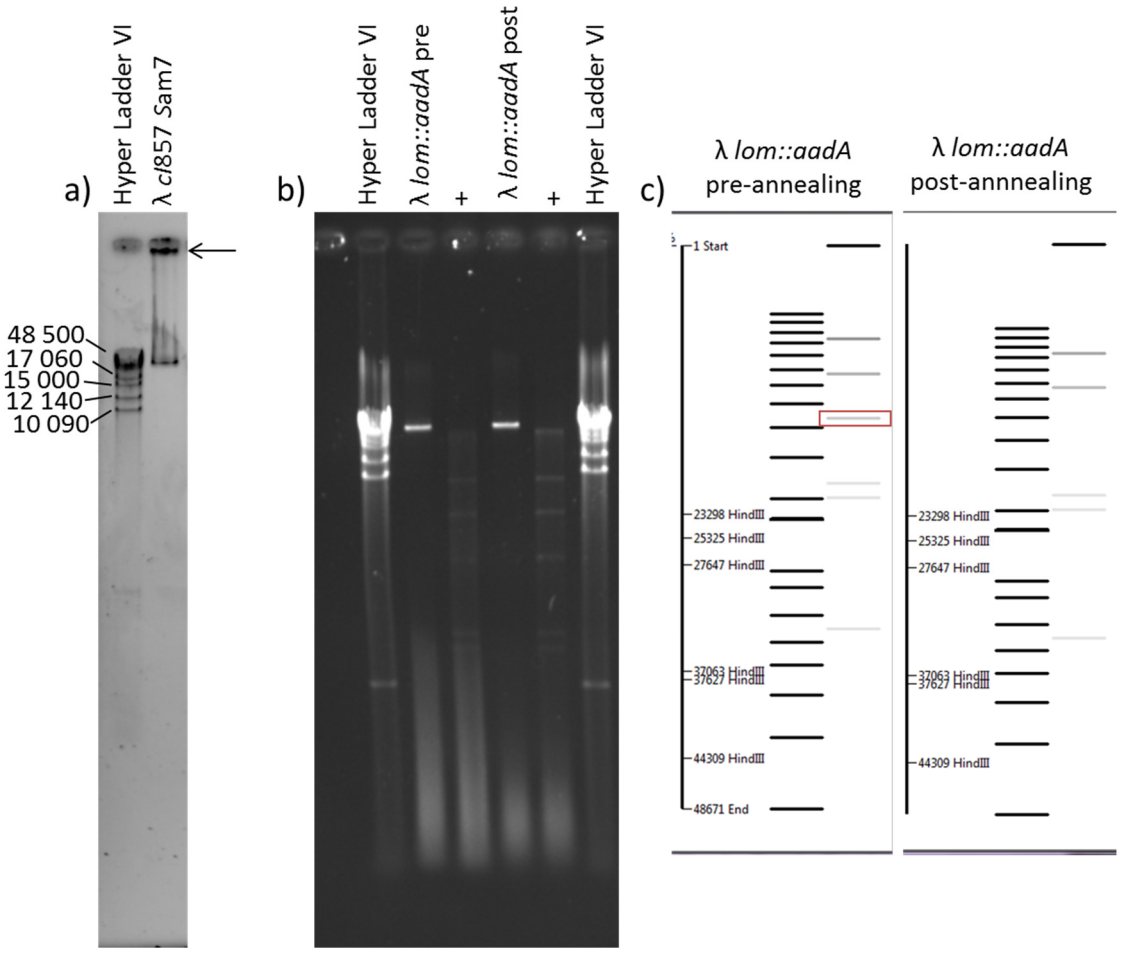

Figure 3.9: Concatemeric λ DNA. a) 0.7% agarose gel of λ *cI*857 *S*am7 DNA post annealing. Arrow indicates large amount of remaining in the well. b) HindIII digest (+) of λ lom::aadA genome pre (λ *lom::aadA* pre) and post (λ *lom::aadA* post) annealing. c) is a predicted band pattern of the linear λ *lom::aadA* (left-hand side) and the predicted band pattern of the circular/concatemeric λ *lom::aadA* (right-hand side), the red box indicates the band at around 4 Kb, which is not visible on the predicted concatemeric sample. On the gel the lower band can't be seen. Predicted banding pattern was produced on ApE 2.0.47, a plasmid editor by M. Wayne Davis, Utah University. Hyper ladder VI is best used for PFGE and the upper band runs at around 48 Kb. The sizes of the visible bands are indicated down the left-hand side of a).

Lysogeny

As well as the concatemeric DNA, in discussions with Maggie Smith at York University, the importance of the frequency of lysogeny also became apparent. The ability to see the Amp transductants relies on enough lysogens being formed to reveal them. I was expecting to see

recombination rates of around 10^{-7} Amp transductants per PFU (Ikeda *et al.*, 1980). This meant that I needed to have 10^7 lysogens to see one transductant. Although I was making lysogens (Figure 3.7), I was seeing at most 65% lysogeny at worst it was 5%, this would translate to about 10^8 colony forming units (CFU)/mL. Although this rate should have revealed transductants, I still was not seeing any. The number of lysogens was also not constant across assays. In order to improve my protocols to ensure I was getting a high enough and consistent number of lysogens, I switched to the λ *lom::aadA* phage. This spectinomycin-resistant phage provides a better selectable marker than the temperature-sensitive repressor. I also found a strain of *E. coli* MA156 (Table 2.1) that carries the *hfl* mutations which stands for high frequency of lysogeny. Lambda forms lysogens at a high frequency (99% lysogeny) in this host as the mutations cause an accumulation of cII, which selects for lysogeny (Wullff & Rosenberg, 1983). Unfortunately, I ran out of time to test this host in the assay.

Ultimately, alongside the issues outlined above, my lack of experience of working with λ likely contributed to the lack of outcomes where this part of my project was concerned. Despite this, I still think that the λ-based assays should be reproducible and given more time, I would have been able to overcome the challenges associated with the assays.

Non-λ assay

This assay has not been published before and was originally designed by Richard Bowater (UEA) and Tony Maxwell (JIC). Figure 3.5a shows the first iteration of this assay, where a linear 900 bp double-stranded PCR product from pACYC177 was incubated with pBR322*. Here I was looking for the transfer of the Kan resistance into pBR322*. I tested these DNA substrates with and without DNA gyrase, ATP (which is in the supercoiling assay buffer), cell extracts (from *E. coli* MG1655) and OA. With this assay, I found a higher than expected number of Kan resistant and Amp and Kan resistant colonies. When I tested just the Kan PCR product with and without the various other components, the resistance, including the Amp resistance, remained (Table 3.1). Unfortunately, I discovered that the PCR product still contained the parental plasmid in it,

which gave false positives as the pACYC177 plasmid carries both an Amp-resistance cassette and a Kan resistance cassette. I tried to gel extract the fragment but unfortunately this did not yield enough DNA to run the experiment. I was also concerned that the 100 bp flanking region was not sufficient to allow DNA gyrase to bind and potentially mediate exchange the whole Kan cassette from within those 100 bp regions. Especially considering the footprint of DNA gyrase on DNA was found to be about 120 bp (Fisher *et al.*, 1981, Rau *et al.*, 1987, Kirkegaard & Wang, 1981, Morrison & Cozzarelli, 1981, Orphanides & Maxwell, 1994). I designed two sets of primers; one set to make the flanking regions 200 bp and the other to make the flanking regions 400 bp. This, however, would not solve the pACYC177 contamination issue. To overcome this issue, I decided to gel extract the PCR fragment then reamplify the fragment with the original primers. The 400 bp fragment would never reamplify after gel extraction but this solved the contamination issue. However, I still did not observe any recombinants.

Table 3.1: Number of colonies that were ampicillin resistant, kanamycin resistant or both after transformation with 900 bp Kan PCR product.

	Number of colonies			
Sample	**No drug**	**Amp (100 µg/mL)**	**Amp (100 µg/mL) + Kan (50 µg/mL)**	**Kan (50 µg/mL)**
No DNA	Millions	0	0	0
pUC19	n.d.	30	0	0
K-PCR only	n.d.	296	0	2
K-PCR + ScAB	n.d.	18	0	2
K-PCR + RxAB	n.d.	>500	0	0
K-PCR + ScAB + DNA gyrase	n.d.	210	0	3
K-PCR + RxAB + DNA gyrase	n.d.	42	0	6
K-PCR + ScAB + DNA gyrase + OA	n.d.	10	0	7
K-PCR + RxAB + DNA gyrase + OA	n.d.	0	1	1

K-PCR + ScAB + DNA gyrase + CE	n.d.	140	0	4
K-PCR + RxAB + DNA gyrase + CE	n.d.	54	0	5
K-PCR + ScAB + DNA gyrase + OA + CE	n.d.	1	0	8
K-PCR + RxAB + DNA gyrase + OA + CE	n.d.	48	0	8

K-PCR is the 900 bp Kan PCR product from pACYC177; ScAB is supercoiling assay buffer; RxAB is relaxation assay buffer; OA is oxolinic acid; CE is crude cell extracts from *E. coli* MG1655; K-PCR is the *kan*^{r} gene PCR product. n.d. is not done

In order to increase the chance of seeing a recombination event, I decided to switch to looking for the disruption of a gene, instead of the transfer of a resistance cassette. This resulted in the second iteration of this assay (Figure 3.5b) where pUC19 (Figure 3.10a) containing the *lacZ* gene was incubated with the 1200 bp Kan fragment (with the 200 bp flanking regions). The idea was to use blue/white colony screening to look for disruption of the *lacZ* gene. Initially, I still had contamination with pACYC177, however, I managed to get rid of the contamination and got a white colony from a sample that had DNA gyrase, topoisomerase IV, ATP, pUC19, the Kan fragment and 0.1 μg/mL OA. We sent this plasmid for primer walking at Eurofins Genomics with the initial primer starting from within the pUC19 Amp-resistance gene cassette (Table 2.3). The sequence showed that this colony was a result of a recombination event in the pUC19 plasmid, that interrupted the *lacZ* gene, however, it was not a result of topoisomerase-mediated IR but was a DDE transposase (Figure 3.10b). The insert has separated the lac operator from *lacZ* and is stopping the production of β-galactosidase.

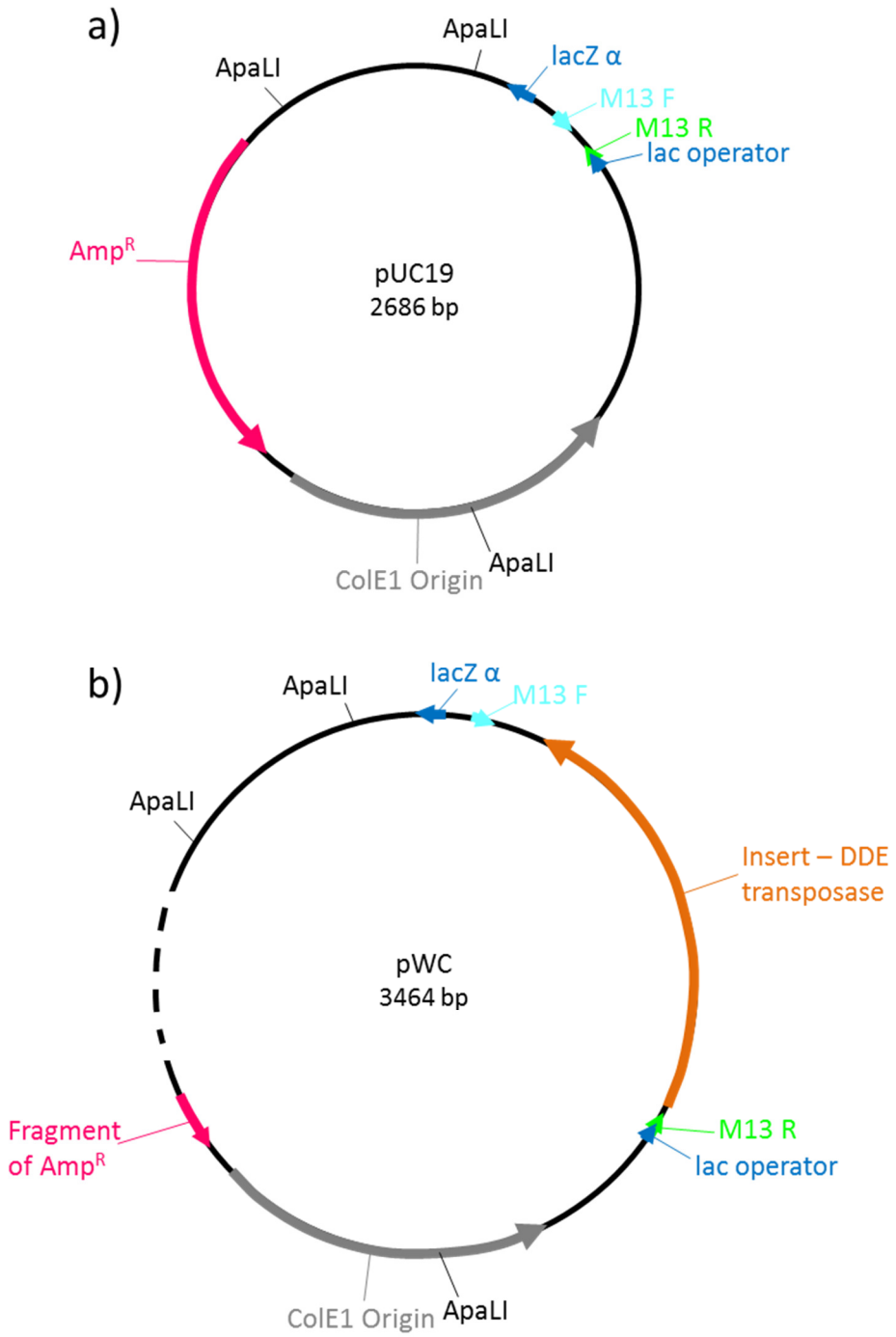

Figure 3.10: Maps of pUC19 and the plasmid from the isolated white colony. a) Plasmid map of pUC19 showing the relative positions of the ColE1 origin (grey), the Ampicillin-resistance cassette (Amp^R in pink), the *lacZ* gene with its operator (Blue), the position of the M13 primer binding site (turquoise and green) and the position of the three ApaLI restriction sites. b) is the plasmid isolated from the white colony with matching features seen in a) except the DDE transposase insert is shown in orange. The Amp^R cassette was not fully sequenced as the primer walking started from within the Amp^R cassette. The dotted lines indicate the area that was not sequenced but is thought to contain the rest of the Amp^R cassette.

I decided at this point to redesign the assay again. As attempts to make a longer (>1200 bp) linear DNA fragment had failed, I designed a fragment (Cam fragment) that was 1896 bp long (Table 2.2 and Appendix I), which contained the chloramphenicol resistance (Cam) cassette as well as two strong-gyrase binding sites (SGS) (one from Mu phage (Pato, 1994), the other from pBR322 (Lockshon & Morris, 1985). The strong-gyrase binding site was identified by fragmentation and sodium dodecyl sulphate (SDS) trapping of the plasmid pBR322 in OA-treated *E. coli*. The SGS was identified by Lockshon and Morris (Lockshon & Morris, 1985) and was identified as: 5' RNNNRNR(T/G)↓GRYC(T/G)YNYN(G/T)NY 3' when averaged across 19 identified sites. N represents any nucleotide, R is a purine, and Y is a pyrimidine. The arrow represents the cutting site. Subsequent investigations have surmised that DNA gyrase cleavage specificity does not always adhere to this sequence (Cove *et al.*, 1997) but alteration of the SGS has been shown to reduce DNA binding by DNA gyrase (Oram *et al.*, 2006). The Cam fragment was fabricated as a linear DNA fragment which could be amplified by PCR. Alongside the Cam fragment, I designed and had fabricated a plasmid with the linear fragment and the pSC101 temperature-sensitive origin (pIR, Appendix I) using GeneArt's plasmid constructor. I also had a MiniCircle made by Twister Biotech (Appendix I) with the same features. This would give two different types of substrate to use in the assay (linear and circular). One with a temperature-sensitive origin and the others without replicons, which mean they cannot replicate in *E. coli*. I also decided to alter my protocol to ensure that I was getting high enough transformation efficiencies to see all potential recombination events. I did this by cleaning up the DNA with phenol-chloroform before buffer exchanging to get rid of any salts and electroporating into high efficiency electrocompetent *E. coli* (Figure 3.5).

The work done with the Cam fragment was completed with the help of an undergraduate Lister summer student, Shannon McKie, who spent 10 weeks working on this assay. Despite removing the pACYC177 from the equation, we still had problems with false positives in this

assay including contamination with two other plasmids. The assay is very sensitive due to the high efficiency of the electrocompetent *E. coli* NEB 5α (> 10^{10} CFU/μg of pUC19) and it picks up contaminating plasmids very easily. The other plasmids were identified as pLysS and pIR (Figure 3.11a and b) (see Appendix I). From Figure 3.11, the digestion patterns from separate plasmids from three Cam-resistant colonies appears to be similar to those of the contaminating plasmids shown in Figure 3.11a. The second plasmid in Figure 3.11b also appears to have a second plasmid present, which is evident by the extra larger DNA bands seen in lane 3 as opposed to the lane 3 of the pBR322* sample seen in Figure 3.11a. The pIR was believed to have been a cross contaminant picked up during DNA quantification. The pLysS was presumed to be a contaminant from the *E. coli* expression host that was used in the expression of the DNA gyrase subunits. It did not appear in every sample containing DNA gyrase but the only source of this plasmid in the lab comes from the expression host JM109 pLysS, in which the subunits of DNA gyrase are expressed.

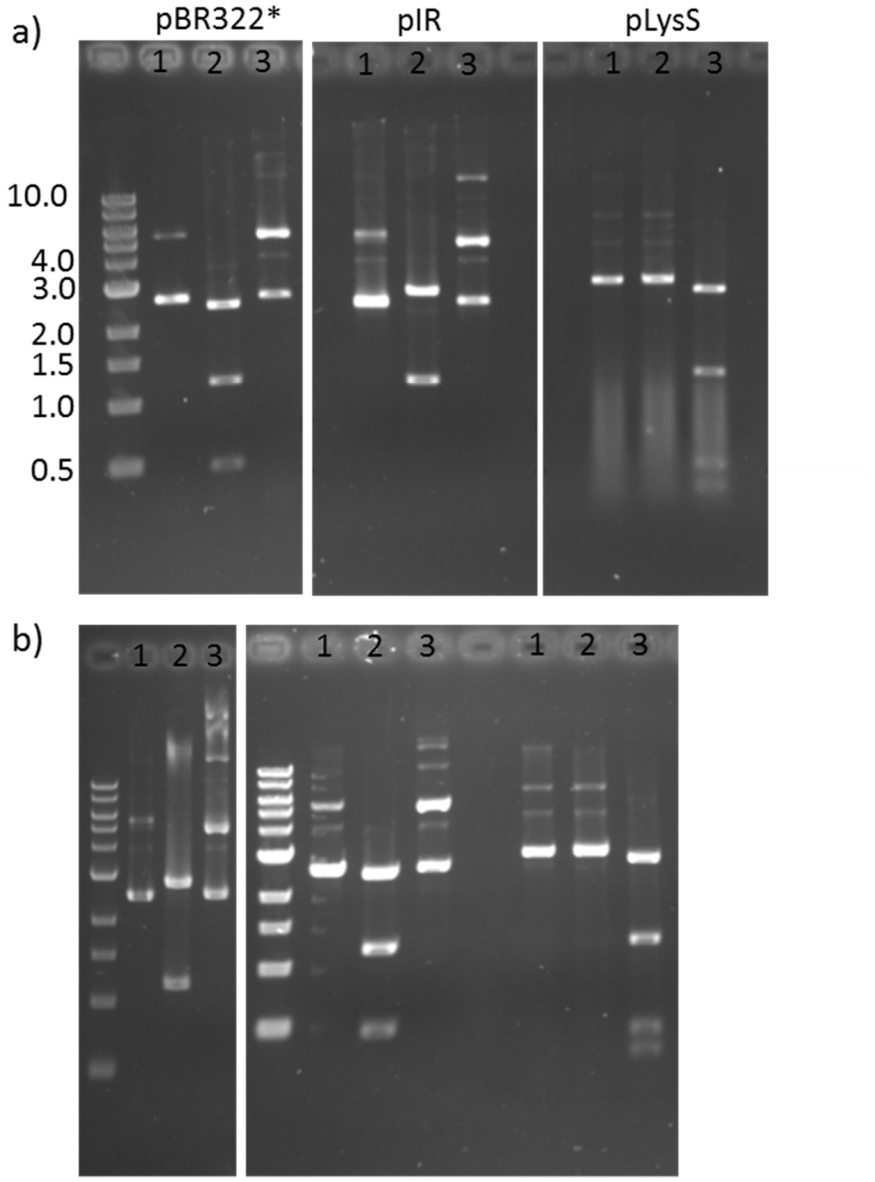

Figure 3.11: Restriction digests of chloramphenicol-resistant plasmids. a) ApaLI (2) and AgeI (3) digests of the parental plasmid pBR322* and two potential contaminating plasmids pIR and pLysS. Undigested plasmid is 1. b) Representative ApaLI and AgeI digests of plasmids isolated from 3 separate chloramphenicol-resistant colonies from non-λ assay. A 1 Kb (NEB) ladder was used with the sizes of the bands in Kb indicated on the left-hand side of a). All samples were resolved on a 1% agarose gel at 90 V for 2 h.

The MiniCircle proved to be unfeasible in the assay as well because of contamination. These MiniCircles are made by using λ recombinase to excise the MiniCircle from a larger plasmid (Fogg *et al.*, 2006). This larger plasmid has a functional replication origin and when we added the

MiniCircle to the assay we got a large number of Cam-resistant colonies. We could not see the larger plasmid on a 1% agarose gel prior to electroporation, but when we extracted the plasmid from one of the Cam-resistant colonies there was a very large plasmid of over 10 Kb (Figure 3.12). We presumed this was the parent plasmid as there was no other source of a plasmid of that size carrying Cam resistance, and it is bigger than a potential fusion between pBR322* and the MiniCircle (this would be ~ 6000 bp).

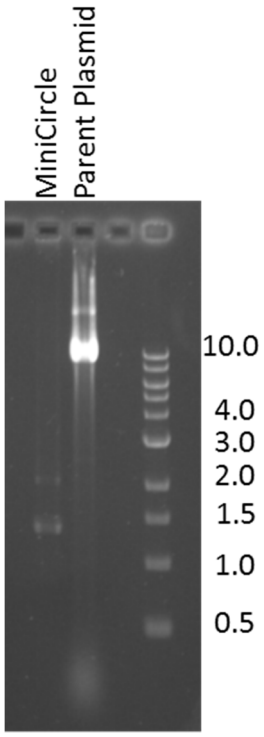

Figure 3.12: Contamination by MiniCircle parent plasmid. MiniCircle (lane 1) and suspected parental plasmid (lane 2). A 1 Kb (NEB) ladder was used with the sizes of the bands in Kb indicated on the left-hand side of a) and d). All samples were resolved on a 1% agarose gel at 90 V for 2 h.

The other source of false positives were double transformants. The high efficiency of the electrocompetent cells allowed for more than one plasmid to be transformed (Figure 3.13, also see Figure 3.11). From Figure 3.11 and 3.13, two plasmids are visible in the uncut lanes (numbered 1). The pBR322* plasmid is a high-copy number plasmid whereas, pLysS is a low copy number plasmid and this is reflected in the relative amounts of each plasmid present on the

agarose gel. This added to the confusion by making the Cam-resistant colonies resistant to Amp as well.

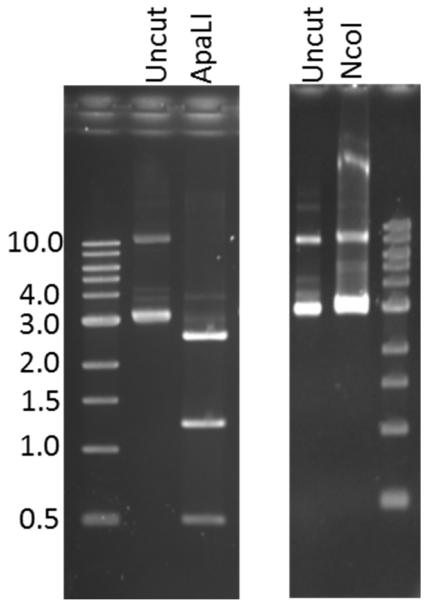

Figure 3.13: Representative ApaLI (left-hand side) and NcoI (4 – right-hand side) digests of a plasmid isolated from a chloramphenicol-resistant colony that also showed ampicillin resistance as a result of cotransformations of pBR322* and pLysS from non-λ assay. A 1 Kb (NEB) ladder was used with the sizes of the bands in Kb indicated on the left-hand side of a) and d). All samples were resolved on a 1% agarose gel at 90 V for 2 h.

A further problem experienced in all iterations of the assay was much lower transformation efficiencies in samples treated with cell extracts. The cell extracts were added to try and identify/provide the extra factor that is needed in DNA gyrase-mediated IR. Previous work indicated that DNA gyrase could not mediate IR alone and some other factor from the packaging extracts was needed for the recombination to occur (Ikeda & Shiozaki, 1984). It is likely to be a factor that is produced during the SOS response which often induced upon phage induction (Greer, 1975, Campoy *et al.*, 2006). A consequence of this is a lower probability of seeing any recombination events and is possibly a result of endonucleases in the cell extracts (Figure 3.12). To ameliorate this problem, I selected DH5α (Table 2.1), an *E. coli* strain that is *endA* (endonuclease-deficient, often used in cloning strains) to make the cell extracts. However, this

strain also has mutations in *gyrA* and *recA* which means that it is resistant to OA. For that reason, I switched to using *E. coli* MM293 which are wild type for *gyrA* and *recA* but are have an endonuclease mutation. With these cell extracts I maintained the same or similar transformation efficiencies in all samples.

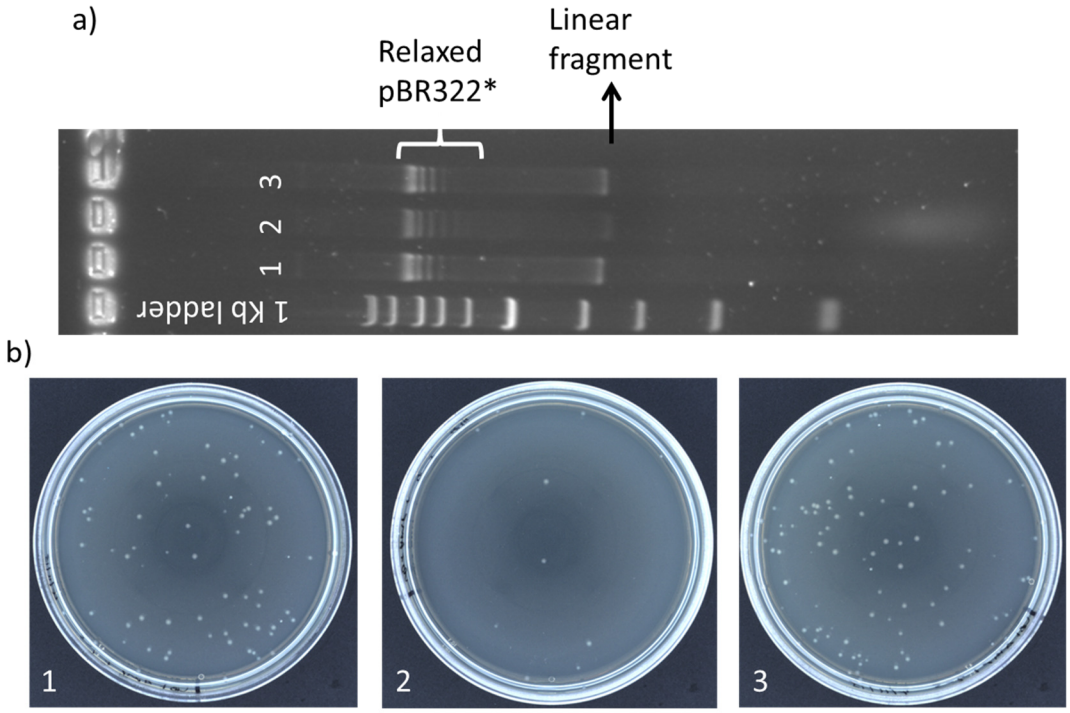

Figure 3.14: Effect of endonuclease-competent strain on transformation efficiencies. a) 1% agarose gel showing the DNA after concentrating with the Amicon concentrators, before electroporation from 3 assays, 1 and 3 have no cell extracts added, 2 has cell extracts from *E. coli* MG1655 added. Although, all started with the same initial amount of DNA, sample 2 had the cell extracts added and seems to have less DNA present b) is the resulting number of Amp-resistant colonies all diluted 10^{-5} from the transformations with the DNA from a). 2 clearly has fewer colonies present.

Whilst preparing the pIR plasmid for use in the assay, a *Bacillus subtilis* plasmid (pGV1) that is not capable of replicating in *E. coli* was brought to my attention (Table 2.2, Appendix I) (Sarkar *et al.*, 1997). This plasmid also carries a Cam-resistance gene and had been used in a similar

assay before with no false positives (Dr. Abhimanyu Sarkar JIC, personal communication, 2015). This substrate would likely be a better option than pIR due to the incompatibility of pGDV1 with *E. coli* and would help solve the problem of cotransformants. In all of the original (λ-based) work done on topoisomerase-mediated IR, the substrates used were all greater than 4 Kb, not linear and were likely to have some degree of supercoiling (Bae *et al.*, 1988, Ikeda, 1986a, Ikeda, 1986b, Ikeda *et al.*, 1984, Ikeda *et al.*, 1980, Ikeda & Shiozaki, 1984). To this effect, I believed a circular substrate would be a much more likely substrate to see recombination with. Hence, the investment in the pIR plasmid and the MiniCircle. Thus, the last iteration of this assay was run with pGDV1 as a substrate. These assays gave colonies that were resistant to Cam and both Cam and Amp but had no contamination with pIR, however there was still some very minor contamination with pLysS. There was no pGDV1 visible. Samples that came from the assay run with supercoiled pBR322*, pGDV1, ATP, OA and DNA gyrase yielded colonies that were Amp and Cam resistant but the plasmid present did not resemble pBR322* or any of the contaminants. Unfortunately, I did not have time to continue working on this assay but Monica Agarwal (JIC) has continued this work and she has found colonies that confer Amp and Cam resistance. When she extracts the plasmids, she does seem to see more than one plasmid present in the sample. To resolve this, she has gel extracted specific bands from the gel and transformed those in to *E. coli*. These gel-extracted plasmids still confer Cam resistance. However, primers designed from the pGDV1 Cam-resistance gene, do not form a product with these plasmids. Neither do primers from within the Amp-resistance gene of pBR322*. One of these plasmids was been sent for sequencing with a primer walking service from Eurofins. Preliminary data suggests that it is possibly pLysS.

The non-λ assay has been plagued with contamination issues and has had a big problem with false positives. Although Monica's work has yielded some unexplained results, the potential problem of cotransformation could be a significant issue with this assay. If a recombination event does occur, it may be contransformed with other plasmids that are wild type or with a

range of plasmids that all have different recombination events. These may be, at best, difficult to disentangle. Equally, it is important to use high efficiency competent cells to ensure that transformation efficiencies are high enough to see prospective transformants (potentially around 10^{-7} recombinants per CFU) (Ikeda *et al.*, 1980). This is one way that the λ-based assays are in theory advantageous as there is certainty that any transfer of resistance is due to infection with a single phage unit. This is due to the immunity against superinfection by other λ phage (Kaiser, 1957) and the fact that λ phage can only package between 78% – 105% of its genome length (Feiss *et al.*, 1977).

3.4 Conclusions

These assays have unfortunately not been fruitful in the investigation of topoisomerase-mediated IR. The λ-based work has proven more difficult to replicate than originally anticipated and the non-λ based assays have been optimised to a point where we may be observing IR, but these events are proving difficult to disentangle.

λ-based assay

With the difficulties reproducing the λ-based assay, the legitimacy of the work has come in to question, however, due to the extensive publications on this subject (Asami *et al.*, 2002, Ashizawa *et al.*, 1999, Bae *et al.*, 1991, Bae *et al.*, 1988, Chiba *et al.*, 1989, Ikeda, 1986a, Ikeda, 1994, Ikeda, 1986b, Ikeda *et al.*, 1982, Ikeda *et al.*, 1984, Ikeda *et al.*, 1980, Ikeda *et al.*, 1995, Ikeda & Shiozaki, 1984, Kato & Ikeda, 1996, Kobayashi & Ikeda, 1977, Kumagai & Ikeda, 1991, Miura-Masuda & Ikeda, 1990, Naito *et al.*, 1984, Sabourin *et al.*, 2003, Saing *et al.*, 1988, Shanado *et al.*, 1998, Shimizu *et al.*, 1997, Shimizu *et al.*, 1995, Tomono *et al.*, 1989) as well as many collaborations with external laboratories (Bae *et al.*, 1988, Ikeda *et al.*, 1984, Sabourin *et al.*, 2003), I doubt that it is a fabrication. It may possibly be an artefact due to the high amount of DMSO present in the packaging extracts but further work is necessary to investigate this as

there is currently no experimental evidence to support this. There are also still many lines of enquiry that have not been fully resolved to explain why this assay has not been reproducible, such as the concatemeric DNA and consistent levels of lysogeny.

non-λ assay

The non-λ assay, although theoretically sound, has proven to be difficult to optimise, mostly due to the sensitivity of the assay. Despite there being no scientific record of this assay working, with some further optimisations, it may still work. The biggest problem I see is the potential for cotransformants. The best way to deal with this would be to use a mini-F' plasmid or something similar where only one plasmid is present in the cell due to compatibility (see Chapter 4). Thomas Germe (JIC) is working on a suicide substrate where only an IR event would result in a plasmid that would not kill the cell. This however, has not been tested yet, but could, in theory, solve this problem.

Unfortunately, time required me to put both the λ and non-λ assays to one side to focus on other assays that were producing more promising results. However, I do feel that given enough time, the challenges that have been described for these assays would be overcome. Particularly where the λ assay is concerned.

3.5 Future work

λ-based assay

I would like to continue trying to reproduce this assay. First, I would resolve the issues around making concatemeric DNA, then I would like to optimise a method which would result in a consistent number of lysogens being produced per infection. Thirdly, I would investigate why the λ phage did not produce plaques in the *E. coli* Y-Mel host. I would also work on recreating the packaging extracts using the method outlined by Kobayashi and Ikeda (Kobayashi

& Ikeda, 1977). Once all of these issues were addressed (and hopefully resolved), I would then reattempt to run the assay again.

non-λ assay

With this assay, I may try and redesign the assay with a mini-F' plasmid, which is a low copy number plasmid (1 or 2 per cell) (Kato & Ikeda, 1996). I would incubate this with the pGDV1 plasmid and look for recombinants. I would also purify DNA gyrase subunits from a non-pLysS strain to eliminate this as a source of false positives. This assay has become a collaborative endeavour between myself, Monica Agarwal (JIC) and Thomas Germe (JIC) and between us, a non-λ, *in vitro* assay could be optimised to study topoisomerase-mediated IR.

Chapter 4: DNA Gyrase Hyper-Recombination Mutants

4.1 Introduction

Mutations in GyrA have been found that increase the frequency of illegitimate recombination (Ashizawa *et al.*, 1999, Shimizu *et al.*, 1997). These mutations caused the aberrant excision of the λ prophage in the presence of the mutagenized *gyrA* gene. They were identified using a plasmid shuffling method developed by Kato and Ikeda (1996). This method uses mini-F plasmids, which are low copy number plasmids (1 – 2 copies per cell) that, due to their stringent copy number control, allows for one mini-F plasmid to easily be replaced by another carrying a different selection marker. In this instance, the gene of interest, *gyrA*, was disrupted in the presence of a mini-F plasmid carrying a functional wild-type gene. The disruptant is then transformed with another mini-F plasmid that carries a mutated *gyrA* gene and a different selection marker (Figure 4.1).

Shimizu *et al.* (1997) mutagenized the *gyrA* gene by PCR in the presence of Mn^{2+} before ligating the product into a mini-F plasmid carrying ampicillin resistance (Amp^R). From 10 000 Amp^R transductants, 130 temperature-sensitive colonies were isolated and the corresponding mini-F plasmid was transformed into a strain with the disrupted *gyrA* gene and carrying a λ *cI*857 lysogen. These were then tested for their ability to induce spontaneous illegitimate recombination by the formation of λ *bio* transductants (Figure 4.1). These transductants were identified by their capacity to form plaques on *E. coli* P2 lysogens (Spi^- phenotype) (Shimizu *et al.*, 1997, Ashizawa *et al.*, 1999).

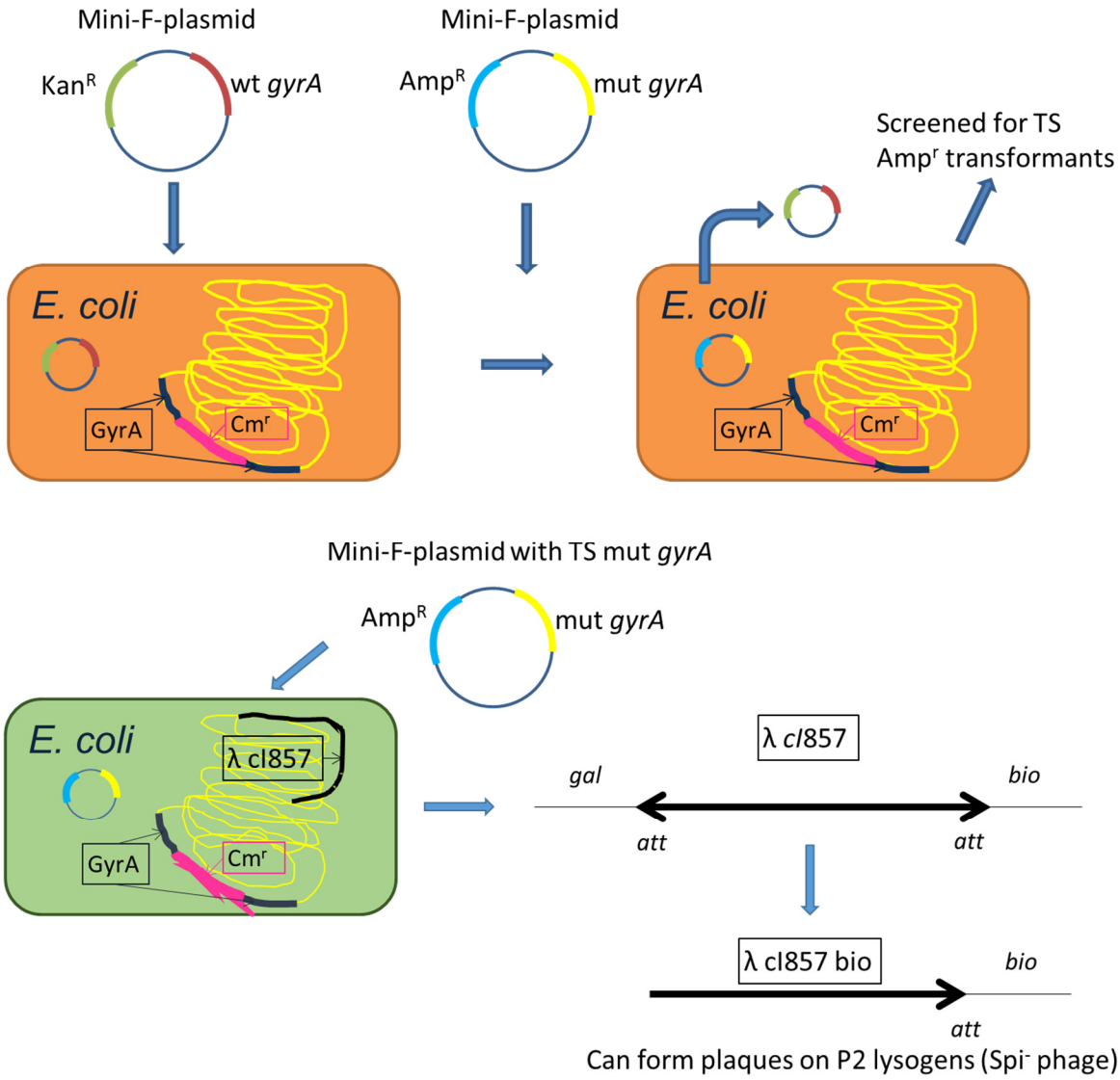

Figure 4.1: **Diagram showing plasmid shuffling system set up by Kato and Ikeda. Briefly, the wild-type *gyrA* gene is disrupted by a chloramphenicol resistance cassette in the presence of a mini-F plasmid carrying a functional wild-type gene. A mini-F plasmid containing a mutagenized *gyrA* gene and an ampicillin-resistance (Amp^R) cassette is transformed into the disruptant (*gyrA::*Cm^R) (orange *E. coli*) and temperature-sensitive Amp^R transductants are selected. The associated mini-F plasmid is then transformed into a λ *cI*857 lysogen with the disrupted *gyrA* gene (green *E. coli*). Illegitimate recombination is measured by the number of λ *cI*857 *bio* transductants that are formed. These transductants have the Spi$^-$ phenotype meaning they can form plaques on *E. coli* P2 lysogens. The black lines indicate the position of the λ *cI*857 on the *E. coli* genome, flanked by the *gal* and *bio* genes. *att* indicates the *att* sites where the λ genome integrates into the *E. coli* genome.**

Occasionally during induction of the lytic phase of the λ life cycle (described in the introduction to Chapter 3), aberrant excision of the prophage can result in specialised transducing phage (Campbell, 1971). This is a type of illegitimate recombination where a portion of the *E. coli* genome is excised along with the λ genome whilst a portion of the λ genome remains in the chromosome. The resulting phage must be able to be packaged into the λ head (it must be a suitable length for packaging to occur) and the cos ends must be maintained (Franklin, 1971). This generally results in the transduction of either the *E. coli gal* or *bio* genes. The concomitant loss in the λ genome with *bio* transductants includes red^-, γ^- and δ^- genes and the lack of these genes enables the λ *bio* transductants to form plaques on P2 lysogens (Zissler *et al.*, 1971). This was also shown to be stimulated by oxolinic acid treatment (Tomono *et al.*, 1989).

Of the 130 temperature-sensitive colonies that were identified, five showed an increase in temperature-induced formation of *bio* transducing phage at frequencies of 74, 53, 30, 30 and 28-fold over wild type. These were GyrA D216G, L492P, L488P, N165S/P215L and I203V/I205V respectively (Ashizawa *et al.*, 1999). However, when these mutations were introduced into mini-F Amp^R plasmids by PCR and transformed into *E. coli* HI2487 *gyrA*::Cmr λ *cI857* only three showed an increase in the frequency of spontaneously induced *bio* transducing phage. These were GyrA I203V/I205V, L488P and L492P at 3.4, 2.5 and 12.5-fold increase over wild type respectively (Ashizawa *et al.*, 1999). When the recombinant junctions were sequenced, all the mutants were shown to induce recombination at greater frequencies at non-hotspot sites over wild type and the junctions were shown to share less than 1 bp homology (Ashizawa *et al.*, 1999). The "hyper-recombination" alleles where shown to be dominant over wild type for the spontaneous induction of λ *bio* transducing phage, however, although they were shown to increase the spontaneous induction of wild-type λ, the mutant alleles were not dominant in this case (Ashizawa *et al.*, 1999).

Figure 4.2 shows the position of the mutations on GyrA. The mutations are located on the 59 kDa N-terminal domain of GyrA which is the domain responsible for the breaking and religating of the double-stranded DNA during the DNA gyrase reaction cycle (Horowitz & Wang, 1987). Specifically, the I203V/I205V mutations are in the winged-helix domain, on the α18 helix, and the two single mutations (L488P, L492P) are on the α10 helix on the coiled-coil domains (Morais Cabral *et al.*, 1997, Berger *et al.*, 1996, Dong & Berger, 2007, Schoeffler & Berger, 2008).

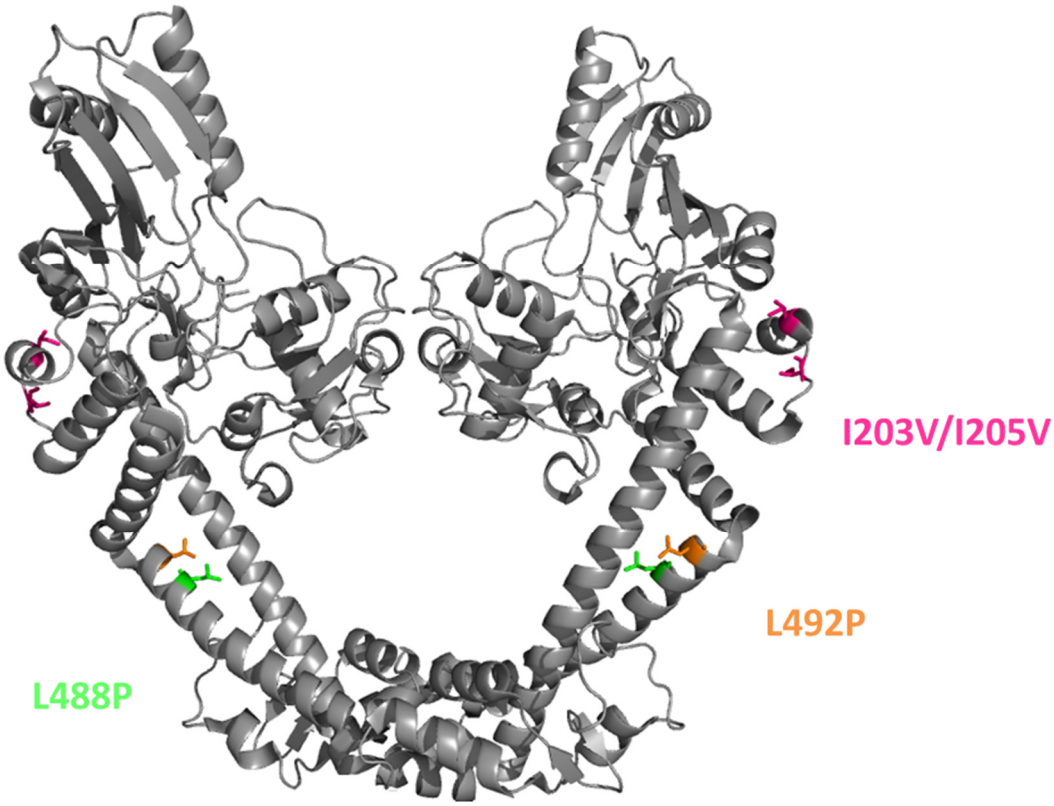

Figure 4.2: Structure of truncated DNA gyrase (GyrA 55; PDB: 4CKK) (grey) with hyper-recombination mutations highlighted. Pink show the residues 203 and 205 from the I203V/I205V double mutant. Green shows the 488 residue from the L488P mutant and orange shows the 492 residue from the L492P mutant.

Ashizawa *et al.* (1999) purified the GyrA L492P mutant and characterised its supercoiling activity alongside the formation of cleavage complexes during supercoiling. They found that under non-permissive conditions a higher amount of cleaved complex was visible (Figure 4.3). They proposed that this indicated that these proteins were either deficient in their ability to

religate DNA or in dimer formation and this would result in double-stranded breaks (DSB) in the chromosome which could confer the hyper-recombination phenotype.

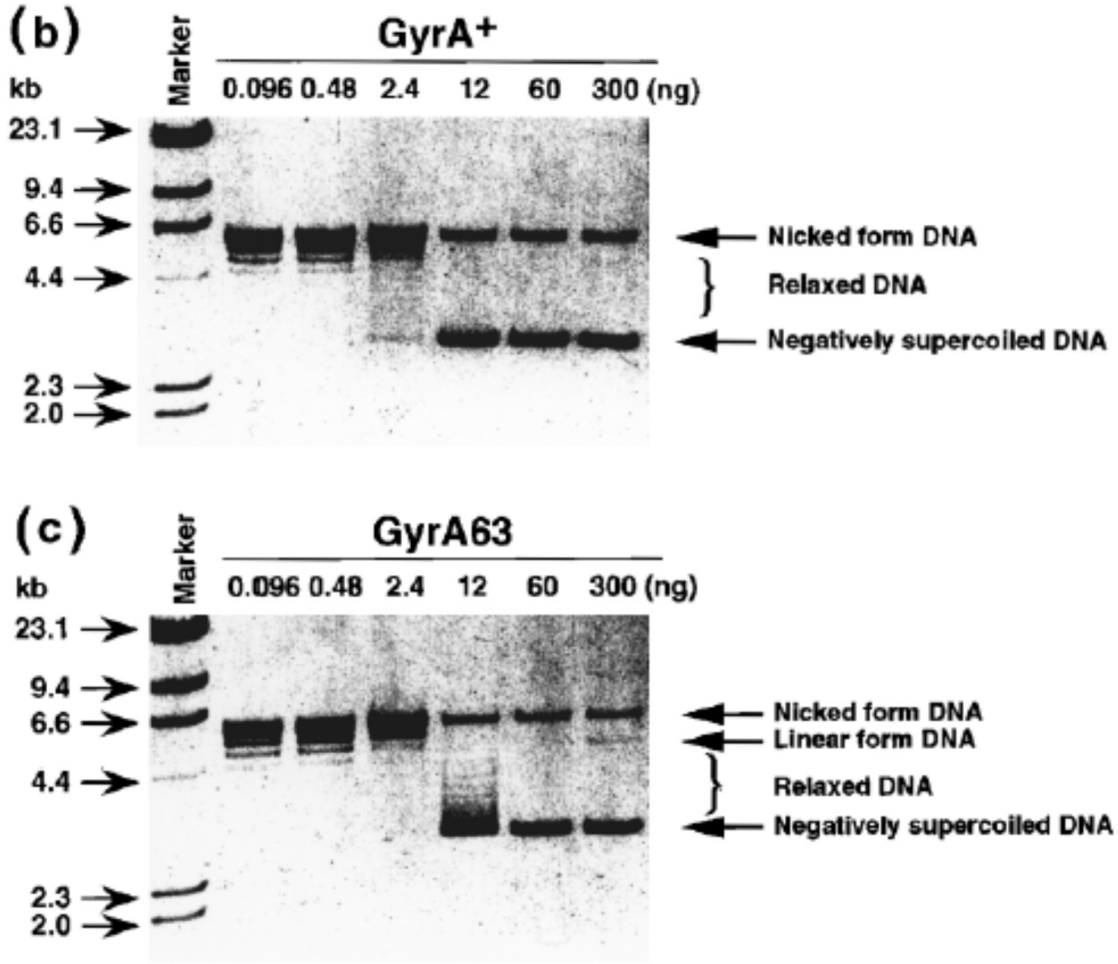

Figure 4.3: Figure from Ashizawa *et al.* (Ashizawa *et al.*, 1999) showing the supercoiling reaction with L492P mutant (GyrA63). (Original Legend: Cleavage of DNA by the GyrA63 protein. (a) – (not shown here) The GyrA$^+$ and GyrA63 proteins were subjected to SDS/12% polyacrylamide gel electrophoresis and stained with Coomassie brilliant blue R250. (b) and (c) Relaxed pACYC184 was incubated with various amounts of (b) GyrA$^+$ or (c) GyrA63 proteins and with a fixed amount (200 ng) of GyrB$^+$ protein at 42°C for 30 minutes. The reaction products were analysed by agarose gel electrophoresis).

Given that the *in vitro* activity of only one of these hyper-recombination mutants had been partially investigated, I set out to investigate the *in vitro* characteristics of all three mutations in order to clarify why they would confer a hyper-recombination phenotype *in vivo*. I did this by

analysing their supercoiling, relaxation, and cleavage activities under various conditions and by evaluating their ability to form complexes *in vitro*. I also attempted to move these mutations into the *E. coli* MG1655 chromosome to further investigate their phenotype *in vivo* (see Chapter 6).

4.2 Specific materials and methods

Site-Directed Mutagenesis

Site-Directed Mutagenesis (SDM) uses mismatched synthetic oligonucleotides that will insert specific mutations into your gene of interest during PCR (Carter, 1986). Using the SDM primers listed in Table 2.3 I set up PCR reactions with pPH3 (GyrA over expression plasmid (Hallett *et al.*, 1990)) as the template, Phusion DNA polymerase (NEB®), Phusion HF buffer (NEB®) in 50 µL PCR reactions, using the PCR conditions in Table 4.1 (see Chapter 2 for more information). The I203V/I205V mutant was made step-wise with the I205V mutation made first. Following this, the I203V mutant was made in the plasmid carrying the I205V mutant. The products were analysed using gel electrophoresis. Any positive hits were digested with DpnI for 1 h at 30°C before transforming into Bioline α-Select (Table 2.1 for genotype) Gold efficiency chemically-competent *E. coli* as per manufacturer's instructions. Fifty microlitres of the transformations were plated onto 9 cm diameter LB 1.1% agar plates with 100 µg/mL ampicillin, as pPH3 has an Amp^R-cassette. Three to five colonies from each mutant were selected and inoculated into 5 mL LB media with 100 µg/mL ampicillin with a sterile toothpick. These were incubated overnight at 30°C. From these overnight cultures, I extracted the plasmids using a Qiagen QIAprep Spin Miniprep Kit, using the manufacturer's instructions. The DNA concentrations were ascertained using UV absorbance and sent for Sanger sequencing by Eurofins Genomics using their overnight Mix2Seq kits. The sequencing primers used are in Table 2.3 and cover the whole *gyrA* gene in pPH3 including the genes' flanking regions and were

designed by Thomas Germe (JIC). Plasmids containing the correct sequences were taken forward for expression trials.

Table 4.1: Polymerase Chain Reaction conditions for Site-Directed Mutagenesis of *gyrA* gene.

Step	Temperature	Time	No. of cycles
Initial Denaturation	98°C	30 s	1
Denaturation	98°C	10 s	35
Annealing	59°C	10 s	35
Extension	72°C	8 min	35
Final Extension	72°C	10 min	1

Supercoiling reactions

The standard supercoiling reaction is run as follows: 0.25 µg of relaxed pBR322* was incubated at either 30°C (permissive) or 42°C (non-permissive) with ScAB (see Chapter 2) and varying concentrations (0 – 44.33 nM) of either wild-type GyrA (wtA) or the mutants in a 15 µL volume. Each sample was made up as a 30 µL sample and then halved after the addition of the enzyme. The GyrA subunits (WT and mutants) were mixed with the WT GyrB subunit at a concentration ratio of 1:1. After 30 min an equal volume of chloroform:isoamyl alcohol (24:1) and 15 µL of 2 × STEB was added and then briefly vortexed. The samples were then centrifuged at 16000 g for 1 min and 10 µL was analysed by gel electrophoresis at 90 V for 2 – 3 h or at 16 V overnight. The standard supercoiling reaction was also stopped with SDS as a repetition of the assay performed by Ashizawa *et al.* (Ashizawa *et al.*, 1999). The assay was run as above except after the 30 min incubation, 3.75 µL of a 1% (w/v) SDS solution (0.25% final concentration) was added, briefly vortexed before the addition of 10 × Invitrogen Loading Buffer (to a final concentration of 1 ×) and 15 µL of chloroform:isoamyl alcohol (24:1).

A supercoiling time course was run in a similar way to the standard supercoiling reaction at both 30°C and 42°C, except that 60 ng/15 µL (10.64 nM) of enzyme (WT and mutants) was added to each reaction and a 15 µL sample was taken at the following time points: 0 s, 10 s, 30 s, 1 min,

2 min, 5 min, 10 min, 15 min, 30 min, 1 h and 2 h. All supercoiling reactions were repeated at least 3 times.

Relaxation reactions

These were run in much the same way as the supercoiling reactions except 0.25 µg supercoiled pBR322* (purchased from Inspiralis Ltd) was incubated with relaxation assay buffer (35 mM Tris.HCl (pH 7.5), 24 mM KCl, 4 mM $MgCl_2$, 2 mM DTT, 6.5 % (w/v) glycerol, and 0.1 mg/ml albumin) which does not have spermidine or ATP in it. Again, all samples were made up as 30 µL reaction volumes and then halved after the addition of the enzyme. In the relaxation time course, 100 ng/15 µL (17.73 nM) of enzyme (A_2B_2 – both wtA and mutants) was added and samples were taken at 0 s, 30 s, 1 min, 2 min, 5 min, 10 min, 15 min, 30 min, 1 h and 2 h. Titrations of the wild-type enzyme and L488P mutant were done in the relaxation assay from 0 - 600 ng and 0 - 1.2 µg for each respectively over a 1 h incubation. The wild type titration was also analysed on a 1% agarose gel with 1 µg/mL chloroquine. The relaxation time courses were repeated at least three times and the titration with L488P was only performed once.

Cleavage reactions

A number of different cleavage reactions were performed. For the drug-induced cleavage reactions 0.25 µg supercoiled pBR322* was incubated with relaxation assay buffer (or relaxation assay buffer with 1 mM ATP for the +ATP reactions) and 50 µM of either ciprofloxacin (CFX) or oxolinic acid (OA) along with either wtA or the mutants in 15 µL reactions. These were incubated at 30°C and 42°C for 30 min. SDS (3.75 µL of 1% (w/v) solution) was added to each reaction, briefly vortexed, and 1.5 µL of 10 mg/mL proteinase K was added before briefly vortexing again. These were then returned to either 30°C or 42°C (i.e. back to their original incubation temperature) for a further 30 min. Following this incubation an equal volume of chloroform:isoamyl alcohol (24:1) and 15 µL of 2 × STEB was added and then briefly vortexed. The samples were the centrifuged at 16000 g for 1 min before loading 10 µL onto a 1% agarose

gel which was run at 90 V for 2 – 3 h or at 16 V overnight. For the CFX – induced cleavage 150 ng (13.3 nM) of either WT or mutant enzyme was added in a 30 µL reaction which was halved after the first incubation. To one set, EDTA was added to 8 mM and vortexed briefly before the addition of the SDS and proteinase K.

For the Mg^{2+} - mediated cleavage, 0.25 µg of relaxed pBR322* was incubated with relaxation buffer without the $MgCl_2$ (35 mM Tris.HCl (pH 7.5), 24 mM KCl, 2 mM DTT, 6.5 % (w/v) glycerol, and 0.1 mg/ml albumin), 375 ng (66.49 nM) of enzyme (WT and mutant), 1 mM ATP, and increasing concentrations of $MgCl_2$ (0, 1 mM, 2 mM, 4 mM, 8 mM, 16 mM and 32 mM) in 15 µL reaction volumes. The 1% agarose gels were run with 0.5 µg/mL EtBr in the gel and running buffer and thus were imaged without needing to be stained. Gel scans were performed using SynGene Gene Tools software using the manual band quantification. The mean pixel value minus background was acquired for all DNA bands present. The percentage of linear DNA was ascertained as a percentage of the total DNA present. A binomial best fit line was generated in Microsoft Excel 2016.

The Ca^{2+}-induced cleavage was run as per the Mg^{2+}-mediated cleavage except a fixed concentration of $CaCl_2$ (4 mM) was added to the samples and 0.5 µg or 1.5 µg of enzyme was added.

Cleavage induced by the non-hydrolysable ATP analogue 5'-adenylyl-β,γ-imidodiphosphate (ADPNP) was set up as per the Mg^{2+} and Ca^{2+} - based assays except relaxation buffer was used with the $MgCl_2$ present and ADPNP was added to 1 mM.

All cleavage reactions were performed in triplicate, except for the cleavage assays done in the presence of Mg^{2+}, which were run twice, and the assay with OA, which was only done once.

Circular Dichroism

Circular Dichroism (CD) is a spectroscopic technique that uses the differential absorption of left and right-handed polarised light to examine the secondary structure of proteins in

solution (Figure 4.4) (Kelly *et al.*, 2005). CD spectra can be used to assess whether a protein is folded correctly and give insight into the overall secondary structure of a protein (Kelly *et al.*, 2005).

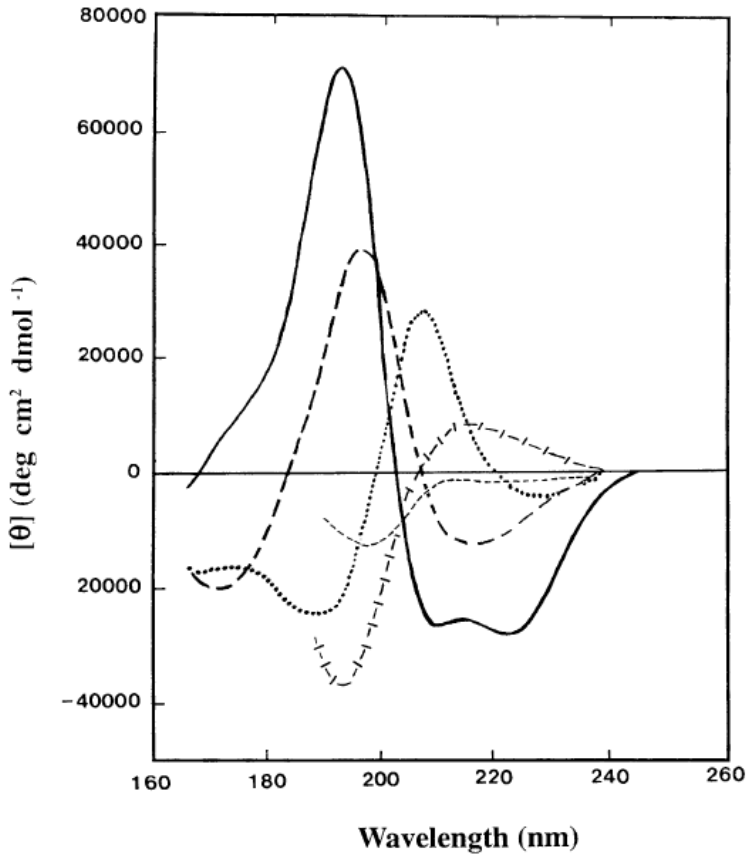

Figure 4.4: Far UV CD spectra associated with various types of secondary structure. Solid line, α-helix; long dashed line, anti-parallel β-sheet; dotted line, type I β-turn; cross dashed line, extended 31-helix or poly (Pro) II helix; short dashed line, irregular structure. From (Kelly *et al.*, 2005) with permission from publisher

The purified wtA and mutant hyper-recombination GyrA proteins were buffer exchanged in 20 mM sodium phosphate buffer (pH 7.5) using ultrafiltration in Amicon® Ultra 0.5 mL centrifugal filters with a 30 kDa cut off. The proteins were diluted to 200 µg/mL. Far UV spectra were obtained using a Chirascan-Plus CD spectrometer (Applied Photophysics) at 30°C and 42°C. This was done with in a quartz glass cell with a 0.5 mm path length, using wavelength scans between 180 nm and 260 nm using a 2 nm bandwidth, 0.5 nm steps and a time per point of 1 s.

The spectra were collected over four repeats and averaged then converted to mean residue ellipticity [θ] using the following equation:

$$[\theta]_{\mathrm{mrw},\lambda} = \mathrm{MRW} \times \theta_\lambda / (10 \times d \times c)$$

Where MRW is the mean residue weight (molecular mass/no. of peptide bonds), θ_λ is the observed ellipticity (degrees) at wavelength λ, *d* is the path length (cm), and *c* is the concentration (mg/ml).

4.3 Results and discussion

Expression and purification

The hyper-recombination mutations were made by site-directed mutagenesis of the GyrA overexpression plasmid pPH3 and were confirmed by Sanger sequencing (Figure 4.5). The plasmids were transformed into the *E. coli* expression strain BL21(DE3) (Table 2.1) and the proteins were expressed in LB with induction by IPTG. Purification of the wild type and mutant proteins involved an initial Q-Sepharose column, followed by a Phenyl Superpose column and finally a MonoQ column (Figure 4.6). For the I203V/I205V and L488P mutants, the MonoQ and Phenyl-Superose steps were reversed. The L492P protein was purified twice to check that the *in vitro* activity of the enzymes was similar across preparations. No difference in activity was visible (data not shown). All proteins used had approximately the same level of purity (~70%) (Figure 4.6e).

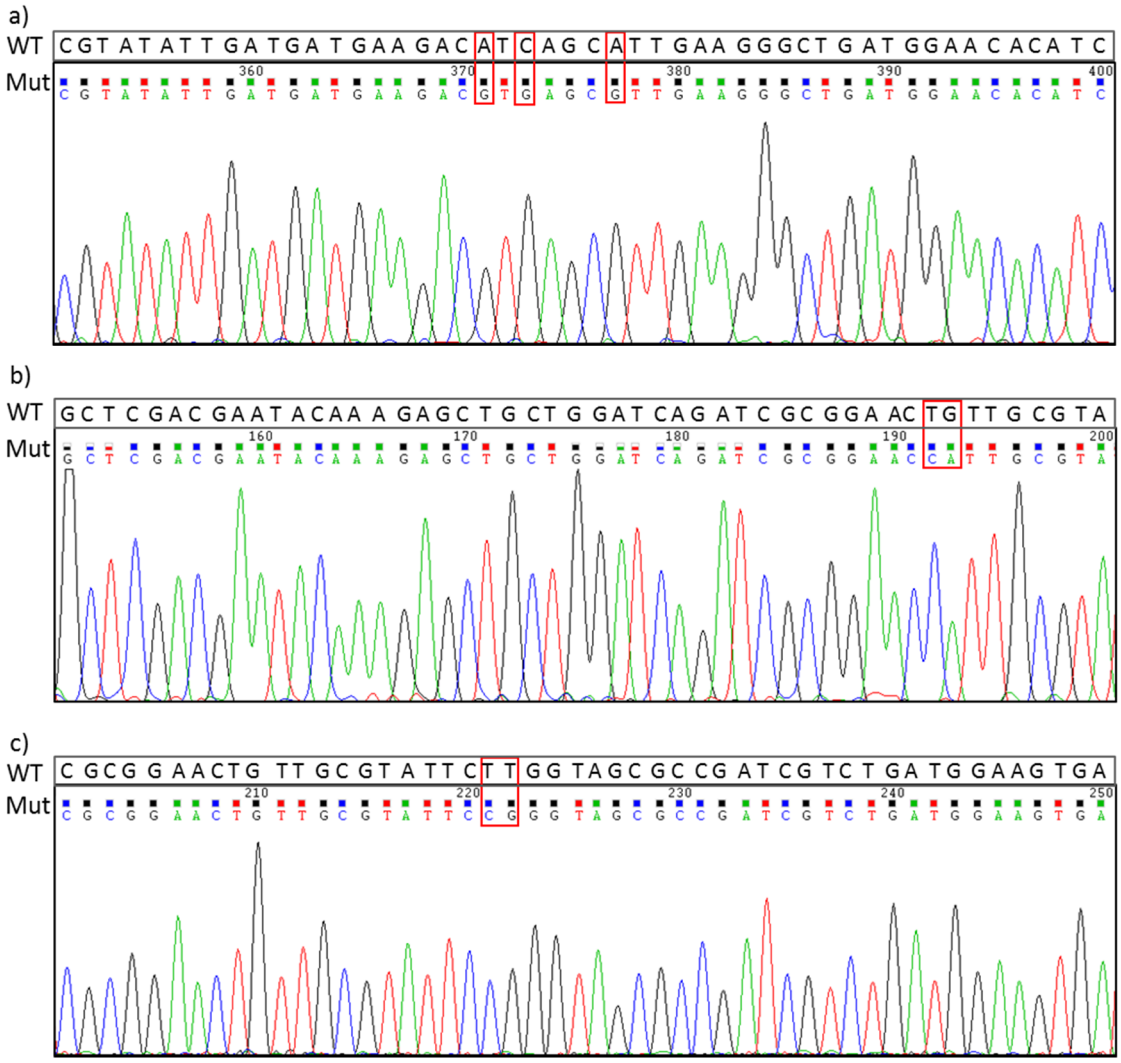

Figure 4.5: Sequencing Chromatograms of *gyrA* mutations in pPH3 aligned with the wild-type sequence. WT is the wild-type pPH3 *gyrA* sequence. Mut is the mutated pPH3 *gyrA* sequence. Red boxes indicate the position of the mutations. a) is the I203V/I205V mutations. b) is the L488P mutation and c) shows the base changes of the L492P mutations.

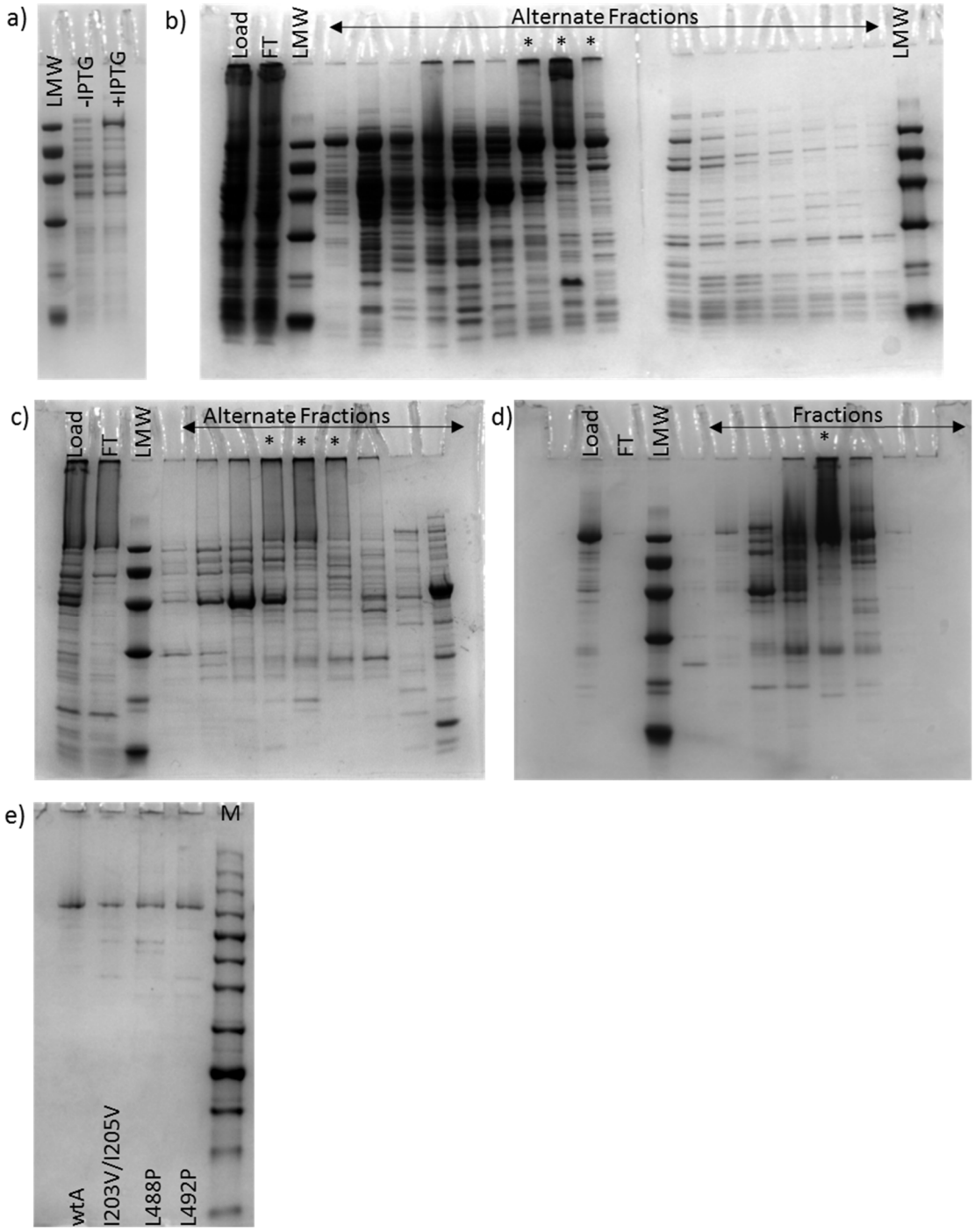

Figure 4.6: Purification GyrA L492P mutant. LMW is the low molecular weight protein marker; Load is a sample of the extract loaded onto the column, FT is the flow through from the column, i.e. the fraction that did not stick to the column. * indicates the fractions (and the fractions between) pooled. a) Overexpression of the protein. Briefly *E. coli* BL21(DE3) transformed with the overexpressing plasmid was grown in LB media until an OD_{600} of 0.4 was reached. A 1 mL sample was removed (-IPTG) and incubated separately. IPTG (IPTG+) was added to the remaining culture and incubated for 18 h before analysis with SDS PAGE. b) Q-Sepharose. After overexpression, the cell extract was applied to a Q-Sepharose and fractions

collected over a NaCl gradient. Alternative fractions were analysed by SDS PAGE. c) Phenyl-Superose. Ammonium sulphate was added to 1 M to the pooled fractions from the Q-Sepharose column and applied to a Phenyl-Superose column. Fractions were collected over a reverse $(NH_4)_2SO_4$ gradient and alternate fractions analysed by SDS PAGE. d) MonoQ. Pooled fractions were dialysed in TGED over night before loaded onto a MonoQ column. Fractions were collected over a NaCl gradient and fractions analysed by SDS PAGE. e) Shows 1 µg of the purified proteins (concentration based on Bradford Assay measurements). wtA is the wild-type GyrA subunit, I203V/I203V, L488P and L492P are the hyper-recombination mutants, amino acid changes are referred to by their single letter codes.

Structural information and complex formation

To check if the mutant proteins were folded correctly CD spectra between 180 nm and 260 nm were measured. As these mutants were identified in a temperature-sensitive screen, the spectra were collected at both permissive (30°C) and non-permissive (42°C) temperatures. From Figure 4.7, there appears to be no difference in the overall shape of the spectra between the wild type and the mutants as well as any difference between the temperatures. This suggests that the mutants have no significant deviations in structure or folding in comparison to wild type or at non-permissive temperatures.

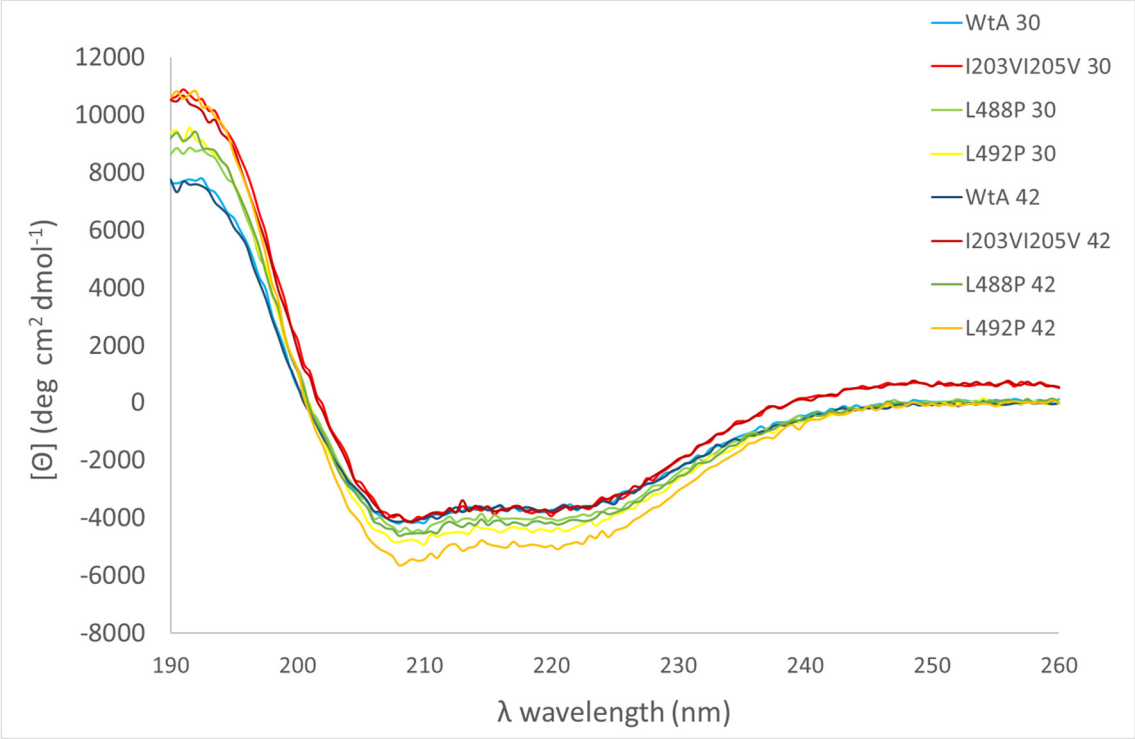

Figure 4.7: Far UV (190 nm – 260 nm) CD spectra of wild-type GyrA and the GyrA hyper-recombination mutants. WtA is the wild-type protein, I203V/I203V, L488P and L492P are the hyper-recombination mutants, amino acid changes are referred to by their single letter codes. 30 and 42 indicate the spectrum at either the permissive or non-permissive temperature (30°C or 42°C respectively).

Ashizawa *et al.* (1999) suggested that one reason that these hyper-recombination mutants present this phenotype may be because they are flawed in subunit dimerisation. To address this, I looked at the native complexes of the subunits using Blue-Native PAGE (BN-PAGE) (Figure 4.8). From the BN-PAGE it appears that like the wild-type GyrA, the hyper-recombination mutants appear to be primarily dimers and do form complexes with GyrB. This is evident as there is no band where a GyrA monomer would run and they seem to have the same banding pattern as the wild type. However, they do not seem to form the higher tetrameric species (A_4) in comparison to the wild-type protein. From the gels, it is apparent that the molecular weights of the marker and the protein complexes do not match up. This is probably because of the limitations of BN-PAGE in ascertaining molecular mass for water soluble proteins with isoelectric

points (pI) below 8.6 (Schagger *et al.*, 1994, Wittig *et al.*, 2006). The measured pI for GyrA is between 4.5 – 5.5 (calculated pI is 4.98) and GyrB is about 6 (calculated pI is 5.52) (Reece & Maxwell, 1991a) and can result in up to a 20% deviation from the actual molecular mass (Schagger *et al.*, 1994). Estimated pI's were calculated using the IPC (Isoelectric Point Calculator) tool online (Kozlowski, 2016). There is also no difference is banding patterns at the different temperatures.

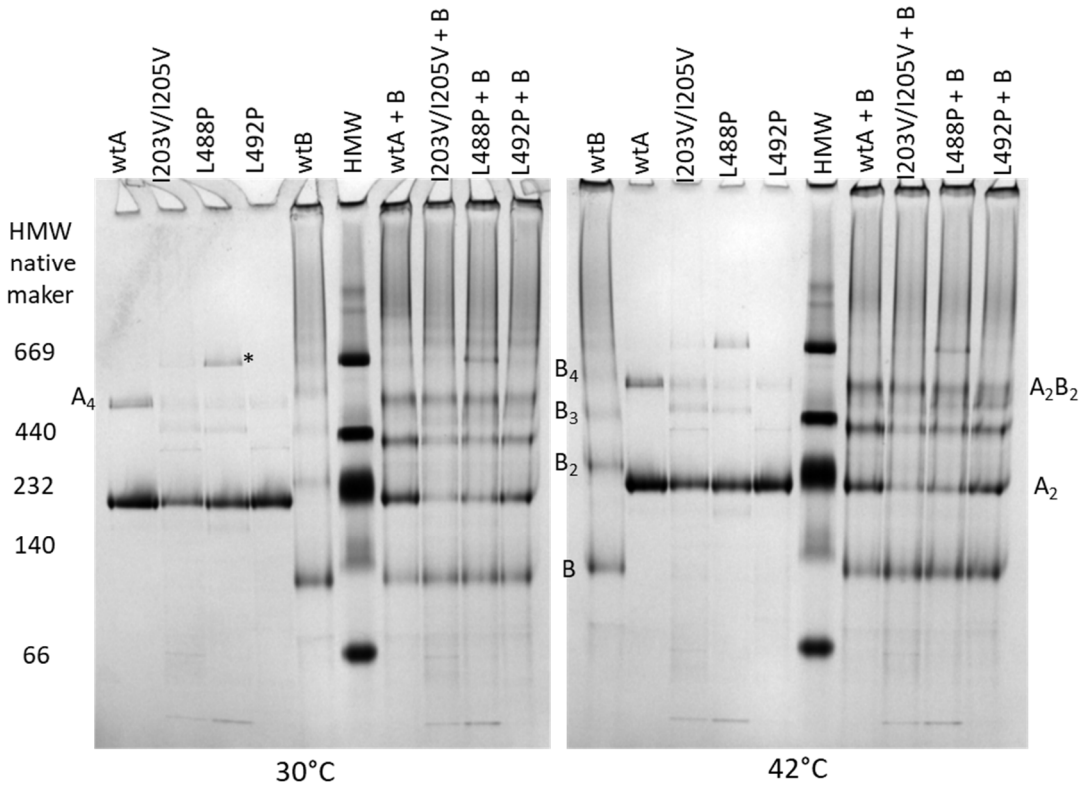

Figure 4.8: Blue-Native PAGE of GyrA wild-type and hyper-recombination mutants. Samples were incubated at 30°C or 42°C for 40 min, either alone or with GyrB (+B samples) before running on a 4-16% gradient polyacrylamide gel. WtA is the wild-type protein, I203V/I203V, L488P and L492P are the hyper-recombination mutants, amino acid changes are referred to by their single letter codes. The High Molecular Weight native size marker (HMW) is indicated on the left-hand side in kDa. A_2 shows the GyrA dimer, A_4 is the GyrA tetramer. B is the GyrB monomer, B_2, B_3 and B_4 show the GyrB dimer, trimer and tetramer. A_2B_2 is the full-length DNA gyrase (GyrA, GyrB tetramer). * is likely a contaminant as it does not show up in a western blot probing with antiGyrA monoclonal antibodies (data not shown).

The BN-PAGE data along with the CD spectra suggests that there are no structural reasons, in terms of folding or complex formation, for these proteins to show a hyper-recombination phenotype.

Supercoiling activity

To investigate the hyper-recombination mutants' *in vitro* activity, I initially looked at their supercoiling activity. Supercoiling is an ATP-dependent activity and involves the wrapping of the DNA around the enzyme to present a T-segment in a positive node. This T-segment is then passed through a G-segment which is bound along the GyrA/GyrB interface and is cleaved during the reaction cycle.

I repeated the assay Ashizawa *et al.* (1999) ran with the L492P mutant (GyrA63 in Figure 4.3) where the enzyme is titrated into the assay and the enzyme-DNA complex is trapped with SDS before analysis on an agarose gel. This should give an indication of the DNA damage caused by the enzyme during the reaction cycle. If the enzyme is inefficient in DNA religation activity a greater amount of cleaved (linear or OC) DNA should be visible. In Figure 4.9, there is no such increase over wild type by any of the mutants, at either permissive or non-permissive temperatures. This contrasts with the conclusions drawn by Ashizawa *et al.* (1999) who suggested that there is an increase in linear DNA present (Figure 4.3). However, I do not entirely concur with their analysis of the gel (Figure 4.3). I would not say that the mutant shows a significant increase in linear DNA over wild type, and further analysis is needed. Ultimately, this assay does not suggest that these hyper-recombination mutants have hyper-cleavage activity.

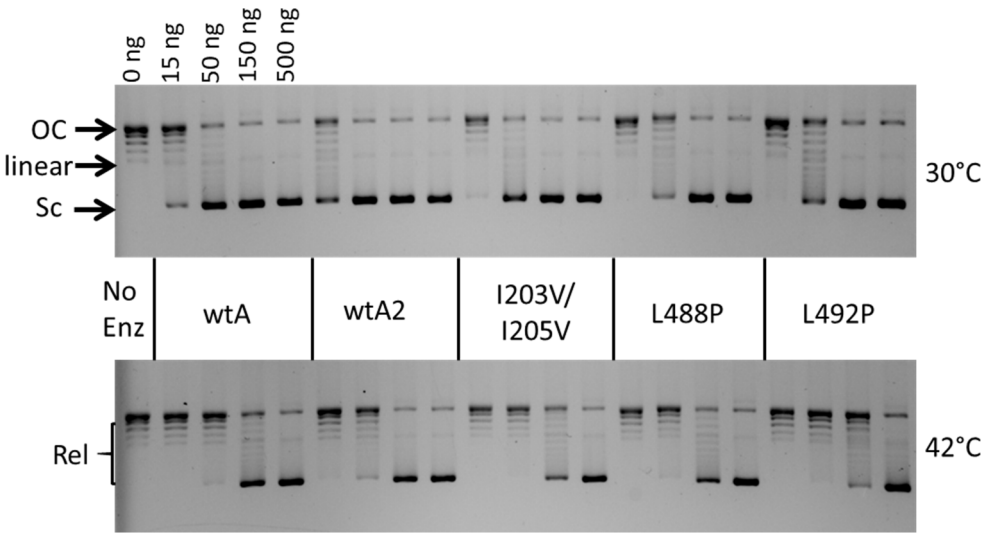

Figure 4.9: SDS-trapping of DNA during supercoiling by DNA gyrase with hyper-recombination mutations. Cleavage activity during supercoiling of the three hyper-recombination GyrA mutants were compared to wild-type GyrA, all with equimolar wild-type GyrB, with between 15 ng and 500 ng (1.33 nM and 44.33 nM) of enzyme at permissive (30°C) and non-permissive (42°C) temperatures. The reactions were stopped by adding 0.25% (w/v) SDS before analysing samples on a 1% agarose gel. OC indicates the open-circular or nicked DNA, linear indicates the cleaved or linear DNA, Sc indicates the supercoiled DNA and Rel indicates the relaxed topoisomers. No Enz is the no enzyme control. wtA and wtA2 are two separate wild-type GyrA controls. I203V/I205V, L488P and L492P are the respective GyrA hyper-recombination mutants.

Under normal supercoiling activity, it appears that the mutants are marginally less active than wild type. When the enzymes are titrated into the assay, the I203V/I205V and L492P mutants do not show much difference to wild type, and the L488P mutant is slightly less active (Figure 4.10). When a time course is run where the amount of enzyme is fixed at 60 ng (10.64 nM), and the wild type shows full supercoiling after 30 min (Figure 4.11), the mutants are less active with the L488P and I203V/I205V mutants only reaching full supercoiling after 30 min and only after 1 h with the L492P mutant. This suggests that the enzymes are slower at supercoiling than wild type.

In all three of these assays, all the enzymes, wild type included, show lower activity at 42°C. This is clear in the time course where the wild type activity is greatly reduced at the non-permissive temperature. This indicates that the mutant enzymes are no more temperature sensitive in their *in vitro* supercoiling activity than wild type. In the previous work (Ashizawa *et al.*, 1999), the L492P mutant was only tested at the non-permissive temperature so no comparison at the permissive temperature can be done. From their data, it seems that these purified enzymes are slightly less active than the Ashizawa *et al.* (1999) GyrA63 at the relevant concentrations. This may be due to the different purification techniques or the slightly different assay conditions.

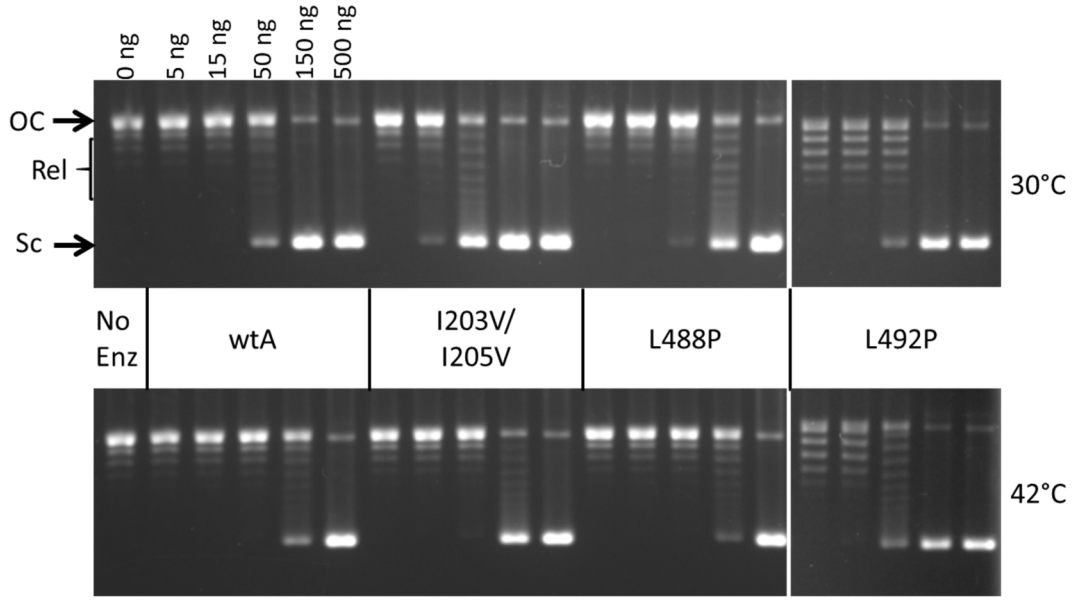

Figure 4.10: Supercoiling activity at increasing concentrations of DNA gyrase with hyper-recombination mutations. Supercoiling activity of the three hyper-recombination GyrA mutants were compared to wild-type GyrA, all with equimolar wild-type GyrB, at enzyme concentrations between 5 ng and 500 ng (1.33 nM and 44.33 nM) at permissive (30°C) and non-permissive (42°C) temperatures. Samples were analysed on a 1% agarose gel. OC indicates the open-circular or nicked DNA, Rel indicates the relaxed topoisomers and Sc indicates the supercoiled DNA. No Enz is the no enzyme control. wtA is the wild-type GyrA control. I203V/I205V, L488P and L492P are the respective GyrA hyper-recombination mutants.

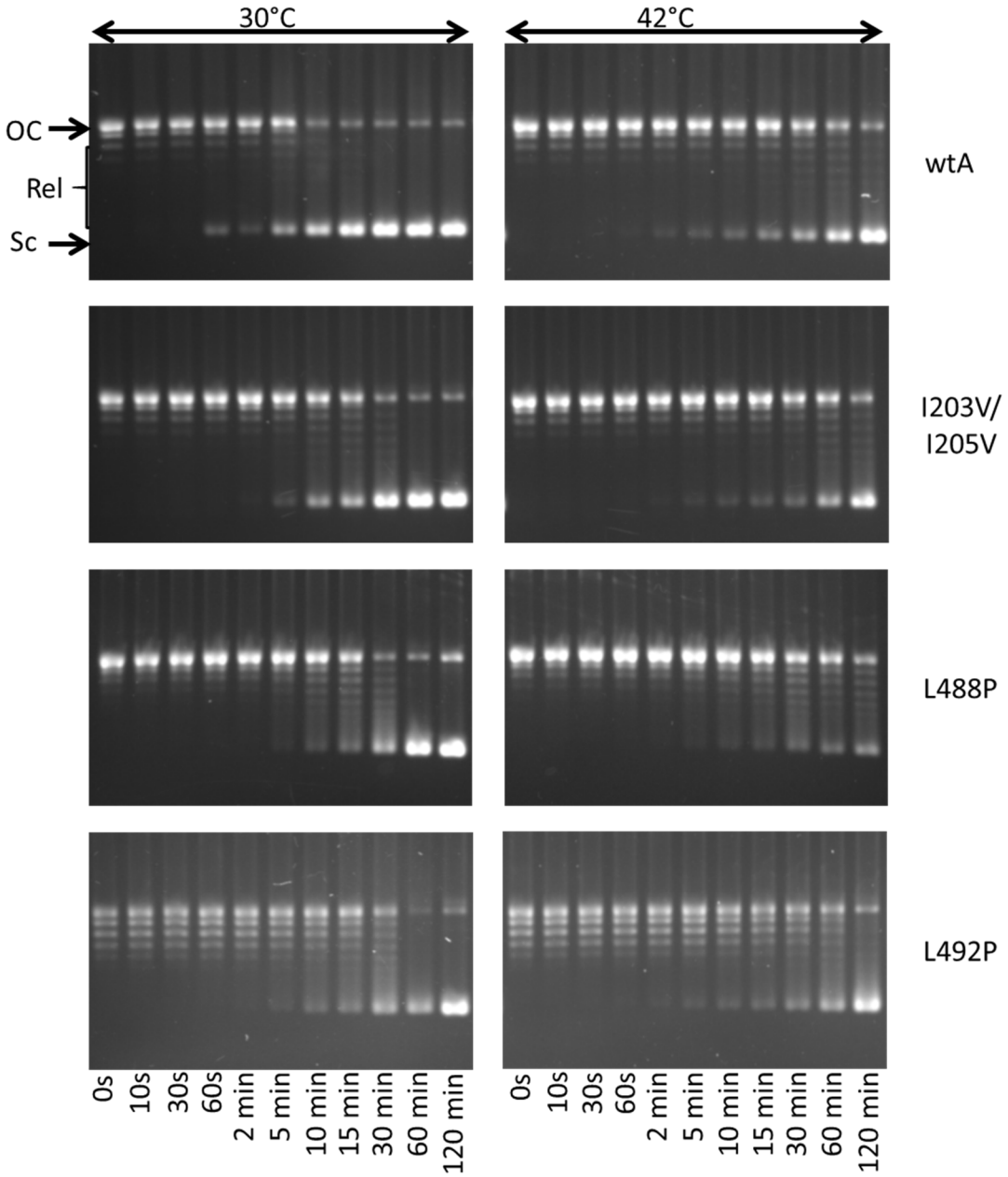

Figure 4.11: Supercoiling activity time-course of GyrA hyper-recombination mutants. Supercoiling activity of the three hyper-recombination GyrA mutants were compared to wild-type GyrA, all with equimolar wild-type GyrB, over 2 h at a fixed enzyme concentration (60 ng or 10.64 nM) at permissive (30°C) and non-permissive (42°C) temperatures. Samples were analysed on a 1% agarose gel. OC indicates the open-circular or nicked DNA, Rel indicates the relaxed topoisomers and Sc indicates the supercoiled DNA. The time points are indicated below each lane. wtA is the wild-type GyrA control. I203V/I205V, L488P and L492P are the respective GyrA hyper-recombination mutants.

DNA supercoiling has been shown to affect transcription *in vivo* (Bagel *et al.*, 1999, Lilley *et al.*, 1996) with different levels of chromosomal supercoiling affecting protein expression in bacteria (Bagel *et al.*, 1999, Webber *et al.*, 2013). Alteration of the superhelical density by perturbations in the expression of topoisomerase I or inhibition of DNA gyrase *in vivo* has been shown to effect site-specific recombination in the *fimA* promoter (Dove & Dorman, 1994). Although supercoiling activity *in vitro* does not directly correlate to the superhelical density of the chromosome *in vivo*, a mutation that shows much lower supercoiling activity would presumably also have an effect *in vivo*. These mutants are less active than the wild type which may have an effect *in vivo*, however, the *in vivo* activity of these mutants would have to be evaluated to draw any conclusions.

Relaxation activity

Relaxation of negative supercoils by DNA gyrase is an ATP-independent process (Gellert *et al.*, 1976b, Higgins *et al.*, 1978, Nollmann *et al.*, 2007b). It is thought to occur by reverse strand-passage (or bottom-up strand passage) (Williams & Maxwell, 1999b).

A relaxation activity time course (Figure 4.12) shows that the I203V/I205V mutant is not to dissimilar to wild type, conversely the L488P and L492P mutants appear to have no relaxation activity. This lack of relaxation activity has not been consistent across all repetitions of the relaxation time-course assay; in some replications, these enzymes have both shown complete relaxation by a mid-timepoint (data not shown). The cause of this effect is not clear. The L488P mutant was titrated into the assay to see if any relaxation could be seen (Figure 4.13), it takes nearly 6-fold more enzyme to achieve full relaxation.

The ATP-independent relaxation by DNA gyrase may not be biologically relevant as it is unlikely that there would be no ATP present in the cell. However, it can give us insights into the structural or functional integrity of the C-gate or exit gate. Williams and Maxwell (1999b) have shown that when the exit gate is cross-linked, the enzyme is no longer able to relax negatively-supercoiled DNA. The L488P and the L492P mutants are not completely deficient in relaxation

but at times have shown very poor relaxation activity. These two mutations are found on the α-helix of the coiled-coil domains near the exit gate (Figure 4.2). The introduction of a proline in the helix could result in a kink in the helix due to the specific structure and chemistry of the amino acid. Altogether, this implies that the L488P and L492P mutants affect the normal functioning of the exit gate.

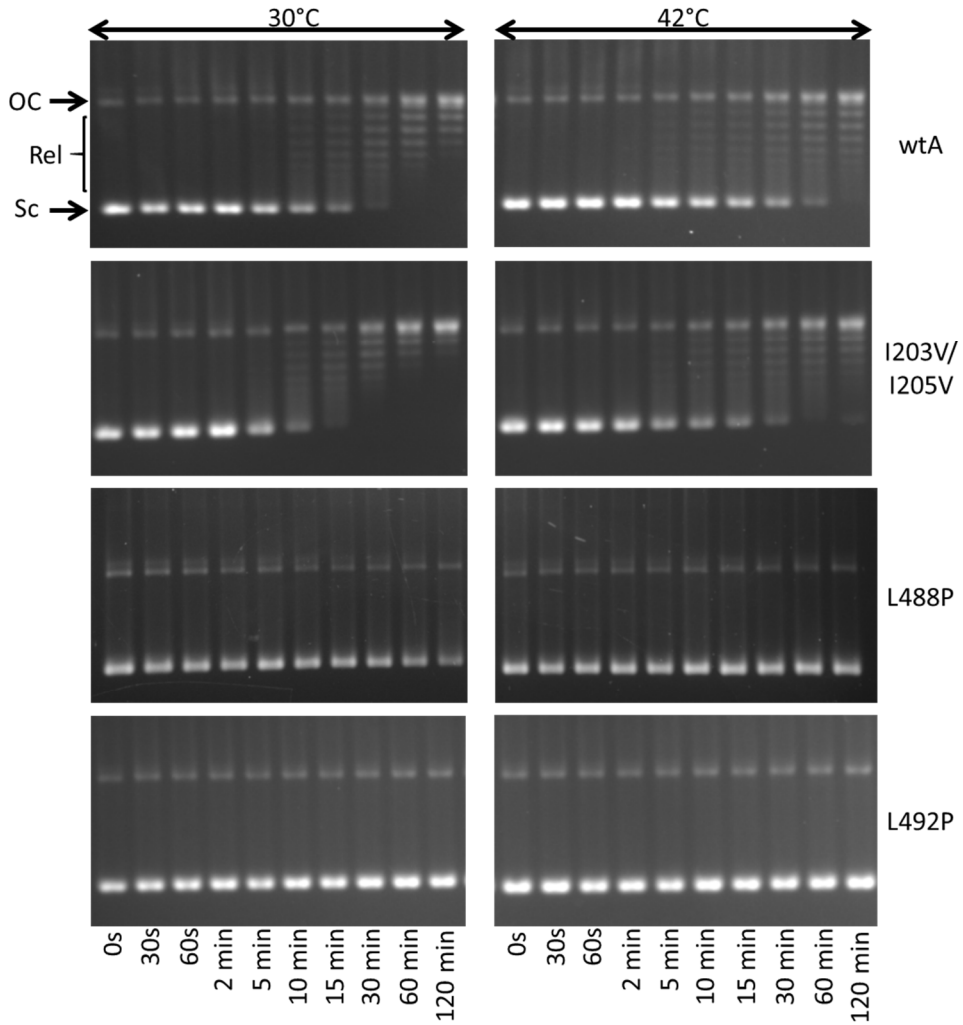

Figure 4.12: Relaxation activity time-course of GyrA hyper-recombination mutants. ATP-independent relaxation activity of the three hyper-recombination GyrA mutants were compared to wild-type GyrA, all with equimolar wild-type GyrB, over 2 h at a fixed amount of enzyme (200 ng or 17.73 nM) at permissive (30°C) and non-permissive (42°C) temperatures. Samples were analysed on a 1% agarose gel. OC indicates the open-circular or nicked DNA, Rel indicates the relaxed topoisomers and Sc indicates the supercoiled DNA. The time points are indicated below each lane. wtA is the wild-type GyrA control. I203V/I205V, L488P and L492P are the respective GyrA hyper-recombination mutants.

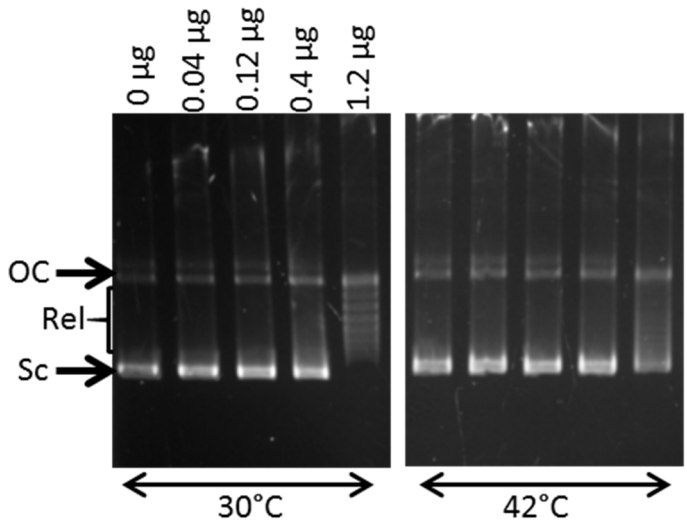

Figure 4.13: Relaxation activity at increasing concentrations of DNA gyrase with L488P hyper-recombination mutation. ATP-independent relaxation activity of the L488P hyper-recombination GyrA mutant, with equimolar wild-type GyrB, at enzyme concentrations between 0.04 µg and 1.2 µg (3.55 nM and 106.38 nM), at permissive (30°C) and non-permissive (42°C) temperatures. These were incubated for 1 h before samples were analysed on a 1% agarose gel. OC indicates the open-circular or nicked DNA, Rel indicates the relaxed topoisomers and Sc indicates the supercoiled DNA.

Cleavage activity

Cleavage assays allow us to see the trapped transient DSBs caused by the enzyme. The cleavage-religation domain has been shown to be primarily in a closed conformation (Gubaev *et al.*, 2009) and double-stranded cleavage is thought to be extremely transient, unless it is stabilised by drugs or denaturants (Maxwell, 1997, Chan *et al.*, 2017). Ashizawa *et al.* (1999) suggested that the hyper-recombination phenotype was due to these mutations causing religation defects. To directly test this, I looked at cleavage with different metal ions, ADPNP-induced cleavage and drug-induced cleavage using quinolone antibiotics (Figure 1.16) that stabilise the cleavage complex between the enzyme and DNA.

I first analysed drug-induced cleavage with oxolinic acid (OA) as it is the quinolone that Ikeda *et al.* (1980) used to identified DNA gyrase-mediated IR with. Figure 4.15 shows the cleavage

assay with OA. With OA, the hyper-recombination mutants do not show more cleavage than wild type. All enzymes show a concentration-dependent increase in linear DNA, with wild type showing the most cleavage at the highest enzyme concentration. Again, all enzymes showed much less activity at 42°C.

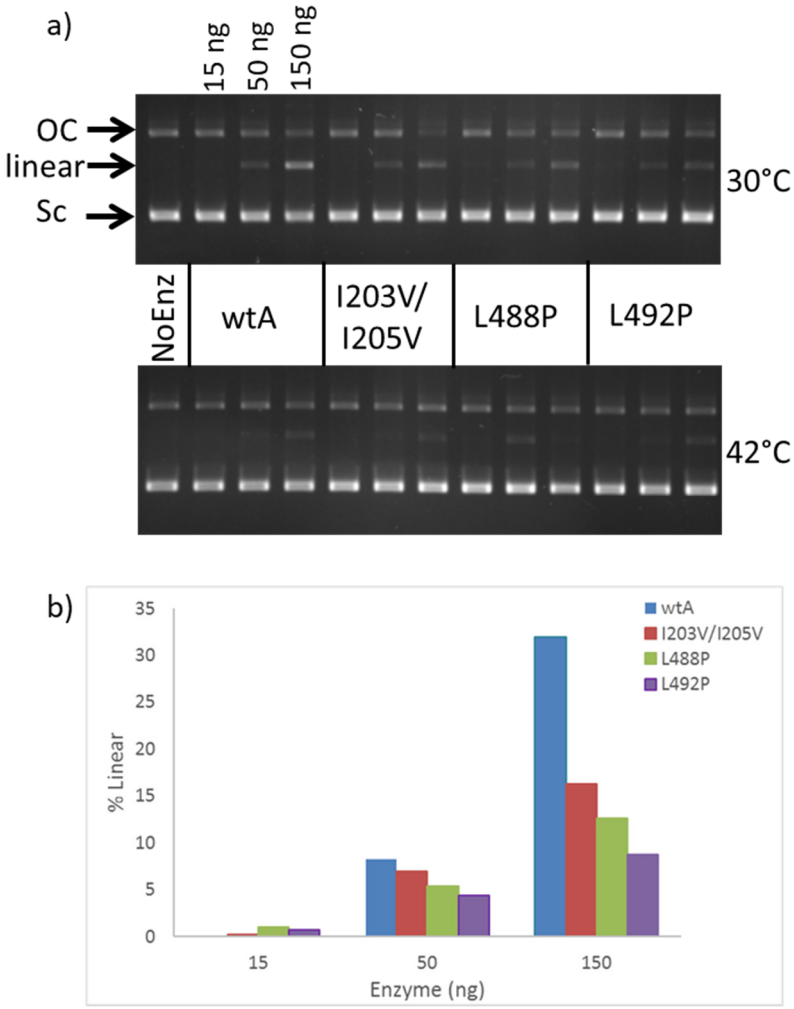

Figure 4.14: Oxolinic acid-induced cleavage by GyrA hyper-recombination mutants. a) ATP-dependent (+ATP) oxolinic acid (OA)-induced cleavage activity of the three hyper-recombination GyrA mutants were compared to wild-type GyrA, all with equimolar wild-type GyrB, at permissive (30°C) and non-permissive (42°C) temperatures. Samples were analysed on a 1% agarose gel. OC indicates the open-circular or nicked DNA, Linear indicates the cleaved DNA and Sc indicates the supercoiled DNA. b) Column Graph showing percentage of linear DNA present. The mean pixel value minus background was acquired for all DNA bands present from the samples in the 30°C assay gel. The percentage of linear DNA (% Linear) was ascertained as a percentage of the total DNA present. wtA is the wild-type GyrA control. I203V/I205V, L488P and L492P are the respective GyrA hyper-recombination mutants.

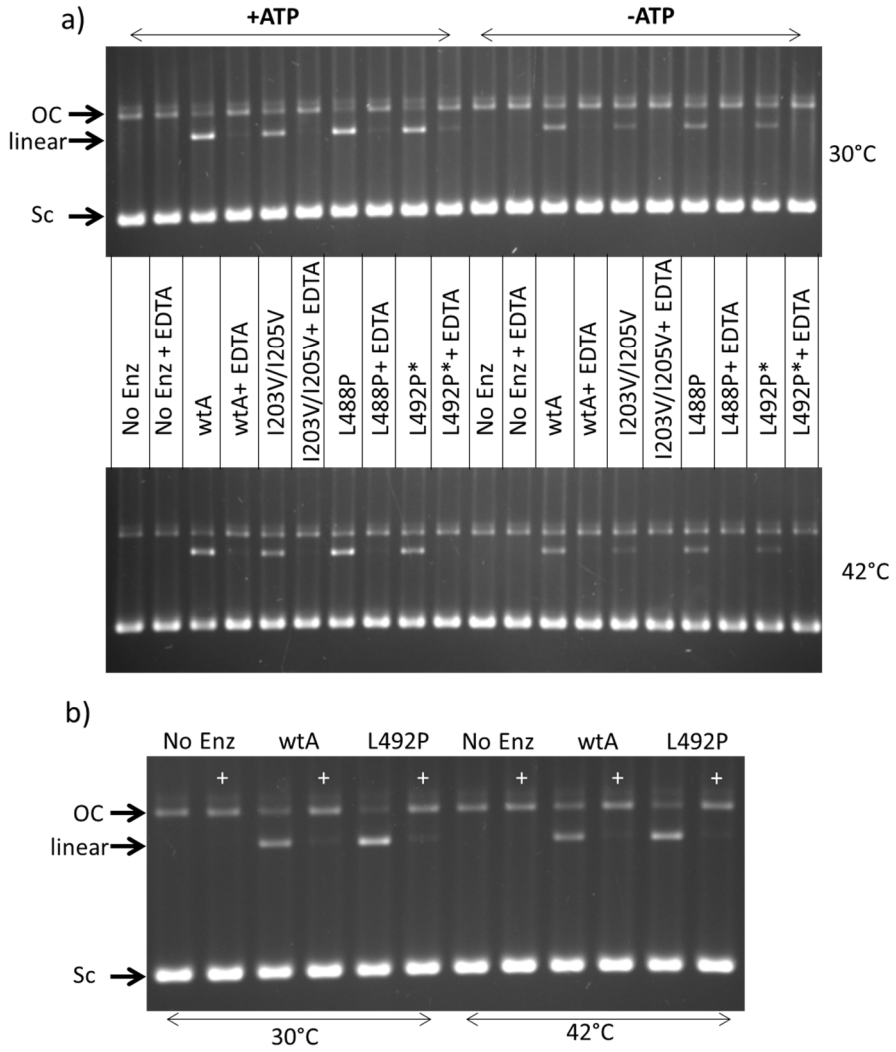

Figure 4.15: Ciprofloxacin-induced cleavage by GyrA hyper-recombination mutants. a) ATP-dependent (+ATP) and independent (-ATP) ciprofloxacin (CFX)-induced cleavage and resealing activity of the three hyper-recombination GyrA mutants were compared to wild-type GyrA, all with equimolar wild-type GyrB, at permissive (30°C) and non-permissive (42°C) temperatures. L492P* is the L492P mutant at a quarter of the wild-type concentration. b) is ATP-dependent (+ATP) CFX-induced cleavage and resealing activity of the L492P hyper-recombination GyrA mutant (at the same concentration as wild-type GyrA) compared to wild-type GyrA. EDTA was added (+EDTA in panel a, and + in panel b) to samples pre-trapping with SDS to strip out the Mg^{2+} ions that mediate the stabilisation of the cleavage complex with CFX in order to test the enzymes ability to reseal cleaved complexes. Samples were analysed on a 1% agarose gel. OC indicates the open-circular or nicked DNA, Linear indicates the cleaved DNA and Sc indicates the supercoiled DNA. wtA is the wild-type GyrA control. I203V/I205V, L488P and L492P are the respective GyrA hyper-recombination mutants.

CFX-induced cleavage was tested in a similar way to the OA-induced cleavage, except the enzymes ability to religate drug-induced cleavage was also measured. CFX is believed to poison via the water-metal ion bridge (Aldred *et al.*, 2016, Aldred *et al.*, 2014a, Aldred *et al.*, 2013) and thus when EDTA is used to strip out the metal ion (Mg^{2+}), the drug can no longer stabilise the cleavage complex and the enzyme can religate the DNA (Gellert *et al.*, 1977, Sugino *et al.*, 1977, Drlica *et al.*, 2014). If these mutants were defective in religation then they would likely show more cleavage after the drug-induced cleavage was repaired.

In the presence of ATP, both the L488P and L492P mutants show more CFX-induced cleavage than wild type (Figure 4.16), at both permissive and non-permissive temperatures, while the I203V/I205V shows slightly less. Without ATP, the differences are not as striking and all enzymes show less cleavage. This is not unexpected as ATP has been shown previously to accelerate CFX-induced cleavage (Li & Liu, 1998, Chan *et al.*, 2017). Cleavage induced by norfloxacin (Figure 1.16), another fluoroquinolone, has also been shown to increase in the presence of ATP (Shen *et al.*, 1989). Considering the poor supercoiling and relaxation activity, it may be expected that the mutants show reduced cleavage activity. This is not necessarily the case as DNA cleavage induced by the quinolones has been shown to be independent of the normal activity of the enzyme (Kampranis & Maxwell, 1998b). Furthermore, when the drug is bound, it favours a conformational change that results in a slow religation step (Kampranis & Maxwell, 1998b). To determine whether the decreased drug-induced cleavage seen with the I203V/I205V mutant is due to the reduced activity of the enzyme overall, or if it is only affecting cleavage activity would require further investigation.

Looking at the effect of the mutations on the enzymes' ability to religate drug-induced cleavage, the L488P and L492P mutations at 30°C, have slightly more linear DNA present after the addition of EDTA but only in the presence of ATP (Figure 4.16). This implies the mutations either cause the enzyme to release the double-stranded ends, or they have a reduced religation

activity. With the former it could indicate that the dimers are coming apart and so the religation cannot happen, or with the latter, that the DSBs are more stable than with wild type and thus take longer to reseal. The best way to probe these interactions would be to look at the cleavage and resealing kinetics.

Although drug-based cleavage can reveal alterations in conformational changes, the drugs themselves can affect the natural conformations during reaction cycle. Thus, the natural cleavage activity was investigated. This was done by titrating Mg^{2+} into the assay and trapping the enzyme/DNA complexes with SDS (Figure 4.17), by substituting Mg^{2+} ions for Ca^{2+} ions in the reaction mix (Figure 4.18), and trapping the whole enzyme with ADPNP (Figure 4.19).

When Mg^{2+} is titrated into the assay there is concentration-dependent increase in linear DNA to 16 mM with the wild type and the I203V/I205V mutant (Figure 4.17 and 4.18). Whereas, the L488P and L492P mutants have much lower levels of cleavage and the amount of linear DNA appears to reach a maximum at 2 mM for the L488P mutant and 8 mM with the L492P mutant (Figure 4.17 and 4.18). However, this maximum is about 6-fold lower than both the wild type and the I203V/I205V mutant. Lane 4 in Figure 4.17 is the reaction with 4 mM $MgCl_2$ which is the standard concentration of Mg^{2+} in the assay buffers. There is less linear DNA present with the I203V/I205V mutant (~3%) and both the L488P and the L492P mutants (~0.5 and 1% respectively) in comparison to wild type (~6%) (Figure 4.18). I was unable to perform gel scans on the 42°C samples as they had an extra, unidentified band running below the open-circular band. The differences with 4 mM $MgCl_2$ show that under standard assay conditions, all three mutants show less cleavage activity in comparison to wild type.

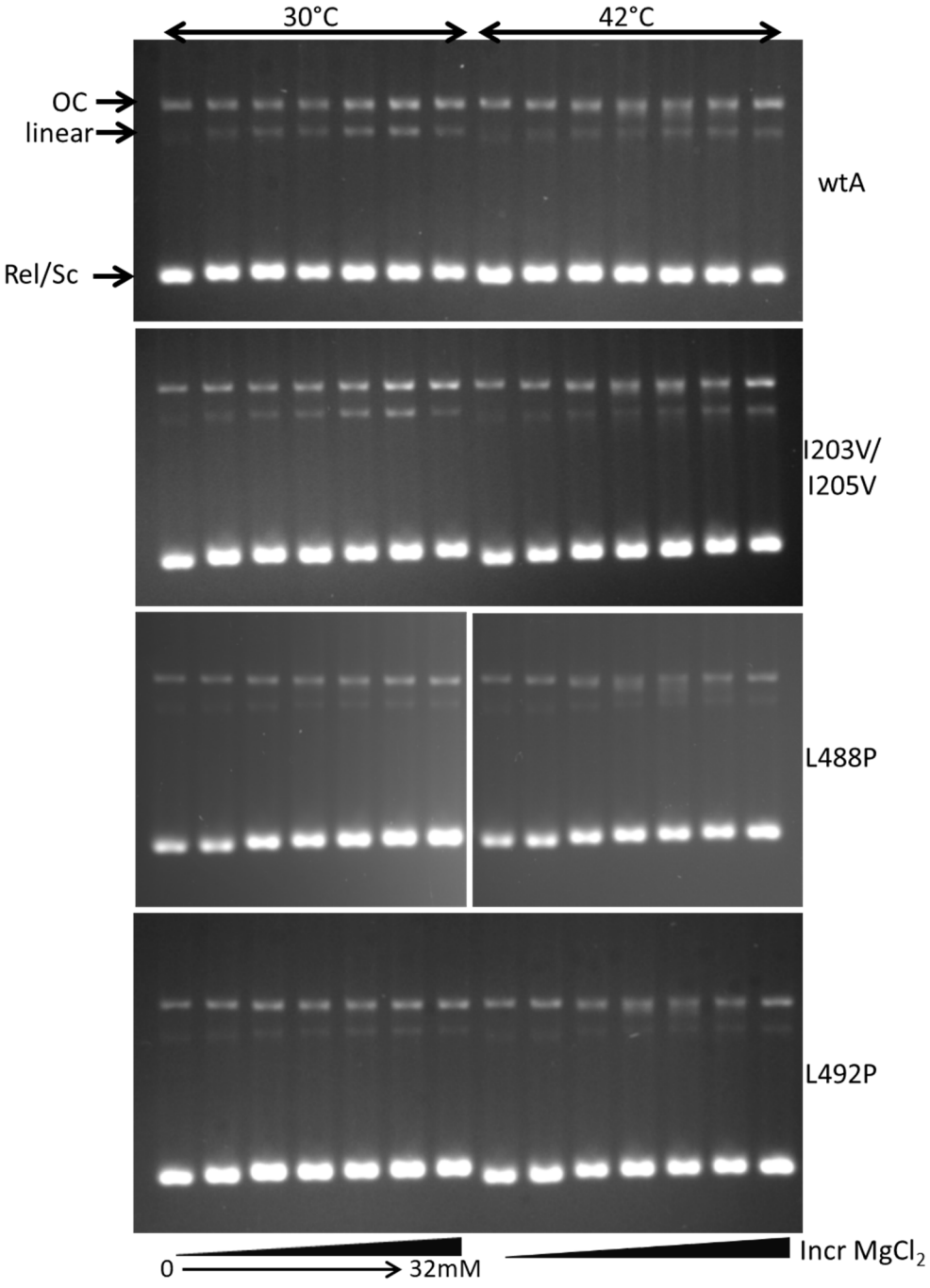

Figure 4.16: Cleavage activity of GyrA hyper-recombination mutants in the presence of increasing concentrations of Mg^{2+}. The effect of increasing Mg^{2+} ions (0 – 32 mM $MgCl_2$) on the cleavage activity of the three hyper-recombination GyrA mutants were compared to wild-type GyrA, all with equimolar wild-type GyrB, at permissive (30°C) and non-permissive (42°C) temperatures. Samples were analysed on a 1% agarose gel with 0.5 µg/mL Ethidium Bromide. OC indicates the open-circular or nicked DNA, Linear indicates the cleaved DNA and Rel/Sc indicates the supercoiled and relaxed DNA. wtA is the wild-type GyrA control. I203V/I205V, L488P and L492P are the respective GyrA hyper-recombination mutants.

The lack of Mg^{2+} concentration-dependent increase seen with the L488P and L492P mutants could be a result of their lower activity, or it could imply that they are defective in cleavage. It has been shown that cleavage (opening of the DNA-gate) and opening of the C-gate are mutually exclusive, so that the C-gate does not open if the DNA-gate is open (preventing the enzyme from falling apart) (Rudolph & Klostermeier, 2013). Thus, if these mutations affect the normal functioning of the C-gate, then it is likely that it would affect the DNA-gate (and cleavage) as well. This suggests that the C-gate possibly spends more time in an open conformation, which would result in the DNA-gate spending more time closed. This in turn would cause the enzyme to be unaffected by the increase in Mg^{2+} as it is not rate-limiting.

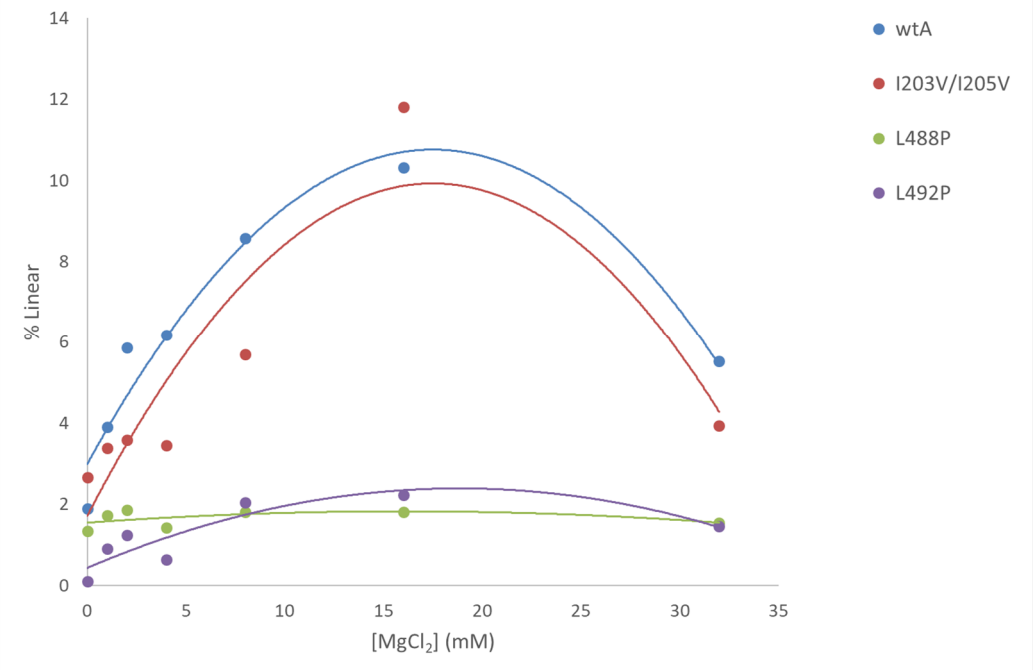

Figure 4.17: Proportion of double-stranded cleavage by GyrA hyper-recombination mutants in the presence of increasing concentrations of Mg^{2+}. The effect of increasing Mg^{2+} ions (0 – 32 mM MgCl2) on the cleavage activity of the three hyper-recombination GyrA mutants were compared to wild-type GyrA. The mean pixel value minus background was acquired for all DNA bands present from the samples in the 30°C assay gel. The percentage of linear DNA (% Linear) was ascertained as a percentage of the total DNA present. wtA is the wild-type GyrA control. I203V/I205V, L488P and L492P are the respective GyrA hyper-recombination mutants.

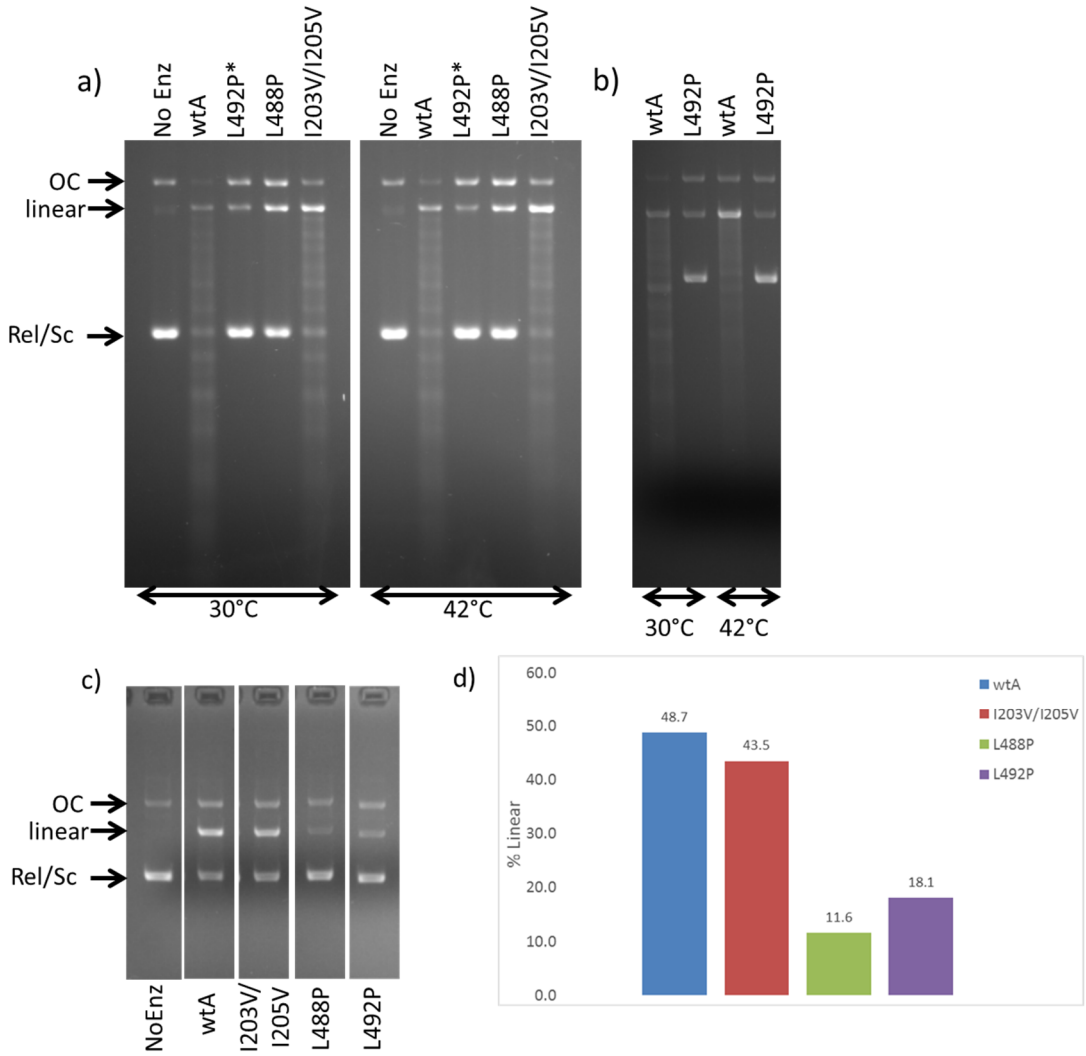

Figure 4.18: Cleavage activity of GyrA hyper-recombination mutants in the presence of Ca^{2+}. Ca^{2+}-induced cleavage activity of the three hyper-recombination GyrA mutants were compared to wild-type GyrA (at 1.5 µg in 30 µL or 132.98 nM), all with equimolar wild-type GyrB, at permissive (30°C) and non-permissive (42°C) temperatures. a) and b) are the same except for the concentration of the L492P mutant. L492P* indicates the L492P mutant but used at a quarter of the wild type concentration. c) is the same as a) except 0.5 µg of enzyme was used. Samples were analysed on a 1% agarose gel with 0.5 µg/mL Ethidium Bromide. OC indicates the open-circular or nicked DNA, Linear indicates the cleaved DNA and Rel/Sc indicates the supercoiled and relaxed DNA. d) Column Graph showing percentage of linear DNA present in c). The mean pixel value minus background was acquired for all DNA bands present from the samples in the 30°C assay gel. The percentage of linear DNA (% Linear) was ascertained as a percentage of the total DNA present. wtA is the wild-type GyrA control. I203V/I205V, L488P and L492P are the respective GyrA hyper-recombination mutants.

Ca^{2+} has been shown to stabilise cleavage with DNA gyrase (Reece & Maxwell, 1989, Kampranis & Maxwell, 1998a, Hockings & Maxwell, 2002) and it can support negative DNA supercoiling, although at a much lower rate (Noble & Maxwell, 2002). From Figure 4.19 we can see a similar result to cleavage with Mg^{2+}. The I203V/I025V mutant does not show as much cleavage with Ca^{2+} as wild type but it is not as deficient as the L488P and L492P mutants (wtA>I203V/I205V>L488P>L492P). This supports the idea that these mutants affect the closing of C-gate. In a study by Williams and Maxwell (1999a), when the DNA-gate was cross-linked, Ca^{2+}-based cleavage was only 10% of wild-type. When the C-gate was cross-linked it too was shown to have reduced Ca^{2+}-induced cleavage but it was much higher, 60% of wild type, than when the DNA-gate was cross-linked (Williams & Maxwell, 1999b). There was no effect of temperature with equal amounts of cleavage visible at both permissive and non-permissive temperatures.

ADPNP (5´-adenylyl-β,γ-imidodiphosphate) is a non-hydrolysable analogue of ATP. It has been shown to support negative supercoiling by DNA gyrase, although at a lower efficiency and is dependent on the topological state of the DNA (Sugino *et al.*, 1978, Bates *et al.*, 1996). ADPNP is thought to effectively stall the enzyme (due to the slow off rate), allowing a single round of supercoiling (Tamura *et al.*, 1992, Kampranis *et al.*, 1999a).

The L488P and L492P mutants show very little to no ADPNP-mediated cleavage (Figure 4.20). In effect, it takes three times more enzyme to see any cleavage over background with the L488P mutant and the L492P mutant doesn't show any increase cleavage over background, even with three times more enzyme. The I203V/I205V mutant does show cleavage with ADPNP, but it is less than wild type (Figure 4.20). Again, there is less cleavage at the non-permissive temperatures with all enzymes.

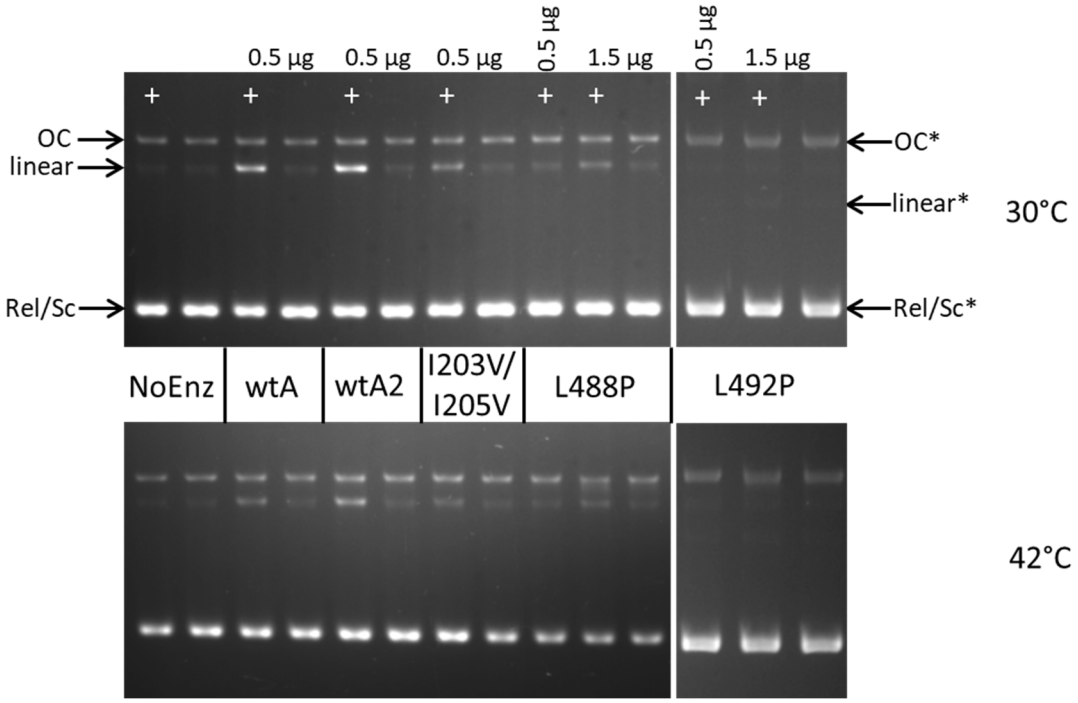

Figure 4.19: ADPNP (5´-adenylyl-β,γ-imidodiphosphate)-induced cleavage by GyrA hyper-recombination mutants. ADPNP-induced cleavage activity of the three hyper-recombination GyrA mutants were compared to wild-type GyrA, all with equimolar wild-type GyrB, at permissive (30°C) and non-permissive (42°C) temperatures. wtA and I203V/I205V were added to 0.5 µg (44.33 nM) and L488P and L492P were added to 0.5 and 1.5 µg (44.33 and 132.98 nM). Samples were analysed on a 1% agarose gel with 0.5 µg/mL Ethidium Bromide. + indicates samples containing 1 mM ADPNP. OC indicates the open-circular or nicked band, Linear indicates the cleaved band and Sc indicates the supercoiled band * indicates bands associated to the L492P gels only. No Enz is the no enzyme control. wtA and wtA2 are two separate wild type GyrA controls. I203V/I205V, L488P and L492P are the respective GyrA hyper-recombination mutants.

The hyper-recombination mutants were identified as temperature-sensitive alleles (Ashizawa *et al.*, 1999, Shimizu *et al.*, 1997). In spite of this, *in vitro*, none of them appear to be more sensitive to the non-permissive temperature than wild type (Figures 4.9 – 4.20). However, they are all less active at the non-permissive temperatures, this may be due to the *in vitro* ATPase activity of the GyrB protein being affected at the higher temperature (Maxwell & Gellert, 1984). Another gyrase mutation, a GyrB mutation R436S was also identified in a temperature-

sensitive screen (Gari *et al.*, 1996) however, when the enzyme was characterised *in vitro* it was found not to be temperature sensitive (Pang *et al.*, 2005). It was shown to have a poor k_{cat} relative to wild type and upon further *in vivo* investigations was shown not to be temperature sensitive at all, i.e. the enzyme was shown to be functional at the higher temperature. However, this poorer activity was demonstrated to cause supercoil disruption near the terminus of the replication *dif* site. The authors argued that at the higher temperature where replication rates are faster, this would have many implications downstream such as replication fork collapse and refiring of the origins, which could then lead to release of DSBs and induction of SOS response (Pang *et al.*, 2005). This 'Terminal Chaos' hypothesis could be applied to the hyper-recombination mutants as well, however, it would not explain the particular hyper-recombination phenotype observed (Ashizawa *et al.*, 1999, Shimizu *et al.*, 1997).

4.4 Conclusions

Table 4.2: Summary of the biochemical data from the hyper-recombination mutants. Values are in relation to wild type.

		I203V/I205V	L488P	L492P
Supercoiling	titration	NSD	~3-fold lower	NSD
	time course[#]	~3-times slower	~3-times slower	~3-times slower
Relaxation		NSD	deficient	deficient
Cleavage	OA^*_1	~2-fold lower	~3-fold lower	~4-fold lower
	CFX_1	~2-fold lower	NSD	NSD
	$Mg^{2+}{}_1$	NSD	~5-fold lower	~5-fold lower
	$Ca^{2+}{}_{1,2}$	NSD	~4-fold lower	~3-fold lower
	$ADPNP_1$	2-fold lower	20-fold lower	17-fold lower

NSD – not significantly different; # based on time point that wtA reached ~50% supercoiling; * at 150 ng of enzyme; 1 – differences based on mean pixel values from gel scans; 2 – at 0.5 µg of enzyme.

Ashizawa *et al.* (1999) and Shimizu *et al.* (1997) suggested the hyper-recombination mutants were causing DSBs in the chromosome and this was inducing illegitimate recombination in the form of spontaneous excision of specialised λ *bio* transducing phage and induction of spontaneous excision of λ prophage. They proposed this based on limited biochemical data from

one of the mutants showing an increase in linear DNA during the mutant's reaction cycle. From the biochemical characterisations I have performed on all three mutants, it seems that the I203V/I205V mutations do not have a large effect on the enzyme (Table 4.2) and the L488P and L492P mutations seem to affect the operation of the C-gate.

Taken together, it appears that the I203V/I205V mutations result in slightly defective DNA gyrase (Table 4.2). This is most evident from all the cleavage assays (Figures 4.15-4.20) where it always seems to show lower levels of cleavage than wild type, although this is marginal. In the gyrase reaction cycle, ATP hydrolysis, not cleavage, is thought to be rate limiting (Tamura *et al.*, 1992, Bates *et al.*, 1996, Kampranis *et al.*, 1999a, Bates & Maxwell, 2007), which explains why the I203V/I205V mutant would appear to be competent in supercoiling whilst having a slower or defective cleavage activity. Relaxation, despite the weaker cleavage activity, would appear to be near wild type levels as ATP-independent relaxation of negative supercoils by DNA gyrase is a much less efficient process than supercoiling (Higgins *et al.*, 1978). A similar GyrA mutant, G214E, was identified *in vivo* which resulted in resistance to the bacterial toxin CcdB (Miki *et al.*, 1992). This mutant and the G214A mutant were purified and their activity was analysed (Smith & Maxwell, 2006). The G214E mutant was shown to be mostly misfolded but the G214A mutant was said to have equivalent supercoiling activity as well as comparable cleavage in the presence of CcdB and CFX. This raised questions as to why this mutant would confer *in vivo* resistance to CcdB (Smith & Maxwell, 2006). This is similar to the I203V/I205V mutants in that the biochemical assays do not reveal an *in vitro* phenotype that would explain the *in vivo* phenotype.

Conversely, the L488P and L492P mutations appear to be affecting the C-gate of DNA gyrase. A mutation thought to destabilise the C-gate (GyrA T467S – *Salmonella* Typhimurium numbering) has been shown to rescue a GyrB mutation in *Salmonella* Typhimurium (Blanc-Potard *et al.*, 2005). The GyrB mutation was shown to be resistant to nalidixic acid, hypersensitive to novobiocin and have reduced supercoiling activity *in vivo*. The mutation in GyrA (T467S) reduced the sensitivity to novobiocin and partially restored the supercoiling

activity to the enzyme but increased the resistance to nalidixic acid. This could confirm destabilisation of the C-gate as it would likely show lower activity. However, the *in vitro* activity of this enzyme was not analysed making it difficult to evaluate how the mutation really affected the activity of the enzyme. Another C-gate mutation GyrA R462C, which was identified as a CcdB-resistance mutation *in vivo* (Bernard & Couturier, 1992, Bernard *et al.*, 1993) and shown to obstruct binding of the bacterial toxin *in vitro* (Kampranis *et al.*, 1999c, Dao-Thi *et al.*, 2005), was demonstrated to have normal supercoiling and drug-induced cleavage activities but the relaxation and natural cleavage activity was not investigated (Smith & Maxwell, 2006). This would mirror the L488P and L492P mutations which did not really affect the supercoiling or drug-based cleavage activity (Table 4.2).

Overall the C-gate in DNA gyrase appears to be vital for the stability of DNA gyrase and attempts to delete it have been unsuccessful (Maxwell and Mitchenall, unpublished data). Martinez-Garcia *et al.* (2014) have successfully made a topoisomerase II with a truncation in the C-gate (83 amino acids between L1039 and W1122), although this enzyme was shown to be 100-fold less active than wild type. Here I have shown that the L488P and L492P mutants have reduced relaxation activity, and reduced Mg^{2+}, Ca^{2+} and ADPNP-induced cleavage activity (Table 4.2). This may suggest that that these mutations are destabilising the C-gate. Upon discussion with David Lawson (Structural Biologist, JIC), the leucine to proline substitution in the α-helix could disrupt hydrogen bonding that could result in a kink in the helix (however, the true structural effects of these mutations could only be determined by crystallography). If this were the case, it could result in a situation where the gate either doesn't open efficiently, doesn't close effectively or cause a problem transducing information between the C-gate and the DNA-gate. Notionally, if the C-gate were to dwell in an open conformation, this could intrinsically cause the DNA-gate to remain closed maintaining the stability of the enzyme, which could result in reduced relaxation activity (reverse strand-passage) and lower cleavage activity. If the C-gate was predominantly in a closed conformation, it is unlikely that there would be reduced cleavage

activity under these conditions, as demonstrated by Williams and Maxwell (1999b) who showed cleavage activity with Ca^{2+} when the C-gate was cross-linked. Further to this, they showed that CFX-mediated cleavage can still occur when the DNA-gate is cross linked (Williams & Maxwell, 1999a). Similarly, the L488P and L492P mutants also showed wild-type levels of CFX-mediated cleavage (Figures 4.15 and 4.16). This indicates that CFX-induced cleavage may work by disrupting the cleavage-religation equilibrium of the enzyme, rather than stopping religation. Moreover, DNA cleavage has been shown to not be essential for drug binding (Critchlow & Maxwell, 1996). The slightly increased amount of cleavage with the L488P and L492P mutants in comparison to wild type after religation demonstrated in Figure 4.16 could be a result of the subunits coming apart as a result of the lack of stability in the C-gate during cleavage. This could also occur when a T-segment is captured and the DNA-gate doesn't open, the subunits could be forced apart and cause double-stranded DNA breaks. This is evident by the increase in ADPNP cleavage demonstrated by Williams and Maxwell (1999a) when the DNA-gate is permanently closed by cross-linking. However, this is in contrast to my data which shows reduced ADPNP-dependent cleavage by the L488P and L492P mutants to wild-type. An explanation for this is that the DNA-gate in these mutants is not permanently shut so this would occur at a much-reduced frequency than that seen by Williams and Maxwell (1999a). It would be difficult to resolve how much of the ADPNP-induced cleavage seen with the mutants was due to the presence of the nucleotide favouring cleavage (Kampranis *et al.*, 1999a) or how much was due to the subunits coming apart. However, this could explain the *in vivo* hyper-recombination phenotype.

4.5 Future work

To confirm this hypothesis, I would do further analysis of these mutations *in vivo* by moving them into the *E. coli* chromosome; this has been attempted and is discussed in Chapter 6. By evaluating their supercoiling activity as well as replication fork collapse, it may give more insight

into the effect these mutants could be having *in vivo*. It would also be good to directly probe for DSBs during log and stationary phases. I would also like to finish the *in vitro* characterisation of the mutants by looking at their cleavage and resealing kinetics and to evaluate the L488P and L492P effects on dimer stability when treated with CFX and ADPNP. It may also be interesting to use single-molecule techniques, such as FRET to investigate the opening of the C-gate of the L488P and L492P mutations. Further biochemical characterisations should include analysis of relaxation of positively supercoiled DNA by these mutants and further characterisation of the anomalous relaxation activity.

Chapter 5: Subunit Exchange

5.1 Introduction

Subunit exchange is often essential for the stability of molecular machines, allowing them to work continuously. It has been demonstrated in various systems and across species. This has been demonstrated during replication where the of Pol III* subassembly in *E. coli* was shown to frequently undergo subunit exchange with free subunits *in vivo* (Beattie *et al.*, 2017). Similarly, subunit exchange in *E. coli* Pol V allows for the error-prone polymerase to be in an inactive state when not needed (Shen *et al.*, 2003). In flagellar motor proteins, the rotor subunits FliN and FliM have been demonstrated to undergo subunit exchange with free FliN and FliM subunits, even while the rotor is functioning (Fukuoka *et al.*, 2010). In plants, the subunits of two docecameric small heat shock proteins from wheat and pea have been shown to undergo subunit exchange (Sobott *et al.*, 2002) and exchange of the αA- and αB-/crystallin with other small heat shock proteins have been shown to alter chaperone activity as a result of physiological heat stress (Bakthisaran *et al.*, 2015). Defective subunit exchange has also been implicated in disease, including cataracts (Fujii *et al.*, 2001), amyloidosis (Keetch *et al.*, 2005), and Neuropathies such as Alzheimer's, Parkinsons, Huntingindon's, Creutzfeldt–Jakob disease and Amyotrophic Lateral Sclerosis (Sun & MacRae, 2005, Shi *et al.*, 2016). It has also been suggested to be a potential mechanism behind certain cancers caused by chromosomal translocations (Ahuja *et al.*, 2000, Aplan, 2006).

The role of subunit exchange in site-specific recombination has been well studied in the Serine Recombinases. These enzymes, including the λ integrase and the cre recombinases, form tetramers and work by cleaving double-stranded DNA. Each subunit forms a phosphodiester bond with the 5´ end of the double-stranded DNA with 2 bp overhangs, before one dimer rotates 180° relative to the dimer, causing a crossover when the DNA is religated (Xiao *et al.*, 2016, Stark, 2014) (Figure 5.1). These enzymes play various roles from antigenic variation, to the movement

of mobile genetic elements, to phage integration and phage host range specificity (Johnson, 2015).

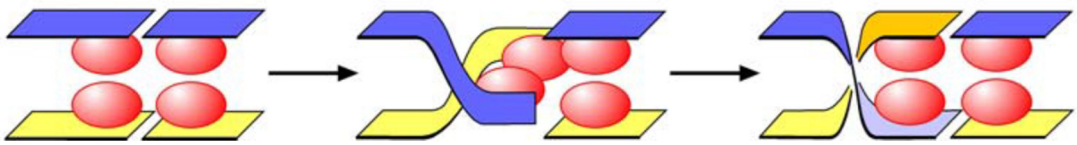

Figure 5.1: Cartoon demonstrating proposed subunit exchange of serine recombinases. Subunit exchange is thought to occur by rotation of one dimer 180° relative to the other resulting in a crossover when the DNA is religated. Figure Taken from (Stark, 2014) with permission

In order to explain topoisomerase-mediated IR, Ikeda *et al.* (1982) proposed a subunit exchange model. They suggested that when DNA gyrase binds and transiently cleaves DNA during the cleavage-religation reaction, it could be possible that another gyrase molecule in a similar position in the reaction cycle, but on an adjacent molecule of DNA, could bind to the original gyrase complex in an A_4B_4 conformation. Occasionally, when this intermediate dissociates, one subunit could be exchanged for the other resulting in a concomitant exchange of DNA strands followed by the religation reaction. Alternatively, subunit exchange may occur by the dissociation of the A_2B_2 complex resulting in heterodimers attached to DNA that could reassociate with another heterodimer in a similar situation, but attached to a different strand of DNA, leading to recombination (Figure 5.2) (Ikeda, 1994, Ikeda *et al.*, 1982, Ikeda *et al.*, 2004). Although this model was suggested, they never verified it experimentally. However, it has been suggested that it may be the mechanism behind the translocations associated with t-AML and some childhood leukaemias (Ahuja *et al.*, 2000, Azarova *et al.*, 2010). Although, this too has not been demonstrated.

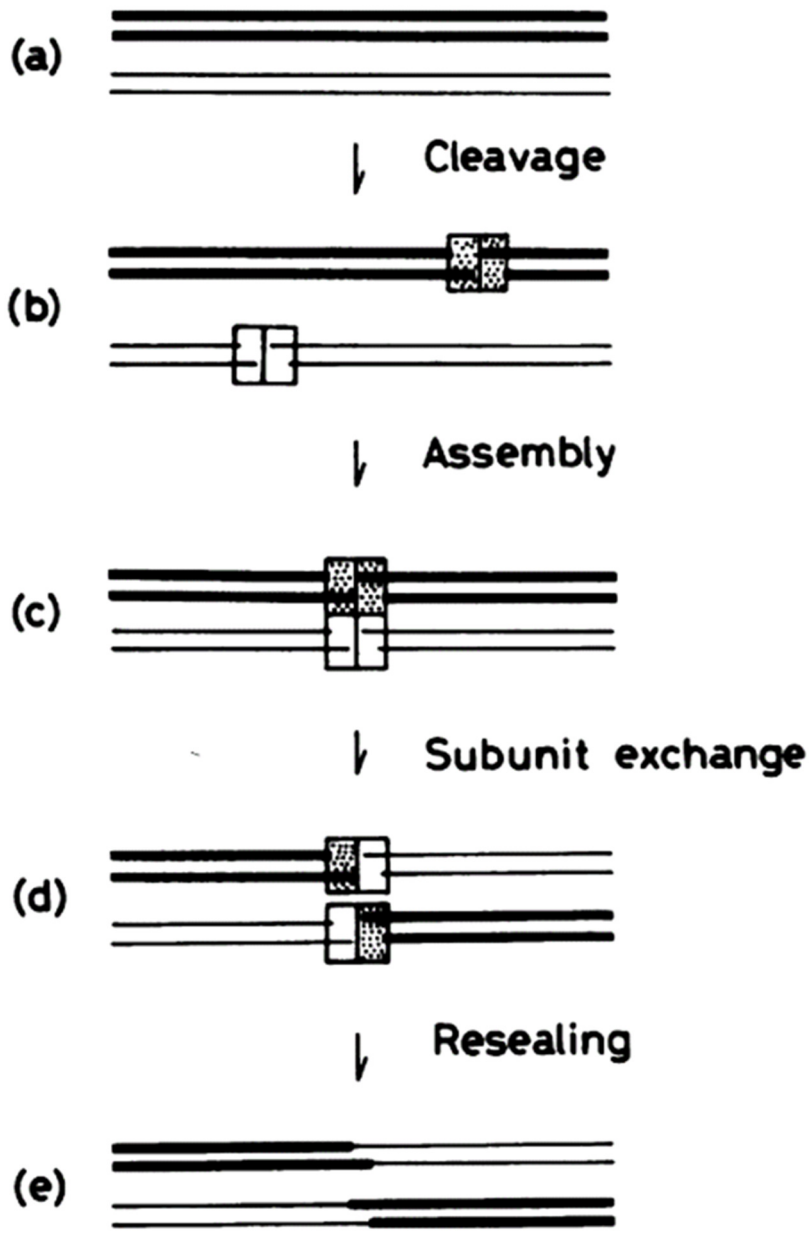

Figure 5.2: The proposed gyrase subunit-exchange model for illegitimate recombination. Each rectangle represents the AB heterodimer of DNA gyrase, composed of one gyrase A subunit and one gyrase B subunit. Two combined rectangles constitute the complete heterotetramer (A_2B_2) of the functional enzyme. The gyrase-DNA complex (b) assembles with another gyrase-DNA complex, forming the A_4B_4 conformation (c). The dissociation of the A_4B_4 conformation to the heterotetramer results in the subunit exchange that leads to the exchange of DNA strands (d). Figure taken from (Ikeda *et al.*, 1982) with permission from publisher

Given that the subunit-exchange model of topoisomerase-mediated IR was never fully examined, and because the λ-based assays were proving unsuccessful, a more direct investigation into subunit exchange was taken. This was done by examining the complexes formed by the GyrA subunits and trying to see if they are perturbed during the reaction cycle. I did this using native PAGE to look at how the complexes changed after incubation either alone or with various components of a supercoiling reaction (see Chapter 4 for method). We also looked at the complexes using native electrospray ionization mass spectrometry (ESI-MS) in collaboration with Prof. Justin Benesch at the University of Oxford.

5.2 Specific materials and methods

Native PAGE

Native polyacrylamide gel electrophoresis is a non-denaturing technique using tris-glycine polyacrylamide gels to look at native protein complexes. Discontinuous gels were run with a 7% resolving gel with a 3% stack (Table 5.1). Unless otherwise stated, 1 µg of protein in 1 x nondenaturing sample buffer (50% glycerol, 0.1 M Tris.HCl pH 6.8 and 0.002% bromophenol blue) was loaded into the stacking gel and samples were run partially submerged in a nondenaturing running buffer (50 mM Tris.HCl pH 8.9, 380 mM glycine), at 110 V for 2 h. Blue-Native PAGE gels are described in the General Methods (Chapter 2).

Table 5.1: Native PAGE gel components.

	7% Resolving gel	3% Stacking gel
30% Polyacrylamide (Severn Biotech Ltd, acrylamide:bisacrylamide 37.5:1)	1.4 mL	0.3 mL
1 M Tris.HCl (pH 8.9) (377 mM final)	2.6 mL	-
1 M Tris.HCl (pH 6.8) (130 mM final)	-	0.39 mL
TEMED (N,N,N´,N´-tetramethylethylenediamine) (Sigma)	10 µL	10 µL
10% Ammonium Persulphate (Sigma)	100 µL	50 µL
Ultrapure H_2O	2 mL	2.31 mL

Denaturation and refolding of GyrA and GyrA59

This is a modification of the protocol outlined in Hockings and Maxwell (Hockings & Maxwell, 2002). Wild-type GyrA and the truncated form, GyrA59, were diluted to 1 mg/mL in EB buffer without glycerol. Two millilitres of each protein were pooled together (4 mL final volume). To the pooled proteins, as well as 2 mL of each protein individually, Guanidine.HCl was added to 8.6 M before incubating at 37°C for 3 hours. Glycerol was added to 10% and then all three samples were transferred to SnakeSkin™ dialysis tubing. These were dialysed against 2 L of EB with 8 M urea overnight at 4°C. The dialysis was then transferred to 2 L of EB at room temperature for two rounds of 4 h, each round with fresh EB. A final dialysis step was performed overnight in 2 L of EB at 4°C. The refolded proteins were then analysed by native PAGE (7% resolving and 3% stack) and SDS PAGE (12.5% resolving and 4% stack).

Assays

Full-length wild-type GyrA or the truncated GyrA59 were either incubated alone or together, with or without: GyrB, pBR322* (relaxed or supercoiled), supercoiling assay buffer (see Chapter 4), 50 µM CFX (ciprofloxacin). Incubation times ranged from 30 min to 14 days at 37°C. Native sample buffer (see General Methods) was added before loading and resolving on Blue-Native PAGE gels (see General Methods). The hyper-recombination mutants were also analysed in a similar way, except they were only incubated for 48 h.

A supercoiling reaction (titration) was performed as described in Chapter 4 except an acetate-based assay buffer, AcAB, was used (250 mM Ammonium acetate, 4 mM magnesium acetate (pH 7.4)) with 1 mM ATP. Before this assay was run, GyrA and GyrB proteins were buffer exchanged into 1 x AcAB using ultrafiltration in Amicon® Ultra 0.5 mL centrifugal filters with a 30 kDa cut off. GyrA and GyrB were used at equimolar concentrations.

2D-PAGE

Bands from BN-PAGE (first dimension) were excised from the BN-PAGE gel and soaked in a solution of 1% SDS and 1% β-mercaptoethanol (Sigma) for 45 min before being briefly washing with H_2O. SDS PAGE gels were made as described in Chapter 2 except, 1.5 mm gels were poured with a single well comb in the stack and the denatured 1st dimension strip was cast in the stacking gel. Gels were run at 90 - 100 V for 3 h.

Western blot

Polyacrylamide gels were transferred to PVDF membranes using the BioRad Trans-Blot® Turbo™ system at 20 V, 2.5 mA, for 15 min. After transfer, membranes were briefly washed with Ponceau S then rinsed with ultrapure MilliQ H_2O. The membrane was blocked in TBS-T (50 mM Tris.HCl pH 7.6, 150 mM NaCl, 0.1% Tween-20) with 5% milk solids (Marvel Dry Skimmed Milk powder) for 10 min before incubating at 4°C overnight with monoclonal antibody (either anti-GyrA-CTD – 4D3 or anti-GyrB-CTD – 9G8; a gift from Alison Howells, Inspiralis) diluted 1/1000 in TBS-T 5% milk. The membrane was then rinsed briefly with TBS-T before washing three times for 10 min each at room temperature. The membrane was then incubated at room temperature for 1 h with secondary antibody (1/5000); rabbit polyclonal antimouse-HRP conjugate (Dako). This was then washed as described above. The membrane was flooded with Pierce™ ECL Western Blotting Substrate and left for 1 min at room temperature before covering with Clingfilm and exposed for 5 – 10 min onto Amersham Hyperfilm ECL Auto Radiography film before developing in a Konica Minolta SRX101A developer.

Native ESI-MS

This was performed and analysed by Justin Benesch at the University of Oxford. Native mass spectra were obtained on a Q-ToF 2 (Waters UK, Ltd) according to a protocol described previously (Kondrat *et al.*, 2015). Samples were infused by nanoelectrospray in 200 mM ammonium acetate, at protein concentrations in the range of 20-40 µM. Instrument conditions were as follows. Capillary: 1.7 kV, sample cone 200 V, extractor cone 20 V, accelerating potential

into the collision cell 50-150 V, collision cell pressure 35 µbar (argon), and backing pressure 0.007 mbar. All spectra were calibrated externally (using CsI as a reference) and processed using MassLynx software (Waters UK Ltd), and are displayed without background subtraction, and with minimal smoothing.

Glossary

Table 5.2: Glossary of terms used to describe various oligomers and samples of GyrA, GyrA59 and GyrB

Term	Definition
A + A59*	The denatured and refolded GyrA and GyrA59 which made the heterodimer
A & A59	The GyrA and GyrA59 subunits mixed together
A_2	The GyrA dimer
$A59_2$	The GyrA59 dimer
(AA59)	The heterodimer
(AA59) + A_2	A heterotetramer of the GyrA dimer and the heterodimer
(AA59) + $A59_2$	A heterotetramer of the GyrA59 dimer and the heterodimer
A_4	The GyrA tetramer
$A59_4$	The GyrA59 tetramer
$(AA59)_2$	A tetramer of the heterodimer (or a tetramer and the GyrA and GyrA59 dimers)
B	GyrB
A_2B_2	DNA gyrase heterotetramer

* contains GyrA and GyrA59 homodimers in the sample as well.

5.3 Results and discussion

To investigate whether the subunit-exchange model of topoisomerase-mediated IR is valid, I set up an assay looking for the creation of heterodimers of the full-length GyrA subunit and a C-terminal deletion (38 kDa), GyrA59 (Reece & Maxwell, 1991b, Kampranis & Maxwell, 1996) (Figure 5.3). In all assays, the GyrA and GyrA59 proteins were more than 95% pure (Figure 5.4).

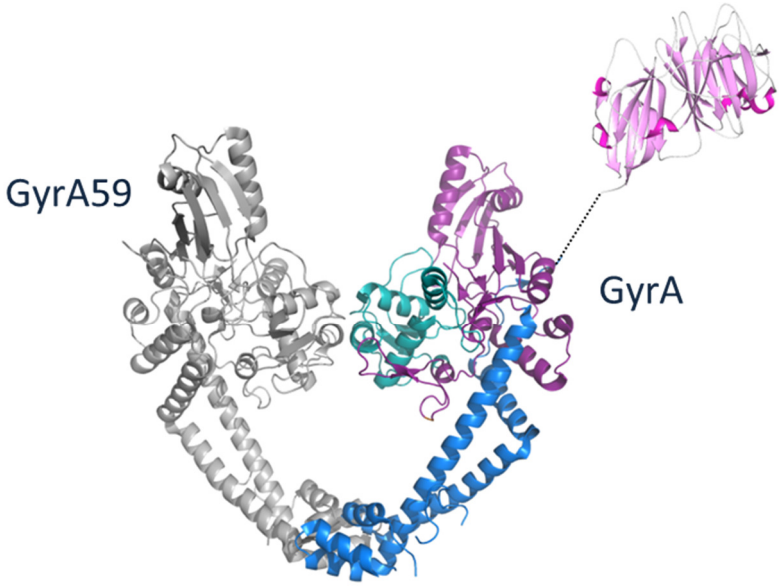

Figure 5.3: Model of proposed heterodimer of GyrA and GyrA59. The coloured subunit is the full-length wild-type GyrA subunit (GyrA). The grey subunit is the truncated GyrA59, it has the 38 kDa C-terminal domain deleted (pink domain on GyrA).

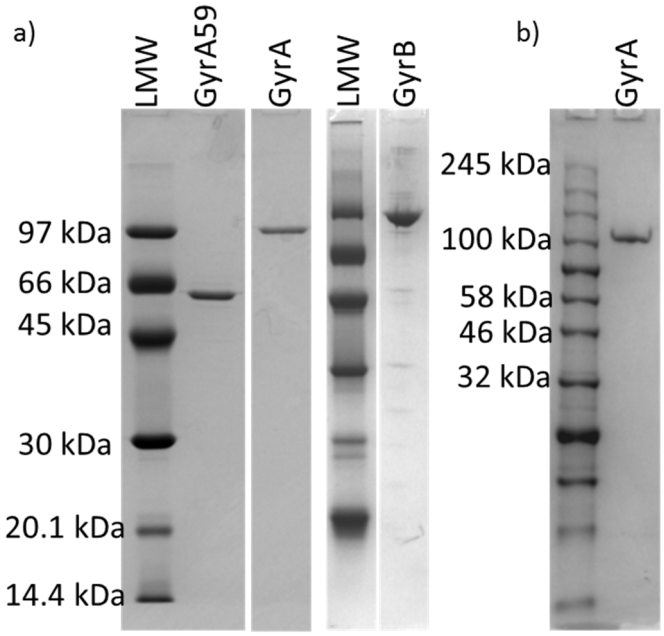

Figure 5.4: SDS PAGE of GyrA, GyrA59 and GyrB proteins used. a) is the GyrA and GyrA59 proteins at about 1 µg. GyrB is about 2 µg based on Bradford measurements. LMW is the low molecular weight marker with the sizes indicated on the left. b) is another preparation of GyrA, also at 1 µg. This GyrA was used for everything except the denaturing and refolding experiment. The molecular weights of the Broad Range, Color Prestained Protein Standard (New England BioLabs®$_{Inc}$) are indicated to the left.

To start with I made the heterodimer by denaturing in Guanidine.HCl and Urea and then refolding the GyrA and GyrA59 subunits together (Figure 5.5). From the native PAGE gel, you can see the appearance of a new band between the GyrA dimer and the GyrA59 dimer. The GyrA dimer is about 194 kDa, the heterodimer should be 156 kDa and the GyrA59 dimer is about 118 kDa. This gel indicates that the heterodimer was stable as a dimer and that the heterodimer was easily resolved from the GyrA and Gyr59 dimer by native PAGE. However, I found that the discontinuous native PAGE was not consistent as when I reran the heterodimer sample; sometimes the GyrA dimer or the GyrA59 dimer would not be visible on the gel. GyrB also did not show up on the gel occasionally (data not shown). It was for these reasons that I switched to running Blue-Native PAGE (BN-PAGE).

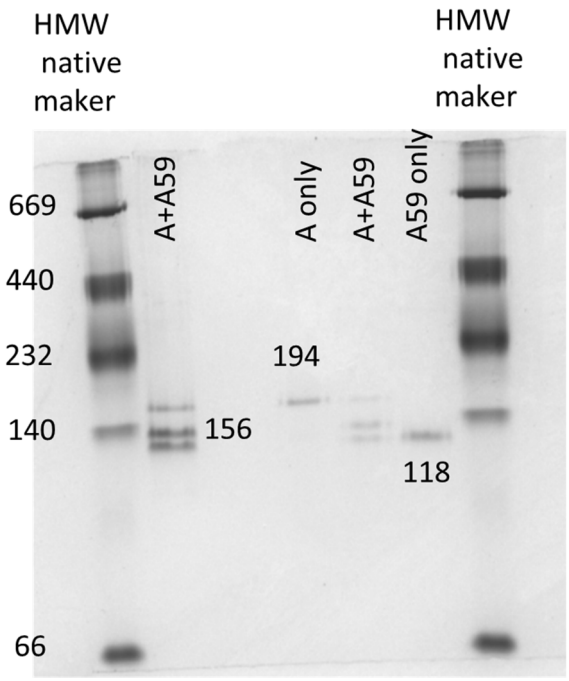

Figure 5.5: 7.0% Native PAGE gel with refolded GyrA and GyrA59 proteins after denaturation in 8.6 M Guanidine.HCl and 8 M urea. A is the GyrA subunit alone, A59 is the GyrA59 subunit alone, A+A59 is a mixture of the GyrA and GyrA59 subunits. HMW is the Native high molecular weight marker and the sizes of the bands in kDa are down the left side.

Figure 5.6 shows the GyrA, GyrA59, the refolded heterodimer and GyrB on a BN-PAGE gel. In this figure, you can see that there are a number of bands associated with all samples (see Table 5.2 for glossary). That is, dimers and tetramers with GyrA and GyrA59 and various complexes with GyrA/GyrA59 (Figure 5.6 b). I believe these are likely higher-order species of the samples as these proteins were greater than 95% pure (Figure 5.4). They are also present in the western blot when the Gyr(AA59) sample was probed with the anti-GyrA-CTD monoclonal antibody (Figure 5.6c). As the GyrA59 protein has the GyrA-CTD deleted (Figure 5.4) it will not be detected by the antibody thus the $A59_2$ or $A59_4$ complexes will not be seen. These higher complexes have also been seen previously, by me and others (Edwards, 2009) on the 7% native PAGE gels (data not shown). Again, it is important to note that with BN-PAGE, there can be as much as a 20% discrepancy between the actual molecular weight and the molecular weight observed on the gel (Schagger *et al.*, 1994, Wittig *et al.*, 2006) (discussed in Chapter 4).

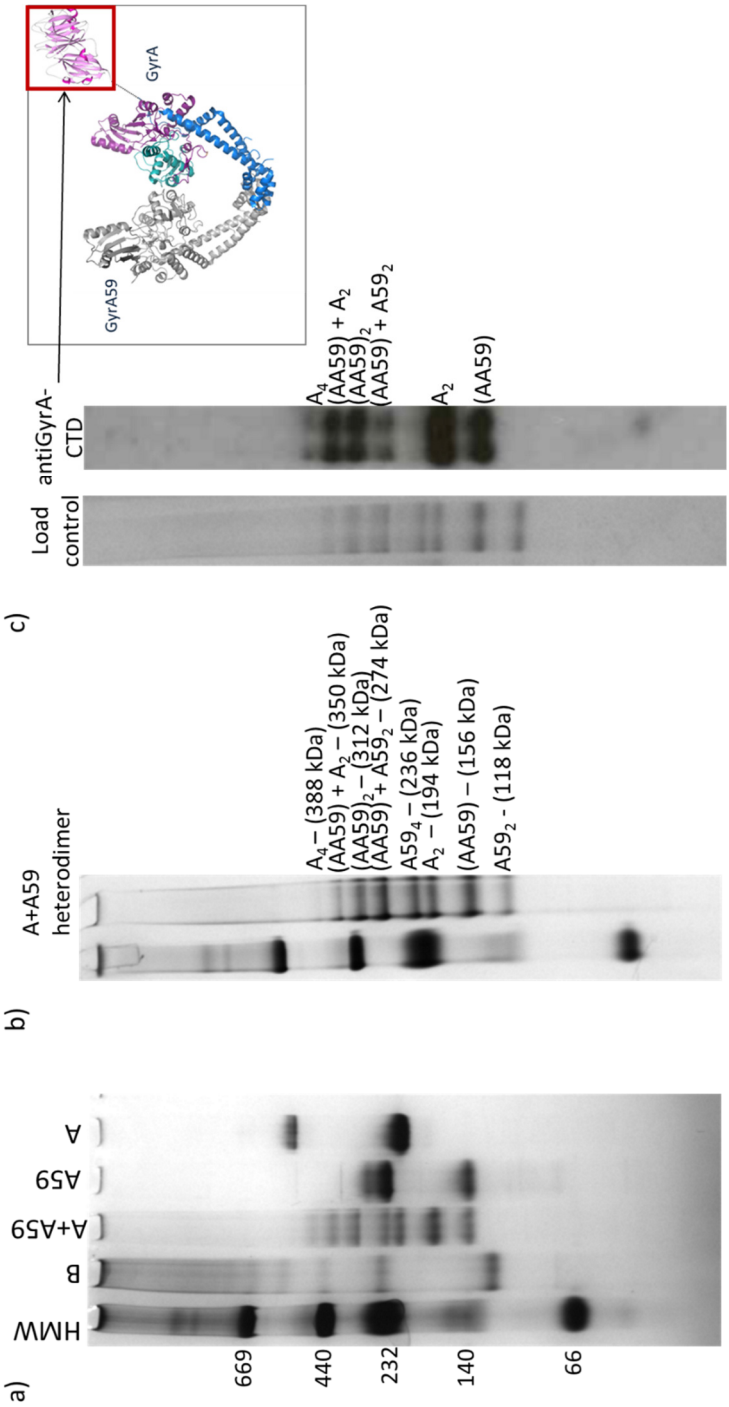

Figure 5.6: Blue-Native PAGE and Western blot of the GyrA/GyrA59 heterodimer. a) is a BN-PAGE of the GyrA (A), GyrA59 (A59), the refolded heterodimer (A+A59) and GyrB (B) run on a 4-12% gradient gel. HMW is the high molecular weight marker with the size of each band in kDa down the left-hand side. b) shows the refolded heterodimer with the higher-order complexes highlighted alongside, with their predicted molecular weights. c) is the refolded heterodimer stained with coomassie alongside the western blot probing for the GyrA-CTD (exposure time 10 min). The arrow indicates the domain the antibody was raised against on the heterodimer (panel in the grey box) with the GyrA-CTD highlighted by the red box. A_4 is

the GyrA tetramer, $A59_4$ is the GyrA59 tetramer, $(AA59)_2$ is the GyrA/GyrA59 heterotetramer, (AA59) is the heterodimer, A_2 is the GyrA dimer, $A59_2$ is the GyA59 dimer.

These higher-order complexes have also been demonstrated by native ESI-MS in collaboration with Justin Benesch (Figure 5.7). Figure 5.7a shows that DNA gyrase is still active in AcAB (as compared with normal supercoiling assay buffer) which was used in the native ESI-MS experiments. In Justin's data, it can be seen that the GyrA and GyrA59 associate into dimers, tetramers, hexamers and octamers (Figure 5.7b) and that GyrB associates in dimers, trimers, tetramers and pentamers (Figure 5.6 and 5.7c). From the data (Figure 5.6 and 5.7), it can be seen that GyrA and GyrA59 are primarily dimers in solution, agreeing with previously published data and crystal structures (Klevan & Wang, 1980, Morais Cabral *et al.*, 1997) but will associate into multimeric complexes in steps of two (Figure 5.7b). GyrB is primarily a monomer in solution in BN-PAGE, agreeing with previously published data (Liu & Wang, 1978, Ali *et al.*, 1993, Ali *et al.*, 1995, Costenaro *et al.*, 2007). In the spectra we can see it associates in dimers, but it does also appear to form multimeric complexes but seemingly only in steps of one (Figure 5.7c). Higher oligomeric species have also been demonstrated with yeast topoisomerase II, which was shown to form multimeric complexes up to octamers (Vassetzky *et al.*, 1994); these authors also showed that these multimeric complexes either associated in aggregates or in more regular rosette structures. From Figure 5.8, it is evident that the refolded GyrA/GyrA59 higher-order oligomeric species seen by BN-PAGE is also evident by ESI-MS. In this figure, the spectra show oligomeric species up to hexamers and various mass species can be resolved that reveal diverse associations between the GyrA and GyrA59 subunits, such as a tetrameric species consisting of the heterodimer (AA59) and the GyrA dimer A_2 (A_3:$A59_1$ in Figure 5.8). This corroborates the data obtained from the BN-PAGE (Figure 5.6).

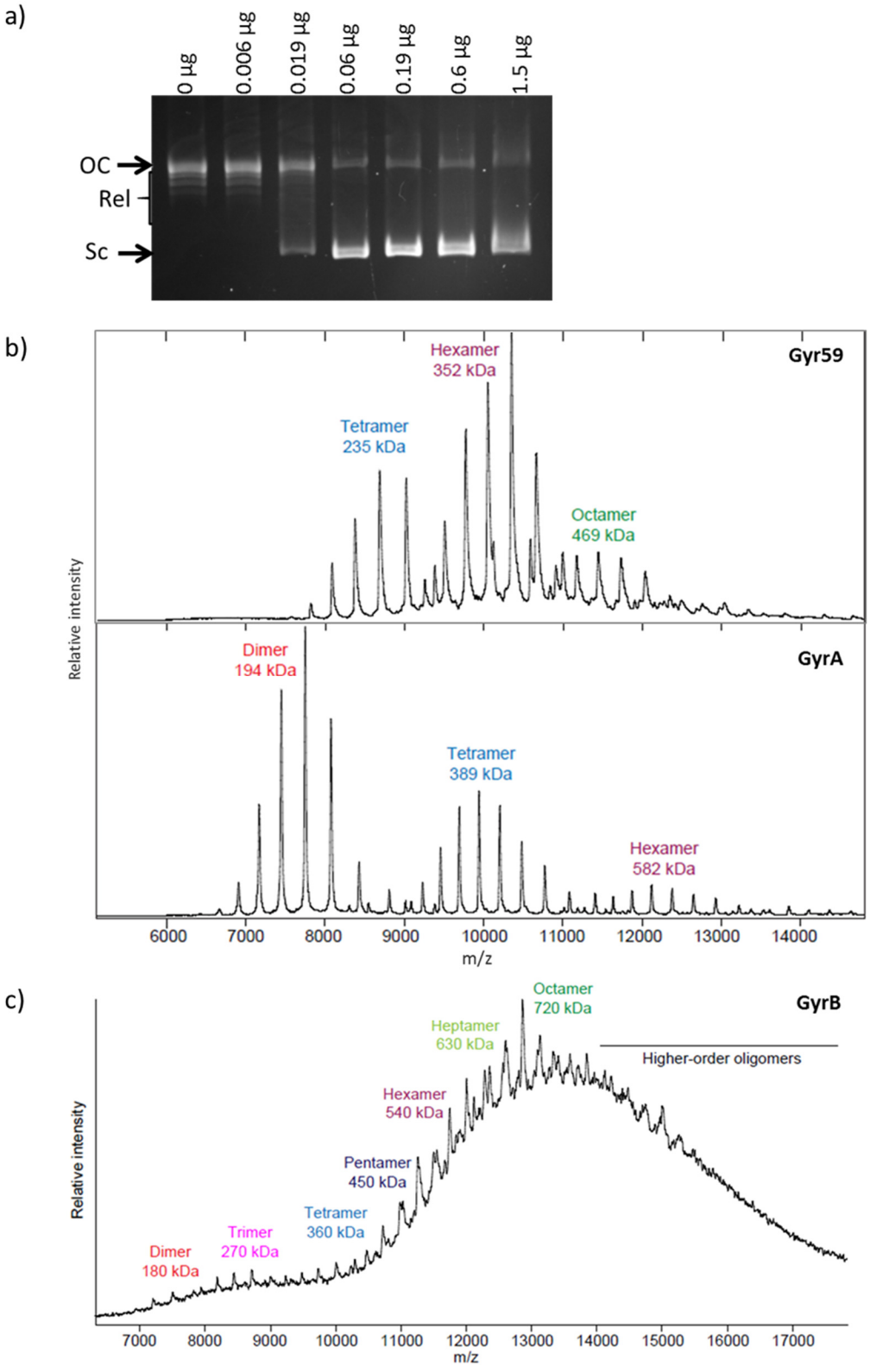

Figure 5.7: Electrospray ionization mass spectra from subunits of DNA gyrase. a) DNA gyrase supercoiling assay in acetate buffer, amount of enzyme (A_2B_2) added is in µg above. OC is the position of the nicked or open-circular band, Rel indicates the relaxed topoisomers, Sc indicates the supercoiled band. b) Mass spectra of GyrA and GyrA59 showing the different

oligomeric species. c) Mass Spectra of GyrB showing higher-order oligomers. ESI-MS was performed and the graphs assembled by Justin Benesch, University of Oxford.

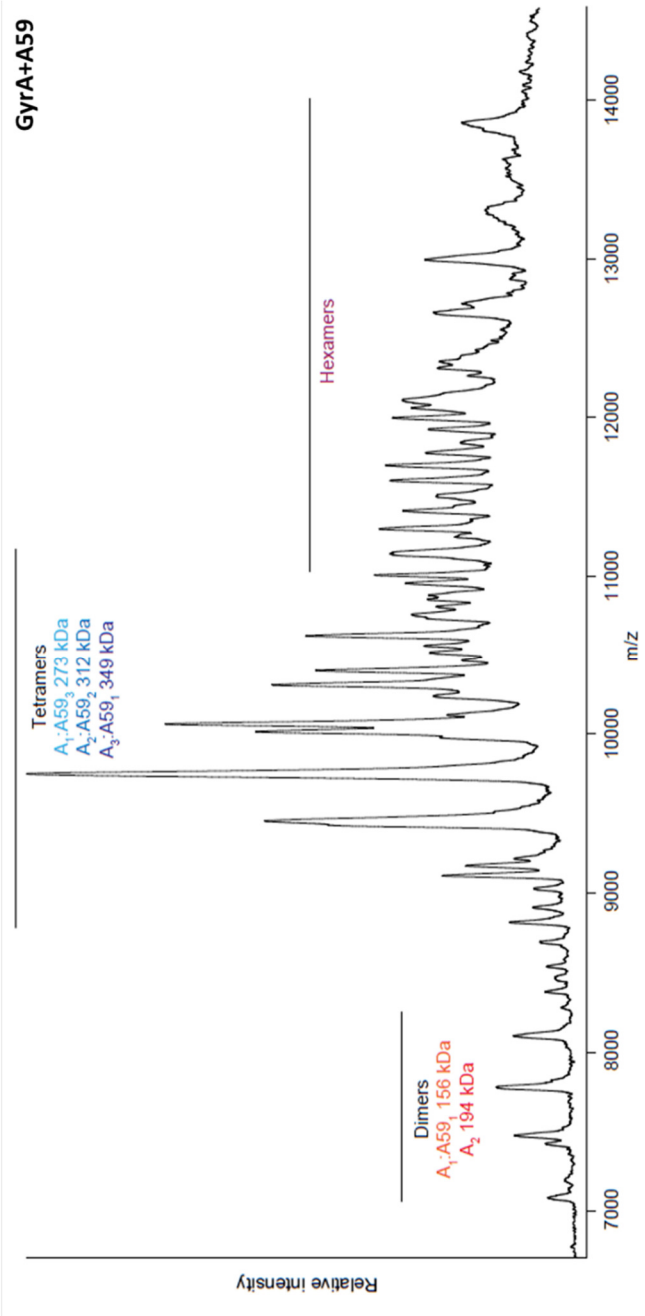

Figure 5.8: Electrospray ionization mass spectra from the refolded GyrA/GyrA59 subunits. Mass Spectra of the denatured and refolded GyrA + GyrA59 sample showing higher-order oligomers. ESI-MS was performed and the figure assembled by Justin Benesch, University of Oxford.

Seeing that the various complexes, including the heterodimer could be resolved using BN-PAGE, I incubated GyrA, GyrA59 and GyrB under supercoiling assay conditions (Figure 5.9) to investigate whether subunit exchange occurs during strand passage. Again, the antibody used in the blot in Figure 5.8b will only bind the full-length GyrA protein.

Firstly, from this figure in the A & A59 lane, we can see a band where we would expect to see the GyrA/GyrA59 heterotetramer ($(AA59)_2$ in the refolded heterodimer, Figure 5.6) however, this could be A_2A59_2 as opposed to $(AA59)_2$ (Table 5.2). Despite this, we don't see the formation of the heterodimer, in either the subunit-only samples or under assay conditions (1 or 3). Secondly, we can see that A_2B_2 forms high molecular weight aggregates visible by the smears running high up on the gel, which are also visible in 1, 2 and 3 on both western blots. In Figure 5.9a, in 1 and 3 we do see a band between where the GyrA dimer and GyrA/Gyr59 heterotetramer run (indicated by arrows on the figure), this is also present in Figure 5.9b but not seen in Figure 5.9c. Based on the proposed oligomers outlined in Figure 5.6, I suggest it is potentially a heterotetramer of (AA59) + $A59_2$. Further to this on the antiGyrA-CTD blot (Figure 5.9b), in samples 1 and 3 there is a band between the GyrA/Gyr59 heterotetramer and the GyrA tetramer (indicated by the asterisk) which is present in the refolded heterotetramer sample (sample A+A59 in the figure). This could be a heterotetramer of the GyrA dimer and GyrA/Gyr59 heterodimer, that is (AA59) + A_2. This could indicate that subunit exchange is occurring. However, it is not definitive as with the band indicated by the arrow ((AA59) + $A59_2$), we don't see an equivalent band in the refolded heterodimer (A+A59) sample. This may be due to the addition of GyrB which seems to have shifted the banding profile of the heterodimer sample, meaning the (AA59) + $A59_2$ heterotetramer in the refolded heterodimer sample may have formed other complexes with GyrB causing the original complex to be below detection levels. Again, we don't see any GyrA, or GyrA59 monomers.

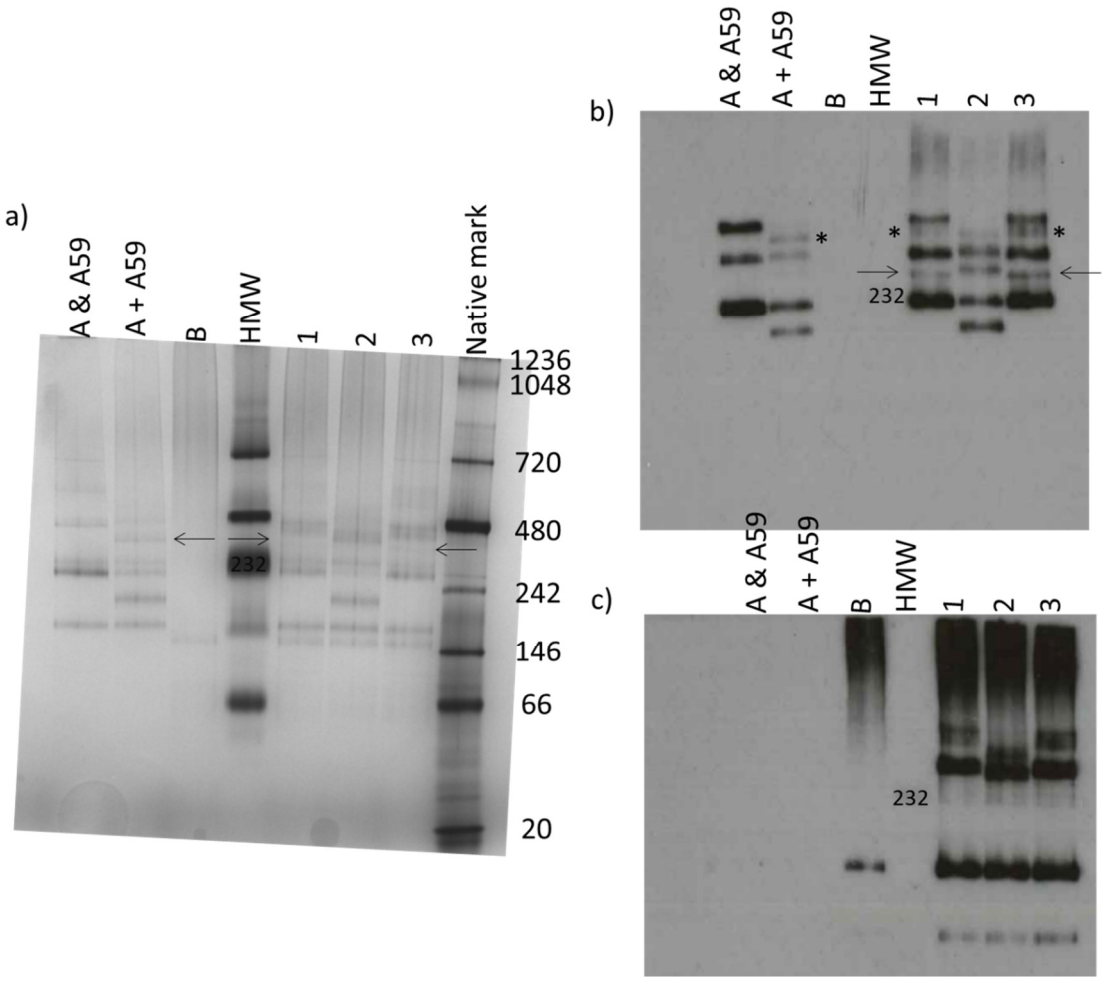

Figure 5.9: Blue-Native PAGE and western blots of gyrase subunits under supercoiling assay conditions. a) Coomassie stained 4-12% gradient BN-PAGE gel. HMW is the native high molecular weight marker. Native mark is the NativeMark™ Protein Ladder with the respective molecular weights down the right-hand side in kDa. b) & c) Western blots probing with the anti-GyrA-CTD monoclonal antibody and anti-GyrB-CTD monoclonal antibody respectively. A 5-min exposure time was done for both blots. A & A59 is GyrA and GyrA59 subunits together, A + A59 is the refolded GyrA/GyrA59 heterodimer sample, B is GyrB, 232 is the band at 232 kDa, 1 and 3 is A & A59 with B, relaxed plasmid pBR322*, and ATP (supercoiling assay buffer). 2 is the refolded heterodimer sample A + A59 with B, relaxed plasmid pBR322*, and ATP (supercoiling assay buffer). Samples were incubated for 2 h at 37°C. The arrows indicate the band seen between the GyrA dimer and GyrA/Gyr59 heterotetramer. * indicates the new band between the GyrA/Gyr59 heterotetramer and the GyrA tetramer.

As no GyrA/GyrA59 heterodimers or monomers were seen after a two-hour incubation, a longer time course was performed. It was run over 14 days, with and without GyrB, relaxed

pBR322*, ATP (supercoiling assay buffer) and CFX, taking samples at various time points (Figure 5.10).

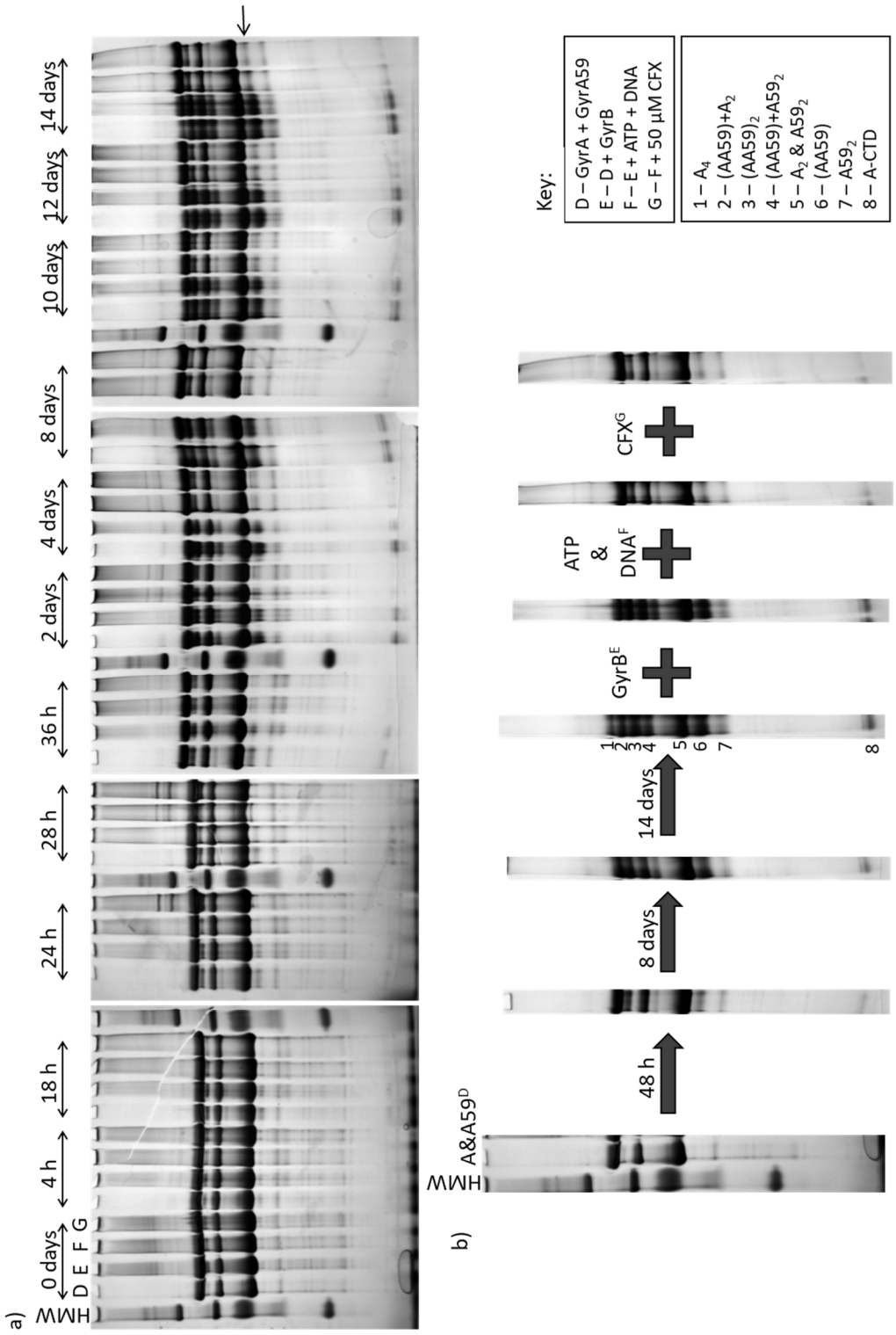

Figure 5.10: Effect of long-term incubation on subunit exchange. a) BN-PAGE experiment run over 14 days with samples taken at time points indicated above the double arrows. D is sample with GyrA and GyrA59 (A & A59) only; E is the sample with A & A59 and GyrB; F is the sample with A, A59, GyrB with ATP and relaxed pBR322* (DNA); G is the sample with A, A59,

B, ATP, DNA and 50 µM ciprofloxacin (CFX). b) is a diagram of a), it shows the A&A59 sample at different time points up to 14 days, then the samples taken of E, F, and G at the 14-day time point. The arrow indicates the position of the heterodimer. 1 – 8 indicate the proposed GyrA/GyrA59 species. HMW is the native high molecular weight marker.

From Figure 5.10 we can see the appearance of the heterodimer in the GyrA and GyrA59 only and the GyrA, GyrA59 and GyrB samples at 18 h, while it is only evident at two days when ATP, DNA and CFX are present. With the GyrA and GyrA59 only and GyrA, GyrA59 and GyrB samples (lanes 1 (D) and 2 (E) from each time point), at 14 days they appear to have a very similar banding pattern to the refolded heterodimer, indicating that there could be some subunit rearrangement occurring. To confirm this a 2D PAGE was run with the 14-day time point of GyrA and GyrA59 only sample (Figure 5.11).

Blue-Native-SDS 2D PAGE has been shown to be a useful techniques in studying membrane protein complexes and protein assembly (Schagger *et al.*, 1994, Wittig *et al.*, 2006, Reisinger & Eichacker, 2007). The premise is that protein complexes that have been resolved by BN-PAGE can be further refined into their subunits in the second dimension using SDS PAGE. Analysis of the second dimension separates the complexes by size allowing us to see which subunits are in the complexes observed in the BN-PAGE (Reisinger & Eichacker, 2007). The lane containing the GyrA and GyrA59 only sample at 14 days was cut out of the BN-PAGE gel and resolved in the second dimension on a 12% Tris-glycine-SDS gel (Figure 5.11). The SDS PAGE shows two distinct bands, one at around 100 kDa, and the second at around 58 kDa. Based on their sizes they would be GyrA (97 kDa) and GyrA59 (59 kDa) respectively. This is confirmed by the GyrA59 dimer from the BN-PAGE only showing a band at about 58 kDa in the second dimension. There are bands visible at around 35 kDa which could be the GyrA-CTD indicating that the full-length GyrA may be degrading over time. This is clear from the A_4 band (1 in Figure 5.11) which has a small amount of GyrA59 and a concomitant band at 35 kDa. For the bands containing both GyrA and GyrA59, the 2D PAGE further corroborates the suggested complexes (numbered in the box in Figure 5.11)

as the amounts of each subunit present on the 2D PAGE appear to be proportional to the ratio of subunits in the complex it is suggested to be in. That is, there is more GyrA59 present on the gel than GyrA from the band suspected to be the (AA59) + $A59_2$ heterotetramer.

Again, in Figure 5.9, we do not see the dimers dissociating to form monomers. This is not surprising as previous work on the related yeast topoisomerase II enzyme showed that this enzyme is a stable dimer and their work suggested that no subunit exchange occurs in the enzyme (Tennyson & Lindsley, 1997). In other work, conversely, heterodimers of the two isoforms of the human enzymes, topoisomerase IIα and topoisomerase IIβ have been shown to exist in HeLa cell lines and in other mammalian cells (Gromova *et al.*, 1998). However, these are thought to be associating during expression and were shown not to be due to subunit exchange (Biersack *et al.*, 1996).

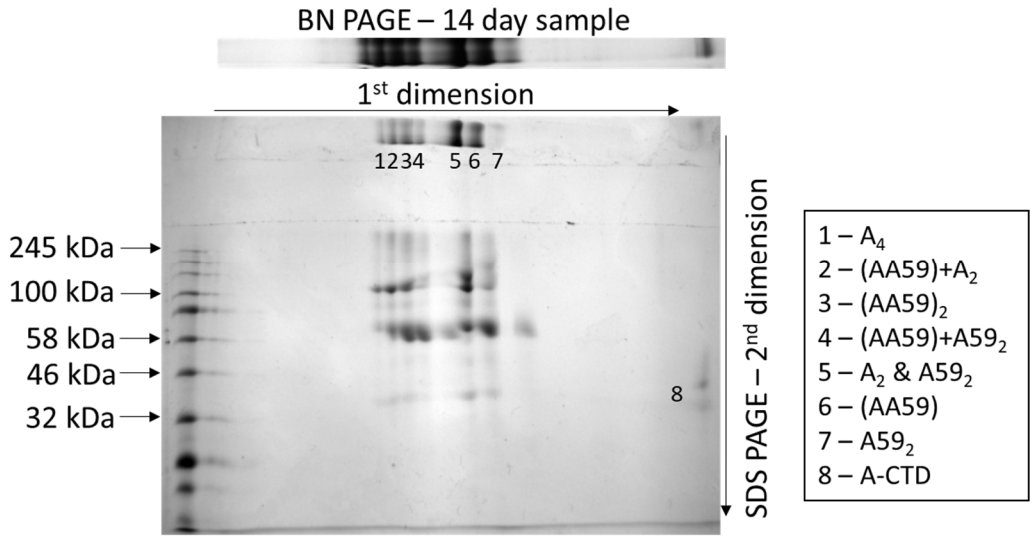

Figure 5.11: 2D-PAGE of GyrA and GyrA59 incubated over 14 days. The first dimension was the 14-day time point from the GyrA and GyrA59 only sample resolved on BN-PAGE. This lane was excised from the BN-PAGE gel and soaked in a solution of 1% SDS and 1% β-mercaptoethanol before running in the second dimension on a denaturing 12% Tris-glycine SDS PAGE gel with a 4% stack and stained with coomassie. The original BN-PAGE sample is shown above. The molecular weights of the Broad Range, Color Prestained Protein Standard (New England BioLabs®Inc) are indicated on the left. The suggested complexes from the BN-PAGE are in the box on the right. A indicates GyrA, and A59 indicates GyrA59. CTD is C-terminal domain.

In Figure 5.10, the samples with ATP and DNA, and ATP, DNA and CFX (lanes 3(F) and 4(G) from each time point) by 14 days do not show the level of rearrangement that is seen with the sample with just the subunits. This suggests that the presence of ATP and DNA reduce exchange, even in the presence of CFX which we would assume would cause more exchange considering the increase in IR seen by Ikeda *et al.* (Ikeda *et al.*, 1982, Ikeda *et al.*, 1984, Ikeda *et al.*, 1980) in the presence of oxolinic acid. To further investigate this, a time course was done over 7 days with the three subunits (GyrA, GyrA59, and GyrB) with and without DNA and CFX. Samples with ATP were run in duplicate over 48 h (Figure 5.12).

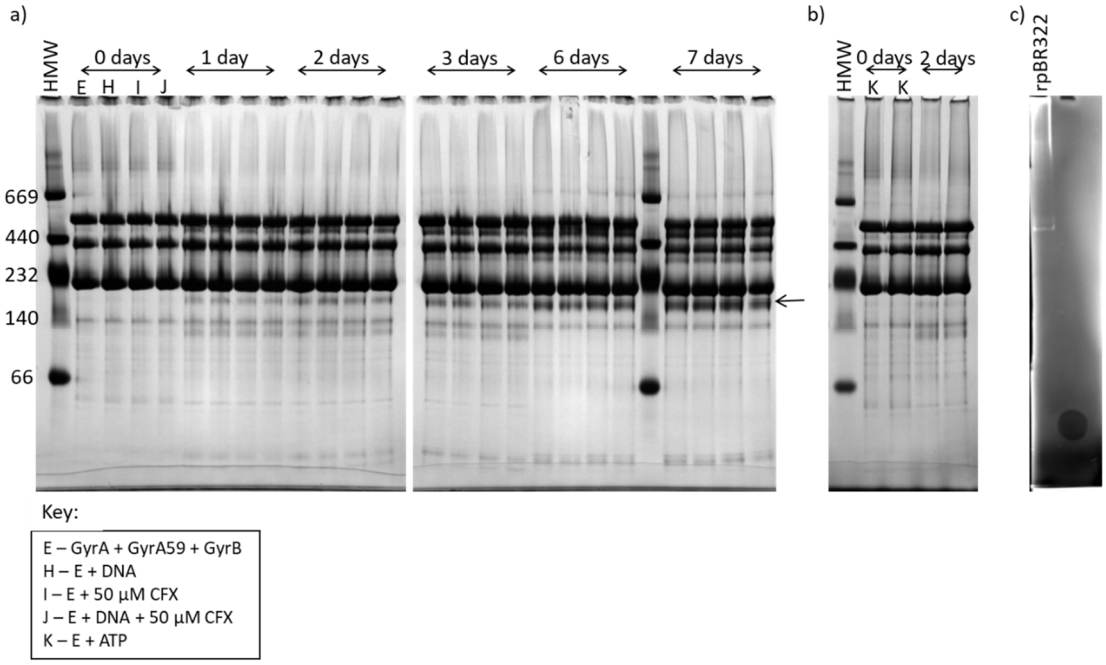

Figure 5.12: Effect of DNA, ATP and ciprofloxacin on subunit exchange. a) BN-PAGE subunit exchange experiment run over 7 days with samples taken at time points indicated above the double-headed arrows. E is GyrA & GyrA59 with GyrB; H is A, A59, GyrB with relaxed pBR322* (DNA); I is A, A59, B, 50 µM ciprofloxacin (CFX), and J is A, A59, B, with DNA and CFX. b) BN-PAGE of 48 h experiment with is A, A59, B, and ATP (indicated by K). c) 0.5 µg of relaxed pBR322* (rpBR322) run on a BN-PAGE gel then stained with ethidium bromide for 30 mins. The arrow indicates the position of the heterodimer. HMW is the native high molecular weight marker with the molecular weights of each band in kDa on the left-hand side.

From Figure 5.12, it is evident that the DNA doesn't reduce the formation of the heterodimer and it is also clear that CFX has no effect on heterodimer formation. However, ATP reduces the amount of heterodimer formed (Figure 5.12b). The reduction in exchange by ATP may suggest an additional role that ATP has during the reaction cycle. DNA gyrase uses the free energy of ATP binding and hydrolysis to introduce negative supercoils into DNA (Bates & Maxwell, 2007, Bates *et al.*, 1996). Here it also suggests that it may have some role in reducing subunit exchange. Vassetzky *et al.* (1994) found that ATP increased the presence of multimers of yeast topoisomerase II. This does not seem to be the case here, as the addition of ATP to the subunits did not seem to affect the formation of the complexes, with dimers and tetramers remaining as the major species on the BN-PAGE.

Figure 5.12c shows where the relaxed pBR322* DNA runs on the BN-PAGE. It is unlikely that the observed bands seen in the gels stained with coomassie or in the western blots are due to the protein binding to DNA. Particularly as there is a band evident with coomassie staining where the DNA runs, with the no DNA samples.

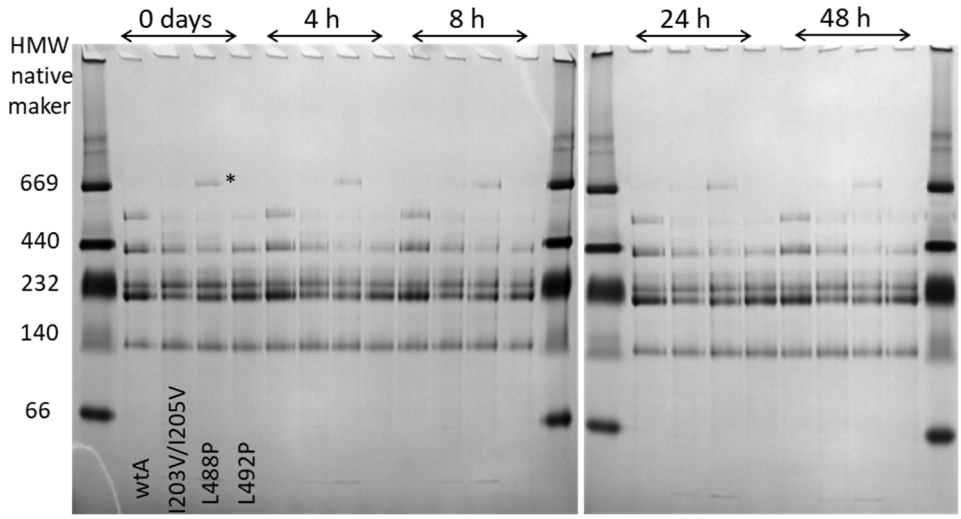

Figure 5.13: Subunit exchange with the hyper-recombination mutants. BN-PAGE with wild-type GyrA and the hyper-recombination mutants with GyrA59, all added to 1 µg. Samples were incubated at 37°C and removed from incubation at various time points up (indicated above the double arrows) up to 48 h. HMW is the high molecular weight marker with the molecular weights of the bands indicated on the left in kDa. wtA is the wild-type protein, I203VI203V, L488P and L492P are the hyper-recombination mutants, amino acid changes are referred to by their single letter codes. * is likely a contaminant as it does not show up in a western blot probing with anti-GyrA monoclonal antibodies (data not shown).

The hyper-recombination mutants discussed in Chapter 4 were also tested in the subunit exchange assay. None of them showed any increase over wild type in subunit rearrangement and, again (see Figure 4.8), they seem to form the higher oligomeric forms at a lower frequency. Interestingly, the subunit rearrangements seen in Figure 5.9 is not visible in Figure 5.13. The difference here is that half the amount of protein was used in the assay in Figure 5.13. This may suggest that the subunit rearrangement is dependent on concentration, although a significant effect by two-fold change in concentration is improbable. Thus, whether, in this particular situation, this is due to subunit exchange being concentration-dependent or whether it is below detection levels due to the lower starting concentrations, remains to be investigated. Vassetzky *et al.* (1994) showed that in yeast topoisomerase II, the appearance of the multimers was concentration dependent. Thus, to see the rearrangements and the higher-order oligomeric

species, higher concentrations of the proteins or a longer incubation period may be necessary. Further to this, where the hyper-recombination mutants are concerned, it may be necessary to have these mutations in the GyrA59 subunit to get a clear idea about whether these mutations could increase subunit rearrangements.

The data presented here may at first appear to conflict with work done by Gubaev *et al.* (2016) and Tennyson and Lindsley (1997). However, the assays and conditions used may explain the contrasting outcome. Both of these papers have looked for subunit exchange using a fluorescence based assay and biochemical assays using inactivated subunits. Gubaev *et al.* (2016) used FRET and fusion proteins that either had a cleavage defective GyrA subunit, or an ATPase deficient GyrB subunit. If subunit exchange occurred the resulting complexes would be inactive for either cleavage or ATPase activity, rendering the enzymes catalytically dead. Both the FRET and activity assays indicated that no subunit exchange was taking place. However, the assays presented were only run for 5 min (Gubaev *et al.*, 2016). Tennyson and Lindsley (1997) used cleavage inactivated yeast topoisomerase II and incubated it with wild-type protein up to 48 h. Here, they looked for a reduction in activity as the cleavage-deficient subunit recombined with the wild-type subunit, the pool of active enzyme would be decreased. They also used an immunotagged subunit exchange assay with two yeast topoisomerase II, one His-tagged, the other Ha-tagged. These were incubated together for up to two weeks before the samples were bound to a Ni^{2+}-chelating spin column. The eluted fraction was then immunoblotted. Here only complexes that had both the His-tag and the Ha-tag would be detected. Neither of these experiments showed any subunit exchange (Tennyson & Lindsley, 1997). Both Tennyson and Lindsley and Gubaev *et al.* looked for subunit exchange under assay conditions with ATP present. In fact, Tennyson and Lindsley (1997) used an ATP-regeneration mixture of phosphoenolpyruvate, pyruvate kinase, NADH, and lactate dehydrogenase in their assays. This would mean that the effect of ATP in the assay would be constant. In my assays, ATP reduced subunit rearrangements which could explain why no subunit exchange was evident in Tennyson

and Lindsley's work, even after two weeks. This is still not to say that it doesn't happen, it may just be below detection level in the assays presented.

5.4 Conclusions

Quaternary structure in proteins in the form of dimers and the formation in multimers is ubiquitous in biology (Marianayagam *et al.*, 2004). It has been shown to regulate function and activate enzymes. It plays an important role in the assembly of big protein complexes such as transmembrane channels or cell-surface receptors. Many DNA-binding proteins such as those involved in recombination, replication, transcription and DNA repair are functional as dimers or higher-order multimers (Marianayagam *et al.*, 2004).

It is well established that DNA gyrase functions as an A_2B_2 heterotetramer (Higgins *et al.*, 1978, Sugino *et al.*, 1980, Klevan & Wang, 1980, Maxwell & Gellert, 1986, Reece & Maxwell, 1991a). Here, I present data that suggests that DNA gyrase may associate in higher-order complexes (Figures 5.6 – 5.13 and Figure 5.14) such as tetramers, hexamers and octamers as well, although the predominant species is always the dimer. This would concur with published work by Vassetzky *et al.* (1994) who found that multimers of yeast topoisomerase II were enzymatically active.

In this work, I have demonstrated that full-length GyrA can reassociate with the truncated GyrA59 to form heterodimers (Figure 5.14). However, in all of the work done to date on DNA gyrase, including that done here, GyrA has not been reported as a monomer. This may be because the monomeric species is too transient to be seen with the methods used to date. However, I believe that subunit exchange is occurring in the higher-order oligomers formed by DNA gyrase. Whether this is a direct subunit exchange as seen with serine recombinases (Stark, 2014, Xiao *et al.*, 2016) or whether it is due to rearrangements within the oligomers, is yet to be

determined. It also appears that the rearrangements may be concentration dependent (Figure 5.13), although further work needs to be done to confirm this.

The presence of plasmid DNA seems to have no protective effect against these rearrangements, however, ATP does (Figure 5.11 and Figure 5.14). Since it is unlikely that a cell would not have ATP available, whether this is biologically relevant may be up for debate. This subunit exchange may reflect a labile quaternary structure, especially considering it is stabilised by ATP. This may also suggest an additional role for ATP; as well as driving the reaction cycle, it may also have a protective role, ensuring that rearrangements of the subunits does not occur during the reaction cycle.

Addition of CFX did not show any increase in rearrangement of the subunits (Figure 5.11 and Figure 5.14). Although at first this may be surprising as quinolones have been shown to increase DNA gyrase-mediated IR (Ikeda *et al.*, 1982, Ikeda *et al.*, 1984, Ikeda *et al.*, 1980), however, the quinolones themselves may have no bearing on the actual subunit rearrangement. CFX would however, stabilise a cleaved-DNA state on the protein which could result in DNA recombination during subunit rearrangement.

In summary, I have demonstrated that subunit exchange is possible with DNA gyrase although it seems to occur in higher-order oligomers, not through the dissociation of the dimers.

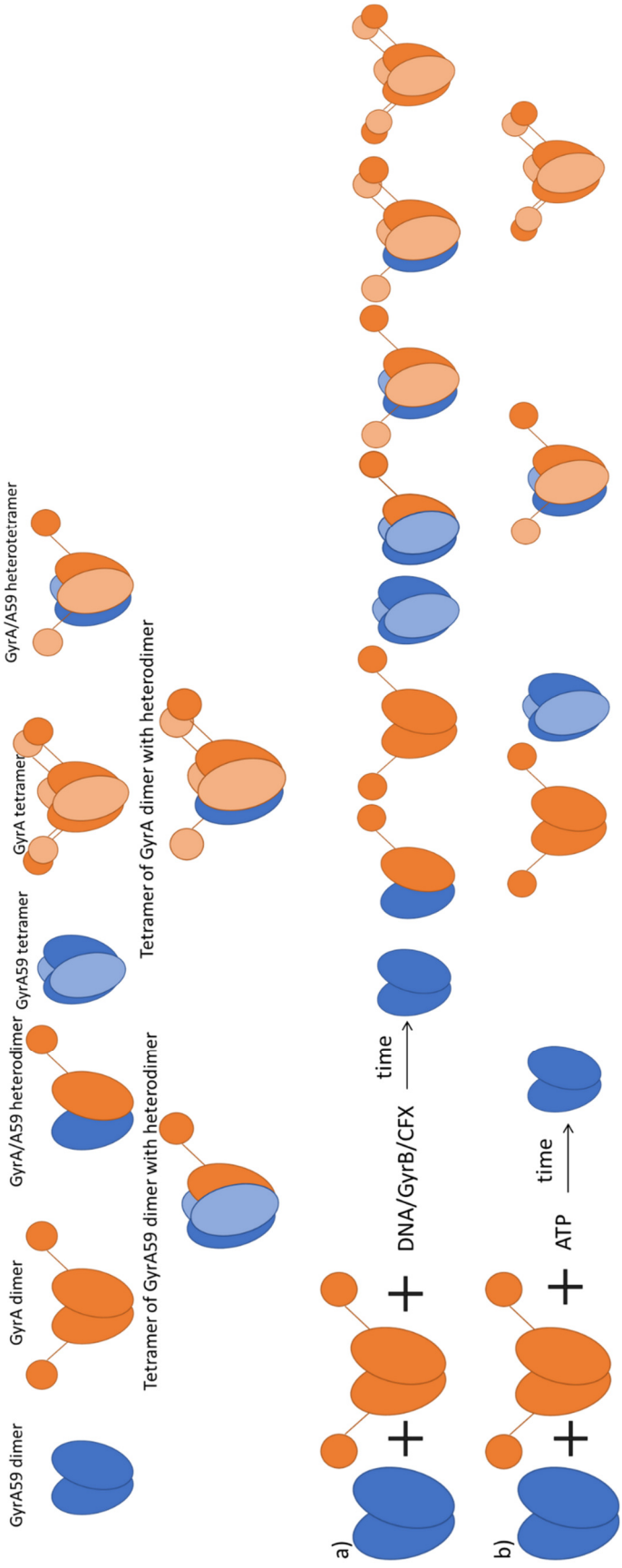

Figure 5.14: Summary Diagram of formation of heterodimers and oligomeric species. Top two lines shows the various species seen. The bottom three lines show the species observed

with a) just the GyrA and GyrA59 subunits (D from Figure 5.10) or with DNA (H from Figure 5.12), CFX (I from Figure 5.12) or DNA and CFX (J from Figure 5.12) incubated long term (arrow with time above). b) with ATP (K from Figure 5.12). The blue shows the GyrA59 subunit and the orange is the GyrA subunit.

5.5 Future work

In future work, I would like to investigate the concentration dependence of the rearrangements, either using BN-PAGE and immunodetection or by ESI-MS. It would be good to assess whether subunit rearrangements occur with the hyper-recombination mutations if more protein is used, and if the mutations in GyrA59 would increase the rearrangements. It would be interesting to see if I get a similar result to Tennyson and Lindsley by having an ATP regenerating system during the long-term incubation of these proteins. Alternatively, to see if ADP stimulates the rearrangements. We have also recently made GyrA subunits that are fluorescently tagged which may provide an alternative way of investigating subunit exchange with both the species being full-length GyrA subunits. I also feel it is important to further investigate if the higher-order oligomers are also seen *in vivo* and to try and ascertain whether this model is biologically relevant.

Chapter 6: Quinolone-Induced Antimicrobial Resistance

6.1 Introduction

Antibiotic resistance is a growing global threat with resistance to all classes of antibiotics now reported worldwide. This issue is compounded by a lack of innovation and few new structural classes of antibiotics brought to the clinic (see Chapter 1) (Bush *et al.*, 2011, Walsh & Wencewicz, 2014, Lewis, 2012). To tackle antibiotic resistance, we need to review our antibiotic stewardship and discover new antibiotics that are not susceptible to known resistance mechanisms. Additionally, we need to understand how resistance develops and how bacteria evolve under the selection pressure of antibiotic killing. Many complex biochemical and physiological processes are involved in the development of resistance and often our fundamental understanding of these processes is lacking (Davies & Davies, 2010).

Another complexity is the effect sublethal doses have on the development and selection of resistance. There are a number of studies and reviews (Andersson & Hughes, 2014, Gullberg *et al.*, 2011, Hughes & Andersson, 2012) describing and discussing the mutagenic effect of low concentrations of antibiotics on bacteria. They have shown that sublethal doses of antibiotics can select for resistance by promoting homologous recombination (Lopez & Blazquez, 2009) and horizontal gene transfer (Laureti *et al.*, 2013), by induction of the SOS response (Blázquez *et al.*, 2012, Thi *et al.*, 2011), or by RpoS induction (Gutierrez *et al.*, 2013). Exposure to sublethal concentrations of antimicrobials has also been shown to increase the number of persister cells (Dörr *et al.*, 2009, Goneau *et al.*, 2014), as well as to the enrichment of resistance genes within the population (Gullberg *et al.*, 2011). Bacteria can be subjected to subinhibitory levels of antibiotics in a variety of environments. These include concentration gradients due to spatial variation within a human body (Hermsen *et al.*, 2012), excretion of unabsorbed antibiotics into the natural environment (Pletz *et al.*, 2004, Mathieu *et al.*, 2016) or as a result of non-medical

uses of antibiotics, such as the agricultural use (ter Kuile *et al.*, 2016, Hughes & Andersson, 2012) or through effluent from pharmaceutical plants (Andersson & Hughes, 2014). Bacteria are also often exposed to natural environmental concentration antibiotic gradients produced by other bacteria and fungi (Andersson & Hughes, 2014). There is also the effect that long-term use of antibiotics in prophylactic treatment of recurrent infections has had on the rise of antibiotic resistance (Goneau *et al.*, 2015, Sethi *et al.*, 2010).

As discussed more widely in the introduction (Chapter 1), quinolones are a potent class of synthetic antibiotics that target DNA gyrase and DNA topoisomerase IV. They are the most successful class of topoisomerase inhibitors with fluoroquinolones being widely prescribed in the United States of America and Europe (Linder *et al.*, 2005, Pitiriga *et al.*, 2017). This, however, has led to an increase in resistance to quinolones including upregulation of efflux pumps, plasmid-based resistance or mutations in the gyrase or topo IV genes (Hooper, 2003, Redgrave *et al.*, 2014). This widespread resistance has resulted in revised stewardship for quinolones (Pitiriga *et al.*, 2017) as well as the WHO categorizing quinolones as a highest priority 'Critically Important Antimicrobial' (WHO, 2017).

Although the rise of quinolone resistance is well-documented (discussed in Chapter 1), there is also evidence that subinhibitory treatment with quinolones can lead to multidrug and non-quinolone resistance. However, this is not well-documented and the cause is not yet fully established. One study shows an increase in the resistance of quinolone-susceptible methicillin-resistant *Staphylococcus aureus* to nafcillin when exposed to subinhibitory doses of ciprofloxacin or levofloxacin (Tattevin *et al.*, 2009). A later study by Kohanski *et al.* (Kohanski *et al.*, 2010) demonstrated that treatment of *E. coli* MG1655 with norfloxacin led to increased resistance to kanamycin and ampicillin. The authors suggest that the mechanism behind this resistance is due to an increase in mutagenesis as a result of oxidative stress caused by the antibiotic. The legitimacy of this has been discussed directly by two other papers (Keren *et al.*, 2013, Liu & Imlay, 2013) (discussed further in Chapter 1). Along with this continued argument on the mechanism

behind this quinolone-induced resistance, further evidence is provided in a paper on *E. coli* isolates from preweaned dairy calves. These were treated with enrofloxacin or the cephalosporin ceftiofur for diarrhoea and respiratory diseases. They found that in the isolates from the quinolone-treated calves, 77% showed resistance to 3 or more antimicrobials. These included ciprofloxacin, streptomycin, tetracycline, ampicillin, cetiofur and chloramphenicol. The cetiofur-treated isolates also showed resistance to 3 or more antibiotics. These included ampicillin, cetiofur, cefoxitin, chloramphenicol, neomycin, streptomycin, tetracycline and trimethoprim sulfamethoxazole (Pereira *et al.*, 2014). A similar study in Spain on the effect of enrofloxacin on the commensal *E. coli* populations in healthy chickens found that after treatment with the quinolone there was an increase in the number of isolates resistant to doxycycline and amoxicillin as well as the enrofloxacin (Jurado *et al.*, 2015). Although these papers provide evidence (although not very robust evidence) for quinolone-induced antibiotic resistance, there are other papers that show that sublethal treatment with quinolones increases mutation rates, mutation frequencies and recombination (Lopez & Blazquez, 2009, Lopez *et al.*, 2007, Cirz *et al.*, 2007, Cirz *et al.*, 2006, Gillespie *et al.*, 2005, O'Sullivan *et al.*, 2008). Some of these papers looked for specific single point mutations in specific genes that would confer resistance to rifampicin or trimethoprim, further indicating the potential of fluoroquinolone-induced resistance. The cause of the increase in mutation rates has been linked to induction of the SOS response and concomitant derepression of the error-prone polymerases (Ysern *et al.*, 1990, Cirz *et al.*, 2007, Cirz *et al.*, 2006, Cirz & Romesberg, 2006, Thi *et al.*, 2011, Tattevin *et al.*, 2009), however, not all of the mutations observed have been linked to this, with some shown to be independent of the SOS response (Lopez & Blazquez, 2009, Lopez *et al.*, 2007, Song *et al.*, 2016).

Many of these papers suggest that treatment with subinhibitory levels of quinolones could have significant effects on general antibiotic resistance but within the literature, no one seems to have engaged the question directly. There is also a question of whether the use of CFX may

induce chromosomal rearrangements similar to those seen with etoposide (Negrini *et al.*, 1993, Lovett *et al.*, 2001, Baldwin & Osheroff, 2005). To try and address these, I have designed an *in vivo* assay looking at the effect of treating *E. coli* MG1655 with sublethal concentrations of antibiotics.

6.2 Specific materials and methods

Number of CFU's from OD_{600}

The number of colony forming units (CFU's) was determined for OD_{600} of 1.0. A single colony of *E. coli* MG1655 (see Table 2.1) was inoculated into 5 mL of LB under sterile conditions and incubated at 37°C overnight. Fifty microlitres of this was inoculated into two universals containing 10 mL LB in each. These were incubated at 37°C. The OD_{600} was measured at intervals and samples were removed at ODs of around 0.6, 0.8 and 1.0. The samples were diluted 10^{-5}, 10^{-6}, and 10^{-7}, and 50 µL of these dilutions were plated onto 9 cm LB 1.5% agar plates. The plates were incubated at 37°C overnight. The colonies were counted and plates that had between 30 and 300 colonies were kept. The CFU/mL was calculated from these at each OD_{600} and averaged across the replicates. The CFU/mL for all samples were converted to CFU/mL at an OD_{600} of 1.0 and an average CFU/mL was calculated as well across the 6 replicates.

MIC testing

Broth and solid-agar MICs were ascertained using the method in Andrews (2001), which is an updated version of the BSAC Guide to Sensitivity Testing (1991). Except, instead of IsoSensitest agar or broth, LB (General Methods) was used. Briefly, under sterile conditions, a single colony of the *E. coli* strain was inoculated into 10 mL of LB and incubated overnight at 37°C (unless otherwise stated). Either the OD_{600} of the overnight culture was ascertained and then diluted or 50 µL of the overnight culture was inoculated into 10 mL of LB and incubated for 2 – 3 h before the OD_{600} was read. The OD_{600} was converted to CFU/mL based on the measured

CFU/mL for and OD_{600} of 1.0 (see above – about 1.5×10^8 CFU/mL). For the solid-agar MICs, the cultures were diluted to between 10^7 and 10^8 CFU/mL whilst for the broth dilution MICs, the inoculum was diluted to 10^5 CFU/mL. Once the cultures were prepared, they were used within 30 min. Each antibiotic or strain was tested in triplicate, for the broth MICs, these were microdilution broth MICs were done in 96-well microtitre plates. For the solid-agar MICs, the LB 1.5% agar supplemented with the appropriate antibiotics at specific dilutions were prepared in square 10 cm petri dishes (Sterilin™). Dilutions of the antibiotics were done based around reported MICs for *E. coli* ATCC 25922 and thus were slightly different for each antibiotic. Stock solutions of the antibiotics were made up as directed in Andrews (Andrews, 2001), these were aliquoted and stored at -20°C. Each antibiotic stock was only used once. From these stocks, the antibiotic was diluted appropriately and added to the microtitre plate (or added to warm (<50°C) LB 1.5% agar for solid MICs). For the solid MICs, once the plates were poured and dried, 2 µL of the prepared inoculum was added in triplicate to each plate. For the broth MICs, the 8 dilution points were made up in 75 µL of LB each and added to the plates in triplicate with 4 wells of 12 set aside for controls. These were two sterile controls (LB only) and 2 growth (0 antibiotic) controls per replicate. For the growth controls and the antibiotic dilutions, 75 µL of the prepared inoculum was added to each well, whilst 75 µL of LB was added to the sterile controls. The lid was placed on the microtitre plate and these were incubated at 37°C (unless otherwise stated) for between 18 – 20 h. For the solid MICs, the 'drops' were left to dry before the plates were inverted and incubated at 37°C for between 18 – 20 h. The MICs were determined by eye as the lowest antibiotic concentration where visible growth was inhibited.

Quinolone-induced antimicrobial resistance assay

An overview of this assay is depicted in Figure 6.1. A colony from an *E. coli* strain was inoculated into 5 mL of LB and incubated overnight at 37°C (unless otherwise stated). Fifty to 100 µL (50 µL for incubations >24 h, 100 µL for 7 h incubations) of the overnight culture was inoculated into 50 mL of LB with either 0, 0.25×, 0.5×, or 1× MIC of an antibiotic. If DMSO was

the solvent that the antibiotic was made in, then it was added to all samples at the same percentage as the highest percentage used with addition of drug. With the plasmid-based hyper-recombination mutants, the GyrA proteins were overexpressed in the presence 0.5 mM IPTG, thus an extra control was run where no drug but 0.5 mM IPTG alone was added. These samples were also run with 20 μg/mL Amp for the maintenance of the plasmid. The samples were incubated at 37°C (unless otherwise stated) for 7 or 24 h (although with CFX it was up to 72 h). After incubation, 12.5 mL of the cultures was decanted into sterile 50 mL centrifuge tubes (Corning™ Falcon™) and centrifuged for 30 min at 3000 g. The supernatant was discarded and the pellet resuspended in 2.5 mL LB. This resuspended culture was used within 30 min of preparation. Serial dilutions were made from 10 μL of this prepared culture (10^{-2} – 10^{-8}) and 100 μL of the dilutions (usually 3, i.e. 10^{-6}, 10^{-7} and 10^{-8}) were plated onto 9 cm LB 1.5% agar plates. The remaining resuspension was plated (400 μL per plate ~ 10^{8} – 10^{10} cells) on 15 cm LB 1.5% agar plates supplemented with either 50 μg/mL Amp, 50 μg/mL Kan, 30 μg/mL Cam, 12 μg/mL Tet, 10 - 15 μg/mL Tri or 0.35 μg/mL CFX (usually about 20× the measured MIC, although for some, concentrations were used at those suggested for selection during cloning). All the plates were incubated for 22 – 24 h at 37°C (unless otherwise stated). After the incubation, at 37°C, the plates were left on the bench (~ 22°C) for a further 8 – 20 h. Any colonies that appeared on the selection plates were restreaked back onto the antibiotic that they were identified on to confirm resistance using sterile 0.5 -10 μL tips before incubating for 20 – 22 h at 37°C. The plates without antibiotic were used to calculate the number of colonies that survived the incubation, any plate that had between 30 and 300 CFU were counted using a ProtoCOL 3 Colony Counter (Synbiosis). To calculate resistance frequencies, the number of colonies that survived the restreaking step were divided by the number of colonies on the LB only plates multiplied by the dilution factor, multiplied by 4 (to scale the amount plated to 400 μL).

For some of the assays, the restreaked colonies were then also streaked onto the other antibiotics to check for cross resistance. To check whether the resistance was due to mutation

or persistence, selected resistant colonies were inoculated into 5 mL of LB and incubated at 37°C for 18 h, after which 50 µL of this was inoculated into 5 mL of LB and incubated at 37°C for a further 8 h. I then took 50 µL of this and inoculated it into 5 mL of LB and incubated at 37°C for a further 18 h. The cells were subcultured again and incubated for a further 8 h as before. These cultures were then streaked back onto the antibiotic that they were identified on and incubated overnight at 37°C. Any colonies that survived were assumed to have some fixed mutation that conferred the resistance.

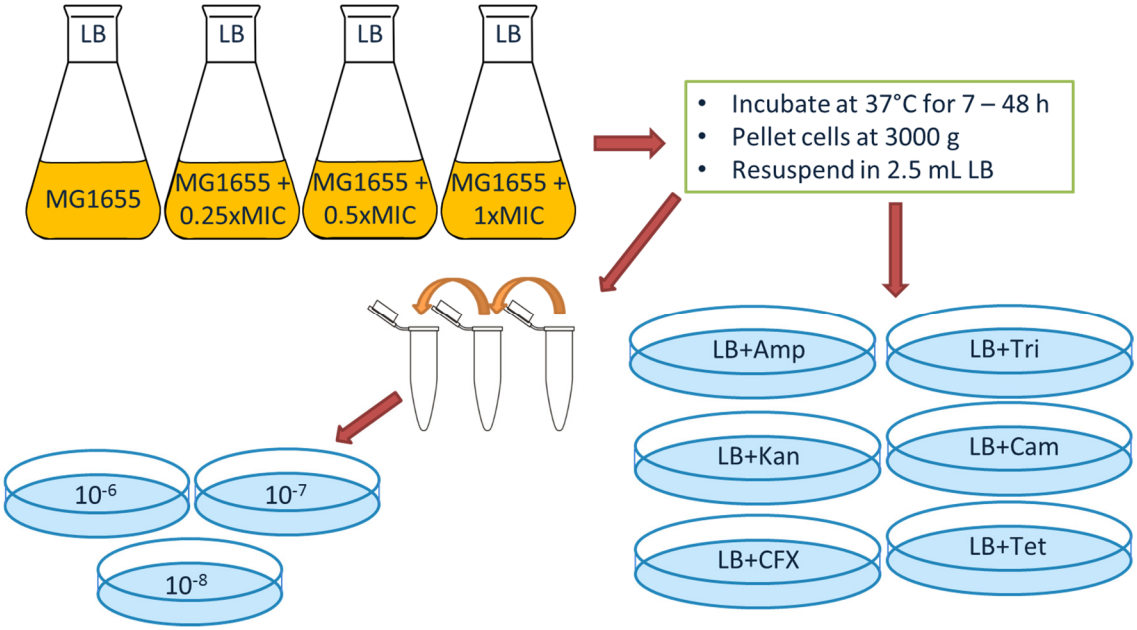

Figure 6.1: Diagram showing *in vivo* quinolone-induced antibiotic resistance assay. *E. coli* MG1655 (or another *E. coli* strain) is incubated with 0, 0.25×, 0.5×, and 1× MIC of an antibiotic at 37°C for 4 – 72 h. The cells are the concentrated and diluted in fresh LB before plating on 9 cm LB 1.5% agar plates at various dilutions (between 10^{-6} – 10^{-8}) to check the number of CFU (cell survival) and then on 15 cm LB 1.5% agar with various antibiotics (~10^{8} – 10^{10} cells plated) to check for any antibiotic resistance. Amp is ampicillin, Tri is triclosan, Kan is kanamycin, Cam is chloramphenicol, and Tet is tetracycline.

Whole genome sequencing

Resistant colonies and non-selected colonies (colonies from dilution plates) where sent for whole genome sequencing (WGS). This was performed by MicrobesNG

(http://www.microbesng.uk), which is supported by the BBSRC (grant number BB/L024209/1). The colonies were prepared according to MicrobesNG's specifications. Colonies that were sent for sequencing were streaked out onto the antibiotic they were identified on or just LB if there was no selection. A singly colony from the restreaked plate was resuspended in 100 µL of sterile PBS (phosphate buffered saline – see Chapter 4). This was streaked onto an LB 1.5% agar plate with 1/3 of the plate as a lawn and then streaks from this lawn to single colonies were done to ensure the culture is pure. These were incubated overnight at 37°C. A large sterile loop was then used to take all of the bacterial culture off the plate, which was mixed into the microbead tubes supplied by Microbes NG. These were sent to MicrobesNG for DNA extraction and library preparation. Sequencing was done on either Illumina® MiSeq or Hiseq 2500 platforms.

Bioinformatics

The bioinformatics was done with support from and in collaboration with Bernardo Clavijo (Earlham Institute). The trimmed reads were used for analysis. These were assembled against the published *E.* coli MG1655 sequence (Blattner *et al.*, 1997). The GenBank and Fasta files of the reference sequence were downloaded from GenBank (NCBI - Accession: NC_000913.3) (Benson *et al.*, 2013). Assemblies and variant calling were performed using Snippy v3.1 (Seeman T., 2015) (https://github.com/tseemann/snippy) using Perl v5.16.2, BioPerl v1.6.923, SamTools v1.3.1, bwa-mem v0.7.5, and Java v7.21. Assemblies and alignments were visualised using Tablet (v1.17.08.17; 17th August 2017) (Milne *et al.*, 2013). A further set of assemblies on two of the samples was done using W2rap Contigger (https://github.com/bioinfologics/w2rap) (Clavijo *et al.*, 2017) using the -gfa dump option. Bandage v0.8.1 was used to visualise these assemblies (https://github.com/rrwick/Bandage) (Wick *et al.*, 2015). Specific nodes of the assemblies done with W2rap were run in BLAST® (NCBI) using their nucleotide blast tool (BLASTN v2.7.0+) using the default settings (run on the 17th of August 2017 and 30th if August 2017) (Zhang *et al.*, 2000, Morgulis *et al.*, 2008). All information about the various genes identified with mutations was obtained from EcoCyc database online (accessed 2017) (Karp *et al.*, 2014).

ssOligo recombineering

I attempted to make the hyper-recombination mutants (Chapter 4) in the *E. coli* MG1655 genome by ssOligo recombineering. This is a method based on λ- red recombineering (Datsenko & Wanner, 2000) which uses a single or double-stranded DNA oligo to insert or delete genetic sequences, or introduce nucleotide polymorphisms into bacterial chromosomes. Double-stranded DNA recombineering uses the λ Exo, Beta and Gam proteins to introduce these novel mutations. Single-stranded recombineering only requires Beta and uses a single-stranded oligo (ssOligo) which pairs with the lagging strand during replication, mimicking an Okazaki fragment (Wang & Church, 2011). ssOligo recombineering can be a quick and scarless way to make mutations in the chromosome. The most important step of the ssOligo recombineering protocol is that of the design of the nucleotide to evade the mismatch repair (MMR) mechanisms in the bacteria. The oligo needs to match the lagging strand (in terms of replication) of the area of the genome you wish to mutate, it should be between 40 and 90 nt in length and it should have a folding energy of no less than -12.5 kcal/mol (as predicted by MFold (Markham & Zuker, 2005)) (Sawitzke *et al.*, 2011, Wang & Church, 2011), .

I designed the hyper-recombination mutation ssOligo's using an online program called MODEST (Bonde *et al.*, 2014). The oligos that were designed by MODEST were then further optimised to evade MMR. The oligos (Table 2.3) were synthesised by Sigma-Aldrich using a desalting purification only and contained four phosphorothioated bases on the 5' end to stop them from being degraded by exonucleases in the cell.

The rest of the protocol was essentially as described by Wang and Church (2011) apart from the following exceptions:

- *E. coli* MG1655 carrying the recombineering plasmid pKD46 (Table 2.2 and Appendix I) (Datsenko & Wanner, 2000) was used.
- 30 mL Sterilin™ Polypropylene 30mL Universal Containers were used instead of glass culture tubes and were incubated in a shaking incubator at 300 rpm.

- Standard colony PCR was used instead of genotyping by multiplex allele specific colony PCR verification.

Colony PCR was set up with the primers shown in Table 2.3. Between 47 and 63 colonies were selected from the colony isolation plates and one colony from the "no oligo" (wild type) control plate (*E. coli* MG1655 (pKD46) without electroporation of any oligo) for each mutation. The colonies were resuspended in 8 µL sterile water in 96-well plates. PCR reactions were set up using GoTaq™ Green mix (Promega), which is a ready-to-use premix of *Taq* polymerase, dNTPs and $MgCl_2$, with either the wild-type GyrA gene forward primer (wt) or the mutant forward primer (mut) as well as the same reverse primer (R400, R500 or R600) for both (Table 2.3), and 1 µL of the resuspended colony. Thus, for each colony, two PCR reactions were set up; one with the primers for the wild-type sequence and one with the primers for the mutant sequence. The PCR reactions were set up in 96-well plates and run using the PCR conditions in Table 6.1. For each colony selected, after addition to the PCR reaction, the colony was restreaked onto another plate and incubated at 30°C overnight.

Table 6.1: Polymerase Chain Reaction conditions for colony PCR.

Step	Temperature	Time	No. of cycles
Initial Denaturation	94°C	2 min	1
Denaturation	94°C	1 min	25
Annealing	65°C	1 min	25
Extension	72°C	1 min	25
Final Extension	72°C	10 min	1

The colony PCR reactions were analysed using the QIAxcel Advanced System using a High-Resolution Kit and the ML400 program. Any colonies that showed a band with the mutant primers or no band with the wild type primers, were reconfirmed by colony PCR. Any confirmed colonies underwent colony PCR with primers upstream from the mutation (see Table 2.3) and this PCR product was sent for sequencing. Any colonies that had the desired mutations were then cured of the pKD46 plasmid by growing them in liquid culture for 24 hours at 37°C without

the ampicillin selection. The culture was then diluted and plated on LB agar plates and incubated overnight. Individual colonies were then selected and streaked on two LB agar plates, one with ampicillin and one LB only. Any colony that grew on the LB only plate but not on the LB with ampicillin were believed to no longer carry the pKD46 plasmid.

6.3 Results and discussion

MICs

Microbroth MICs for the antibiotics used in the assay were determined for the *E. coli* MG1655 strain (Table 6.2). For the other *E. coli* strains used, only the MIC of CFX was ascertained (Table 6.3). All MICs were done in triplicate and the MIC used was an average of the triplicates. For the *E. coli* MG1655, solid-agar MICs (Table 6.4) were also determined for CFX, OA, Amp, Tet, Kan, and Cam. The MIC for CFX against MG1655 was determined to be 0.016 µg/mL, which is almost the same as the published MIC for *E. coli* ATCC 25922 which was 0.015 µg/mL (Andrews, 2001). It was also within a factor of 2 from another study measuring the CFX MIC of MG1655 (Cirz *et al.*, 2005) and it was the same as the MIC reported in (Mo *et al.*, 2016), except that study used the resazurin method to determine MICs. The other MICs measured either matched reported (if applicable) MICs or they were within a factor of 2; except for the BW25113 strain, which, in my hands, had a 4-fold lower MIC than previously reported (Tamae *et al.*, 2008). The solid-agar MICs were calculated from two separate iterations (apart from the OA solid MIC, which was only run once). With the solid MICs, a sheen of growth or individual colonies were ignored in the analysis as prescribed in Andrews (Andrews, 2001).

Table 6.2: Minimum Inhibitory Concentrations (MICs) for all antibiotics used in the QIAR assay against *E. coli* MG1655.

	MIC (μg/mL)								
***E. coli* Strain**	**CFX**	**SFX**	**MFX**	**NFX**	**OA***	**5931**	**$CouA_1$**	**Amp***	**Kan***
MG1655	0.016	0.016	0.032	0.032	0.4	1.0	16.0	6.0	4.0

* these were solid-agar MICs; CFX – ciprofloxacin, SFX – sparfloxacin, MFX – moxifloxacin, NFX – norfloxacin, OA – oxolinic acid, 5931 – REDX05931, $CouA_1$ – coumermycin A_1, Amp – ampicillin, Kan – kanamycin

Table 6.3: Minimum Inhibitory Concentrations (MICs) for ciprofloxacin (CFX) used in the QIAR assay. Broth-based MICs were determined for CFX used in the QIAR assay against all *E. coli* strains used.

***E. coli* Strain**	**MIC (μg/mL)**
MLS83L	0.256
BW25113	0.004
NGB345	0.008
MG1655 (pPH3)[a]	0.004
MG1655 (pI203V/I205V)	0.004
MG1655 (pL492P)	0.004
MG1655 (pL488P)	0.004

a – brackets indicate the strain with a plasmid.

Table 6.4: Solid-agar minimum inhibitory concentrations (MICs) for antibiotics used in the QIAR assay.

	Solid-agar MIC (μg/mL)					
	Kan	**Amp**	**Cam**	**Tet**	**CFX**	**OA**
E. coli MG1655	4.0	6.0	8.0	4.0	0.016	0.4

CFX – ciprofloxacin, Amp – ampicillin, Kan – kanamycin, Tet – tetracycline, Cam – chloramphenicol, OA – oxolinic acid

QIAR assay

This assay investigated the effect of CFX on different *E. coli* hosts (for genotypes see Table 2.1) as well as the effect of other quinolone and non-quinolone antibiotics on *E. coli* MG1655 alone. Whole genome sequencing was only performed on colonies that arose during the assays with MG1655. The number of times the assay was performed with each strain or antibiotic is detailed in Table 6.5. Due to time constraints, some of the strains or antibiotics were only tested

once or twice. This means that some of the data is not as robust as hoped, it also means that the conclusions drawn do not have statistical support.

Table 6.5: Number of times the QIAR assay was run with each strain or antibiotic for each incubation period (h).

E. coli Strain	Antibiotic	No. of times performed for each incubation period			
		7 h	24 h	48 h	72 h
MG1655	CFX	3	7	1	1
	Amp	2	1	-	-
	$CouA_1$	1	1	-	-
	5931	1	3	-	-
	Kan	1	1	-	-
	OA	1	1	-	-
	SFX	-	1	-	-
	MFX	1	1	-	-
	NFX	-	1	-	-
MLS83L	CFX	1	1	-	-
BW25113	CFX	1	2	-	-
NGB345	CFX	-	1	-	-
MG1655 (pPH3)	CFX	1	3	-	-
MG1655 (pI203V/I205V)	CFX	-	1	-	-
MG1655 (pL488P)	CFX	-	2	-	-
MG1655 (pL492P)	CFX	-	1	-	-

- is not determined; CFX – ciprofloxacin, SFX – sparfloxacin, MFX – moxifloxacin, NFX – norfloxacin, OA – oxolinic acid, 5931 – REDX05931, $CouA_1$ – coumermycin A_1, Amp – ampicillin, Kan – kanamycin

With *E. coli* MG1655

I chose *E. coli* MG1655 for these assays as it is a non-virulent, near wild-type *E. coli* K12 strain that has a fully annotated genome sequence available (Blattner *et al.*, 1997). When this strain was incubated with sublethal concentrations of CFX for 7 h or more, resistant colonies were isolated on the non-quinolone antibiotic selection plates. Many (between 20% and 100%; on average ~60%) of these colonies survived when they were restreaked back onto the antibiotic they were identified on; an example of these in shown in Figure 6.2. Analysis of all replicates of the assay showed that when MG1655 was treated with sublethal concentrations of CFX, there was an increase in the frequency of resistance to all non-quinolone antibiotics tested (Table 6.6 and 6.7). The most common non-quinolone resistance identified was to Cam and Kan. Resistance

to Amp and Tet were not as common, and resistance to Tri was only really identified once (see below). This resistance was also shown not to be due to contaminating plasmids as after plasmid preparations (see General Methods) were performed on selected colonies with Amp, Kan and Cam resistance, no plasmids were observed by gel electrophoresis (data not shown).

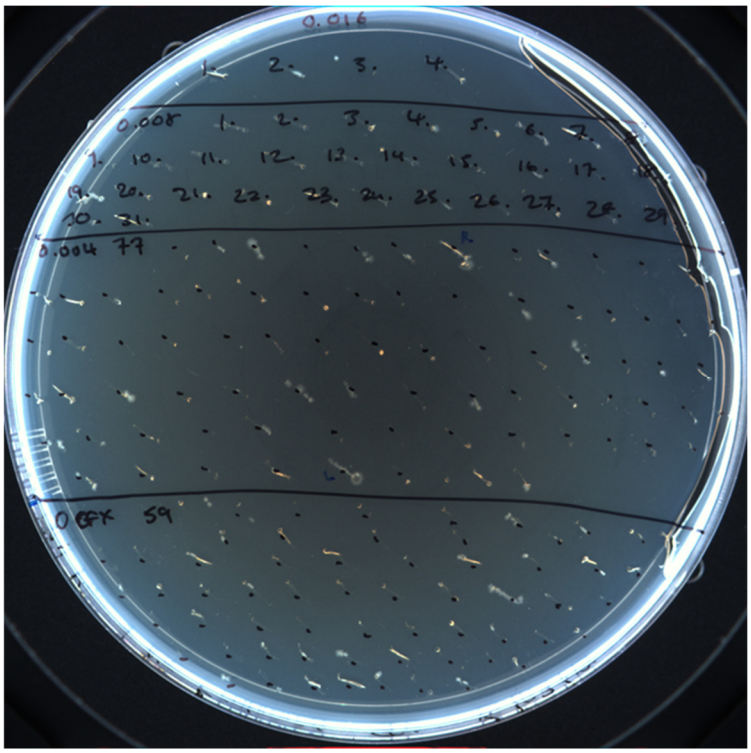

Figure 6.2: Example of restreaked colonies isolated on selection plates post incubation with sublethal ciprofloxacin (CFX). All kanamycin (Kan) resistant colonies (Kan^R) isolated from a Kan selection plate after a 24 h incubation with sublethal CFX (0, 0.004, 0.008 and 0.016 µg/mL) were streaked back onto a LB 1.5% agar plate supplemented with 50 µg/mL Kan and incubated for 20 h at 37°C.

Table 6.6: Range of antibiotic resistances identified for all assays run with *E. coli* MG1655

Treatment		Selection Antibiotic											
	n	Kan	Amp	Cam	Tet	Tri	CFX	$CouA_1$	OA	5931	SFX	MFX	NFX
CFX	7	✓	✓	✓	✓	✓	✓						
Kan	2	✓	0	0	0	0	0						
Amp	2	✓	✓	0	0	0	0						

CouA$_1$	2	✓	0	0	0	0	0	✓					
OA	2	✓	✓	0	0	0	✓		✓				
5931	4	✓	0	✓	0	0	✓			✓			
SFX	1	✓	0	✓	✓	0					✓		
MFX	2	✓	0	0	0	0						✓	
NFX	1	✓	0	✓	0	0							✓

✓ - present; 0 – absent; if blank, then it was not determined; CFX – ciprofloxacin, SFX – sparfloxacin, MFX – moxifloxacin, NFX – norfloxacin, OA – oxolinic acid, 5931 – REDX05931, CouA$_1$ – coumermycin A$_1$, Amp – ampicillin, Kan – kanamycin, Cam is chloramphenicol, Tet is tetracycline, and Tri is triclosan

Table 6.7: Frequency of antibiotic resistance per CFU (×10^{-10}) for *E. coli* MG1655 treated with sublethal antibiotics over a 24 h incubation.

Treatment		**Antibiotic Resistance/CFU (×10^{-10})**										
Antibiotic	**×MIC**	**Kan**	**Amp**	**Cam**	**Tet**	**CFX**	**CouA$_1$**	**5931**	**OA**	**SFX**	**MFX**	**NFX**
CFX[a]	**0**	34	0.4	0	0	0						
	0.25	86	0	0.7	0	0						
	0.5	806	0	63	0	1480						
	1.0	25	16	203	0.2	60						
Kan	**0**	98	0	0	0	0						
	0.25	79	0	0	0	0						
	0.5	921	0	0	0	0						
	1.0	3176	0	0	0	0						
Amp	**0**	0	0	0	0	0						
	0.25	0	0	0	0	0						
	0.5	0	0.8	0	0	0						
	1.0	0	0	0	0	0						
CouA$_1$	**0**	5	0	0	0	0	0					
	0.25	22	0	0	0	0	14					
	0.5	0	0	0	0	0	0					
	1.0	0	0	0	0	0	0					
5931[a]	**0**	62	0	0	0	0		1				
	0.25	145	0	0	0	0		>167				
	0.5	312	0	7	0	46		>288				
	1.0	57	0	69	0	>117		>217				
OA	**0**	77	0	0	0	0			8			
	0.25	109	3	0	0	0			3			
	0.5	83	5	0	0	0			0			
	1.0	0	0	0	0	17			97			
SFX	**0**	44	0	0	0					0		
	0.25	67	0	0	0					0		
	0.5	62	0	0	0					0		
	1.0	27	0	218	17					62		

MFX	**0**	162	0	0	0	0	
	0.25	118	0	0	0	0	
	0.5	44	0	0	0	0	
	1.0	89	0	0	0	0	
NFX	**0**	15	0	0	0		0
	0.25	15	0	0	0		0
	0.5	27	0	0	0		2
	1.0	223	0	2	0		49

a – these are averages across replicates, CFX = average across 6 replicates, 5931 = average across 3 replicates. All the others are single data points. If blank, then it was not determined; CFX – ciprofloxacin, SFX – sparfloxacin, MFX – moxifloxacin, NFX – norfloxacin, OA – oxolinic acid, 5931 – REDX05931, $CouA_1$ – coumermycin A_1, Amp – ampicillin, Kan – kanamycin

Some of the resistant colonies were tested for multidrug resistance by streaking onto all antibiotics used. Those tested did not show cross resistance to the other antibiotics, that is colonies identified as Kan resistant were only resistant to Kan and not any other antibiotic tested (data not shown). However, testing for cross resistance was only performed twice, and thus instances of multidrug resistance could have been missed, especially considering some of the WGS data (see below).

Several resistant colonies were incubated without selection (in LB only) over 3 days, with subculturing twice daily (18 h incubation followed by an 8 h incubation for 3 days). The cultures were then streaked back onto the antibiotic the original colony was identified on, in order to determine whether the resistance was maintained over generations. Some of the colonies did not retain resistance, some showed reduced resistance while with others the resistance was maintained (Figure 6.3). This indicated that in some cases the resistance was heritable and unlikely to be due to tolerance or epigenetic factors.

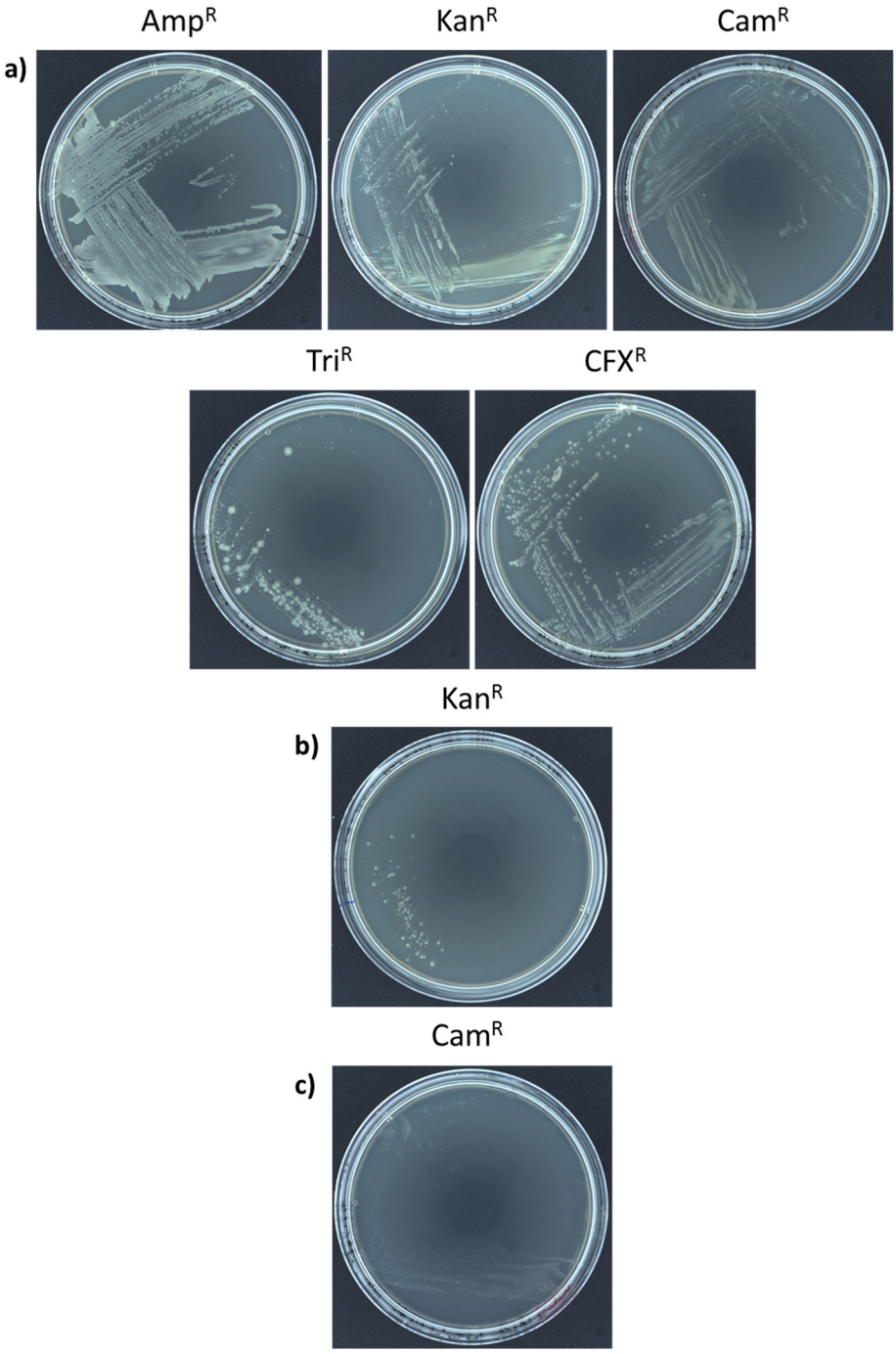

Figure 6.3: LB agar plates showing that resistance is still maintained after growth in LB only. Several resistant colonies were inoculated into LB and incubated for 3 days, with subculturing into LB twice daily (after 8 h and 18 h). The resultant culture was then streaked back onto the antibiotic they were originally identified on. a) Examples of cultures that maintained resistance; Amp^R indicates a colony that was resistant to ampicillin (Amp) and is still resistant to Amp, likewise with Kan^R, Cam^R, Tri^R, and CFX^R (kanamycin, chloramphenicol, triclosan and ciprofloxacin respectively). b) Example of a colony that was initially Kan resistant but upon subculturing only showed partial Kan resistance. c) Example of a colony that was initially Cam resistant but upon subculturing is now no longer resistant.

From Table 6.7, the 0.5 × MIC (0.004 µg/mL) treatment appears to have the greatest effect over a 24 h period with highest frequency of resistance/CFU observed. Here resistance frequencies of 8.0×10^{-8} were seen for Kan, and 1.4×10^{-7} for CFX, as opposed to the 0.25 × MIC and 1 × MIC samples where the greatest frequency observed was 2×10^{-8} for Cam. However, a greater diversity in the resistance profile is seen with the 1 × MIC (0.016 µg/mL) samples, with resistance to all antibiotics tested observed at least once across the 7 iterations (Table 6.6 and 6.7). The treatment with 0.5 × MIC has been previously reported to have greater effect on recombination and mutation rates (Lopez *et al.*, 2007, Thi *et al.*, 2011). Increased frequencies of resistance with sublethal CFX treatment have been demonstrated previously and concurs with the results seen here. In particular, incubation of methicillin-susceptible *S. aureus* with sub-MIC CFX has been shown to increase resistance to methicillin (Tattevin *et al.*, 2009). Gullberg *et al.* (2011) (reviewed in (Hughes & Andersson, 2012)) have also demonstrated an increase in fluoroquinolone resistance when *E. coli* was incubated with 0.1 × MIC of CFX. Subinhibitory levels of CFX have also been shown to increase the mutation rates in *E. coli* and *Mycobacterium fortuitum* (Gillespie *et al.*, 2005, Mo *et al.*, 2016, Song *et al.*, 2016).

In Table 6.6 and Figure 6.3, resistance to triclosan (Tri) is seen but it is not reported in Table 6.7. Despite this biocide being used for selection of resistance in all assays, resistance was only ever isolated in one of the assays run over both the 7 h and 24 h incubations, and it was isolated from the no-CFX control (as well as in the 0.5 × MIC and 1 × MIC treatments). In this particular assay, I did not see colonies on the LB only (non-selective) plates at the dilutions I plated the 1 × MIC sample on. This was either due to an error in plating or the inappropriate dilutions being plated. This meant that I could not work out a frequency of resistance for this assay and thus it was left out of the analysis for Table 6.6. I expected to see the Tri resistance again, however, in later assays, I increased the amount of Tri to 15 µg/mL (in error) which may explain why I didn't see any other Tri resistance. The colony isolated from the 1 × MIC treated sample was sent for

WGS (see below) and it did align to the no-CFX control except for a single point mutation, indicating that it is unlikely to be a contaminant. Recently, mutations that confer quinolone resistance in DNA gyrase were shown to increase resistance to Tri (Webber *et al.*, 2013, Webber *et al.*, 2017). This was found to be upregulation of stress-response genes due to the altered supercoiling caused by these mutations (Webber *et al.*, 2017). Thus, here, it was expected that with increasing CFX-resistant mutations in GyrA could lead to more Tri resistance.

Although the data is incomplete (the total number of times the assay was incubated for the various time periods is not the same, i.e. 7 times for 24 h vs 3 times at 7 h), there does seem to be a greater number of resistant colonies after the 24 h period as opposed to the 7 h period (Table 6.8). However, to fully evaluate the effect that incubation time has on the rise in resistance, time courses should be run.

Table 6.8: Average number of resistant colonies identified per assay for *E. coli* MG1655 treated with sublethal CFX after various incubation times.

	Incubation Time	
×MIC	**7 h[a]**	**24 h[b]**
0	7	11
0.25	5	12
0.5	4	42
1.0	3	15

a – is an average of 3 replicates, b – is an average of 7 replicates

Indications from the literature, suggested that multidrug resistance could be induced by a non-quinolone antibiotics as well (Kohanski *et al.*, 2010), so to ascertain whether this was a general characteristic of treatment with subinhibitory levels of antibiotics, the assay was run with Amp and Kan. The same variety of resistance induced by sub-MIC CFX treatment is not seen when the assay is run with sub-MIC concentrations of Amp or Kan (Table 6.5 and 6.6). Resistant colonies were isolated with these two antibiotics but the colonies were only resistant to the incubation antibiotic (i.e. only Amp-resistant colonies were seen with the treatment with sublethal Amp). This is in contrast to previous work, that showed the rise of multidrug resistance

after incubation with sublethal levels of Amp and increased mutation rates when treated with Amp or Kan (Kohanski *et al.*, 2010). Other studies have shown that β-lactam antibiotics such as Amp increase mutations either via induction of the RpoS regulon, leading to an increase in resistance to fosfomycin, Tet, and rifampicin (Gutierrez *et al.*, 2013), or via induction of the SOS response (Shaw *et al.*, 2003, Miller *et al.*, 2004), both of these pathways can result in the upregulation of the error-prone polymerase Pol IV (*dinB*) (Pérez-Capilla *et al.*, 2005). The discrepancies between my work and published work may be down to experimental differences, such as with Kohanski *et al.* (Kohanski *et al.*, 2010), they were looking for an increase in MIC (I was looking for resistant colonies at a fixed selection concentration), and with their mutation assays they left their plates at 37°C for 48 h, whereas at most my incubations were for 22 h at 37°C (although occasionally, I left the plates for a further 18 h at 22°C). This is also true for study conducted by Gutierrez *et al.* (2013) who also only scored colonies after a 48-h incubation at 37°C.

When the assay was run in the presence of a non-cleavage-stabilising DNA gyrase inhibitor $CouA_1$, there was also no increase in resistance except to $CouA_1$ itself (Table 6.5 and 6.6). Coumermycin A_1 is a non-quinolone antimicrobial that targets the GyrB protein of DNA gyrase and competitively inhibits the ATPase reaction (Gellert *et al.*, 1976b). The Kan resistance seen in Table 6.6 and 6.7 is shown in Figure 6.4 not to be greatly different to the no-$CouA_1$ control. Coumermycin was shown by Ikeda et al (Ikeda *et al.*, 1980) to reduce the frequency of IR both in the presence (down by 20%) and absence (down 70%) of OA. Another aminocoumarin antibiotic novobiocin has also been shown to inhibit the SOS response, in the presence and absence of CFX, and it reduced the frequency of recombination in *S. aureus* (Schröder *et al.*, 2013). This all implies that merely inhibiting DNA gyrase does not cause an increase in resistance indicating that it may be due to the stabilisation of the cleavage complex.

To address this, and in collaboration with my CASE partner Redx Anti-Infectives, I tested a compound, RedX05931 (5931), which inhibits DNA gyrase by stabilising the cleavage complex

but is not a quinolone antibiotic and does not seem to share the quinolone-binding site (Savage *et al.*, 2016a, Savage *et al.*, 2016b). This compound did show resistance to other antibiotics as well as to itself, specifically Cam and CFX (Table 6.6 and 6.7) and possibly Kan (I will deal with this separately), but across the four iterations, the levels of resistance and the extent of the resistance were not equivalent to that of CFX (Table 6.6 and 6.7). This drug has been shown to have a lower frequency of resistance in *S. aureus*, which may suggest that doesn't induce the formation of spontaneous mutations to the same level as CFX. This raised the question of whether the effect seen is peculiar to CFX or whether it is common to all quinolones?

For that reason, I tested OA, SFX, MFX and NFX. All but MFX showed resistance to at least two other antibiotics (Table 6.6 and 6.7). Due to time constraints, the other quinolones were only tested once for each incubation period (OA and MFX) or only once over 24 h (SFX and NFX). Looking at OA first, resistance was seen to Kan, Amp, CFX and to itself. Although, the increased resistance to CFX is not surprising as certain types of quinolone resistance are often effective to some degree across all quinolones (Yoshida *et al.*, 1990). Oxolinic acid is the antibiotic that Ikeda *et al.* (1980) identified DNA gyrase-mediated IR with. He saw a 13-fold increase in IR when he added OA to his assay. Oxolinic acid is a first-generation quinolone whilst CFX, SFX and MFX are second third and fourth-generation fluoroquinolones respectively (see Chapter 1). Sparfloxacin, although only tested once showed increased resistance to Kan, and resistance to Cam and Tet (Table 6.6, 6.7 and Figure 6.4). This is in contrast to MFX which did not show any increase in resistance to Kan over a 24 h period, and no resistance to any other antibiotic, including itself (Table 6.6). When the assay was run over a 7 h incubation period, however, one MFX-resistant colony was identified with the 1 × MIC sample. This is in line with other studies that have demonstrated that resistance is less frequently isolated against MFX (Malik *et al.*, 2012, Dalhoff, 2012, Dong *et al.*, 1998, Sethi *et al.*, 2010). Against *E. coli*, MFX was shown to have a mutation rate 100-fold less than that seen with CFX at 4 × MIC (Schedletzky *et al.*, 1999). This may be because MFX has been shown to target both topo IV and DNA gyrase equally in *Streptococcus*

pneumoniae and thus two mutations are required to cause resistance (Houssaye *et al.*, 2002). Further to this, in *S. aureus*, gatifloxacin, which like MFX is an 8-methoxyfluoroquinolone, was also shown to target both topo IV and DNA gyrase equally (Ince & Hooper, 2001). Despite MFX apparently showing decreased induction of resistance in this work, it has been shown to increase the selection of resistant mutants in comparison to the β-lactam ceftriaxone when tested against *S. pneumoniae*, although in this same study, it had the lowest selection frequencies in comparison to the other quinolones tested (Browne *et al.*, 2002).

Norfloxacin has been used extensively to study the effect that subinhibitory concentrations of antibiotics have on resistance. This is despite NFX having been demonstrated to affect killing in cells by a different mechanism than most other fluoroquinolones (Drlica *et al.*, 2008, Drlica *et al.*, 2009). Specifically, killing with NFX appears to be sensitive to Cam and it has been suggested to upregulate ROS which results in cell death. However, it has also been shown to be lethal under anaerobic conditions making the mode of killing by this quinolone complex (Malik *et al.*, 2007). Considering the debate surrounding the hypothesis that the lethality of antibiotics is due to ROS killing and the role that NFX has played in that, I felt it was necessary to test this quinolone in my assay. However, due to time constraints, I was only able to run the assay once with a 24 h incubation period. Thus, preliminary results do not suggest that this antibiotic is too different to SFX or CFX in initiating an increase in the frequency of resistance when MG1655 was treated with sublethal concentrations (Table 6.6 and 6.7). It does show the third greatest increase in Kan resistance after Kan and CFX (Figure 6.4). Unfortunately, due to time constraints the colonies obtained were not assessed for cross resistance.

The Kan resistance profile of the assay changed in February of this year (2017). Before February the only time Kan resistance was seen with the no-drug control was when the assay was run in the presence of DMSO. After February, however, despite repeated decontamination, making fresh Kan stocks from a new stock of kanamycin sulphate (Sigma), and streaking out MG1655 from a separate glycerol, the colonies repeatedly appeared in the no-drug control.

Many of these colonies did not survive restreaking (on average - 0 × MIC = 48% survival, 0.25 × MIC = 62% survival, 0.5 × MIC = 84% survival, and 1 × MIC = 54% survival). The ones that did survive would often not grow in liquid culture, regardless of whether there was Kan in the media or not. In order to use the Kan data, I took the number of colonies that survived restreaking and calculated the frequency of resistance per CFU. I then calculated the fold change in resistance to the no-drug control. That meant the no-drug control gave a fold-change value of 1.0, in other words, no change. In Figure 6.6, the red line indicates this value, that is, a fold-change value of 1.0. Any bars above this red line indicate a greater change in the frequency of resistance whilst any bars below this red line indicate a lower frequency of resistance than the no-drug control. From Figure 6.4, it is evident that CFX, Kan and NFX show the greatest increase in frequency of Kan resistance over the other antibiotics tested. However, it is important to note that the $CouA_1$, SFX and NFX data is from a single experiment with a 24 h incubation period.

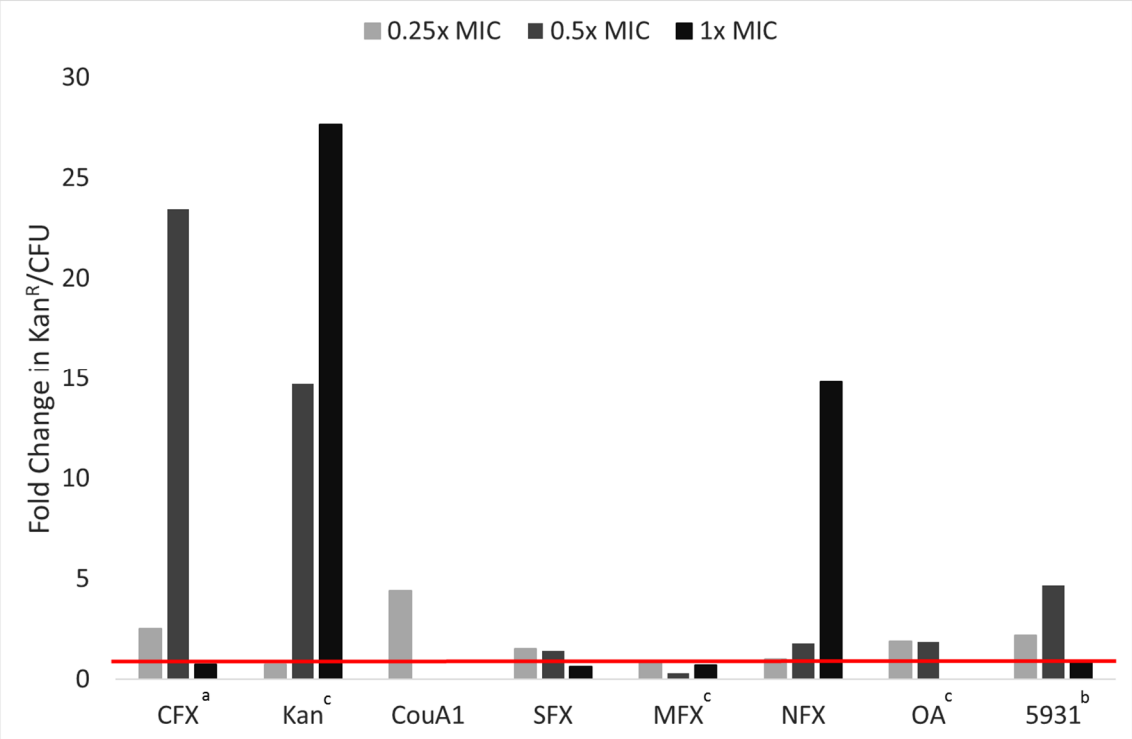

Figure 6.4: Fold change in the frequency of kanamycin resistance to the no-drug control. *E. coli* MG1655 was treated with sublethal antibiotics over a 7 h and a 24 h period before selection of LB 1.5% agar plates supplemented with 50 µg/mL kanamycin (Kan). Resistant colonies were isolated and restreaked back on to Kan. Colonies that regrew were used to calculate the frequency of resistance per CFU and the fold change in resistance was calculated in respect to the no-drug control. The red line shows the fold change in the frequency of resistance of one, i.e. no change over the no-drug control. a is data that was calculated as an average over 2 replicates of the 7 h and 6 replicates of the 24 h period incubation. b is data that was calculated as an average over a 7 h incubation period and 3 replicates of the 24 h period incubation. c indicates data that was calculated as an average of a single run of the 7 h and 24 h results. CouA1, SFX and NFX sample data was calculated from a single experiment incubated over 24 h. CFX is ciprofloxacin, CouA1 is coumermycin A_1, SFX is sparfloxacin, MFX is moxifloxacin, NFX is norfloxacin, OA is oxolinic acid and 5931 is RedX05931.

With other *E. coli* hosts

To investigate whether DNA gyrase was involved in this increase in resistance, the quinolone-resistant *E. coli* strain MLS83L (see Table 2.1) was used in the assay with CFX. This strain has the clinically-relevant quinolone-resistant GyrA S83L mutation in the MG1655

background (Parks, 2004). From Table 6.9 and 6.10 and Figure 6.5, it is evident that the MLS83L strain treated with sublethal CFX does not seem to show the same increase in antibiotic resistance as observed with MG1655 and CFX (shown above in Table 6.6, 6.7 and Figure 6.4). This may confirm that DNA gyrase is involved in the observed increase in resistance, however further replicates of the assay with this strain are needed. It also suggests that the effect is stimulated by DNA gyrase rather than topo IV in this strain. I tested this strain using the MIC of the susceptible strain (0.016 μg/mL). Although I did not have the time to test this, I would predict that I would observe an increase in resistance if I ran the experiment with this strain using 0.25, 0.5 and 1 × its own MIC (0.064, 0.128 and 0.256 μg/mL respectively).

Table 6.9: Range of antibiotic resistances identified when *E. coli* MG1655, MLS83L and BW25113 were treated with sublethal concentrations of ciprofloxacin.

		Selection Antibiotic					
***E. coli* strain**	**n**	**Kan**	**Amp**	**Cam**	**Tet**	**Tri**	**CFX**
MG1655	7	✓	✓	✓	✓	✓	✓
MLS83L	2	✓	0	0	0	0	
BW25113	3	✓	0	✓	✓	0	✓

✓ - present; 0 – absent; if blank, then it was not determined or it was not applicable; CFX – ciprofloxacin, Amp – ampicillin, Kan – kanamycin, Cam is chloramphenicol, Tet is tetracycline, and Tri is triclosan

Table 6.10: Frequency of antibiotic resistance per CFU ($\times 10^{-10}$) for *E. coli* strains MG1655, MLS83L, and BW25113 treated with sublethal CFX over a 24 h incubation

Treatment		**Antibiotic Resistance/CFU ($\times 10^{-10}$)**				
***E. coli* strain**	**×MIC**	**Kan**	**Amp**	**Cam**	**Tet**	**CFX**
MG1655[a]	**0**	34	0.4	0	0	0
	0.25	86	0	0.7	0	0
	0.5	806	0	63	0	1480
	1	25	16	203	0.2	60
MLS83L[b]	**0**	28	0	0	0	
	0.25	37	0	0	0	
	0.5	5	0	0	0	
	1	39	0	0	0	
BW25113[c]	**0**	17	0	0	0	0.8

	0.25	18	0	0	0	7
	0.5	31	0	32	0	96
	1	11	0	0	3	3

a – average across 6 replicates, b – data from a single experiment, c – average across 2 replicates. If blank, then it was not determined; CFX – ciprofloxacin, Amp – ampicillin, Kan – kanamycin, Cam is chloramphenicol, and Tet is tetracycline.

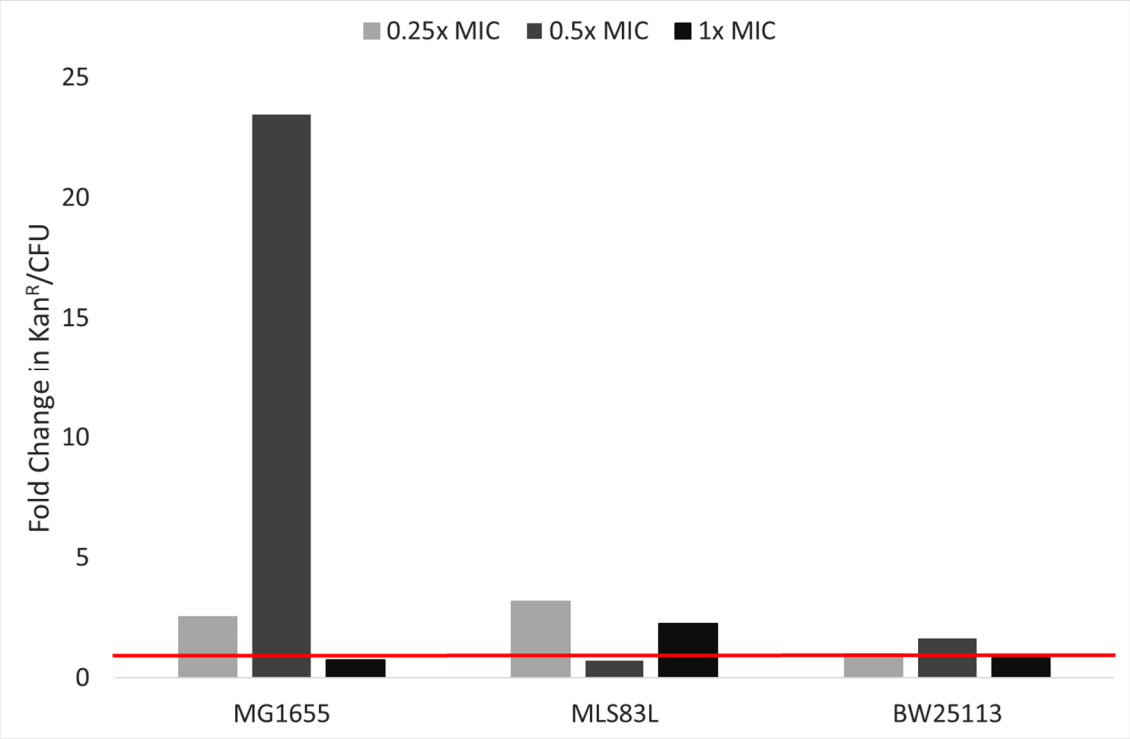

Figure 6.5: Fold change in the frequency of kanamycin resistance to the no-drug control for *E. coli* strains MG1655, MLS83L and BW25113 treated with sublethal concentrations of ciprofloxacin (CFX). Strains were treated with sublethal CFX over a 7 h and a 24 h period before selection on LB 1.5% agar plates supplemented with 50 µg/mL kanamycin (Kan). Resistant colonies were isolated and restreaked back on to Kan. Colonies that regrew were used to calculate the frequency of resistance per CFU and the fold change in resistance was calculated in respect to the no-drug control. The red line shows the fold change in the frequency of resistance of one, i.e. no change over the no-drug control. The data presented from MLS83L is an average of the 7h and 24 h incubation data, BW25113 is an average over the 7 h and 2 replicates of the 24 h incubation data and MG1655 is calculated as an average over 2 replicates of the 7 h and 6 replicates of the 24 h period incubation.

E. coli BW25113 (see Table 2.1) is the parental strain that all deletion mutations were made from in the Keio collection (Baba *et al.*, 2006). The ultimate aim was to use specific strains from

the Keio collection to investigate the other proteins or genes involved in the increase in resistance caused by sublethal treatment with CFX. Unfortunately, I ran out of time to attempt any of this but I did use the parent strain, BW25113, as a further control to test whether the same effect was visible with another strain of *E. coli*. This strain had an MIC lower than that measured for MG1655 (0.004 μg/mL). However, colonies were isolated that were resistance to Cam (0.5 × MIC, frequency of 3.2×10^{-9}), Tet (1 × MIC, frequency of 3×10^{-10}) and CFX (0 – 1 × MIC) (Table 6.9 and 6.10) but did not show the same increase in resistance to Kan (Figure 6.5). This implies that the increase in resistance may not be peculiar to MG1655 but it would be good to test clinically-isolated strains and other species of bacteria to see if it is relevant in a clinical setting. Overall the BW25113 strain was more resistant to CFX with CFX resistance identified in the no-drug control (frequency of 0.8×10^{-10}).

With the hyper-recombination mutants

The hyper-recombination mutants were identified by Ashizawa *et al.* (1999) as mutations in GyrA that increase the frequency of illegitimate recombination *in vivo* (see Chapter 4). In order to test their *in vivo* phenotype and to see if they affect the increase in the frequency of resistance, I transformed the overexpression plasmids (made by site-directed mutagenesis of pPH3) that were used to produce the proteins in Chapter 4, into MG1655 (pPH3 – wild-type GyrA, pI203V/I205V - GyrA I203V/I205, pL488P – GyrA L488P and pL492P – GyrA L492P). I also attempted to move these mutations into the MG1655 *gyrA* gene on the chromosome by ssOligo Recombineering. Regrettably, I was unable to make the L488P or the L492P mutations due to time constraints. Although I managed to move the I203V/I205V mutations into the chromosome, I accidently added an extra mutation leaving me with I203V/S204R/I205V (*E. coli* NGB345 – Table 2.1) (Figure 6.6). This was due to a mistake in the oligo (Table 2.3) not as a result of spontaneous mutation.

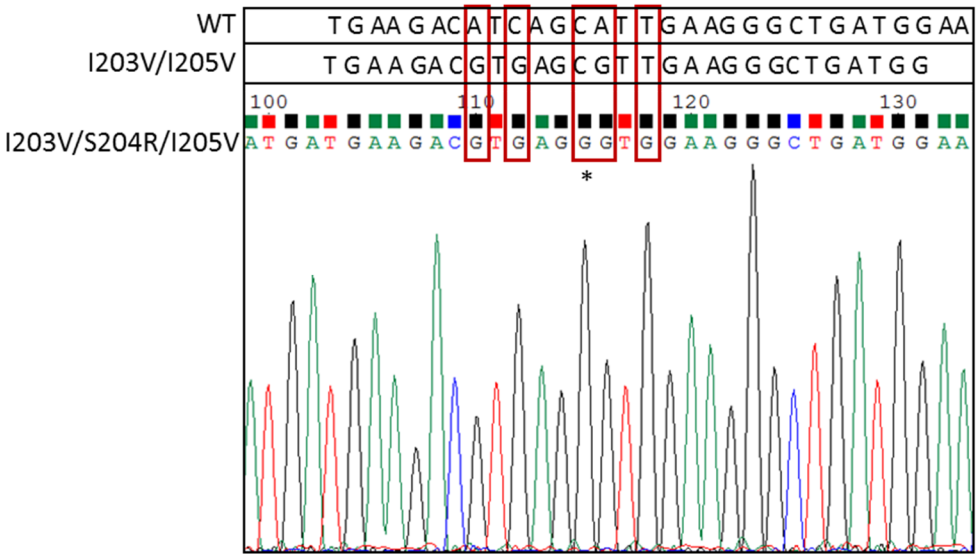

Figure 6.6: Sequencing chromatogram of the *E. coli* MG1655 *gyrA* mutations (I203V/S204R/I205V) after ssOligo recombineering aligned with the expected sequence (I203V/I205V) and the wild-type (WT) sequences. Red boxes indicate the positions of the base changes and the star indicates the erroneous base. Amino acid changes are referred to by their single letter codes.

Although these assays were only run once for the hyper-recombination mutants, the preliminary results suggest that overexpressing the GyrA subunit with the hyper-recombination mutants appears to have little effect on the frequency of mutation when compared to the WT MG1655 (Table 6.11 and Figure 6.7). There is no increase in the frequency of resistance with NGB345 when compared with WT MG1655. There is also very little difference in the frequency of resistance observed with the overexpressed hyper-recombination mutants in comparison with the overexpressed wt-GyrA (pPH3). In terms of the range of resistances seen, the MG1655 (pL492P) showed resistance is against Kan, Cam and CFX whilst with MG1655 (pI203V/I205V) resistance is seen to Kan, Cam and Tet. With MG1655 (pPH3) resistance was observed against Kan and Cam, however only Kan resistance was obtained with the MG1655 (pL488P) mutant. Overall with these mutants, less resistance to CFX was observed (Table 6.11). The frequency of resistance appears to be higher with the pI203V/I205V than that of the strain NGB345 (especially at 1×MIC) (Table 6.11 and Figure 6.7). This may be because the extra mutation (S204R) has

altered the effect the other two mutations have on the protein or that overexpression of this mutation is needed to see the effect. This protein would have to be tested *in vitro* to see what effect the extra mutation has on the activity of the enzyme. All things considered, the actual I203V/I205V, L488P and L492P mutations need to be made in MG1655 to definitively assess the *in vivo* phenotypes with regards to sublethal treatment with CFX. Furthermore, these assays would need to be repeated to get a realistic idea of the effect these mutations could be having. Moreover, these assays were run at permissive temperatures and increasing the temperature may yield very different results. Ultimately, further work with these mutations in this assay is needed to fully explore whether they do increase IR in this assay.

Table 6.11: Frequency of antibiotic resistance per CFU ($\times 10^{-10}$) for *E. coli* strains MG1655, NGB345, and MG1655 carrying the wt-GyrA and hyper-recombination overexpression plasmids, all treated with sublethal CFX over a 24 h incubation.

Treatment		Antibiotic Resistance/CFU ($\times 10^{-10}$)				
***E. coli* strain**	**×MIC**	**Kan**	**Amp**	**Cam**	**Tet**	**CFX**
MG1655[a]	**0**	34	0.4	0	0	0
	0.25	86	0	0.7	0	0
	0.5	806	0	63	0	1480
	1	25	16	203	0.2	60
NGB345[b]	**0**	52	0	0	0	0
	0.25	15	0	0	0	2
	0.5	48	0	0	0	0
	1	30	0	6	0	0
MG1655 (pPH3)[b]	**0**	19		0	0	0
	+IPTG	10		0	0	0
	0.25	13		1	0	0
	0.5	40		2	0	0
	1	26		7	0	0
MG1655 (pI203V/I205V)[b]	**0**	6		9	0	0
	+IPTG	4		0	0	0
	0.25	2		0	0	0
	0.5	3		0	0	0
	1	186		46	23	0
MG1655 (pL488P)[b]	**0**	1		0	0	0
	+IPTG	0		0	0	0

	0.25	14	0	0	0
	0.5	2	0	0	0
	1	386	0	0	0
MG1655 (pL492P)[b]	**0**	9	0	0	0
	+IPTG	12	1	0	0
	0.25	55	0	0	0
	0.5	75	0	0	0
	1	6	3	0	3

a – average across 6 replicates, b – data from a single experiment; if blank, then it was not determined; CFX – ciprofloxacin, Amp – ampicillin, Kan – kanamycin, Cam is chloramphenicol, and Tet is tetracycline.

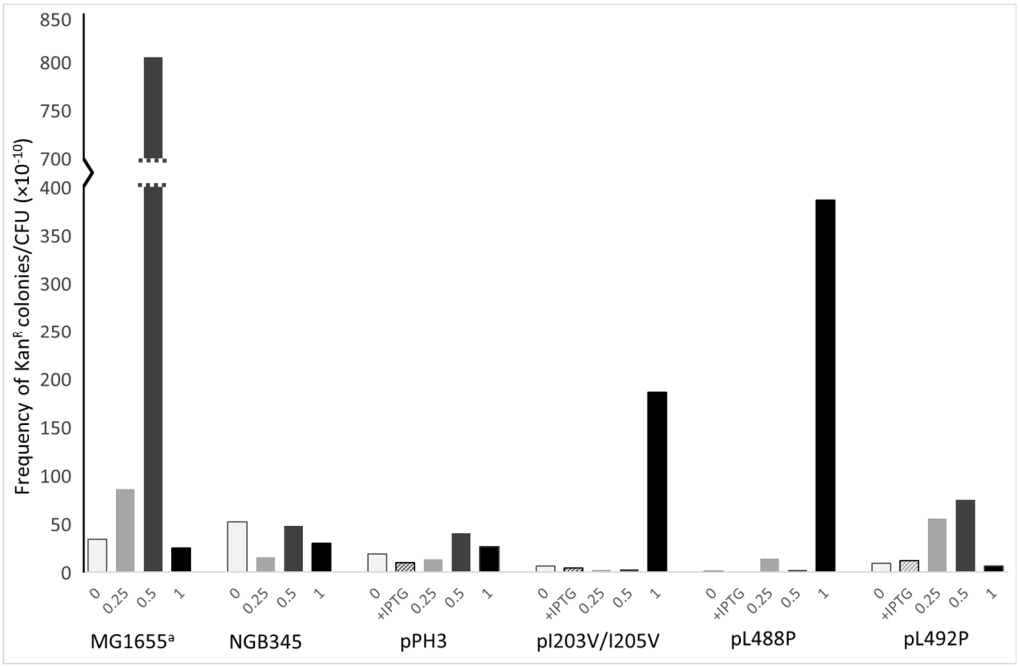

Figure 6.7: Frequency of kanamycin resistant colonies per CFU (×10^{-10}) for the *E. coli* strains MG1655, NGB345, and MG1655 carrying the wt-GyrA and hyper-recombination overexpression plasmids treated with sublethal concentrations of ciprofloxacin (CFX). Strains were treated with sublethal CFX over a 7 h (CFX only) and a 24 h period before selection of LB 1.5% agar plates supplemented with 50 µg/mL kanamycin (Kan). Resistant colonies were isolated and restreaked back on to Kan. Colonies that regrew were used to calculate the frequency of resistance per CFU. On the X-axis, the 0, 0.25, 0.5 and 1 are × MIC and the +IPTG is the sample that had 0.5 mM IPTG added but no CFX. A indicates that the data presented from MG1655 is calculated as an average over 2 replicates of the 7 h and 6 replicates of the 24 h period incubation. NGB345, and MG1655 carrying the wt-GyrA and hyper-recombination overexpression plasmids sample data was calculated from a single experiment incubated over 24 h. pPH3 is the plasmid carrying the wild-type *gyrA* gene; pI203V/I205V, pL488P and pL492P are the hyper-recombination mutations of *gyrA* in pPH3.

Whole genome sequencing

A variety of strains from the assays run with *E. coli* MG1655 and sublethal CFX were sent for WGS. A total of 24 strains were sent and included resistant and non-selected strains. The non-selected strains were those that had been incubated with 0.25, 0.5, or 1 × MIC CFX but were taken from the LB only plates and therefore had not been selected on any antibiotic. Control strains were sent from LB only plates from samples that had been incubated without any CFX and one parental strain was sent that had not been run in the assay.

Firstly, from Table 6.12 it is evident that there are specific mutations that are found in all of the strains sent for sequencing. These include a CC deletion (bp 2173360) in *gatC,* a G insertion (bp 3560455) in *glpR* and a CG insertion (bp 4296380) in a repeat region that is non-coding. These are all known variants of this strain (Freddolino *et al.*, 2012, Graves Jr *et al.*, 2015). Two different sources of MG1655 were used in these assays. Initially, a lab strain of MG1655 was used (assays from October 2015 until January 2016) before the strain from CGSC arrived. This initial lab strain had a SNP in *yieP* and it was found to have a 4.5 kb deletion (confirmed by PCR) from bp 1397239 – 1401771 across *ynaJ*, *uspE*, *fnr*, *ogt*, *agbT* and *rrlD* (data not shown). The resistant strains that were sent for sequencing that were derived from this parent include the Amp, and Tri strains, a CFX strain (CFX-1 – Table 6.12), a Cam strain (Cam-1 – Table 6.12) and a Kan strain (Kan with 0.5 × MIC in Table 6.12). Whether the deletions in this parental strain has played a role in the development of the resistance or the associated chromosomal deletions (Δ*marR* or Δ*leuP*) is unknown. The strain obtained from CGSC developed a spontaneous SNP in *dppD* (probably during the preparation of the strain for sequencing) and later also had one in *nfo* (possibly developed in the process of making the initial glycerols of the strain for long-term storage). This mutation may have more serious consequences as the *nfo* gene codes for endonuclease IV. This mutation resulted in an amino acid change from valine to phenylalanine on β-sheet 6 at position 176, which appears to be a conserved residue in the protein, however

it does not appear to be in or near the active site of the enzyme (Hosfield *et al.*, 1999, Daley *et al.*, 2010). Endonuclease IV is one of the apurinic/apyrimidinic (AP) endonucleases that is involved in the DNA repair of oxidative damage. It removes apurine or apyrimidine bases during base excision repair. Mutations at AP sites are often A>T transversion mutations with *E. coli* mutants deficient in AP site repair also showing an increase in A>T transversion mutations (Daley *et al.*, 2010). In all of the unique mutations found when this parent MG1655 was used in the assays, only one (out of the 11 SNPs) showed an A>T transversion (Kan resistant without CFX, Table 6.12). This may suggest that the majority of the SNPs seen may not have been influenced by this mutation. Ultimately the effects of this *nfo* mutation are not really known and although endonuclease IV has not been shown to play a significant role in the repair of DNA damage by CFX, I cannot say for certain that it has not affected the outcomes of this assay. Suffice to say that an increase in the frequency of resistance was observed regardless of the parental strain used and the hallmark A>T transversion mutation of AP sites was not a considerable contributor to the SNPs seen (11% of the SNPs). Furthermore, it is also unlikely that the mutation in endonuclease IV would affect the large genome mutations (e.g. the large deletions) that have been observed. Having said that, all of this should be repeated with a wild-type *nfo* strain.

Table 6.12: All variants and mutations identified from whole genome sequencing of 24 *E. coli* MG1655 strains from QIAR (quinolone-induced antibiotic resistance) assay.

Resistance	Mutation type	Genotype		Chromosome position	Gene	Notes
		Reference	Strain			
None - No incubation	deletion	ACCC	AC	2173360	*gatC*	known MG1655 variant
	insertion	CC	CGC	3560455	*glpR*	known MG1655 variant
	SNP	G	A	3703260	*dppD*	dipeptide ABC transporter
	insertion	AC	ACGC	4296380	Non-coding	RIP321 element (repetitive extragenic palindromic)
	deletion	ACCC	AC	2173360	*gatC*	

None - Incubated without CFX - 4 strains	SNP	G	T	2251365	*nfo*	Endonuclease IV - V176F
	insertion	CC	CGC	3560455	*glpR*	
	insertion	AC	ACGC	4296380	Non-coding	
None - Incubated with 0.25 or 0.5 × MIC - 4 strains	deletion	ACCC	AC	2173360	*gatC*	
	SNP	G	T	2251365	*nfo*	
	insertion	CC	CGC	3560455	*glpR*	
	insertion	AC	ACGC	4296380	Non-coding	
None - Incubated with 1 × MIC - 2 strains	deletion	ACCC	AC	2173360	*gatC*	
	SNP	G	T	2251365	*nfo*	
	SNP	G	A	2339173	*gyrA*	DNA gyrase A subunit S83L – known resistance
	insertion	CC	CGC	3560455	*glpR*	
	insertion	AC	ACGC	4296380	Non-coding	
Amp - incubated with 0.5 × MIC	deletion	ACCC	AC	2173360	*gatC*	
	insertion	CC	CGC	3560455	*glpR*	
	SNP	C	A	3941164	*yieP*[f]	Predicted transcriptional regulator
	insertion	AC	ACGC	4296380	Non-coding	
	SNP	A	T	4379035	*frdD*	Lies within the promoter of *ampC*
Tri - incubated with 0.5 × MIC	SNP	C	A	1350762	*fabI*	G93V - known Tri resistance mutation
	SNP	C	T	1351063	Non-coding	
	deletion	ACCC	AC	2173360	*gatC*	
	insertion	CC	CGC	3560455	*glpR*	
	SNP	C	A	3941164	*yieP*	
	insertion	AC	ACGC	4296380	Non-coding	
Tet - incubated with 1 × MIC	deletion	CTC	CC	458566	*clpX*	ClpX ATP-dependent protease specificity component and chaperone

	deletion	GAA	GA	459223	*lon*	Protease
	insertion	GAAAAAAAT	GAAAAAAAT	468358	Non-coding	
	SNP	C	T	1619468	*marR*	DNA-binding transcriptional repressor
	deletion	ACCC	AC	2173360	*gatC*	
	SNP	G	T	2251365	*nfo*	
	insertion	CC	CGC	3560455	*glpR*	
	insertion	AC	ACGC	4296380	Non-coding	
CFX-1 - incubated with 1 × MIC[a]	deletion	ACCC	AC	2173360	*gatC*	
	SNP	G	C	2339173	*gyrA*	S83W
	insertion	GTGGTCA	GTGGTCTGGTCA	2664136	*suhB*	Inositol-phosphate phosphatase
	insertion	CC	CGC	3560455	*glpR*	
	SNP	C	A	3941164	*yieP*	
	insertion	AC	ACGC	4296380	Non-coding	
CFX-2 - incubated with 1 × MIC[b]	SNP	G	T	1619370	*marR*	
	deletion	ACCC	AC	2173360	*gatC*	
	SNP	G	T	2251365	*nfo*	
	SNP	G	A	2339173	*gyrA*	S83L
	insertion	CC	CGC	3560455	*glpR*	
	insertion	AC	ACGC	4296380	Non-coding	
Cam - incubated with 0.5 × MIC	complex	N/A	N/A	883585 - 932177		possible loop or amplification See Figure 6.11
	deletion	ACCC	AC	2173360	*gatC*	
	SNP	G	T	2251365	*nfo*	
	insertion	CC	CGC	3560455	*glpR*	
	insertion	AC	ACGC	4296380	Non-coding	
Cam-1 - incubated with 1 × MIC[c]	deletion	N/A	N/A	1619098 - 1619552	*ΔmarR*	See Figure 6.10
	SNP	A	T	1792432	*nlpC*	
	insertion	CC	CGC	3560455	*glpR*	
	SNP	C	A	3941164	*yieP*	
	insertion	AC	ACGC	4296380	Non-coding	

Cam-2 - incubated with 1 × MIC[d]	complex	N/A	N/A	870751 - 899202		possible loop or amplification See Figure 6.12
	deletion	N/A	N/A	1196375 - 1211411	e14 prophage	Excision of cryptic phage
	SNP	C	T	1619468	*marR*	
	deletion	ACCC	AC	2173360	*gatC*	
	SNP	G	T	2251365	*nfo*	
	insertion	CC	CGC	3560455	*glpR*	
	insertion	AC	ACGC	4296380	Non-coding	
Cam -3 - incubated with 1 × MIC[e]	SNP	T	G	883616	Non-coding	found between *mdfA* and its promoter
	SNP	T	G	1619370	*marR*	
	deletion	ACCC	AC	2173360	*gatC*	
	SNP	G	T	2251365	*nfo*	
	insertion	CC	CGC	3560455	*glpR*	
	insertion	AC	ACGC	4296380	Non-coding	
Kan - Incubated without CFX	SNP	C	A	516710	*fetB*	putative iron ABC exporter
	deletion	ACCC	AC	2173360	*gatC*	
	SNP	G	T	2251365	*nfo*	
	SNP	G	A	3471539	*fusA*	elongation factor G - known Kan resistance gene
	insertion	CC	CGC	3560455	*glpR*	
	SNP	A	T	4104443	*cpxA*	sensory histidine kinase – part of CpxAR two-component signal transduction system
	insertion	AC	ACGC	4296380	Non-coding	
Kan - incubated with 0.5 × MIC	deletion	ACCC	AC	2173360	*gatC*	
	SNP	G	C	2400681	*nuoF*	NADH:quinone oxidoreductase subunit F
	SNP	G	A	3471686	*fusA*	
	insertion	CC	CGC	3560455	*glpR*	
	SNP	C	A	3941164	*yieP*	
	insertion	AC	ACGC	4296380	Non-coding	

	deletion	N/A	N/A	4606166 - 4606314	Δ*leuP*	tRNA – see Figure 6.10
Kan - Incubated with 1 × MIC	SNP	T	G	1619370	*marR*	
	deletion	ACCC	AC	2173360	*gatC*	
	SNP	G	T	2251365	*nfo*	
	insertion	CCTGC	CCTGC TGC	3471824	*fusA*	
	insertion	CC	CGC	3560455	*glpR*	
	deletion	CTG	CG	3991578	*cyaA*	adenylate cyclase - suggested to play a role in persistence
	insertion	AC	ACGC	4296380	Non-coding	

0.25, 0.5 and 1 × MIC CFX is 0.004, 0.008 and 0.016 µg/mL respectively. Grey blocks indicate unique mutations. a & b are different strains identified from different replicates that share CFX resistance. c - e are different strains identified from different replicates that share Cam resistance. f the variant of *yieP* was found in all resistant strains from the first batch of WGS, the parental MG1655 strain these assays were run with was a lab strain that likely carried this variant.

The strains that were incubated with CFX but were not selected against another antibiotic did not show any other mutations other than the SNP mutations in *gyrA* seen when MG1655 was incubated with 1 × MIC CFX (Table 6.12). This perhaps is not surprising considering the chance of selecting of selecting a colony with various mutations at random is quite low considering the low frequencies of resistance (1 in 10^7 for CFX-resistant mutations, 1 in 10^{10} for Tet-resistant mutations). However, having said that, this does raise the question about whether the non-CFX mutations arise during the initial incubation with sublethal CFX or if they are a result of the secondary selection. This would imply that pre-exposure to CFX makes bacteria more predisposed to becoming resistant when exposed to a secondary antibiotic. To the best of my knowledge, there is no evidence in the literature that this has been directly tested, however, Torres-Barceló *et al.* (2015) have argued that the induction of the SOS-induced response by CFX does not increase evolvability, but competitive fitness, implying that for mutations to become fixed in the population, continued selection is needed. This was also demonstrated by Gullberg *et al.* (2011) who showed in competition experiments that continued selection with sublethal antibiotics gave individuals with resistance mutations a competitive advantage over those

without. Despite these studies however, there are papers that show that sublethal treatment with CFX increases recombination between homologous sequences (Lopez & Blazquez, 2009) and between non-homologous sequences independently of the SOS response (Lopez *et al.*, 2007), implying that treatment with CFX is enough to cause significant chromosomal modifications.

The CFX-resistant mutations seen here are in the *gyrA* gene (at bp 2339173), and all lead to the mutation of the S83. Mutations that cause this residue to be mutated are well known (Collin *et al.*, 2011, Aldred *et al.*, 2014b). It is the residue that is involved in the binding of CFX through the water-metal ion bridge (Aldred *et al.*, 2014a, Aldred *et al.*, 2013, Hooper & Jacoby, 2015) and the S83L and S83W mutations identified here are well characterised (Redgrave *et al.*, 2014).

For the Amp- and Tri- resistant strains, both contain SNPs that explain the resistance phenotype (Table 6.12). The Amp resistance comes from an A>T transversion (bp 4379035) mutation in the promoter region of *ampC*. This promoter in *E. coli* overlaps with the end of the *frdD* gene (Grundström & Jaurin, 1982) and is not generally inducible (Livermore, 1995) resulting in Amp susceptibility in *E. coli*. However, there are examples of mutations in this promoter region that increase the production of this gene which encodes a β-lactamase (class C cephalosporinase) including an amplification of the *ampC* gene (Normark *et al.*, 1977, Briñas *et al.*, 2002, Corvec *et al.*, 2002). The Tri resistance comes from a known C>A transversion mutation (bp 1350762) in *fabI* resulting in the G93V amino acid change (Heath *et al.*, 1999).

The Tet resistance appears to be a synergistic outcome of two mutations, the deletion in the *lon* gene (ΔA at bp 459223), and the C>T transition mutation in *marR* (bp 1619468) as neither of the individual mutations would have been enough to see the observed resistance (Nicoloff & Andersson, 2013, Nicoloff *et al.*, 2007). This may explain why only low levels of Tet resistance have been seen in this assay as the probability of the formation of two mutations is much lower than that of just one mutation. Mutations in *lon* have also been demonstrated in *Pseudomonas*

aeruginosa when treated with sublethal CFX (Brazas *et al.*, 2007). Lon protease has also been suggested to be involved in the repair of quinolone-induced DNA damage (Drlica *et al.*, 2009).

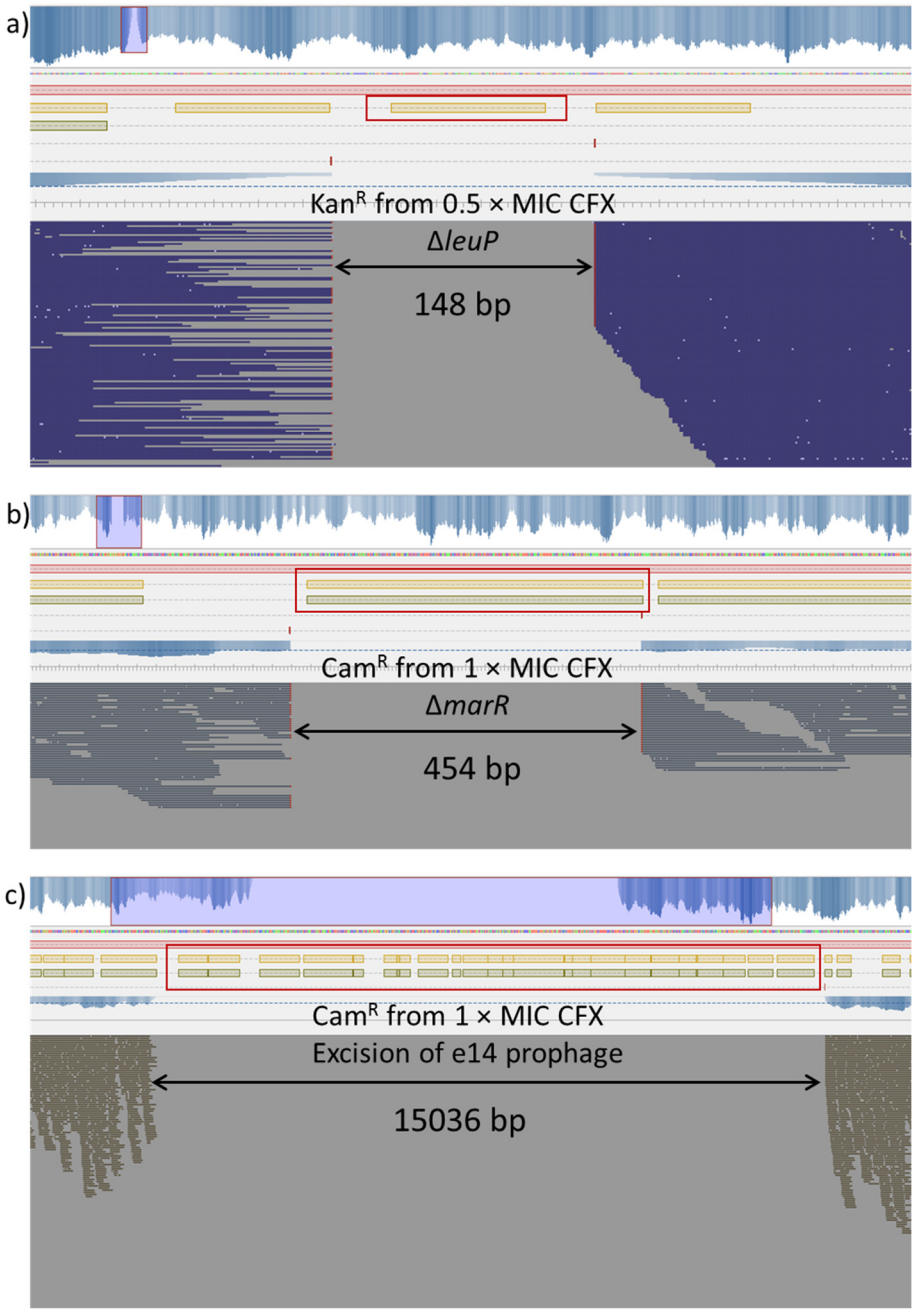

Figure 6.8: Large-scale (> 100 bp) deletions from antibiotic-resistant strains obtained after sublethal treatment with ciprofloxacin (CFX). Trimmed reads were assembled and aligned to the published *E. coli* MG1655 sequence and scanned by eye for large-scale genomic changes in Tablet (Milne *et al.*, 2013), with deletions indicated by gaps in coverage (double-headed arrows). Kan^R is a kanamycin-resistant strain with a deletion of *leuP* (red box Δ*leuP*), Cam^R are chloramphenicol-resistant strains, one showing a deletion of *marR* (red box Δ*marR*) and the other the excision of the cryptic prophage e14.

Cam resistance was often obtained after MG1655 treatment of sublethal CFX and 4 of the 24 strains sent for WGS were Cam resistant. Three of those had mutations in *marR*, including the complete deletion of the gene (Figure 6.8b) and two SNPs, one C>T transition (bp 1619468) and one T>G transversion (bp 1619370). All of these *marR* mutations were identified from MG1655 treated with 1 × MIC CFX. The Mar operon (Multiple Antibiotic Resistance) contains 3 genes *marR*, *marA*, and *marB*. MarR is the transcriptional repressor of *marA* and *marB* and derepression of these results in multidrug resistance through MarA which itself regulates a number of efflux pumps and porins. Mutations in *marR* are known to give rise to resistance to various antibiotics including tetracycline, chloramphenicol and fluoroquinolones (Cohen *et al.*, 1993, Alekshun & Levy, 1997, Alekshun & Levy, 2007). Considering these mutations should give multidrug resistance, I should have seen resistance to more than just Cam when I tested for cross resistance, however, there may have been a decreased susceptibility of these strains to the other antibiotics that was not visible at the concentrations of the antibiotics that were used. If MICs were performed on these strains, I expect that higher MICs would be obtained for all of the antibiotics tested. The high number of *marR* mutations obtained, particularly with treatment at 1 × MIC CFX, may imply that the resistance is induced to reduce the effects of the CFX, and the Cam resistance may be a secondary effect observed. Especially as specific resistance to fluoroquinolones mediated by *marOR* mutations have been identified in *E. coli* isolated from patients with urinary tract infections (UTI's) that were treated with various fluoroquinolones (Komp Lindgren *et al.*, 2003) and demonstrated under treatment with sub-MIC NFX (Long *et al.*, 2016).

One of the strains with a *marR* SNP and the Cam-resistant strain from the 0.5 × MIC treatment showed a large jump in coverage after assembly with Snippy (Figures 6.9a and 6.10a) (1 × MIC Cam^R – CV jump from ~50 to ~450; 0.5 × MIC Cam^R – CV jump from ~50 to ~250). In order to try and address whether or not this was a sequencing or PCR error, Bernardo

reassembled the reads from these two strains using W2rap Contigger. When the newly assembled reads were visualised in Bandage, both of the assemblies had large loops visible that mapped to the same area as the previously assemblies (Figures 6.9b and 6.10b). The small unitigs from the loops (398 bp unitig and 394 bp unitig from Figures 6.9b and 6.10b) were then run in BLAST. The sequences in these unitigs aligned to the edges of the "duplications" with exactly half of the sequence aligning to the front end of the area with high coverage and the other half to the far end (Figures 6.9c and 6.10c). This suggests that this is a loop or plasmid or it is an amplification made up of a number of concatemers of this region. This still needs to be confirmed by PCR or sending these strains for further sequencing using a long-read sequencer such as PacBio® or MinION. The interesting thing about this duplication is that in both strains it contains the *mdfA* gene, also known as the *cmr* gene. This gene encodes a transmembrane ATPase multi-drug efflux pump (Edgar & Bibi, 1997) which was initially identified by its ability to confer resistance to Cam when over expressed (Nilsen *et al.*, 1996). It has also been found to increase resistance to a number of molecules as well as several clinically-relevant antibiotics including fluoroquinolones (Edgar & Bibi, 1997), however, clinically significant increases in resistance to fluoroquinolones has been shown to require over expression of more than one efflux pump, such as *mdfA* and *acrAB* (Swick *et al.*, 2011). With the Cam-resistant isolate from the 0.5 × MIC CFX treatment, this amplification of the *mdfA* gene is the only genetic explanation for the Cam resistance that is observed. Here is appears that the copy number of this gene has increased 9-fold in the 1 × MIC Cam^R isolate and 5-fold in the 0.5 × MIC Cam^R isolate.

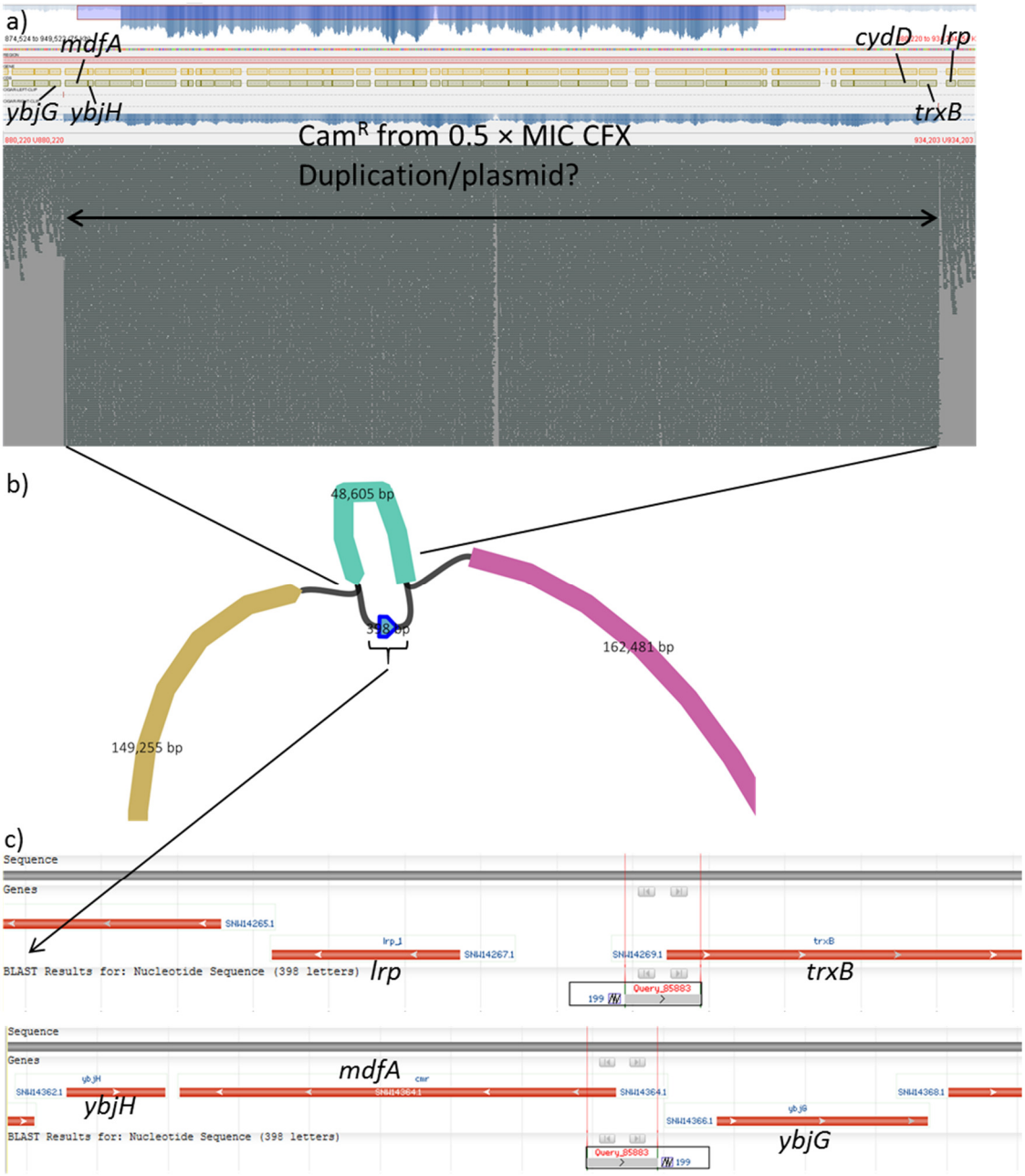

Figure 6.9: Putative plasmid or duplications of bp 883585 – 932177 in a chloramphenicol-resistant strain isolated after treatment with sublethal (0.5 × MIC) ciprofloxacin. a) Trimmed reads were assembled and aligned to the published *E. coli* MG1655 sequence (using Snippy) and scanned by eye for large-scale genomic changes in Tablet (Milne *et al.*, 2013), with the duplication/plasmid indicated by a large jump in coverage (double-headed arrows). Important genes and the flanking genes are shown above the assembled reads. b) The assemblies were redone using W2rap Contigger (Clavijo *et al.*, 2017) and visualised using Bandage, with the duplications/plasmid indicated by the 48605 bp and 398 bp unitigs. c) The 398 bp unitig was run in BLASTN. The query sequence aligned to *E. coli* sequences in two places, splitting the query sequence in half and these are graphically presented here (screen shots of the BLAST graphic).

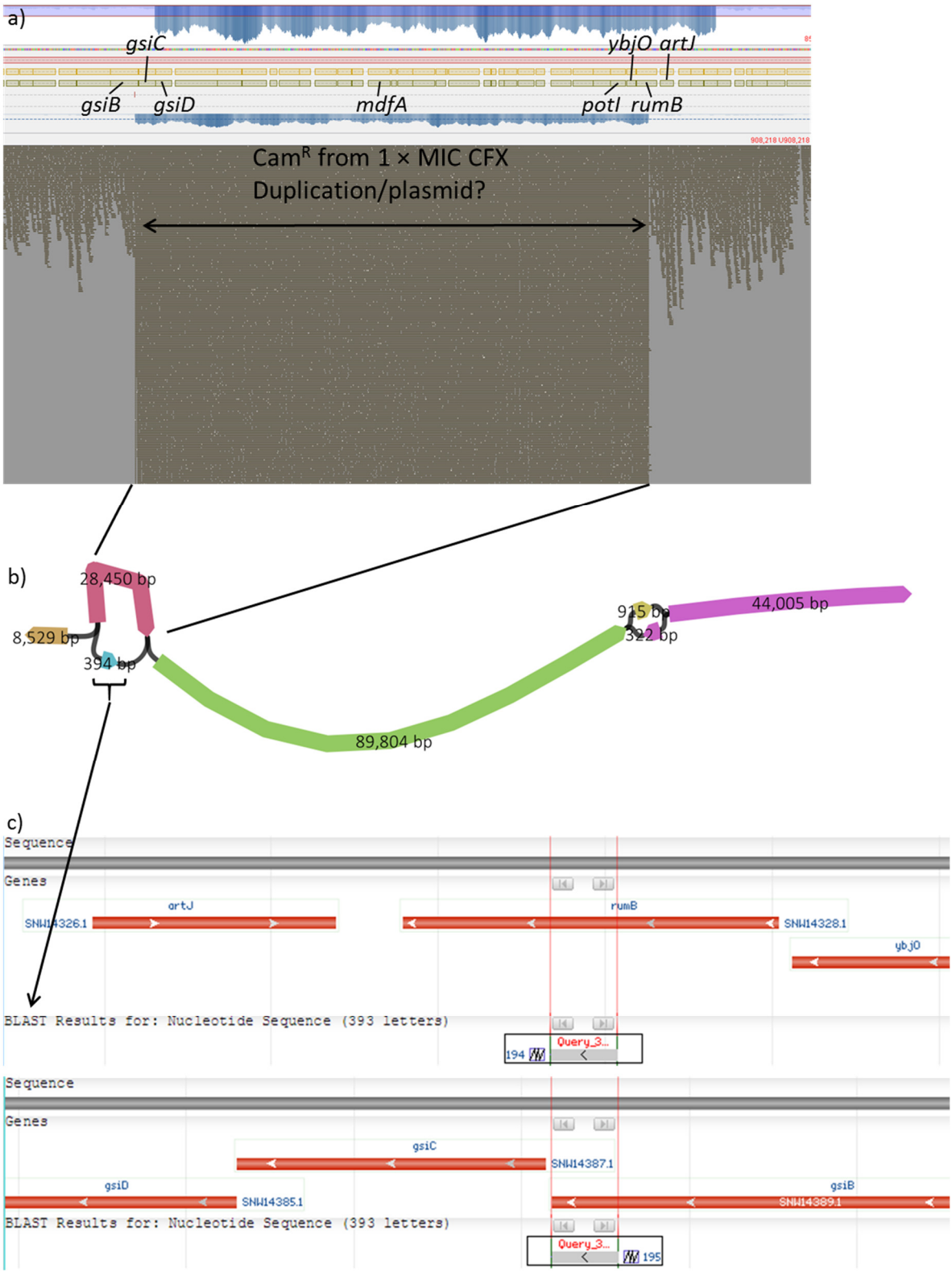

Figure 6.10: Putative plasmid or duplications of bp 870751 – 899202 in a chloramphenicol-resistant strain isolated after treatment with sublethal (1 × MIC) ciprofloxacin. a) Trimmed reads were assembled and aligned to the published *E. coli* MG1655 sequence (using Snippy) and scanned by eye for large-scale genomic changes in Tablet (Milne *et al.*, 2013), with the duplication/plasmid indicated by a large jump in coverage (double-headed arrows). Important

genes and the flanking genes are shown above the assembled reads. b) The assemblies were redone using W2rap Contigger (Clavijo *et al.*, 2017) and visualised using Bandage, with the duplications/plasmid indicated by the 28450 bp and 394 bp unitigs. c) The 394 bp unitig was run in BLASTN. The query sequence aligned to *E. coli* sequences in two places, splitting the query sequence in half and these are graphically presented here (screen shots of the BLAST graphic).

Gene duplications and amplifications (GDA) have been suggested to be found frequently in bacteria populations (including those not under any selection (Brochet *et al.*, 2008, Roth *et al.*, 2006)) and have been implicated in resistance previously in a number of bacterial species (Andersson & Hughes, 2009, Conrad *et al.*, 2009, Hjort *et al.*, 2016, Slager *et al.*, 2014, Sun *et al.*, 2009) including some clinical isolates (Gao *et al.*, 2015, McGann *et al.*, 2014). In particular, MG1655 was shown to have gene duplications of 12 kb – 140 kb after short-term laboratory evolution experiments in lactate minimal media. Here they demonstrated a 1 – 4-fold increase in coverage in their assemblies in areas of the amplifications (Conrad *et al.*, 2009). The first reported gene amplification that was linked with resistance was found in an ampicillin-resistant *E. coli* that had amplifications of the *ampC* gene (Normark *et al.*, 1977). Slager *et al.* (Slager *et al.*, 2014) showed that antibiotics that target DNA replication increased gene dosage near *oriC* in *S. pneunomiae* which was a result of stalled replication forks and refiring of the replication origin. Tandem duplications of 98 kb were found in MRSA clinical isolates as well as 20 kb amplifications that included *mprF* that confers resistance to antimicrobial peptides were identified in vancomycin-intermediate *S. aureus* (Gao *et al.*, 2015). Due to GDA being found in a population of bacteria under no particular selection, it has been suggested that these mutations are often the first selected for when a selection pressure is applied (such as antibiotics) (Andersson & Hughes, 2009, Roth *et al.*, 2006). Further to this, GDA may be a short-term solution (as GDA's have been shown to generally be unstable in a population (Hjort *et al.*, 2016)) to a selection pressure until a stable mutation is established. Thus, GDA's may facilitate antibiotic resistance by allowing populations time to accumulate point mutations that may confer stable

resistance (Andersson & Hughes, 2009). GDA's have been demonstrated to arise through RecA-dependent and -independent routes (Andersson & Hughes, 2009). The RecA-dependent routes include non-equal homologous recombination between long directly repeats (Anderson & Roth, 1981), transposable or insertion elements (Nicoloff *et al.*, 2007) or repeat regions (Shyamala *et al.*, 1990). The RecA-independent routes include DNA secondary structure (Trinh & Sinden, 1993) or crossovers between sister chromatids (Lovett *et al.*, 1993) that may direct recombination between direct repeats or through illegitimate recombination by DNA gyrase (Ikeda *et al.*, 2004). Alternatively, they could happen as a result of double-strand DNA breaks and rolling circle replication (Andersson & Hughes, 2009). There is no evidence that transposons or insertion elements played a role in the amplifications demonstrated here and the closest repeat is 400 bps away (most are >1 kb away) nor are there any repeat regions in the join points (Figure 6.9c and 6.10c). This suggests that these amplifications occurred via a RecA-independent pathway, however this would need further analysis and experimentation to confirm this.

All of the Kan-resistant isolates have mutations in the elongation factor G gene *fusA* (Table 6.12). These include an insertion of a TGC at bp 3471824 in the *fusA* gene causing the addition of an alanine at position 564 and two separate G>A transition mutation (bp 3471539 and 3471686 respectively) causing FusA P658L (Kan-resistant isolate from incubation without CFX) and P610L (Kan-resistant isolate from 0.5 ×MIC CFX treatment) respectively. The P610L mutation has been identified previously (Mogre *et al.*, 2014) and the amino acid 658 has been shown to lie within a set of conserved residues on the C-terminus of the protein (Hou *et al.*, 1994). Overall many mutations in *fusA* resulting in Kan resistance have been reported in both *E. coli* (Lázár *et al.*, 2013) and in *S. aureus* (Norström *et al.*, 2007). Two other mutations that have been shown to contribute to Kan resistance are also seen in the Kan-resistant isolate that had no incubation with CFX and in the 1 × MIC CFX treatment isolate. These are the A>T transversion mutation (bp 4104443) in *cpxA* and the single bp deletion in *cyaA* respectively (Lázár *et al.*, 2013, Mogre & Seshasayee, 2017). Mutations in these genes, alongside the *fusA* genes have been shown to

increase MIC of Kan, however, the study by Mogre and Seshasayee (Mogre & Seshasayee, 2017) has not been published in a peer-reviewed journal, only in the Cold Spring Harbour Laboratory hosted BioRxiv. The other mutation of note, is the 148 bp deletion of *leuP* in the Kan-resistant isolate from the 0.5 × MIC CFX treatment (Figure 6.8a).

Large genomic deletions have been demonstrated here with the deletion of *marR* in the Cam-resistant 1 × MIC CFX-treated isolate and the deletion of *leuP* in the Kan-resistant 0.5 × MIC CFX-treatment isolate (Figure 6.8a and b). Another deletion in another Cam-resistant 1 × MIC CFX-treated isolate (Figure 6.8c) was identified to be a potential excision event of the cryptic e14 prophage. The excision of this prophage in response to treatment with sublethal norfloxacin has been demonstrated by Long *et al.* (Long *et al.*, 2016). The e14 prophage is a defective prophage with important phage-related functional genes having been deleted since integration (Mehta *et al.*, 2004). Despite this, the e14 prophage has been shown to excise from the genome if the SOS response is induced (Brody *et al.*, 1985, Wang *et al.*, 2010). The sequence length of e14 prophage is 15.4 kb long (Mehta *et al.*, 2004) which is a bit longer than the deletion seen in the Cam-resistant strain (15.036 kb). This is not too surprising considering the e14 prophage has been demonstrated to form a 14.4 kb circle after excision (Brody *et al.*, 1985). This prophage seems to provide some protection to the bacterium making it more tolerant to nalidixic acid, and acid stress (without the phage there was a 90-fold reduction in % cell survival after pH 2.5 for 30 min), probably due to its role in biofilm formation (Wang *et al.*, 2010). The other genomic deletions are more difficult to explain and to the best of my knowledge no large deletions (>100 bp) have been reported as a response to sublethal treatment with CFX previously. *Salmonella enterica* has been previously shown to naturally decrease the size of its genome over time by a RecA-independent mechanism with deletions from 1 bp to 212 kb reported (Nilsson *et al.*, 2005). However, the deletions seen here though seem to be in response to treatment with antibiotics so it is unlikely to be a natural mechanism of genome size reduction. Sublethal treatment with fluoroquinolones have been demonstrated to induce small deletions (>19 bp) in *E. coli*

previously (Long *et al.*, 2016, Song *et al.*, 2016) and these were suggested to be independent of the SOS response-induced error-prone polymerases. Translesion polymerases (error-prone polymerases) have been shown to introduce spontaneous deletions in *Salmonella enterica* Typhimurium as a result of double-strand break repair. However, the size of these deletions was not discussed (Koskiniemi & Andersson, 2009). Ultimately, the mechanism behind how these deletions have formed is not known.

With all of the SNP mutations present, the vast majority (44%) are G>A or C>T transition mutations. This has been shown to be the dominant type of spontaneous mutation in *E. coli* (Foster *et al.*, 2015). However, an increase in this kind of SNP mutation has also been linked with an increase in 8-oxo-G- and deamination-damage due to ROS (Lind & Andersson, 2008, Foster *et al.*, 2015). However, in another study, an increase in G>A and C>T transition mutations under treatment with norfloxacin was shown not to be as a result of oxidative damage (Long *et al.*, 2016). Studies that have looked at the effect of sublethal antibiotics on the development of mutation, have shown that genes involved in the SOS response are responsible for the elevated mutation rate under sublethal treatment with CFX; including *recA* which when deleted showed reduced mutation rates when incubated with 0.5 × MIC CFX (Thi *et al.*, 2011). The cleavage of LexA and the concomitant derepression of the three error-prone polymerases *polB*, *dinB*, and *umuCD* have also been shown to be necessary for the increase in mutation caused by sublethal treatment with CFX in *E. coli*, *P. aeruginosa* and *S. aureus* (Cirz *et al.*, 2005, Cirz *et al.*, 2007, Cirz *et al.*, 2006, Mo *et al.*, 2016). Further to this, the reduction of mutation induced by CFX seen in SOS response-depleted strains was also observed in SOS response-depleted hypermutator species of *E. coli* (*E. coli* with mutations in mismatch repair) (Cirz & Romesberg, 2006), suggesting the MMR was not involved in the restoration of CFX-induced mutations. Although the involvement of the error-prone polymerases would explain the increase in SNPs and small deletions or insertions seen here, the larger mutations such as the large deletions or the loops/amplifications are unlikely to be caused by the error-prone polymerases. In fact, induction

of recA-mediated homologous recombination by sublethal CFX is only partially dependent on SOS induction (Lopez & Blazquez, 2009), and recombination between divergent sequences induced by treatment with sublethal concentrations of CFX has been shown to be independent of SOS induction (Lopez *et al.*, 2007). In this case, there is some suggestion that the recombination is induced by the RecBCD and RecFOR pathways (Lopez *et al.*, 2007). Overall, more work is needed to fully explain how the deletions and duplications/amplifications reported here have arisen. However, there is no reason to suspect the DNA gyrase-mediated IR is not involved.

6.4 Conclusions

QIAR assay

Treatment of *E. coli* MG1655 with sublethal concentrations of CFX has resulted in an increase in resistance to non-quinolone antibiotics. This was not seen when the competitive DNA gyrase inhibitor $CouA_1$ was used, nor was it demonstrated with Amp or Kan. Other quinolones including SFX, NFX and OA also induced resistance to non-quinolone antibiotics, however MFX did not. The Redx compound 5931, which inhibits DNA gyrase by stabilising the cleavage complex was demonstrated to induce resistance to other antibiotics although not to the same level as the quinolones suggesting the stabilisation of the cleavage complex may be important. Treatment of the Keio collection strain parent *E. coli* BW25113 with sublethal CFX also showed an increase in resistance to non-quinolone antibiotics. When the quinolone-resistant *E. coli* MLS83L strain (MG1655 with the GyrAS83L mutation) was tested with sublethal CFX, there was no increase in resistance. The hyper-recombination mutants when overexpressed on plasmids did not show much difference in resistance over the overexpressed wild-type GyrA and the overexpressed I203V/I205V mutant showed a greater increase in resistance over the chromosomally expressed

I203V/S204R/I205V protein (NGB345 strain). However, all of these strains when treated with sublethal CFX showed resistance to non-quinolone antibiotics.

Whole genome sequencing

Whole genome sequencing revealed a number of SNPs and small deletions that explained most of the resistance seen. It also showed large-scale genomic modifications that explained two of the Cam-resistance mutations. The cause of these large-scale chromosomal modifications is unknown and more work here is needed, but DNA gyrase-mediated IR has not been ruled out as a potential mechanism.

6.5 Future work

This part of my PhD work has the most unresolved questions. So much so, that a new PhD student will be taking up some of this work from October.

Firstly, all of the assays done here need to be repeated with a wild-type *nfo* MG1655 strain. I would reassess the antibiotics used in the second selection step and perhaps look to include more clinically-relevant antibiotics such as rifampicin or vancomycin. I would also try with the antimicrobial peptide microcin B17, which targets DNA gyrase and stabilises the cleavage complex but seemingly not in the same way as quinolone antibiotics. Further repetitions of the other quinolone and non-quinolone antibiotics need to be done to get a true reflection of the induced resistance profile. This is also true for the other strains of *E. coli* and I would like to include some clinically isolated strains in the experiments. I would like to continue to work on getting the hyper-recombination mutations into the MG1655 chromosome and to test these fully. I would also like to design an assay that would allow us to measure mutation rates either by Delbruck and Luria fluctuation assays or through mutation accumulation studies (Pope *et al.*, 2008).

Secondly, I would like to try and work out the mechanism behind the increase in resistance after sublethal treatment by CFX. I would like to systematically delete genes or pathways involved in SOS response, non-homologous end joining, and other DNA repair pathways including the RecBCD and FOR pathways to see how these affect the increase in resistance.

Thirdly, I would like to confirm and establish what the amplifications are by PCR or long-read sequencing. I would also further evaluate the WGS data and try and evaluate the deletion and amplification junctions to see if any further information about the likelihood that they are as a result of DNA gyrase-mediated IR can be obtained. I would also send more strains for WGS to see if the genome modifications continue to occur and do long-read WGS alongside de novo assemblies on these to see if any other rearrangements can be discerned.

Chapter 7: Discussion and Conclusions

7.1 Discussion

IR assays

λ-based assays

This project began with attempts to re-establish the assays that were done by Ikeda *et al.* (Ikeda *et al.*, 1982, Ikeda *et al.*, 1984, Ikeda *et al.*, 1980, Ikeda & Shiozaki, 1984) to further study the molecular and biochemical reasons for the demonstrated topoisomerase-mediated IR. However, the λ-based assays proved to be more problematic than anticipated. There is a notion that gyrase-mediated IR as described previously may be an artefact. The translocations seen may have been due to the high concentrations of DMSO in the packaging extracts (Kobayashi & Ikeda, 1977) and the involvement of gyrase and topoisomerases in IR may be more subtle or indirect.

Non-λ assays

At the same time, I also worked on optimising a separate non-λ assay to study topoisomerase-mediated IR. Despite this assay appearing to be a simpler system in theory, in practise it has proved to be more complicated. This complication arose from the DNA substrates used in the assay. In particular, the pBR322* plasmid substrate which, due to it being a high-copy number plasmid, results in a cotransformants that make it difficult to identify recombinants. In spite of this difficulty, the non-λ assay still has the potential to be a good system for studying IR, particularly if a better DNA substrate can be found. The λ-based assays also still have the potential to work as there are still avenues of enquiry that have not been fully explored. Both the λ-based and non-λ assays had to be put aside due to time constraints and other assays proving more successful.

Hyper-recombination mutants

Ashizawa *et al.* (1999) identified mutations in GyrA that conferred a hyper-recombination phenotype in their assay (*in vivo*). These were I203V/I205V, L488P and L492P. The L492P mutant was purified and tested in an *in vitro* supercoiling assay. The authors suggested that the reason for the hyper-recombination phenotype was that these mutations were causing spontaneous double-stranded breaks (DSBs) in the chromosome. This was due to the mutations causing instability in the GyrA dimer, or by these mutations causing a defect in the cleavage or religation reaction by the enzyme. I had always planned to purify these mutants and use them in the IR assays as well as characterise them using biochemical activity assays. However, when the IR assays were put aside, I worked on characterising the *in vitro* activity of all three mutants.

In Chapter 4, I show that contrary to the phenotype suggested by Ashizawa *et al.* (1999), here none of the mutations increased the amount of natural cleavage of the enzyme, nor were there any defects in religation. Moreover, the mutations do not appear to destabilise the GyrA dimer. The I203V/I205V mutations seem to reduce the activity the enzyme all round, while the L488P and L492P mutations appear to affect the stability of exit gate of the enzyme. How these mutations would induce a hyper-recombination phenotype is not immediately obvious. In fact, the *in vitro* activities of these mutants seem counter to a hyper-recombination phenotype.

I203V/I205V mutations

To rationalise the unexpected phenotype seen with these mutations, I suggest that the reduced activity seen with the I203V/I205V mutations could potentially cause downstream effects leading to an accumulation of DSBs and induction of the SOS response. Here, a build-up of positive supercoils during replication and transcription could result in replication fork collapse and pausing or stalling of both the replication machinery and RNA polymerase. Both of these situations have been demonstrated to lead to an increase in DSBs and induction of the SOS response (Lilley *et al.*, 1996, Michel *et al.*, 2004, Seol & Neuman, 2016). Alternatively, this could also result in a loss of superhelical density in the chromosome. This could affect replication and

transcription which may trigger a general stress response (Peter *et al.*, 2004) leading to the phenotype described by Ashizawa et al (1999). The I203V/I205V mutant could have a particularly severe phenotype when the temperature is increased, as is seen with in the Ashizawa *et al.* (1999) study where the lysogens were shifted to 42°C for induction of the lytic cycle. Transient relaxation of DNA has been demonstrated after heat shock at 42°C *in vivo*, followed by increased negative supercoiling (decrease in linking number) upon the shift to higher temperatures (Camacho-Carranza *et al.*, 1995, Mizushima *et al.*, 1993, Rui & Tse-Dinh, 2003). Although increased relaxation of chromosomal DNA has been shown to increase expression of the subunits of DNA gyrase (Dorman & Dorman, 2016, Menzel & Gellert, 1983, Snoep *et al.*, 2002), it is not known whether the increase in supercoiling post heat shock is due to an increase in the amount of DNA gyrase or whether there is an increase in the activity of the enzyme. In *Streptococcus* sp., there was no significant increase in the presence of *gyrA* or *gyrB* transcripts at 40°C, suggesting no increase in the expression of these genes at higher temperature (Smoot *et al.*, 2001). This may suggest that there is more reliance on the activity of the enzyme at higher temperatures, which would amplify the effects of the I203V/I205V mutant leading to DSBs and the hyper-recombination phenotype seen by Ashizawa *et al.* (1999).

L488P and L492P mutations

With the L488P and L492P mutants, again a seemingly contradictory *in vitro* phenotype was seen with very low natural cleavage activity observed. However, in comparison to the I203V/I205V mutations, these mutants did show a more severe phenotype. The L488P and L492P mutations appear to cause defects in the exit or C-gate in GyrA. This could either be by interfering with the transduction of information from the DNA-gate to the C-gate, or by causing the gate to remain in a closed conformation or to dwell primarily in an open conformation. There is little information on how the opening of the C-gate is controlled. It has been demonstrated that DNA cleavage and strand passage will occur when the C-gate of DNA gyrase and topo II is cross-linked (Roca, 2004, Roca *et al.*, 1996, Williams & Maxwell, 1999b). Moreover, when the C-

gate in topo II was truncated so that it was thought to be unable to close, there was a loss of activity by two orders of magnitude (Martinez-Garcia *et al.*, 2014). This truncated mutant was used to demonstrate that the C-gate is necessary for the type IIA topoisomerases to do topology simplification (Martinez-Garcia *et al.*, 2014). Topology simplification is the observation that the type IIA topoisomerases are able to reduce the level of crossings of DNA through relaxation, decatenation and unknotting, beyond thermal equilibrium (Rybenkov *et al.*, 1997). They showed that the distribution of topoisomers after relaxation with the truncated C-gate resembled that of those after relaxation with topo I, which cannot do topology simplification (Martinez-Garcia *et al.*, 2014). They also demonstrated that this truncated topo II could not mediate reverse strand passage (Martinez-Garcia *et al.*, 2014). This suggests that the DNA-gate does not readily open in this mutant. A similar observation was made by Williams *et al.* (1999a) who showed a 75 – 90% reduction in the relaxation of negative supercoils by DNA gyrase when the DNA-gate was cross-linked. Relaxation of negative supercoils by gyrase has been demonstrated to occur by a reverse-strand passage mechanism (Williams & Maxwell, 1999b). Taking all of this into consideration, I suggest that the L488P and the L492P mutations cause the C-gate to dwell in an open conformation. I also propose that the reason that Martinez-Garcia *et al.* (2014) required so much more enzyme to see relaxation activity with their truncated topo II was because the DNA-gate did not open frequently due to the open C-gate. I also suggest that the DNA-gate may have been forced open occasionally. In this case the dimers of the truncated topo II may have stayed together due to the N-gate of topo II not being a separate subunit and the fact that the NTDs of topo II have been shown to wrap around each other upon dimerisation and strand passage (Schmidt *et al.*, 2012). This is unlike DNA gyrase in which the N-gate is made by GyrB, which is a separate subunit to GyrA which makes up the DNA-gate and C-gate (Reece & Maxwell, 1991a, Reece & Maxwell, 1989). Studies have suggested that having two of the three protein interfaces closed during the "two-gate mechanism" of strand passage provides stability to the enzyme. This prevents the enzyme complex from dissociating during the catalytic cycle which would result in DNA DSBs and chromosome fragmentation (Roca, 2004, Roca *et al.*, 1996,

Rudolph & Klostermeier, 2013, Williams & Maxwell, 1999b). Thus, in gyrase, if the DNA-gate was forced open when the C-gate was also open, this could lead to both subunits dissociating, carrying with it the cleaved DNA. This would cause DSBs which would potentially explain the hyper-recombination phenotype.

Subunit exchange

In Chapter 5, we demonstrated that GyrA, GyrA59 and GyrB can form higher-order oligomeric species. GyrA and GyrA59 form multimers in steps of two, whereas GyrB in steps on one. The full-length DNA gyrase was also shown to associate in higher-order species, however, the stoichiometry of this was not ascertained. The subunits in these higher-order species were also demonstrated to be labile and subunit exchange was possible under certain conditions from within the multimeric species. This was demonstrated by mixing GyrA with GyrA59 and GyrB and incubating them together over at least 18 h. Heterodimers of GyrA and GyrA59 as well as other multimeric species were visible at the 18 h time point. This observed subunit exchange occurred in the presence of DNA, however, no increase was visible when ciprofloxacin (CFX) was added alone or with DNA. The presence of ATP considerably reduced subunit exchange, even in the presence of DNA or DNA and CFX, suggesting that the nucleotide contributes to the stability of the subunits. Still, this stabilisation by ATP did not entirely preclude exchange between the GyrA and GyrA59 subunits as after 48 h there was evidence that heterodimers were formed. This raised the question of what effect a high ADP concentration would have on this observed subunit exchange. The ATP:ADP ratio has been demonstrated to drop in *E. coli* in the transition to stationary phase before ATP levels recovered in stationary phase (Buckstein *et al.*, 2008). This has been demonstrated to have a concomitant relaxation of the chromosome during this time, until ATP levels recover (Reyes-Domínguez *et al.*, 2003, Gutiérrez-Estrada *et al.*, 2014, Hsieh *et al.*, 1991, van Workum *et al.*, 1996). The return to negative supercoiling when the ATP levels recovered was shown to be reliant on the pool of gyrase already present as no increase in the expression of the enzyme was detected (Reyes-Domínguez *et al.*, 2003). The relaxation has also

been shown to be a direct response to the decrease in ATP:ADP ratio and gyrase was implicated in this decrease (van Workum *et al.*, 1996). Taken together, this may suggest that subunit exchange could potentially occur *in vivo*, providing that gyrase associates in these higher-order oligomers *in vivo* as well. GyrA has been previously demonstrated to associate in a hexamer, however, this was an asymmetric unit in a crystal of the *B. subtilis* GyrA subunit (Rudolph & Klostermeier, 2013). An interesting feature of this hexameric asymmetric unit is that the DNA-gate and C-gate of each monomer makes a protein contact with DNA-gate and C-gate of two other monomers, in a domain swapping fashion (PDB: 4DDQ). Nonetheless, higher-order multimers of GyrA or DNA gyrase have not been demonstrated *in vivo*.

Heterodimers of the human topo II isoforms, topo IIα and topo IIβ have been identified *in vivo* and have been found to be active *in vitro* (Biersack *et al.*, 1996, Gromova *et al.*, 1998). However, these have been suggested not to form as a result of subunit exchange and no oligomers of the two enzymes were detected (Biersack *et al.*, 1996, Gromova *et al.*, 1998). Contrary to this, yeast topo II was demonstrated to form multimers *in vitro*. The degree of multimerisation was concentration dependent, although the multimers were not restricted to high concentrations (Vassetzky *et al.*, 1994). When the multimeric species was isolated, it was found to be catalytically active, and arguably, more active than the dimeric species (Vassetzky *et al.*, 1994). Further to this, another study showed that more than one human topo IIα dimer will bind one DNA crossing using atomic force microscopy (AFM) (Alonso-Sarduy *et al.*, 2011). Evidently there is no clear consensus in the literature about the formation of higher-order oligomers of topoisomerase subunits. This may be due to different methods of detection or differing experimental conditions. Vassetzky *et al.* (1994) have shown that the multimers observed with yeast topo II are dependent on a number of factors. Salt concentrations (NaCl) above 150 mM were shown to disrupt multimers as was the addition of $CaCl_2$, however in contrast, $CuSO_4$ was demonstrated to increase the formation of multimers (Vassetzky *et al.*, 1994). Furthermore, the level of phosphorylation of topo II was also demonstrated to be

important in the formation of multimers; phosphorylation with casein kinase II increased aggregation by 20% (Vassetzky *et al.*, 1994).

When the GyrA and GyrA59 subunits were incubated with GyrB, DNA and ATP under supercoiling assay conditions (Chapter 2), there is evidence of a tetrameric species that appears to be a heterodimer (GyrA/GyrA59) with the GyrA59 homodimer ($GyrA59_2$), that is $A59_2$ +AA59. This would imply that low levels of subunit exchange are occurring during the catalytic cycle in the presence of ATP. This appears contrary to work done previously by Tennyson and Lindsley (1997) who showed that eukaryotic topo II is a stable dimer and no subunit exchange occurred during the catalytic cycle of the enzyme. It also appears contradictory to work done by Gubaev *et al.* (2016), who demonstrated that there was no subunit exchange visible between subunits of DNA gyrase. Both of these studies used two different assays, one using fluorescence and the other using inactivated subunits that upon exchange would result in a loss of activity. Two further points on those that I have raised in Chapter 5 with regards to these conflicting results. The first is that Tennyson and Lindsley (1997) purified and stored the subunits of their subunit exchange immunoprecipitation assay in 500 mM NaCl, which, based on the work by Vassetzky *et al.* (1994), would result in a loss of multimers. Based on the work presented here, I suggest that subunit exchange occurs within these multimers, the loss of which would result in no subunit exchange, as demonstrated by Tennyson and Lindsley (1997). The second point is from a discussion with Thomas Germe (JIC). He suggested that based on my multimer theory, and the domain swapping seen in the GyrA crystals by Rudolph and Klostermeier (2013) that the inactivated subunits could still be active if they formed multimers. With regards to the assay presented in Tennyson and Lindsley (1997), subunit exchange could still be occurring in the multimers, however, there would be no loss in activity if the multimers contained at least two wild-type subunits. With regards to the work by Gubaev *et al.* (2016), again, if the enzyme was to found to be active in multimers, then subunit exchange could still occur without the loss of activity. Furthermore, this may also explain the extraordinary results obtained by Gubaev *et al.*

(2016) who proposed that DNA gyrase can negatively supercoil DNA with only one catalytic tyrosine. This, of course, is all speculative as there is no evidence that type IIA topoisomerases typically function in multimers, and the conventional view is that type II topoisomerases function as dimers (Higgins *et al.*, 1978, Klevan & Wang, 1980, Sugino *et al.*, 1980, Vos *et al.*, 2011). I'm not necessarily disputing this fact as, although higher-order oligomers are found, dimers are still the primary species. However, while not conclusive evidence that this is typical, multimers of topo II have been demonstrated to be catalytically active and more than one unit of topo II has been observed at DNA crossings previously (Vassetzky *et al.*, 1994, Alonso-Sarduy *et al.*, 2011).

QIAR

In Chapter 6, I outlined data showing that treating *E. coli* with sublethal concentrations of CFX can cause resistance to other, non-quinolone antibiotics. This was not seen when I ran the assay with the β-lactam ampicillin (Amp) or the aminoglycoside kanamycin (Kan). Nor was it seen when *E. coli* were sublethally treated with the aminocoumarin coumermycin A_1 (a non-quinolone, DNA gyrase inhibitor). This suggested that the stabilisation of cleavage was important to this increase in the frequency of resistance. This was corroborated by other cleavage-stabilising compounds, namely three other quinolones, oxolinic acid, norfloxacin and sparfloxacin, and a compound from our collaborators Redx Anti-Infectives, RedX05931. Interestingly, moxifloxacin did not appear to show the same increase in resistance as seen with the other quinolones. Although this may not be that surprising as it has been shown to be less mutagenic than other quinolones (Malik *et al.*, 2012, Schedletzky *et al.*, 1999). The increase in resistance was not seen when a strain of *E. coli* that has mutations in *gyrA* that confer quinolone resistance was used. This suggests that DNA gyrase plays a primary role in this development of resistance. Although topo IV has also been demonstrated to be a target for quinolones, DNA gyrase has been shown to be the primary target for CFX in *E. coli* (Drlica *et al.*, 2008, Redgrave *et al.*, 2014). Quinolones has have been shown to either target gyrase or topo IV or both depending on the species of bacteria and the quinolone itself (Aldred *et al.*, 2014b, Ferrero *et*

al., 1994, Khodursky *et al.*, 1995, Correia *et al.*, 2017). Thus, this effect may be specific to this quinolone (CFX) in this species of bacteria (*E. coli*). Although these data look promising, they need to viewed with caution. Most of the results presented here are very preliminary and due to time pressures, many of these assays were only run once or twice. To make these data statistically robust many of these assays need to be repeated. I believe this will also provide a more realistic comparison with the data obtained with sublethal CFX. Overall, I think the assay could also be improved to make it more clinically-relevant and to facilitate further study into the processing of quinolones *in vivo*. Despite these caveats, the general trends observed here concur with much of the published data, with a number of studies showing that sublethal treatment with quinolones increase both mutation rate (Gillespie *et al.*, 2005, Komp Lindgren *et al.*, 2003, Thi *et al.*, 2011) and mutation frequency (Andersson & Hughes, 2014, Cirz *et al.*, 2007, Cirz *et al.*, 2006, Cirz & Romesberg, 2006, Kohanski *et al.*, 2010, Martinez & Baquero, 2000, Mo *et al.*, 2016, Tattevin *et al.*, 2009).

A proportion of resistant and non-resistant strains isolated in the assays were sent for whole genome sequencing (WGS) and broadly three types or mutations were observed. The majority of these were SNPs and small insertions or deletions (<5 bp), however there was evidence of greater chromosomal modifications as well, such as larger deletions (>100 bp) and gene amplifications (20 -45 kb). Most of the antibiotic-resistance determinants were identified as due to the SNPs and many of these were known variants. However, two chloramphenicol (Cam)-resistant isolates were found to be resistant as a result of the larger chromosomal modifications, namely the deletion of the *marR* gene in one and the increase in gene copy number (due to the amplification) of *mdfA* in the other. Both of these are known to cause resistance to Cam but they have also been suggested to result in an increase in resistance to a number of antibiotics, including CFX (Alekshun & Levy, 1997, Cohen *et al.*, 1993, Edgar & Bibi, 1997, Nicoloff *et al.*, 2007).

Based on the literature and the information on the development of mutation due to antibiotics therein, I propose that there are two ways resistance develops in response to sublethal treatment with CFX. However, these may not be mutually exclusive and are either via the SOS response pathway or independent of it. In response to sublethal treatment with CFX, the SOS response is upregulated and this results in an increase in survivability alongside an increase in mutagenesis (Martinez & Baquero, 2000, Torres-Barceló *et al.*, 2015). This ultimately results in SNPs in the genes that confer resistance to CFX itself. When the bacteria are then challenged with another antibiotic, this increase in competitive ability under stress as well as the increase in mutability can result in SNPs that confer resistance to the secondary selection antibiotic. In other words, the pre-exposure to CFX, causes upregulation of a stress response that prepares the bacterium to survive further increased stress. Alternatively, the antibiotic-resistance mutation to the secondary antibiotic does arise randomly in the initial incubation, but the fitness of the bacterium that carries this mutation is only increased upon the secondary selection (Martinez & Baquero, 2000). The reason that CFX-resistance mutations are not seen alongside other resistance mutations is probably due to a decrease in the SOS response, which has been found to decline as resistance to CFX is established (Torres-Barceló *et al.*, 2015). Thus, the response that has increased the survivability to stress is decreased leaving the CFX-resistant cells susceptible to the second antibiotic. Resistance to CFX during sublethal CFX treatment was visible in the treated but unselected isolates that were sent for WGS. This suggests that in some cases the CFX resistance could have arisen during the initial sublethal incubation and the secondary CFX selection was not needed for development of resistance. The SOS response can also increase the frequency of resistance via horizontal gene transfer (HGT) (Baharoglu & Mazel, 2014). It has been demonstrated to increase conjugational transfer of antibiotic resistance genes, and increase the incidence of transduction by inducing excision of prophage (Baharoglu *et al.*, 2010, Baharoglu *et al.*, 2013, Long *et al.*, 2016). One of the large chromosomal deletions seen here was the excision of the e14 prophage. Although there was no gain of resistance

through HGT by this, it does reinforce that CFX can contribute to the transfer of resistance from one bacterium to another by HGT.

The second way resistance can be induced by CFX is by recombination. This is evident by the deletion of *marR* and the amplification of *mdfA* seen in this work which caused resistance to Cam. Lopez *et al.* (Lopez & Blazquez, 2009, Lopez *et al.*, 2007) has demonstrated that CFX can induce recombination between homologous and divergent DNA sequences. They show that this is mediated by RecA and RecBCD respectively. RecBCD has been demonstrated to be involved in the processing of quinolone-induced double-strand breaks in preparation of induction of the SOS response (Sutherland & Tse-Dinh, 2010). Although no insertions, inversions or translocations are visible in the data I have presented, this may be due to the type of sequencing and assemblies that were performed on the data. The lack of insertions is probably due to there being no exogenous source of DNA in the bacteria to insert into the chromosome. However, there are deletions and the potential gene amplifications present. Although there is evidence that SOS-induced translesion polymerases (Pol II, Pol IV and Pol V) can mediate spontaneous deletions, the size of these, to the best of my knowledge, is unreported (Andersson *et al.*, 2010). However, in eukaryotes, the translesion polymerases have been shown to mediate deletions up to 200 kb (Roerink *et al.*, 2014). Thus, it is possible that the translesion polymerases could induce the deletions seen here. Gene amplifications are thought to occur randomly in a population of bacteria and are not necessarily as a result of a stress response (Andersson & Hughes, 2009, Sandegren & Andersson, 2009). However, they have been found previously as the meditators of antibiotic resistance as they can cause an increase in gene dosage that can increase resistance (Brochet *et al.*, 2008, Hjort *et al.*, 2016, Sun *et al.*, 2009). Gene amplifications are examples of adaptive evolution as they have been suggested to provide a short-term solution to selection, allowing time for induction of more permanent mutations or potentially the creation of novel biochemical solutions (for example through gene fusions) (Andersson & Hughes, 2009). Whether these gene amplifications are in response to treatment with CFX, or if they are already present

in the population and have been selected for because they decrease susceptibility to CFX, is not yet known. Although they were found in isolates resistant to Cam, the *mdfA* gene is also known to increase resistance to CFX (Edgar & Bibi, 1997). Many of these multidrug resistance mechanisms show variable resistance to different antibiotics, with some being more efficient against specific antibiotics than others (Nilsen *et al.*, 1996, Alekshun & Levy, 1997, Edgar & Bibi, 1997, Nicoloff *et al.*, 2007). The two that feature in this work, the ones controlled by the MarR regulon and the *mdfA* gene are known to be more effective against Cam, although they do decrease susceptibility to CFX and tetracycline (Alekshun & Levy, 1997, Alekshun & Levy, 2007, Edgar & Bibi, 1997, Nicoloff *et al.*, 2007, Swick *et al.*, 2011). Therefore, I propose that in these cases the mutations are a direct response to the treatment with the sublethal CFX and the mitigating effect against Cam is secondary. This implies that in some cases, the quinolone-induced antimicrobial resistance to other antibiotics is a secondary effect. This also raises the issue of the difference between clinical resistance versus microbiological resistance. Clinical antibiotic resistance is defined as a failure to clear an infection after adequate antimicrobial dosage and schedule are followed. It is often defined as a clinical breakpoint (Cantón & Morosini, 2011). Microbiological resistance is defined as an acquired mechanism of resistance that makes an isolate less susceptible to an antimicrobial. This is regardless of the level of resistance and does not necessarily relate to clinical resistance (Cantón & Morosini, 2011). Thus, the resistance mechanism acquired against the sublethal CFX may not make the isolate clinically resistant to CFX. However, it may make it clinically resistant to another antibiotic, depending on the type of resistance. This further emphasises the importance of reducing exposure of bacterial communities to sublethal concentrations of quinolones. One solution that has been suggested, is a move away from minimum inhibitory concentration (MIC) and to focus more on a mutant prevention concentration (Andersson & Hughes, 2010, Andersson & Hughes, 2014, Gullberg *et al.*, 2011).

Ultimately, the data presented here suggest that CFX can induce mutations and IR. However, the exact mechanism behind it has yet to be ascertained and whether DNA gyrase or topo IV are directly involved is unknown.

7.2 Conclusion

From the data presented in this thesis, the question of how DNA gyrase is involved in IR is still unexplained. I have shown that subunit exchange is possible but not necessarily in the way that was expected. I propose that type IIA topoisomerases may be catalytically active in multimers and subunit exchange can occur in these multimers. The hyper-recombination mutations gave results that did not immediately suggest a biochemical reason for their *in vivo* phenotype. Here, I suggest that the I203V/I205V mutant may be perturbing supercoiling which has downstream effects leading to increased recombination. While the L488P and L492P mutations may be disrupting the exit gate of DNA gyrase which can lead to much lower activity and potentially the dissolution of the subunits in extreme circumstances. The treatment of *E. coli* with sublethal CFX has shown that IR may play a role in the increase in the frequency of resistance, however, the role of gyrase in this is not clear. The emerging picture is a complicated one in that topoisomerases seem to be necessary for IR. However, the prominence of this involvement and the molecular details of their role in IR has evaded us. In some cases, it looks to be an incidental role, such as in the accumulation of SNPs that result in antibiotic resistance, and in others it seems to be more direct, such as in the accumulation of larger chromosomal modifications. These may be caused by subunit exchange under the appropriate conditions, however, this is merely speculation. Overall, more work is necessary to ascertain the role of topoisomerases in IR.

List of abbreviations

A_2B_2: GyrA/GyrB heterotetramer (functional unit of DNA gyrase)

ADP: adenosine diphosphate – hydrolysis product of ATP

ADPNP: 5'-adenylyl β,γ-imidodiphosphate

Amp: ampicillin

Amp^R: ampicillin resistance

AP: apurinic/apyrimidinic

ATP: adenosine triphosphate

BN: blue-native

bp: base pair

$CaCl_2$: calcium chloride

Cam: chloramphenicol

Cam^R: chloramphenicol resistant

CFU: colony forming unit

CFX: ciprofloxacin

CFX^R: ciprofloxacin resistant

cou^r: coumermycin A_1 resistance

CD: circular dichroism

CTD: C-terminal domain

DMSO: dimethyl sulfoxide

DNA: deoxyribonucleic acid

DSB: double stranded break

dsDNA: double-stranded DNA

DTT: dithiothreitol

EB: enzyme buffer

EDTA: ethylenediaminetetraacetic acid

EtOH: ethanol

G-segment: gate segment

gyrase: DNA gyrase

GyrA: gyrase A

GyrA59: CTD truncation of GyrA

GyrB: gyrase B

h: hour/s

HCl: hydrochloric acid

HSP90: heat shock protein 90

IR: illegitimate recombination

K-PCR: *Kan*^{R} gene PCR product

Kan: kanamycin

Kan^{R}: kanamycin resistance

kb: kilobase pairs

KCl: potassium chloride

kDa: kilo Dalton

λ: bacteriophage lambda

LB: Luria-Bertani or Lysogeny Broth Media

Liq N_2: liquid nitrogen

Lk: linking number

mAMSA: (9-acridinylamino) methanesulphon-m-anisidide

Mb: megabase pairs

$MgCl_2$: magnesium chloride

$MgSO_4$: magnesium sulphate

MFX: moxifloxacin

MIC: minimum inhibitory concentration

min: minute/s

NaOAc: sodium acetate

NaCl: sodium chloride

nal^{r}: nalidixic acid resistance

$(NH_4)_2SO_4$: ammonium sulphate

NFX: norfloxacin

NTD: N-terminal domain

OA: oxolinic acid

OD_{600}: optical density at wavelength 600 nm

PAGE: polyacrylamide gel electrophoresis

PCR: polymerase chain reaction

PFU: plaque forming unit

QIAR: quinolone-induced antimicrobial resistance

QRDR: quinolone resistance-determining region

RNA: Ribonucleic acid

ROS: reactive oxygen species

s: second/s

ScAB: DNA gyrase supercoiling assay buffer

SDM: site-directed mutagenesis

SDS: sodium dodecyl sulphate

SFX: sparfloxacin

SHDIR: short-homology dependent illegitimate recombination

SHIIR: short-homology independent illegitimate recombination

SNP: single nucleotide polymorphism

ssDNA: single-stranded DNA

t-AML: therapy-related acute myeloid leukaemia

Tet: tetracycline

Tet^R: tetracycline resistant

Tri: triclosan

Tri^R: triclosan resistant

topo I: topoisomerase I

topo II: topoisomerase II

topo III: topoisomerase III

topo IV: topoisomerase IV

topo V: topoisomerase V

topo VI: topoisomerase VI

topo VIII: topoisomerase VIII

TOPRIM: topoisomerase-primase

T-segment: transport segment

Tris.HCl: tris(hydroxymethyl)aminomethane hydrochloride

Tw: twist

WGS: whole genome sequencing

WHD: winged-helix domain

WHO: World Health Organisation

Wr: writhe

WT/wt: wild type

References

Adachi, T., M. Mizuuchi, E.A. Robinson, E. Appella, M.H. O'Dea, M. Gellert & K. Mizuuchi, (1987) DNA sequence of the E. coli gyrB gene: application of a new sequencing strategy. *Nucleic Acids Res.* **15**: 771-784.

Adams, D.E., E.M. Shekhtman, E.L. Zechiedrich, M.B. Schmid & N.R. Cozzarelli, (1992) The role of topoisomerase IV in partitioning bacterial replicons and the structure of catenated intermediates in DNA replication. *Cell* **71**: 277-288.

Ahmed, W., C. Sala, S.R. Hegde, R.K. Jha, S.T. Cole & V. Nagaraja, (2017) Transcription facilitated genome-wide recruitment of topoisomerase I and DNA gyrase. *PLoS Genet.* **13**: e1006754.

Ahuja, H.G., C.A. Felix & P.D. Aplan, (2000) Potential role for DNA topoisomerase II poisons in the generation of t(11;20)(p15;q11) translocations. *Genes Chromosomes & Cancer* **29**: 96-105.

Akimitsu, N., K. Kamura, S. Toné, A. Sakaguchi, A. Kikuchi, H. Hamamoto & K. Sekimizu, (2003) Induction of apoptosis by depletion of DNA topoisomerase IIα in mammalian cells. *Biochem. Biophys. Res. Commun.* **307**: 301-307.

Aldred, K.J., T.R. Blower, R.J. Kerns, J.M. Berger & N. Osheroff, (2016) Fluoroquinolone interactions with Mycobacterium tuberculosis gyrase: Enhancing drug activity against wild-type and resistant gyrase. *Proc. Natl. Acad. Sci. USA* **113**: E839-846.

Aldred, K.J., E.J. Breland, V. Vlckova, M.P. Strub, K.C. Neuman, R.J. Kerns & N. Osheroff, (2014a) Role of the water-metal ion bridge in mediating interactions between quinolones and Escherichia coli topoisomerase IV. *Biochemistry* **53**: 5558-5567.

Aldred, K.J., R.J. Kerns & N. Osheroff, (2014b) Mechanism of Quinolone Action and Resistance. *Biochemistry* **53**: 1565-1574.

Aldred, K.J., S.A. McPherson, C.L. Turnbough, Jr., R.J. Kerns & N. Osheroff, (2013) Topoisomerase IV-quinolone interactions are mediated through a water-metal ion bridge: mechanistic basis of quinolone resistance. *Nucleic Acids Res.* **41**: 4628-4639.

Alekshun, M.N. & S.B. Levy, (1997) Regulation of chromosomally mediated multiple antibiotic resistance: the mar regulon. *Antimicrob. Agents Chemother.* **41**: 2067-2075.

Alekshun, M.N. & S.B. Levy, (2007) Molecular Mechanisms of Antibacterial Multidrug Resistance. *Cell* **128**: 1037-1050.

Ali, J.A., A.P. Jackson, A.J. Howells & A. Maxwell, (1993) The 43-kilodalton N-terminal fragment of the DNA gyrase-b protein hydrolyzes ATP and binds coumarin drugs. *Biochemistry* **32**: 2717-2724.

Ali, J.A., G. Orphanides & A. Maxwell, (1995) Nucleotide-binding to the 43-kilodalton N-terminal fragment of the DNA gyrase-b protein. *Biochemistry* **34**: 9801-9808.

Alonso-Sarduy, L., C. Roduit, G. Dietler & S. Kasas, (2011) Human topoisomerase II–DNA interaction study by using atomic force microscopy. *FEBS Lett.* **585**: 3139-3145.

Aminov, R., (2017) History of antimicrobial drug discovery: Major classes and health impact. *Biochem. Pharmacol.* **133**: 4-19.

Anderson, P. & J. Roth, (1981) Spontaneous tandem genetic duplications in Salmonella typhimurium arise by unequal recombination between rRNA (rrn) cistrons. *Proc. Natl. Acad. Sci. USA* **78**: 3113-3117.

Andersson, D.I. & D. Hughes, (2009) Gene Amplification and Adaptive Evolution in Bacteria. *Annu. Rev. Genet.* **43**: 167-195.

Andersson, D.I. & D. Hughes, (2010) Antibiotic resistance and its cost: is it possible to reverse resistance? *Nat. Rev. Microbiol.* **8**: 260-271.

Andersson, D.I. & D. Hughes, (2014) Microbiological effects of sublethal levels of antibiotics. *Nat. Rev. Microbiol.* **12**: 465-478.

Andersson, D.I., S. Koskiniemi & D. Hughes, (2010) Biological roles of translesion synthesis DNA polymerases in eubacteria. *Mol. Microbiol.* **77**: 540-548.

Andrews, J.M., (2001) Determination of minimum inhibitory concentrations. *J. Antimicrob. Chemother.* **48 Suppl 1**: 5-16.

Aplan, P.D., (2006) Causes of oncogenic chromosomal translocation. *Trends in genetics : TIG* **22**: 46-55.

Appleyard, R.K., (1954) Segregation of New Lysogenic Types during Growth of a Doubly Lysogenic Strain Derived from Escherichia Coli K12. *Genetics* **39**: 440-452.

Aratani, Y., T. Andoh & H. Koyama, (1996) Effects of DNA topoisomerase inhibitors on nonhomologous and homologous recombination in mammalian cells. *Mutat. Res./DNA Repair* **362**: 181-191.

Aravind, L., L.M. Iyer, T.E. Wellems & L.H. Miller, (2003) Plasmodium biology: Genomic gleanings. *Cell* **115**: 771-785.

Aravind, L., D.D. Leipe & E.V. Koonin, (1998) Toprim--a conserved catalytic domain in type IA and II topoisomerases, DnaG-type primases, OLD family nucleases and RecR proteins. *Nucleic Acids Res.* **26**: 4205-4213.

Arber, W., (1983) A Beginner's Guide to Lambda Biology. In: Lambda II. R. Hendrix, J.W. Roberts, F.W. Stahl & R.A. Weisberg (eds). Cold Spring Harbour: Cold Spring Harbour Laboratory, pp. 381-394.

Asami, Y., D.W. Jia, K. Tatebayashi, K. Yamagata, M. Tanokura & H. Ikeda, (2002) Effect of the DNA topoisomerase II inhibitor VP-16 on illegitimate recombination in yeast chromosomes. *Gene* **291**: 251-257.

Ashizawa, Y., T. Yokochi, Y. Ogata, Y. Shobuike, J. Kato & H. Ikeda, (1999) Mechanism of DNA gyrase-mediated illegitimate recombination: Characterization of Escherichia coli gyrA mutations that confer hyper-recombination phenotype. *J. Mol. Biol.* **289**: 447-458.

Ashour, M.E., R. Atteya & S.F. El-Khamisy, (2015) Topoisomerase-mediated chromosomal break repair: an emerging player in many games. *Nat. Rev. Cancer* **15**: 137-151.

Avalos, E., D. Catanzaro, A. Catanzaro, T. Ganiats, S. Brodine, J. Alcaraz & T. Rodwell, (2015) Frequency and Geographic Distribution of gyrA and gyrB Mutations Associated with Fluoroquinolone Resistance in Clinical Mycobacterium Tuberculosis Isolates: A Systematic Review. *PLoS ONE* **10**: e0120470.

Azarova, A.M., R.K. Lin, Y.C. Tsai, L.F. Liu, C.P. Lin & Y.L. Lyu, (2010) Genistein induces topoisomerase IIbeta- and proteasome-mediated DNA sequence rearrangements: Implications in infant leukemia. *Biochem. Biophys. Res. Commun.* **399**: 66-71.

Baba, T., T. Ara, M. Hasegawa, Y. Takai, Y. Okumura, M. Baba, K.A. Datsenko, M. Tomita, B.L. Wanner & H. Mori, (2006) Construction of Escherichia coli K-12 in-frame, single-gene knockout mutants: the Keio collection. *Mol. Syst. Biol.* **2**: 2006.0008-2006.0008.

Bae, Y.S., M. Chiba, M. Ohira & H. Ikeda, (1991) A shuttle vector for analysis of illegitimate recombination in mammalian cells: effects of DNA topoisomerase inhibitors on deletion frequency. *Gene* **101**: 285-289.

Bae, Y.S., I. Kawasaki, H. Ikeda & L.F. Liu, (1988) Illegitimate recombination mediated by calf thymus DNA topoisomerase II *in vitro*. *Proc. Natl. Acad. Sci. USA* **85**: 2076-2080.

Bagel, S., V. Hullen, B. Wiedemann & P. Heisig, (1999) Impact of gyrA and parC mutations on quinolone resistance, doubling time, and supercoiling degree of Escherichia coli. *Antimicrob. Agents Chemother.* **43**: 868-875.

Baharoglu, Z., D. Bikard & D. Mazel, (2010) Conjugative DNA Transfer Induces the Bacterial SOS Response and Promotes Antibiotic Resistance Development through Integron Activation. *PLoS Genet.* **6**: e1001165.

Baharoglu, Z., E. Krin & D. Mazel, (2013) RpoS Plays a Central Role in the SOS Induction by Sub-Lethal Aminoglycoside Concentrations in Vibrio cholerae. *PLoS Genet.* **9**: e1003421.

Baharoglu, Z. & D. Mazel, (2014) SOS, the formidable strategy of bacteria against aggressions. *FEMS Microbiol. Rev.* **38**: 1126-1145.

Baird, C.L., M.S. Gordon, D.M. Andrenyak, J.F. Marecek & J.E. Lindsley, (2001) The ATPase reaction cycle of yeast DNA topoisomerase II. Slow rates of ATP resynthesis and P(i) release. *J. Biol. Chem.* **276**: 27893-27898.

Baker, N.M., S. Weigand, S. Maar-Mathias & A. Mondragon, (2011) Solution structures of DNA-bound gyrase. *Nucleic Acids Res.* **39**: 755-766.

Bakthisaran, R., R. Tangirala & C.M. Rao, (2015) Small heat shock proteins: Role in cellular functions and pathology. *Biochim. Biophys. Acta* **1854**: 291-319.

Baldi, M.I., P. Benedetti, E. Mattoccia & G.P. Tocchini-Valentini, (1980) *In vitro* catenation and decatenation of DNA and a novel eucaryotic ATP-dependent topoisomerase. *Cell* **20**: 461-467.

Baldwin, E.L. & N. Osheroff, (2005) Etoposide, topoisomerase II and cancer. *Curr. Med. Chem.: Anti-Cancer Agents* **5**: 363-372.

Bansal, S., D. Sinha, M. Singh, B. Cheng, Y.C. Tse-Dinh & V. Tandon, (2012) 3,4-dimethoxyphenyl bis-benzimidazole, a novel DNA topoisomerase inhibitor that preferentially targets Escherichia coli topoisomerase I. *J. Antimicrob. Chemother.* **67**: 2882-2891.

Basu, A., A.C. Parente & Z. Bryant, (2016) Structural dynamics and mechanochemical coupling in DNA gyrase. *J. Mol. Biol.* **428**: 1833-1845.

Basu, A., A.J. Schoeffler, J.M. Berger & Z. Bryant, (2012) ATP binding controls distinct structural transitions of Escherichia coli DNA gyrase in complex with DNA. *Nat. Struct. Mol. Biol.* **19**: 538-546, s531.

Bates, A.D., J.M. Berger & A. Maxwell, (2011) The ancestral role of ATP hydrolysis in type II topoisomerases: prevention of DNA double-strand breaks. *Nucleic Acids Res.* **39**: 6327-6339.

Bates, A.D. & A. Maxwell, (2005) *DNA Topology,* p. 216. Oxford University Press, New York.

Bates, A.D. & A. Maxwell, (2007) Energy Coupling in Type II Topoisomerases: Why Do They Hydrolyze ATP?†. *Biochemistry* **46**: 7929-7941.

Bates, A.D., M.H. O'Dea & M. Gellert, (1996) Energy coupling in Escherichia coli DNA gyrase: the relationship between nucleotide binding, strand passage, and DNA supercoiling. *Biochemistry* **35**: 1408-1416.

Bauer, D.L.V., R. Marie, K.H. Rasmussen, A. Kristensen & K.U. Mir, (2012) DNA catenation maintains structure of human metaphase chromosomes. *Nucleic Acids Res.* **40**: 11428-11434.

Beattie, T.R., N. Kapadia, E. Nicolas, S. Uphoff, A.J.M. Wollman, M.C. Leake & R. Reyes-Lamothe, (2017) Frequent exchange of the DNA polymerase during bacterial chromosome replication. *eLife* **6**: e21763.

Bellon, S., J.D. Parsons, Y.Y. Wei, K. Hayakawa, L.L. Swenson, P.S. Charifson, J.A. Lippke, R. Aldape & C.H. Gross, (2004) Crystal structures of Escherichia coli topoisomerase IV ParE subunit (24 and 43 kilodaltons): a single residue dictates differences in novobiocin potency against topoisomerase IV and DNA gyrase. *Antimicrob. Agents Chemother.* **48**: 1856-1864.

Belova, G.I., R. Prasad, I.V. Nazimov, S.H. Wilson & A.I. Slesarev, (2002) The domain organization and properties of individual domains of DNA topoisomerase V, a type 1B topoisomerase with DNA repair activities. *J. Biol. Chem.* **277**: 4959-4965.

Benson, D.A., M. Cavanaugh, K. Clark, I. Karsch-Mizrachi, D.J. Lipman, J. Ostell & E.W. Sayers, (2013) GenBank. *Nucleic Acids Res.* **41**: D36-D42.

Berger, J.M., S.J. Gamblin, S.C. Harrison & J.C. Wang, (1996) Structure and mechanism of DNA topoisomerase II. *Nature* **379**: 225-232.

Bergerat, A., B. de Massy, D. Gadelle, P.C. Varoutas, A. Nicolas & P. Forterre, (1997) An atypical topoisomerase II from Archaea with implications for meiotic recombination. *Nature* **386**: 414-417.

Bergerat, A., D. Gadelle & P. Forterre, (1994) Purification of a DNA topoisomerase II from the hyperthermophilic archaeon Sulfolobus shibatae. A thermostable enzyme with both bacterial and eucaryal features. *J. Biol. Chem.* **269**: 27663-27669.

Bernard, P. & M. Couturier, (1992) Cell killing by the F plasmid CcdB protein involves poisoning of DNA-topoisomerase II complexes. *J. Mol. Biol.* **226**: 735-745.

Bernard, P., K.E. Kézdy, L. Van Melderen, J. Steyaert, L. Wyns, M.L. Pato, P.N. Higgins & M. Couturier, (1993) The F Plasmid CcdB Protein Induces Efficient ATP-dependent DNA Cleavage by Gyrase. *J. Mol. Biol.* **234**: 534-541.

Biersack, H., S. Jensen, I. Gromova, I.S. Nielsen, O. Westergaard & A.H. Andersen, (1996) Active heterodimers are formed from human DNA topoisomerase II alpha and II beta isoforms. *Proc. Natl. Acad. Sci. USA* **93**: 8288-8293.

Binaschi, M., G. Capranico, L. Dal Bo & F. Zunino, (1997) Relationship between lethal effects and topoisomerase II-mediated double-stranded DNA breaks produced by anthracyclines with different sequence specificity. *Mol. Pharmacol.* **51**: 1053-1059.

Birch, R.G. & S.S. Patil, (1985) Preliminary characterization of an antibiotic produced by Xanthomonas albilineans which inhibits DNA synthesis in Escherichia coli. *Microbiology* **131**: 1069-1075.

Bisacchi, G.S., (2015) Origins of the Quinolone Class of Antibacterials: An Expanded "Discovery Story". *J. Med. Chem.* **58**: 4874-4882.

Blanc-Potard, A.-B., G. Labesse, N. Figueroa-Bossi & L. Bossi, (2005) Mutation at the “Exit Gate” of the Salmonella Gyrase A Subunit Suppresses a Defect in the Gyrase B Subunit. *J. Bacteriol.* **187**: 6841-6844.

Blattner, F.R., G. Plunkett, 3rd, C.A. Bloch, N.T. Perna, V. Burland, M. Riley, J. Collado-Vides, J.D. Glasner, C.K. Rode, G.F. Mayhew, J. Gregor, N.W. Davis, H.A. Kirkpatrick, M.A. Goeden, D.J. Rose, B. Mau & Y. Shao, (1997) The complete genome sequence of Escherichia coli K-12. *Science* **277**: 1453-1462.

Blázquez, J., A. Couce, J. Rodríguez-Beltrán & A. Rodríguez-Rojas, (2012) Antimicrobials as promoters of genetic variation. *Curr. Opin. Microbiol.* **15**: 561-569.

Bodley, A.L., H.C. Huang, C. Yu & L.F. Liu, (1993) Integration of simian virus 40 into cellular DNA occurs at or near topoisomerase II cleavage hot spots induced by VM-26 (teniposide). *Mol. Cell. Biol.* **13**: 6190-6200.

Boles, T.C., J.H. White & N.R. Cozzarelli, (1990) Structure of plectonemically supercoiled DNA. *J. Mol. Biol.* **213**: 931-951.

Bolla, J.-M., S. Alibert-Franco, J. Handzlik, J. Chevalier, A. Mahamoud, G. Boyer, K. Kieć-Kononowicz & J.-M. Pagès, (2011) Strategies for bypassing the membrane barrier in multidrug resistant Gram-negative bacteria. *FEBS Lett.* **585**: 1682-1690.

Bollimpelli, V.S., P.S. Dholaniya & A.K. Kondapi, (2017) Topoisomerase IIβ and its role in different biological contexts. *Arch. Biochem. Biophys.* **633**: 78-84.

Bonde, M.T., M.S. Klausen, M.V. Anderson, A.I.N. Wallin, H.H. Wang & M.O.A. Sommer, (2014) MODEST: a web-based design tool for oligonucleotide-mediated genome engineering and recombineering. *Nucleic Acids Res.* **42**: W408-W415.

Boros, I., G. Pósfai & P. Venetianer, (1984) High-copy-number derivatives of the plasmid cloning vector pBR322. *Gene* **30**: 257-260.

Brazas, M.D., E.B.M. Breidenstein, J. Overhage & R.E.W. Hancock, (2007) Role of Lon, an ATP-Dependent Protease Homolog, in Resistance of Pseudomonas aeruginosa to Ciprofloxacin. *Antimicrob. Agents Chemother.* **51**: 4276-4283.

Brenner, S., A.O. Stretton & S. Kaplan, (1965) Genetic code: the 'nonsense' triplets for chain termination and their suppression. *Nature* **206**: 994-998.

Brenner, S. & A.O.W. Stretton, (1964) The amber mutation. *Journal of Cellular and Comparative Physiology* **64**: 43-49.

Briñas, L., M. Zarazaga, Y. Sáenz, F. Ruiz-Larrea & C. Torres, (2002) β-Lactamases in Ampicillin-Resistant Escherichia coli Isolates from Foods, Humans, and Healthy Animals. *Antimicrob. Agents Chemother.* **46**: 3156-3163.

Brochet, M., E. Couvé, M. Zouine, C. Poyart & P. Glaser, (2008) A Naturally Occurring Gene Amplification Leading to Sulfonamide and Trimethoprim Resistance in Streptococcus agalactiae. *J. Bacteriol.* **190**: 672-680.

Brody, H., A. Greener & C.W. Hill, (1985) Excision and reintegration of the Escherichia coli K-12 chromosomal element e14. *J. Bacteriol.* **161**: 1112-1117.

Bron, S., (1990) Plasmids. In: Molecular biological methods for Bacillus. C.R. Harwood & S.M. Cutting (eds). New York: John Wiley & Sons, pp. 75 - 174.

Brown, E.D. & G.D. Wright, (2016) Antibacterial drug discovery in the resistance era. *Nature* **529**: 336-343.

Brown, P. & N. Cozzarelli, (1979) A sign inversion mechanism for enzymatic supercoiling of DNA. *Science* **206**: 1081-1083.

Browne, F.A., C. Clark, B. Bozdogan, B.E. Dewasse, M.R. Jacobs & P.C. Appelbaum, (2002) Single and multi-step resistance selection study in Streptococcus pneumoniae comparing ceftriaxone with levofloxacin, gatifloxacin and moxifloxacin. *Int. J. Antimicrob. Agents* **20**: 93-99.

BSAC, (1991) A guide to sensitivity testing. Report of the Working Party on Antibiotic Sensitivity Testing of the British Society for Antimicrobial Chemotherapy. *J. Antimicrob. Chemother.* **27 Suppl D**: 1-50.

Buckstein, M.H., J. He & H. Rubin, (2008) Characterization of Nucleotide Pools as a Function of Physiological State in Escherichia coli. *J. Bacteriol.* **190**: 718-726.

Buhler, C., J.H. Lebbink, C. Bocs, R. Ladenstein & P. Forterre, (2001) DNA topoisomerase VI generates ATP-dependent double-strand breaks with two-nucleotide overhangs. *J. Biol. Chem.* **276**: 37215-37222.

Bullock, P., J.J. Champoux & M. Botchan, (1985) Association of crossover points with topoisomerase I cleavage sites: a model for nonhomologous recombination. *Science* **230**: 954-958.

Burlison, J.A., L. Neckers, A.B. Smith, A. Maxwell & B.S.J. Blagg, (2006) Novobiocin: Redesigning a DNA Gyrase Inhibitor for Selective Inhibition of Hsp90. *J. Am. Chem. Soc.* **128**: 15529-15536.

Bush, K., P. Courvalin, G. Dantas, J. Davies, B. Eisenstein, P. Huovinen, G.A. Jacoby, R. Kishony, B.N. Kreiswirth, E. Kutter, S.A. Lerner, S. Levy, K. Lewis, O. Lomovskaya, J.H. Miller, S. Mobashery, L.J.V. Piddock, S. Projan, C.M. Thomas, A. Tomasz, P.M. Tulkens, T.R. Walsh, J.D. Watson, J. Witkowski, W. Witte, G. Wright, P. Yeh & H.I. Zgurskaya, (2011) Tackling antibiotic resistance. *Nat Rev Micro* **9**: 894-896.

Bush, N.G., K. Evans-Roberts & A. Maxwell, (2015) DNA Topoisomerases. *EcoSal Plus* **6**.

Calderwood, S.K., (2016) A critical role for topoisomerase IIb and DNA double strand breaks in transcription. *Transcription* **7**: 75-83.

Camacho-Carranza, R., J. Membrillo-Hernández, J. Ramírez-Santos, J. Castro-Dorantes, V. Chagoya de Sánchez & M.C. Gómez-Eichelmann, (1995) Topoisomerase activity during the heat shock response in Escherichia coli K-12. *J. Bacteriol.* **177**: 3619-3622.

Campbell, A., (1971) Genetic Structure. In: The Bacteriophage Lambda. A.D. Hershey (ed). Cold Spring Harbor: Cold Spring Harbor Laboratory, pp. 13-44.

Campoy, S., A. Hervàs, N. Busquets, I. Erill, L. Teixidó & J. Barbé, (2006) Induction of the SOS response by bacteriophage lytic development in Salmonella enterica. *Virology* **351**: 360-367.

Candel, F.J. & M. Peñuelas, (2017) Delafloxacin: design, development and potential place in therapy. *Drug Des. Dev. Ther.* **11**: 881-891.

Cantón, R. & M.-I. Morosini, (2011) Emergence and spread of antibiotic resistance following exposure to antibiotics. *FEMS Microbiol. Rev.* **35**: 977-991.

Capranico, G., J. Marinello & G. Chillemi, (2017) Type I DNA Topoisomerases. *J. Med. Chem.* **60**: 2169-2192.

Capranico, G., S. Tinelli, C.A. Austin, M.L. Fisher & F. Zunino, (1992) Different patterns of gene expression of topoisomerase II isoforms in differentiated tissues during murine development. *Biochim. Biophys. Acta* **1132**: 43-48.

Carter, P., (1986) Site-directed mutagenesis. *Biochem. J.* **237**: 1-7.

Carucci, D.J., M.J. Gardner, H. Tettelin, L.M. Cummings, H.O. Smith, M.D. Adams, S.L. Hoffman & J.C. Venter, (1998) The malaria genome sequencing project. *Expert Rev Mol Med* **1998**: 1-9.

Casali, N., (2003) Escherichia coli Host Strains. In: E. coli Plasmid Vectors: Methods and Applications. N. Casali & A. Preston (eds). Totowa, NJ: Humana Press, pp. 27-48.

Cebrián, J., A. Castán, V. Martínez, M.J. Kadomatsu-Hermosa, C. Parra, M.J. Fernández-Nestosa, C. Schaerer, P. Hernández, D.B. Krimer & J.B. Schvartzman, (2015) Direct evidence for the formation of precatenanes during DNA replication. *J. Biol. Chem.* **290**: 13725-13735.

Champoux, J.J., (1981) DNA is linked to the rat liver DNA nicking-closing enzyme by a phosphodiester bond to tyrosine. *J. Biol. Chem.* **256**: 4805-4809.

Champoux, J.J. & R. Dulbecco, (1972) An activity from mammalian cells that untwists superhelical DNA--a possible swivel for DNA replication (polyoma-ethidium bromide-mouse-embryo cells-dye binding assay). *Proc. Natl. Acad. Sci. USA* **69**: 143-146.

Chan, P.F., T. Germe, B.D. Bax, J. Huang, R.K. Thalji, E. Bacqué, A. Checchia, D. Chen, H. Cui, X. Ding, K. Ingraham, L. McCloskey, K. Raha, V. Srikannathasan, A. Maxwell & R.A. Stavenger, (2017) Thiophene antibacterials that allosterically stabilize DNA-cleavage complexes with DNA gyrase. *Proc. Natl. Acad. Sci. USA* **114**: E4492-E4500.

Chan, P.F., J. Huang, B.D. Bax & M.N. Gwynn, (2014) Recent Developments in Inhibitors of Bacterial Type IIA Topoisomerases. In: Antibiotics: Targets, Mechanisms and Resistance. C.O. Gualerzi, L. Brandi, A. Fabbretti & C.L. Pon (eds). Weinheim, Germany: Wiley-VCH Verlag GmbH & Co, pp. 263 - 297.

Chang, A.C. & S.N. Cohen, (1978) Construction and characterization of amplifiable multicopy DNA cloning vehicles derived from the P15A cryptic miniplasmid. *J. Bacteriol.* **134**: 1141-1156.

Chatterji, M., S. Unniraman, A. Maxwell & V. Nagaraja, (2000) The additional 165 amino acids in the B Protein of Escherichia coli DNA gyrase have an important role in DNA binding. *J. Biol. Chem.* **275**: 22888-22894.

Cheng, B., I.F. Liu & Y.C. Tse-Dinh, (2007) Compounds with antibacterial activity that enhance DNA cleavage by bacterial DNA topoisomerase I. *J. Antimicrob. Chemother.* **59**: 640-645.

Cheng, B., S. Shukla, S. Vasunilashorn, S. Mukhopadhyay & Y.C. Tse-Dinh, (2005) Bacterial cell killing mediated by topoisomerase I DNA cleavage activity. *J. Biol. Chem.* **280**: 38489-38495.

Chiba, M., H. Shimizu, A. Fujimoto, H. Nashimoto & H. Ikeda, (1989) Common sites for recombination and cleavage mediated by bacteriophage T4 DNA topoisomerase *in vitro*. *J. Biol. Chem.* **264**: 12785-12790.

Cho, H.S., S.S. Lee, K.D. Kim, I. Hwang, J.S. Lim, Y.I. Park & H.S. Pai, (2004) DNA gyrase is involved in chloroplast nucleoid partitioning. *Plant Cell* **16**: 2665-2682.

Cirz, R.T., J.K. Chin, D.R. Andes, V. de Crecy-Lagard, W.A. Craig & F.E. Romesberg, (2005) Inhibition of mutation and combating the evolution of antibiotic resistance. *PLoS Biol.* **3**: e176.

Cirz, R.T., M.B. Jones, N.A. Gingles, T.D. Minogue, B. Jarrahi, S.N. Peterson & F.E. Romesberg, (2007) Complete and SOS-mediated response of Staphylococcus aureus to the antibiotic ciprofloxacin. *J. Bacteriol.* **189**: 531-539.

Cirz, R.T., B.M. O'Neill, J.A. Hammond, S.R. Head & F.E. Romesberg, (2006) Defining the Pseudomonas aeruginosa SOS response and its role in the global response to the antibiotic ciprofloxacin. *J. Bacteriol.* **188**: 7101-7110.

Cirz, R.T. & F.E. Romesberg, (2006) Induction and inhibition of ciprofloxacin resistance-conferring mutations in hypermutator bacteria. *Antimicrob. Agents Chemother.* **50**: 220-225.

Clarke, D.J., A.C. Vas, C.A. Andrews, L.A. Diaz-Martinez & J.F. Gimenez-Abian, (2006) Topoisomerase II checkpoints: universal mechanisms that regulate mitosis. *Cell Cycle* **5**: 1925-1928.

Clavijo, B., G. Garcia Accinelli, J. Wright, D. Heavens, K. Barr, L. Yanes & F. Di Palma, (2017) W2RAP: a pipeline for high quality, robust assemblies of large complex genomes from short read data. *bioRxiv*.

Cobbe, N. & M.M.S. Heck, (2000) Review: SMCs in the World of Chromosome Biology— From Prokaryotes to Higher Eukaryotes. *J. Struct. Biol.* **129**: 123-143.

Cohen, S.P., H. Hächler & S.B. Levy, (1993) Genetic and functional analysis of the multiple antibiotic resistance (mar) locus in Escherichia coli. *J. Bacteriol.* **175**: 1484-1492.

Collin, F., S. Karkare & A. Maxwell, (2011) Exploiting bacterial DNA gyrase as a drug target: current state and perspectives. *Appl. Microbiol. Biotechnol.* **92**: 479-497.

Confalonieri, F., C. Elie, M. Nadal, C. de La Tour, P. Forterre & M. Duguet, (1993) Reverse gyrase: a helicase-like domain and a type I topoisomerase in the same polypeptide. *Proc. Natl. Acad. Sci. USA* **90**: 4753-4757.

Conrad, T.M., A.R. Joyce, M.K. Applebee, C.L. Barrett, B. Xie, Y. Gao & B.Ø. Palsson, (2009) Whole-genome resequencing of Escherichia coli K-12 MG1655 undergoing short-term laboratory evolution in lactate minimal media reveals flexible selection of adaptive mutations. *Genome Biol.* **10**: R118.

Corbett, K.D., P. Benedetti & J.M. Berger, (2007) Holoenzyme assembly and ATP-mediated conformational dynamics of topoisomerase VI. *Nat. Struct. Mol. Biol.* **14**: 611-619.

Corbett, K.D. & J.M. Berger, (2003) Structure of the topoisomerase VI-B subunit: implications for type II topoisomerase mechanism and evolution. *EMBO J.* **22**: 151-163.

Corbett, K.D. & J.M. Berger, (2005) Structural dissection of ATP turnover in the prototypical GHL ATPase TopoVI. *Structure* **13**: 873-882.

Corbett, K.D., A.J. Schoeffler, N.D. Thomsen & J.M. Berger, (2005) The structural basis for substrate specificity in DNA topoisomerase IV. *J. Mol. Biol.* **351**: 545-561.

Corbett, K.D., R.K. Shultzaberger & J.M. Berger, (2004) The C-terminal domain of DNA gyrase A adopts a DNA-bending β-pinwheel fold. *Proc. Natl. Acad. Sci. USA* **101**: 7293-7298.

Correia, S., P. Poeta, M. Hébraud, J.L. Capelo & G. Igrejas, (2017) Mechanisms of quinolone action and resistance: where do we stand? *J. Med. Microbiol.* **66**: 551-559.

Corvec, S., N. Caroff, E. Espaze, J. Marraillac & A. Reynaud, (2002) −11 Mutation in the ampC Promoter Increasing Resistance to β-Lactams in a Clinical Escherichia coli Strain. *Antimicrob. Agents Chemother.* **46**: 3265-3267.

Costenaro, L., J.G. Grossmann, C. Ebel & A. Maxwell, (2005) Small-angle X-ray scattering reveals the solution structure of the full-length DNA gyrase a subunit. *Structure* **13**: 287-296.

Costenaro, L., J.G. Grossmann, C. Ebel & A. Maxwell, (2007) Modular structure of the full-length DNA gyrase B subunit revealed by small-angle X-ray scattering. *Structure* **15**: 329-339.

Cove, M.E., A.P. Tingey & A. Maxwell, (1997) DNA gyrase can cleave short DNA fragments in the presence of quinolone drugs. *Nucleic Acids Res.* **25**: 2716-2722.

Cowell, I.G. & C.A. Austin, (2012) Mechanism of generation of therapy related leukemia in response to anti-topoisomerase II agents. *Int. J. Env. Res. Public Health* **9**: 2075-2091.

Crisona, N.J., T.R. Strick, D. Bensimon, V. Croquette & N.R. Cozzarelli, (2000) Preferential relaxation of positively supercoiled DNA by E. coli topoisomerase IV in single-molecule and ensemble measurements. *Genes Dev.* **14**: 2881-2892.

Critchlow, S.E. & A. Maxwell, (1996) DNA Cleavage Is Not Required for the Binding of Quinolone Drugs to the DNA Gyrase−DNA Complex. *Biochemistry* **35**: 7387-7393.

Cunningham, E.L. & J.M. Berger, (2005) Unraveling the early steps of prokaryotic replication. *Curr. Opin. Struct. Biol.* **15**: 68-76.

Daley, J.M., C. Zakaria & D. Ramotar, (2010) The endonuclease IV family of apurinic/apyrimidinic endonucleases. *Mutat. Res. - Rev. Mut. Res.* **705**: 217-227.

Dalhoff, A., (2012) Global Fluoroquinolone Resistance Epidemiology and Implictions for Clinical Use. *Interdisciplinary Perspectives on Infectious Diseases* **2012**: 37.

Daniels, D.L., J.L. Schroeder, W. Syzbalski, F. Sanger & F.R. Blattner, (1983) A Molecular Map of Coliphage Lambda. In: Lambda II. R.W. Hendrix, J.W. Roberts, F.W. Stahl & R.A. Weisberg (eds). Cold Spring Harbour: Cold Spring Habour Laboratory, pp. 469 - 517.

Dao-Thi, M.-H., L. Van Melderen, E. De Genst, H. Afif, L. Buts, L. Wyns & R. Loris, (2005) Molecular basis of gyrase poisoning by the addiction toxin CcdB. *J. Mol. Biol.* **348**: 1091-1102.

Dar, M.A., A. Sharma, N. Mondal & S.K. Dhar, (2007) Molecular cloning of apicoplast-targeted Plasmodium falciparum DNA gyrase genes: unique intrinsic ATPase activity and ATP-independent dimerization of PfGyrB subunit. *Eukaryot. Cell* **6**: 398-412.

Darmon, E. & D.R.F. Leach, (2014) Bacterial Genome Instability. *Microbiol. Mol. Biol. Rev.* **78**: 1-39.

Datsenko, K.A. & B.L. Wanner, (2000) One-step inactivation of chromosomal genes in Escherichia coli K-12 using PCR products. *Proc. Natl. Acad. Sci. USA* **97**: 6640-6645.

Davies, J. & D. Davies, (2010) Origins and evolution of antibiotic resistance. *Microbiol. Mol. Biol. Rev.* **74**: 417-433.

Davis, R.W., D. Botstein & J.R. Roth, (1980) *Advanced Bacterial Genetics: A Manual for Genetic Engineering,* p. 254. Cold Spring Harbour Laboratory, Cold Spring Harbour.

Deibler, R.W., S. Rahmati & E.L. Zechiedrich, (2001) Topoisomerase IV, alone, unknots DNA in E. coli. *Genes Dev.* **15**: 748-761.

Deng, S., R.A. Stein & N.P. Higgins, (2005) Organization of supercoil domains and their reorganization by transcription. *Mol. Microbiol.* **57**: 1511-1521.

Deweese, J.E., M.A. Osheroff & N. Osheroff, (2009) DNA Topology and Topoisomerases. *Biochem Mol Biol Educ* **37**: 2-10.

Digate, R.J. & K.J. Marians, (1989) Molecular cloning and DNA sequence analysis of Escherichia coli topb, the gene encoding topoisomerase III. *J. Biol. Chem.* **264**: 17924-17930.

Digate, R.J. & K.J. Marians, (1992) Escherichia coli topoisomerase III catalyzed cleavage of RNA. *J. Biol. Chem.* **267**: 20532-20535.

Dillingham, M.S. & S.C. Kowalczykowski, (2008) RecBCD Enzyme and the Repair of Double-Stranded DNA Breaks. *Microbiol. Mol. Biol. Rev.* **72**: 642-671.

DiNardo, S., K. Voelkel & R. Sternglanz, (1984) DNA topoisomerase II mutant of Saccharomyces cerevisiae: topoisomerase II is required for segregation of daughter molecules at the termination of DNA replication. *Proc. Natl. Acad. Sci. USA* **81**: 2616-2620.

Dinardo, S., K.A. Voelkel, R. Sternglanz, A.E. Reynolds & A. Wright, (1982) Escherichia coli DNA topoisomerase I mutants have compensatory mutations in DNA gyrase genes. *Cell* **31**: 43-51.

Domagala, J.M., L.D. Hanna, C.L. Heifetz, M.P. Hutt, T.F. Mich, J.P. Sanchez & M. Solomon, (1986) New structure-activity relationships of the quinolone antibacterials using the target enzyme. The development and application of a DNA gyrase assay. *J. Med. Chem.* **29**: 394-404.

Dong, K.C. & J.M. Berger, (2007) Structural basis for gate-DNA recognition and bending by type IIA topoisomerases. *Nature* **450**: 1201-1205.

Dong, Y., C. Xu, X. Zhao, J. Domagala & K. Drlica, (1998) Fluoroquinolone Action against Mycobacteria: Effects of C-8 Substituents on Growth, Survival, and Resistance. *Antimicrob. Agents Chemother.* **42**: 2978-2984.

Dorman, C.J. & M.J. Dorman, (2016) DNA supercoiling is a fundamental regulatory principle in the control of bacterial gene expression. *Biophys Rev* **8**: 209-220.

Dörr, T., K. Lewis & M. Vulić, (2009) SOS Response Induces Persistence to Fluoroquinolones in Escherichia coli. *PLoS Genet.* **5**: e1000760.

Dove, S.L. & C.J. Dorman, (1994) The site-specific recombination system regulating expression of the type 1 fimbrial subunit gene of Escherichia coli is sensitive to changes in DNA supercoiling. *Mol. Microbiol.* **14**: 975-988.

Drake, F.H., G.A. Hofmann, H.F. Bartus, M.R. Mattern, S.T. Crooke & C.K. Mirabelli, (1989a) Biochemical and pharmacological properties of p170 and p180 forms of topoisomerase II. *Biochemistry* **28**: 8154-8160.

Drake, F.H., G.A. Hofmann, S.M. Mong, J.O. Bartus, R.P. Hertzberg, R.K. Johnson, M.R. Mattern & C.K. Mirabelli, (1989b) *In vitro* and intracellular inhibition of topoisomerase II by the antitumor agent merbarone. *Cancer Res.* **49**: 2578-2583.

Drlica, K., (1992) Control of bacterial DNA supercoiling. *Mol. Microbiol.* **6**: 425-433.

Drlica, K., H. Hiasa, R. Kerns, M. Malik, A. Mustaev & X. Zhao, (2009) Quinolones: Action and resistance updated. *Curr. Top. Med. Chem.* **9**: 981-998.

Drlica, K. & M. Malik, (2003) Fluoroquinolones: Action and resistance. *Curr. Top. Med. Chem.* **3**: 249-282.

Drlica, K., M. Malik, R.J. Kerns & X. Zhao, (2008) Quinolone-mediated bacterial death. *Antimicrob. Agents Chemother.* **52**: 385-392.

Drlica, K., A. Mustaev, T.R. Towle, G. Luan, R.J. Kerns & J.M. Berger, (2014) Bypassing Fluoroquinolone Resistance with Quinazolinediones: Studies of Drug–Gyrase–DNA Complexes Having Implications for Drug Design. *ACS Chemical Biology* **9**: 2895-2904.

Duderstadt, K.E., R. Reyes-Lamothe, A.M. van Oijen & D.J. Sherratt, (2014) Replication-Fork Dynamics. *Cold. Spring. Harb. Perspect. Biol.* **6**: a010157.

Durrieu, F., K. Samejima, J.M. Fortune, S. Kandels-Lewis, N. Osheroff & W.C. Earnshaw, (2000) DNA topoisomerase IIalpha interacts with CAD nuclease and is involved in chromatin condensation during apoptotic execution. *Curr. Biol.* **10**: 923-926.

Dutta, R. & M. Inouye, (2000) GHKL, an emergent ATPase/kinase superfamily. *Trends Biochem. Sci.* **25**: 24-28.

Echols, H., (1971) Regulation of Lytic Development. In: The Bacteriophage Lambda. A.D. Hershey (ed). Cold Spring Harbour: Cold Spring Harbour Laboratory, pp. 247-270.

Echols, H., (1986) Bacteriophage λ development: temporal switches and the choice of lysis or lysogeny. *Trends Genet.* **2**: 26-30.

Edgar, R. & E. Bibi, (1997) MdfA, an Escherichia coli multidrug resistance protein with an extraordinarily broad spectrum of drug recognition. *J. Bacteriol.* **179**: 2274-2280.

Edwards, M.J., (2009) The mode of action of Simocyclinone D8; a novel inhibitor of DNA gyrase. In: John Innes Centre, Biological Chemistry. Norwich, United Kingdom: University of East Anglia, pp.

Edwards, M.J., R.H. Flatman, L.A. Mitchenall, C.E. Stevenson, T.B. Le, T.A. Clarke, A.R. McKay, H.P. Fiedler, M.J. Buttner, D.M. Lawson & A. Maxwell, (2009) A crystal structure of the bifunctional antibiotic simocyclinone D8, bound to DNA gyrase. *Science* **326**: 1415-1418.

Edwards, M.J., M.A. Williams, A. Maxwell & A.R. McKay, (2011) Mass Spectrometry Reveals That the Antibiotic Simocyclinone D8 Binds to DNA Gyrase in a "Bent-Over" Conformation: Evidence of Positive Cooperativity in Binding. *Biochemistry* **50**: 3432-3440.

Eisen, H. & M. Ptashne, (1971) Regulation of Repressor Synthesis. In: The Bacteriophage Lambda. A.D. Hershey (ed). Cold Spring Harbour: Cold Spring Harbour Laboratory, pp. 239-245.

El Sayyed, H., L. Le Chat, E. Lebailly, E. Vickridge, C. Pages, F. Cornet, M. Cosentino Lagomarsino & O. Espéli, (2016) Mapping Topoisomerase IV Binding and Activity Sites on the E. coli Genome. *PLoS Genet.* **12**: e1006025.

Elguero, M.E., M. de Campos-Nebel & M. González-Cid, (2012) DNA-PKcs-dependent NHEJ pathway supports the progression of topoisomerase II poison-induced chromosome aberrant cells. *Environ. Mol. Mutag.* **53**: 608-618.

Emmerson, A.M. & A.M. Jones, (2003) The quinolones: decades of development and use. *J. Antimicrob. Chemother.* **51**: 13-20.

Espeli, O. & K.J. Marians, (2004) Untangling intracellular DNA topology. *Mol. Microbiol.* **52**: 925-931.

Fang, F.C., (2013) Antibiotic and ROS linkage questioned. *Nat. Biotechnol.* **31**: 415-416.

Feiss, M. & A. Becker, (1983) DNA packaging and cutting. In: Lambda II. R. Hendrix, J.W. Roberts, F.W. Stahl & R.A. Weisberg (eds). Cold Spring Harbour, New York: Cold Spring Harbour Laboratory, pp. 305-330.

Feiss, M., R.A. Fisher, M.A. Crayton & C. Egner, (1977) Packaging of the bacteriophage lambda chromosome: effect of chromosome length. *Virology* **77**: 281-293.

Fernández, L. & R.E.W. Hancock, (2012) Adaptive and Mutational Resistance: Role of Porins and Efflux Pumps in Drug Resistance. *Clin. Microbiol. Rev.* **25**: 661-681.

Ferrero, L., B. Cameron, B. Manse, D. Lagneaux, J. Crouzet, A. Famechon & F. Blanche, (1994) Cloning and primary structure of Staphylococcus aureus DNA topoisomerase IV: a primary target of fluoroquinolones. *Mol. Microbiol.* **13**: 641-653.

Fisher, L.M., K. Mizuuchi, M.H. O'Dea, H. Ohmori & M. Gellert, (1981) Site-specific interaction of DNA gyrase with DNA. *Proc. Natl. Acad. Sci. USA* **78**: 4165-4169.

Flatman, R.H., A.J. Howells, L. Heide, H.P. Fiedler & A. Maxwell, (2005) Simocyclinone D8, an inhibitor of DNA gyrase with a novel mode of action. *Antimicrob. Agents Chemother.* **49**: 1093-1100.

Fogg, J.M., N. Kolmakova, I. Rees, S. Magonov, H. Hansma, J.J. Perona & E.L. Zechiedrich, (2006) Exploring writhe in supercoiled minicircle DNA. *J Phys Condens Matter* **18**: S145-s159.

Fogg, P.C.M., H.E. Allison, J.R. Saunders & A.J. McCarthy, (2010) Bacteriophage Lambda: a Paradigm Revisited. *J. Virol.* **84**: 6876-6879.

Forterre, P., (2002) A hot story from comparative genomics: reverse gyrase is the only hyperthermophile-specific protein. *Trends Genet.* **18**: 236-238.

Forterre, P., G. Mirambeau, C. Jaxel, M. Nadal & M. Duguet, (1985) High positive supercoiling *in vitro* catalyzed by an ATP and polyethylene glycol-stimulated topoisomerase from Sulfolobus acidocaldarius. *EMBO J.* **4**: 2123-2128.

Foster, P.L., H. Lee, E. Popodi, J.P. Townes & H. Tang, (2015) Determinants of spontaneous mutation in the bacterium Escherichia coli as revealed by whole-genome sequencing. *Proc. Natl. Acad. Sci. USA* **112**: E5990-E5999.

Franklin, N., (1971) Illegitimate Recombination. In: The Bacteriophage Lambda. A.D. Hershey (ed). Cold Spring Harbour, New York: Cold Spring Harbour Laboratory, pp. 175 - 194.

Freddolino, P.L., S. Amini & S. Tavazoie, (2012) Newly Identified Genetic Variations in Common Escherichia coli MG1655 Stock Cultures. *J. Bacteriol.* **194**: 303-306.

Friedman, D.I. & D.L. Court, (2001) Bacteriophage lambda: alive and well and still doing its thing. *Curr. Opin. Microbiol.* **4**: 201-207.

Friedman, D.I. & M.E. Gottesman, (1983) Lytic Mode of Lambda Development. In: Lambda II. R. Hendrix, J.W. Roberts, F.W. Stahl & R.A. Weisberg (eds). Cold Spring Harbor: Cold Spring Harbor Laboratory, pp. 21-51.

Fu, G., J. Wu, W. Liu, D. Zhu, Y. Hu, J. Deng, X.-E. Zhang, L. Bi & D.-C. Wang, (2009) Crystal structure of DNA gyrase B' domain sheds lights on the mechanism for T-segment navigation. *Nucleic Acids Res.* **37**: 5908-5916.

Fujii, N., S. Matsumoto, K. Hiroki & L. Takemoto, (2001) Inversion and isomerization of Asp-58 residue in human αA-crystallin from normal aged lenses and cataractous lenses. *Biochim. Biophys. Acta* **1549**: 179-187.

Fukuoka, H., Y. Inoue, S. Terasawa, H. Takahashi & A. Ishijima, (2010) Exchange of rotor components in functioning bacterial flagellar motor. *Biochem. Biophys. Res. Commun.* **394**: 130-135.

Funnell, B.E., T.A. Baker & A. Kornberg, (1986) Complete enzymatic replication of plasmids containing the origin of the Escherichia coli chromosome. *J. Biol. Chem.* **261**: 5616-5624.

Furniss, K.L., H.J. Tsai, J.A. Byl, A.B. Lane, A.C. Vas, W.S. Hsu, N. Osheroff & D.J. Clarke, (2013) Direct monitoring of the strand passage reaction of DNA topoisomerase II triggers checkpoint activation. *PLoS Genet.* **9**: e1003832.

Gadelle, D., M. Graille & P. Forterre, (2006) The HSP90 and DNA topoisomerase VI inhibitor radicicol also inhibits human type II DNA topoisomerase. *Biochem. Pharmacol.* **72**: 1207-1216.

Gadelle, D., M. Krupovic, K. Raymann, C. Mayer & P. Forterre, (2014) DNA topoisomerase VIII: a novel subfamily of type IIB topoisomerases encoded by free or integrated plasmids in Archaea and Bacteria. *Nucleic Acids Res.* **42**: 8578-8591.

Ganguly, A., Y. del Toro Duany & D. Klostermeier, (2013) Reverse Gyrase Transiently Unwinds Double-Stranded DNA in an ATP-Dependent Reaction. *J. Mol. Biol.* **425**: 32-40.

Gao, W., I.R. Monk, N.J. Tobias, S.L. Gladman, T. Seemann, T.P. Stinear & B.P. Howden, (2015) Large tandem chromosome expansions facilitate niche adaptation during persistent infection with drug-resistant Staphylococcus aureus. *Microbial Genomics* **1**: e000026.

Gari, E., N. Figueroa-Bossi, A.B. Blanc-Potard, F. Spirito, M.B. Schmid & L. Bossi, (1996) A class of gyrase mutants of Salmonella typhimurium show quinolone-like lethality and require rec functions for viability. *Mol. Microbiol.* **21**: 111-122.

Gelband, H., M. Miller-Petrie, S. Pant, S. Gandra, J. Levinson, D. Barter, A. White & R. Laxminarayan, (2015) State of the World's Antibiotics. In. E.a.P. Center for Disease Dynamics (ed). CDDEP: Washington, D.C., pp.

Gellert, M., L.M. Fisher & M.H. O'Dea, (1979) DNA gyrase: purification and catalytic properties of a fragment of gyrase B protein. *Proc. Natl. Acad. Sci. USA* **76**: 6289-6293.

Gellert, M., K. Mizuuchi, M.H. O'Dea, T. Itoh & J.-I. Tomizawa, (1977) Nalidixic acid resistance: A second genetic character involved in DNA gyrase activity. *Proc. Natl. Acad. Sci. USA* **74**: 4772-4776.

Gellert, M., K. Mizuuchi, M.H. O'Dea & H.A. Nash, (1976a) DNA gyrase: an enzyme that introduces superhelical turns into DNA. *Proc. Natl. Acad. Sci. USA* **73**: 3872-3876.

Gellert, M., M.H. O'Dea, T. Itoh & J. Tomizawa, (1976b) Novobiocin and coumermycin inhibit DNA supercoiling catalyzed by DNA gyrase. *Proc. Natl. Acad. Sci. USA* **73**: 4474-4478.

Gensberg, K., Y.F. Jin & L.J. Piddock, (1995) A novel gyrB mutation in a fluoroquinolone-resistant clinical isolate of Salmonella typhimurium. *FEMS Microbiol. Lett.* **132**: 57-60.

Gillespie, S.H., (2016) The role of moxifloxacin in tuberculosis therapy. *Eur. Respir. Rev.* **25**: 19-28.

Gillespie, S.H., S. Basu, A.L. Dickens, D.M. O'Sullivan & T.D. McHugh, (2005) Effect of subinhibitory concentrations of ciprofloxacin on Mycobacterium fortuitum mutation rates. *J. Antimicrob. Chemother.* **56**: 344-348.

Godbole, A.A., W. Ahmed, R.S. Bhat, E.K. Bradley, S. Ekins & V. Nagaraja, (2015) Targeting Mycobacterium tuberculosis Topoisomerase I by Small-Molecule Inhibitors. *Antimicrob. Agents Chemother.* **59**: 1549-1557.

Goldberg, A.R. & M. Howe, (1969) New mutations in the S cistron of bacteriophage lambda affecting host cell lysis. *Virology* **38**: 200-202.

Goneau, L.W., T.J. Hannan, R.A. MacPhee, D.J. Schwartz, J.M. Macklaim, G.B. Gloor, H. Razvi, G. Reid, S.J. Hultgren & J.P. Burton, (2015) Subinhibitory antibiotic therapy alters recurrent urinary tract infection pathogenesis through modulation of bacterial virulence and host immunity. *MBio* **6**.

Goneau, L.W., N.S. Yeoh, K.W. MacDonald, P.A. Cadieux, J.P. Burton, H. Razvi & G. Reid, (2014) Selective Target Inactivation Rather than Global Metabolic Dormancy Causes Antibiotic Tolerance in Uropathogens. *Antimicrob. Agents Chemother.* **58**: 2089-2097.

Gonzalez, R.E., C.U. Lim, K. Cole, C.H. Bianchini, G.P. Schools, B.E. Davis, I. Wada, I.B. Roninson & E.V. Broude, (2011) Effects of conditional depletion of topoisomerase II on cell cycle progression in mammalian cells. *Cell Cycle* **10**: 3505-3514.

Gottesman, M.E. & M.B. Yarmolinsky, (1968) The Integration and Excision of the Bacteriophage Lambda Genome. *Cold Spring Harbor Symp. Quant. Biol.* **33**: 735-747.

Graham, J.E., K.J. Marians & S.C. Kowalczykowski, (2017) Independent and Stochastic Action of DNA Polymerases in the Replisome. *Cell* **169**: 1201-1213.e1217.

Graves Jr, J., M. Tajkarimi, Q. Cunningham, A. Campbell, H. Nonga, S. Harrison & J. E Barrick, (2015) *Rapid Evolution of Silver Nanoparticle Resistance in Escherichia coli,* p. 42.

Greer, H., (1975) The kil gene of bacteriophage lambda. *Virology* **66**: 589-604.

Grenier, F., D. Matteau, V. Baby & S. Rodrigue, (2014) Complete Genome Sequence of Escherichia coli BW25113. *Genome Announcements* **2**: e01038-01014.

Gromova, I., H. Biersack, S. Jensen, O.F. Nielsen, O. Westergaard & A.H. Andersen, (1998) Characterization of DNA topoisomerase II alpha/beta heterodimers in HeLa cells. *Biochemistry* **37**: 16645-16652.

Grundström, T. & B. Jaurin, (1982) Overlap between ampC and frd operons on the Escherichia coli chromosome. *Proc. Natl. Acad. Sci. USA* **79**: 1111-1115.

Gubaev, A., M. Hilbert & D. Klostermeier, (2009) The DNA-gate of Bacillus subtilis gyrase is predominantly in the closed conformation during the DNA supercoiling reaction. *Proc. Natl. Acad. Sci. USA* **106**: 13278-13283.

Gubaev, A. & D. Klostermeier, (2011) DNA-induced narrowing of the gyrase N-gate coordinates T-segment capture and strand passage. *Proc. Natl. Acad. Sci. USA* **108**: 14085-14090.

Gubaev, A. & D. Klostermeier, (2014) The mechanism of negative DNA supercoiling: A cascade of DNA-induced conformational changes prepares gyrase for strand passage. *DNA Repair* **16c**: 23-34.

Gubaev, A., D. Weidlich & D. Klostermeier, (2016) DNA gyrase with a single catalytic tyrosine can catalyze DNA supercoiling by a nicking-closing mechanism. *Nucleic Acids Res.* **44**: 10354-10366.

Gullberg, E., S. Cao, O.G. Berg, C. Ilbäck, L. Sandegren, D. Hughes & D.I. Andersson, (2011) Selection of resistant bacteria at very low antibiotic concentrations. *PLoS Path.* **7**: e1002158.

Gussin, G.N., A.D. Johnson, C.O. Pabo & R.T. Sauer, (1983) Repressor and Cro Protein: Structure, Function, and Role in Lysogenisation. In: Lambda II. R. Hendrix, J.W. Roberts, F.W. Stahl & R.A. Weisberg (eds). Cold Spring Harbour: Cold Spring Harbour Laboratory, pp. 93-121.

Gutiérrez-Estrada, A., J. Ramírez-Santos & M.d.C. Gómez-Eichelmann, (2014) Role of chaperones and ATP synthase in DNA gyrase reactivation in Escherichia coli stationary-phase cells after nutrient addition. *SpringerPlus* **3**: 656.

Gutierrez, A., L. Laureti, S. Crussard, H. Abida, A. Rodríguez-Rojas, J. Blázquez, Z. Baharoglu, D. Mazel, F. Darfeuille, J. Vogel & I. Matic, (2013) β-lactam antibiotics promote bacterial mutagenesis via an RpoS-mediated reduction in replication fidelity. *Nat. Commun.* **4**: 1610.

Guyer, M.S., R.R. Reed, J.A. Steitz & K.B. Low, (1981) Identification of a Sex-factor-affinity Site in E. coli as γδ. *Cold Spring Harbor Symp. Quant. Biol.* **45**: 135-140.

Hallett, P., A.J. Grimshaw, D.B. Wigley & A. Maxwell, (1990) Cloning of the DNA gyrase genes under tac promoter control: overproduction of the gyrase A and B proteins. *Gene* **93**: 139-142.

Halligan, B.D., J.L. Davis, K.A. Edwards & L.F. Liu, (1982) Intra- and intermolecular strand transfer by HeLa DNA topoisomerase I. *J. Biol. Chem.* **257**: 3995-4000.

Hamperl, S. & K.A. Cimprich, (2016) Conflict Resolution in the Genome: How Transcription and Replication Make It Work. *Cell* **167**: 1455-1467.

Han, Y.-H., M.J.F. Austin, Y. Pommier & L.F. Povirk, (1993) Small deletion and insertion mutations induced by the topoisomerase II inhibitor teniposide in CHO cells and comparison with sites of drug-stimulated DNA cleavage *in vitro*. *J. Mol. Biol.* **229**: 52-66.

Hande, K.R., (1998) Etoposide: four decades of development of a topoisomerase II inhibitor. *Eur. J. Cancer* **34**: 1514-1521.

Hartung, F., K.J. Angelis, A. Meister, I. Schubert, M. Melzer & H. Puchta, (2002) An archaebacterial topoisomerase homolog not present in other eukaryotes is indispensable for cell proliferation of plants. *Curr. Biol.* **12**: 1787-1791.

Hartung, F. & H. Puchta, (2000) Molecular characterisation of two paralogous SPO11 homologues in Arabidopsis thaliana. *Nucleic Acids Res.* **28**: 1548-1554.

Heath, R.J., J.R. Rubin, D.R. Holland, E. Zhang, M.E. Snow & C.O. Rock, (1999) Mechanism of Triclosan Inhibition of Bacterial Fatty Acid Synthesis. *J. Biol. Chem.* **274**: 11110-11114.

Heddle, J.G., S. Mitelheiser, A. Maxwell & N.H. Thomson, (2004) Nucleotide binding to DNA gyrase causes loss of DNA wrap. *J. Mol. Biol.* **337**: 597-610.

Heide, L., (2009) The aminocoumarins: biosynthesis and biology. *Nat. Prod. Rep.* **26**: 1241-1250.

Hermsen, R., J.B. Deris & T. Hwa, (2012) On the rapidity of antibiotic resistance evolution facilitated by a concentration gradient. *Proc. Natl. Acad. Sci. USA* **109**: 10775-10780.

Herrero, M., R. Kolter & F. Moreno, (1986) Effects of microcin B17 on microcin B17-immune cells. *Microbiology* **132**: 403-410.

Hershey, A.D. & W. Dove, (1971) Introduction to Lambda. In: The Bacteriohage Lambda. A.D. Hershey (ed). Cold Spring Harbour: Cold Spring Harbour Laboratory, pp. 3-11.

Hiasa, H., D.O. Yousef & K.J. Marians, (1996) DNA Strand Cleavage Is Required for Replication Fork Arrest by a Frozen Topoisomerase-Quinolone-DNA Ternary Complex. *J. Biol. Chem.* **271**: 26424-26429.

Higgins, N.P., (2016) Species-specific supercoil dynamics of the bacterial nucleoid. *Biophys Rev* **8**: 113-121.

Higgins, N.P., C.L. Peebles, A. Sugino & N.R. Cozzarelli, (1978) Purification of subunits of Escherichia coli DNA gyrase and reconstitution of enzymatic activity. *Proc. Natl. Acad. Sci. USA* **75**: 1773-1777.

Higgins, N.P. & A.V. Vologodskii, (2015) Topological Behavior of Plasmid DNA. *Microbiol Spectr.* **3**.

Hiraga, S., H. Niki, T. Ogura, C. Ichinose, H. Mori, B. Ezaki & A. Jaffé, (1989) Chromosome partitioning in Escherichia coli: novel mutants producing anucleate cells. *J. Bacteriol.* **171**: 1496-1505.

Hjort, K., H. Nicoloff & D.I. Andersson, (2016) Unstable tandem gene amplification generates heteroresistance (variation in resistance within a population) to colistin in Salmonella enterica. *Mol. Microbiol.* **102**: 274-289.

Hockings, S.C. & A. Maxwell, (2002) Identification of four GyrA residues involved in the DNA breakage–reunion reaction of DNA gyrase. *J. Mol. Biol.* **318**: 351-359.

Hohn, B., (1979) *In vitro* packaging of lambda and cosmid DNA. *Methods Enzymol.* **68**: 299-309.

Hohn, B. & T. Hohn, (1974) Activity of empty, headlike particles for packaging of DNA of bacteriophage lambda *in vitro*. *Proc. Natl. Acad. Sci. USA* **71**: 2372-2376.

Holmes, V.F. & N.R. Cozzarelli, (2000) Closing the ring: Links between SMC proteins and chromosome partitioning, condensation, and supercoiling. *Proc. Natl. Acad. Sci. USA* **97**: 1322-1324.

Hooper, D.C., (2003) Mechanisms of Quinolone Resistance. In: Quinolone Antimicrobial Agents, Third Edition. American Society of Microbiology, pp.

Hooper, D.C. & G.A. Jacoby, (2015) Mechanisms of drug resistance: quinolone resistance. *Ann. N. Y. Acad. Sci.* **1354**: 12-31.

Horowitz, D.S. & J.C. Wang, (1987) Mapping the active site tyrosine of Escherichia coli DNA gyrase. *J. Biol. Chem.* **262**: 5339-5344.

Hosfield, D.J., Y. Guan, B.J. Haas, R.P. Cunningham & J.A. Tainer, (1999) Structure of the DNA Repair Enzyme Endonuclease IV and Its DNA Complex. *Cell* **98**: 397-408.

Hou, Y., Y.P. Lin, J.D. Sharer & P.E. March, (1994) *In vivo* selection of conditional-lethal mutations in the gene encoding elongation factor G of Escherichia coli. *J. Bacteriol.* **176**: 123-129.

Houssaye, S., L. Gutmann & E. Varon, (2002) Topoisomerase Mutations Associated with *In vitro* Selection of Resistance to Moxifloxacin in Streptococcus pneumoniae. *Antimicrob. Agents Chemother.* **46**: 2712-2715.

Hsiang, Y.H., R. Hertzberg, S. Hecht & L.F. Liu, (1985) Camptothecin induces protein-linked DNA breaks via mammalian DNA topoisomerase I. *J. Biol. Chem.* **260**: 14873-14878.

Hsieh, L.-S., R.M. Burger & K. Drlica, (1991) Bacterial DNA supercoiling and [ATP][ADP]. *J. Mol. Biol.* **219**: 443-450.

Hsieh, T. & D. Brutlag, (1980) ATP-dependent DNA topoisomerase from D. melanogaster reversibly catenates duplex DNA rings. *Cell* **21**: 115-125.

Hsieh, T.J., L. Farh, W.M. Huang & N.L. Chan, (2004) Structure of the topoisomerase IV C-terminal domain: a broken beta-propeller implies a role as geometry facilitator in catalysis. *J. Biol. Chem.* **279**: 55587-55593.

Hsieh, T.J., T.J. Yen, T.S. Lin, H.T. Chang, S.Y. Huang, C.H. Hsu, L. Farh & N.L. Chan, (2010) Twisting of the DNA-binding surface by a beta-strand-bearing proline modulates DNA gyrase activity. *Nucleic Acids Res.* **38**: 4173-4181.

Hughes, D. & D.I. Andersson, (2012) Selection of resistance at lethal and non-lethal antibiotic concentrations. *Curr. Opin. Microbiol.* **15**: 555-560.

Ikeda, H., (1986a) Bacteriophage T4 DNA topoisomerase mediates illegitimate recombination *in vitro*. *Proc. Natl. Acad. Sci. USA* **83**: 922-926.

Ikeda, H., (1986b) Illegitimate recombination mediated by T4 DNA topoisomerase *in vitro*. *Mol. Gen. Genet.* **202**: 518-520.

Ikeda, H., (1994) DNA Topoisomerase-Mediated Illegitimate Recombination. In: Advances in Pharmacology. F.L. Leroy (ed). Academic Press, pp. 147-165.

Ikeda, H., K. Aoki & A. Naito, (1982) Illegitimate recombination mediated *in vitro* by DNA gyrase of Escherichia coli: Structure of recombinant DNA molecules. *Proc. Natl. Acad. Sci. USA* **79**: 3724-3728.

Ikeda, H., I. Kawasaki & M. Gellert, (1984) Mechanism of illegitimate recombination: common sites for recombination and cleavage mediated by Escherichia coli DNA gyrase. *Mol. Gen. Genet.* **196**: 546-549.

Ikeda, H., K. Moriya & T. Matsumoto, (1980) *In vitro* study of illegitimate recombination: involvement of DNA gyrase. *Cold Spring Harbor Symp. Quant. Biol.* **45**: 399-408.

Ikeda, H., H. Shimizu, T. Ukita & M. Kumagai, (1995) A novel assay for illegitimate recombination in Escherichia coli: Stimulation of λbio transducing phage formation by ultra-violet light and its independence from RecA function. *Adv. Biophys.* **31**: 197-208.

Ikeda, H. & M. Shiozaki, (1984) Nonhomologous recombination mediated by Escherichia coli DNA gyrase: possible involvement of DNA replication. *Cold Spring Harbor Symp. Quant. Biol.* **49**: 401-409.

Ikeda, H., K. Shiraishi & Y. Ogata, (2004) Illegitimate recombination mediated by double-strand break and end-joining in Escherichia coli. *Adv. Biophys.* **38**: 3-20.

Ikeda, H. & J.I. Tomizawa, (1965) Transducing fragments in generalized transduction by phage P1. I. Molecular origin of the fragments. *J. Mol. Biol.* **14**: 85-109.

Imlay, J.A., (2015) Diagnosing oxidative stress in bacteria: not as easy as you might think. *Curr. Opin. Microbiol.* **24**: 124-131.

Ince, D. & D.C. Hooper, (2001) Mechanisms and Frequency of Resistance to Gatifloxacin in Comparison to AM-1121 and Ciprofloxacin inStaphylococcus aureus. *Antimicrob. Agents Chemother.* **45**: 2755-2764.

Jain, C.K., H.K. Majumder & S. Roychoudhury, (2017) Natural Compounds as Anticancer Agents Targeting DNA Topoisomerases. *Curr. Genomics* **18**: 75-92.

Janion, C., (2008) Inducible SOS response system of DNA repair and mutagenesis in Escherichia coli. *Int. J. Biol. Sci.* **4**: 338-344.

Johnson, R.C., (2015) Site-specific DNA Inversion by Serine Recombinases. *Microbiol Spectr.* **3**: 1-36.

Jurado, S., A. Medina, R. de la Fuente, J.A. Ruiz-Santa-Quiteria & J.A. Orden, (2015) Resistance to non-quinolone antimicrobials in commensal Escherichia coli isolates from chickens treated orally with enrofloxacin. *Jap. J. Vet. Res.* **63**: 195-200.

Kaiser, A.D., (1957) Mutations in a temperate bacteriophage affecting its ability to lysogenize Escherichia coli. *Virology* **3**: 42-61.

Kampranis, S.C., A.D. Bates & A. Maxwell, (1999a) A model for the mechanism of strand passage by DNA gyrase. *Proc. Natl. Acad. Sci. USA* **96**: 8414-8419.

Kampranis, S.C., N.A. Gormley, R. Tranter, G. Orphanides & A. Maxwell, (1999b) Probing the binding of coumarins and cyclothialidines to DNA gyrase. *Biochemistry* **38**: 1967-1976.

Kampranis, S.C., A.J. Howells & A. Maxwell, (1999c) The interaction of DNA gyrase with the bacterial toxin CcdB: evidence for the existence of two gyrase-CcdB complexes. *J. Mol. Biol.* **293**: 733-744.

Kampranis, S.C. & A. Maxwell, (1996) Conversion of DNA gyrase into a conventional type II topoisomerase. *Proc. Natl. Acad. Sci. USA* **93**: 14416-14421.

Kampranis, S.C. & A. Maxwell, (1998a) Conformational changes in DNA gyrase revealed by limited proteolysis. *J. Biol. Chem.* **273**: 22606-22614.

Kampranis, S.C. & A. Maxwell, (1998b) The DNA gyrase-quinolone complex: ATP hydrolysis and the mechanism of DNA cleavage. *J. Biol. Chem.* **273**: 22615-22626.

Karp, P., D. Weaver, S. Paley, C. Fulcher, A. Kubo, A. Kothari, M. Krummenacker, P. Subhraveti, D. Weerasinghe, S. Gama-Castro, A. Huerta, L. Muñiz-Rascado, C. Bonavides-Martinez, V. Weiss, M. Peralta-Gil, A. Santos-Zavaleta, I. Schröder, A. Mackie, R. Gunsalus, J. Collado-Vides, I. Keseler & I. Paulsen, (2014) The EcoCyc Database. *EcoSal Plus*.

Katayama, T., T. Kubota, K. Kurokawa, E. Crooke & K. Sekimizu, (1998) The Initiator Function of DnaA Protein Is Negatively Regulated by the Sliding Clamp of the *E. coli* Chromosomal Replicase. *Cell* **94**: 61-71.

Kato, J.-i. & H. Ikeda, (1996) Construction of mini-F plasmid vectors for plasmid shuffling in Escherichia coli. *Gene* **170**: 141-142.

Keetch, C.A., E.H. Bromley, M.G. McCammon, N. Wang, J. Christodoulou & C.V. Robinson, (2005) L55P transthyretin accelerates subunit exchange and leads to rapid formation of hybrid tetramers. *J. Biol. Chem.* **280**: 41667-41674.

Kellenberger, E. & R.S. Edgar, (1971) Structure and assembly of phage particles. In: The Bacteriophage Lambda. A.D. Hershey (ed). Cold Spring Harbour, New York: Cold Spring Harbour Laboratory, pp. 271-295.

Kelly, S.M., T.J. Jess & N.C. Price, (2005) How to study proteins by circular dichroism. *Biochim. Biophys. Acta* **1751**: 119-139.

Keren, I., Y. Wu, J. Inocencio, L.R. Mulcahy & K. Lewis, (2013) Killing by Bactericidal Antibiotics Does Not Depend on Reactive Oxygen Species. *Science* **339**: 1213-1216.

Khodursky, A.B., E.L. Zechiedrich & N.R. Cozzarelli, (1995) Topoisomerase IV is a target of quinolones in Escherichia coli. *Proc. Natl. Acad. Sci. USA* **92**: 11801-11805.

Kikuchi, A. & K. Asai, (1984) Reverse gyrase--a topoisomerase which introduces positive superhelical turns into DNA. *Nature* **309**: 677-681.

Kim, N. & S. Jinks-Robertson, (2017) The Top1 paradox: Friend and foe of the eukaryotic genome. *DNA Repair* **56**: 33-41.

Kirkegaard, K. & J.C. Wang, (1981) Mapping the topography of DNA wrapped around gyrase by nucleolytic and chemical probing of complexes of unique DNA sequences. *Cell* **23**: 721-729.

Klevan, L. & J.C. Wang, (1980) Deoxyribonucleic acid gyrase-deoxyribonucleic acid complex containing 140 base pairs of deoxyribonucleic acid and an alpha 2 beta 2 protein core. *Biochemistry* **19**: 5229-5234.

Kobayashi, I. & H. Ikeda, (1977) Formation of recombinant DNA of bacteriophage lambda by recA function of Escherichia coli without duplication, transcription, translation, and maturation. *Mol. Gen. Genet.* **153**: 237-245.

Kohanski, M.A., M.A. DePristo & J.J. Collins, (2010) Sublethal antibiotic treatment leads to multidrug resistance via radical-induced mutagenesis. *Mol. Cell* **37**: 311-320.

Komp Lindgren, P., Å. Karlsson & D. Hughes, (2003) Mutation Rate and Evolution of Fluoroquinolone Resistance in Escherichia coli Isolates from Patients with Urinary Tract Infections. *Antimicrob. Agents Chemother.* **47**: 3222-3232.

Kondrat, F.D.L., W.B. Struwe & J.L.P. Benesch, (2015) Native Mass Spectrometry: Towards High-Throughput Structural Proteomics. In: Structural Proteomics: High-Throughput Methods. R.J. Owens (ed). New York, NY: Springer New York, pp. 349-371.

Koskiniemi, S. & D.I. Andersson, (2009) Translesion DNA polymerases are required for spontaneous deletion formation in Salmonella typhimurium. *Proc. Natl. Acad. Sci. USA* **106**: 10248-10253.

Koskiniemi, S., D. Hughes & D.I. Andersson, (2010) Effect of translesion DNA polymerases, endonucleases and RpoS on mutation rates in Salmonella Typhimurium. *Genetics* **185**: 783-795.

Koster, D.A., A. Crut, S. Shuman, M.A. Bjornsti & N.H. Dekker, (2010) Cellular strategies for regulating DNA supercoiling: A single-molecule perspective. *Cell* **142**: 519-530.

Kottur, J. & D.T. Nair, (2016) Reactive oxygen species play an important role in the bactericidal activity of quinolone antibiotics. *Angew. Chem.* **55**: 2397-2400.

Kozlowski, L.P., (2016) IPC – Isoelectric Point Calculator. *Biology Direct* **11**: 55.

Kramlinger, V.M. & H. Hiasa, (2006) The "GyrA-box" is required for the ability of DNA gyrase to wrap DNA and catalyze the supercoiling reaction. *J. Biol. Chem.* **281**: 3738-3742.

Kreuzer, K.N., (2013) DNA Damage Responses in Prokaryotes: Regulating Gene Expression, Modulating Growth Patterns, and Manipulating Replication Forks. *Cold. Spring. Harb. Perspect. Biol.* **5**: a012674.

Kreuzer, K.N. & N.R. Cozzarelli, (1980) Formation and resolution of DNA catenanes by DNA gyrase. *Cell* **20**: 245-254.

Kumagai, M. & H. Ikeda, (1991) Molecular analysis of the recombination junctions of lambda bio transducing phages. *Mol. Gen. Genet.* **230**: 60-64.

Kumar, R., P. Nurse, S. Bahng, C.M. Lee & K.J. Marians, (2017) The mukB-topoisomerase IV interaction is required for proper chromosome compaction. *J. Biol. Chem.*

Lanz, M.A., M. Farhat & D. Klostermeier, (2014) The acidic C-terminal tail of the GyrA subunit moderates the DNA supercoiling activity of Bacillus subtilis gyrase. *J. Biol. Chem.* **289**: 12275-12285.

Lanz, M.A. & D. Klostermeier, (2011) Guiding strand passage: DNA-induced movement of the gyrase C-terminal domains defines an early step in the supercoiling cycle. *Nucleic Acids Res.* **39**: 9681-9694.

Laponogov, I., D.A. Veselkov, I.M.-T. Crevel, X.-S. Pan, L.M. Fisher & M.R. Sanderson, (2013) Structure of an 'open' clamp type II topoisomerase-DNA complex provides a mechanism for DNA capture and transport. *Nucleic Acids Res.*

Laponogov, I., D.A. Veselkov, M.K. Sohi, X.-S. Pan, A. Achari, C. Yang, J.D. Ferrara, L.M. Fisher & M.R. Sanderson, (2007) Breakage-reunion domain of Streptococcus pneumoniae topoisomerase IV: Crystal structure of a gram-positive quinolone target. *PLoS ONE* **2**: e301.

Laureti, L., I. Matic & A. Gutierrez, (2013) Bacterial Responses and Genome Instability Induced by Subinhibitory Concentrations of Antibiotics. *Antibiotics* **2**: 100.

Laurie, B., V. Katritch, J. Sogo, T. Koller, J. Dubochet & A. Stasiak, (1998) Geometry and physics of catenanes applied to the study of DNA replication. *Biophys. J.* **74**: 2815-2822.

Lázár, V., G. Pal Singh, R. Spohn, I. Nagy, B. Horváth, M. Hrtyan, R. Busa-Fekete, B. Bogos, O. Méhi, B. Csörgő, G. Pósfai, G. Fekete, B. Szappanos, B. Kégl, B. Papp & C. Pál, (2013) Bacterial evolution of antibiotic hypersensitivity. *Mol. Syst. Biol.* **9**: 700-700.

Lesher, G.Y., E.J. Froelich, M.D. Gruett, J.H. Bailey & R.P. Brundage, (1962) 1,8-Naphthyridone derivatives. A new class of chemotherapeutic agents. *J. Med. Chem.* **91**: 1063-1065.

Levine, C., H. Hiasa & K.J. Marians, (1998) DNA gyrase and topoisomerase IV: biochemical activities, physiological roles during chromosome replication, and drug sensitivities. *Biochim. Biophys. Acta* **1400**: 29-43.

Lewin, C.S., B.M.A. Howard, N.T. Ratcliff & J.T. Smith, (1989) 4-Quinolones and the SOS response. *J. Med. Microbiol.* **29**: 139-144.

Lewis, K., (2012) Antibiotics: Recover the lost art of drug discovery. *Nature* **485**: 439-440.

Lewis, R.J., O.M. Singh, C.V. Smith, T. Skarzynski, A. Maxwell, A.J. Wonacott & D.B. Wigley, (1996) The nature of inhibition of DNA gyrase by the coumarins and the cyclothialidines revealed by X-ray crystallography. *EMBO J.* **15**: 1412-1420.

Li, T.-K. & L.F. Liu, (1998) Modulation of Gyrase-Mediated DNA Cleavage and Cell Killing by ATP. *Antimicrob. Agents Chemother.* **42**: 1022-1027.

Lilley, D.M., D. Chen & R.P. Bowater, (1996) DNA supercoiling and transcription: topological coupling of promoters. *Q. Rev. Biophys.* **29**: 203-225.

Lima, C.D., J.C. Wang & A. Mondragon, (1994) Three-dimensional structure of the 67K N-terminal fragment of E. coli DNA topoisomerase I. *Nature* **367**: 138-146.

Lin, T.-Y., S. Nagano & J. Gardiner Heddle, (2015) Functional Analyses of the Toxoplasma gondii DNA Gyrase Holoenzyme: A Janus Topoisomerase with Supercoiling and Decatenation Abilities. *Sci. Rep.* **5**: 14491.

Lind, P.A. & D.I. Andersson, (2008) Whole-genome mutational biases in bacteria. *Proc. Natl. Acad. Sci. USA* **105**: 17878-17883.

Linder, J.A., E.S. Huang, M.A. Steinman, R. Gonzales & R.S. Stafford, (2005) Fluoroquinolone prescribing in the United States: 1995 to 2002. *Am. J. Med.* **118**: 259-268.

Lindsley, J.E., (2001) DNA Topology: Supercoiling and Linking. In: eLS. John Wiley & Sons, Ltd, pp.

Liu, L.F., C.C. Liu & B.M. Alberts, (1980) Type II DNA topoisomerases: enzymes that can unknot a topologically knotted DNA molecule via a reversible double-strand break. *Cell* **19**: 697-707.

Liu, L.F. & J.C. Wang, (1978) Micrococcus luteus DNA gyrase: active components and a model for its supercoiling of DNA. *Proc. Natl. Acad. Sci. USA* **75**: 2098-2102.

Liu, L.F. & J.C. Wang, (1987) Supercoiling of the DNA template during transcription. *Proc. Natl. Acad. Sci. USA* **84**: 7024-7027.

Liu, Y. & J.A. Imlay, (2013) Cell Death from Antibiotics Without the Involvement of Reactive Oxygen Species. *Science* **339**: 1210-1213.

Livermore, D.M., (1995) beta-Lactamases in laboratory and clinical resistance. *Clin. Microbiol. Rev.* **8**: 557-584.

Lockshon, D. & D.R. Morris, (1985) Sites of reaction of Escherichia coli DNA gyrase on pBR322 *in vivo* as revealed by oxolinic acid-induced plasmid linearization. *J. Mol. Biol.* **181**: 63-74.

Long, H., S.F. Miller, C. Strauss, C. Zhao, L. Cheng, Z. Ye, K. Griffin, R. Te, H. Lee, C.-C. Chen & M. Lynch, (2016) Antibiotic treatment enhances the genome-wide mutation rate of target cells. *Proc. Natl. Acad. Sci. USA* **113**: E2498-E2505.

Long, M., (2001) Evolution of novel genes. *Curr. Opin. Genet. Dev.* **11**: 673-680.

Lopez, C.R., S. Yang, R.W. Deibler, S.A. Ray, J.M. Pennington, R.J. DiGate, P.J. Hastings, S.M. Rosenberg & E.L. Zechiedrich, (2005) A role for topoisomerase III in a recombination pathway alternative to RuvABC. *Mol. Microbiol.* **58**: 80-101.

Lopez, E. & J. Blazquez, (2009) Effect of subinhibitory concentrations of antibiotics on intrachromosomal homologous recombination in Escherichia coli. *Antimicrob. Agents Chemother.* **53**: 3411-3415.

Lopez, E., M. Elez, I. Matic & J. Blazquez, (2007) Antibiotic-mediated recombination: ciprofloxacin stimulates SOS-independent recombination of divergent sequences in Escherichia coli. *Mol. Microbiol.* **64**: 83-93.

Lovett, B.D., L. Lo Nigro, E.F. Rappaport, I.A. Blair, N. Osheroff, N. Zheng, M.D. Megonigal, W.R. Williams, P.C. Nowell & C.A. Felix, (2001) Near-precise interchromosomal recombination and functional DNA topoisomerase II cleavage sites at MLL and AF-4 genomic breakpoints in treatment-related acute lymphoblastic leukemia with t(4;11) translocation. *Proc. Natl. Acad. Sci. USA* **98**: 9802-9807.

Lovett, S.T., P.T. Drapkin, V.A. Sutera-Jr & T.J. Gluckman-Peskind, (1993) A Sister-Strand Exchange Mechanism for Reca-Independent Deletion of Repeated DNA Sequences in Escherichia Coli. *Genetics* **135**: 631-642.

Luijsterburg, M.S., M.F. White, R. van Driel & R.T. Dame, (2008) The Major Architects of Chromatin: Architectural Proteins in Bacteria, Archaea and Eukaryotes. *Crit. Rev. Biochem. Mol. Biol.* **43**: 393-418.

Lynn, R., G. Giaever, S.L. Swanberg & J.C. Wang, (1986) Tandem regions of yeast DNA topoisomerase II share homology with different subunits of bacterial gyrase. *Science* **233**: 647-649.

Madhusudan, K. & V. Nagaraja, (1996) Alignment and phylogenetic analysis of type II DNA topoisomerases. *J. Biosci. (Bangalore)* **21**: 613-629.

Malik, M., K. Chavda, X. Zhao, N. Shah, S. Hussain, N. Kurepina, B.N. Kreiswirth, R.J. Kerns & K. Drlica, (2012) Induction of Mycobacterial Resistance to Quinolone Class Antimicrobials. *Antimicrob. Agents Chemother.* **56**: 3879-3887.

Malik, M., S. Hussain & K. Drlica, (2007) Effect of Anaerobic Growth on Quinolone Lethality with Escherichia coli. *Antimicrob. Agents Chemother.* **51**: 28-34.

Malik, M., X. Zhao & K. Drlica, (2006) Lethal fragmentation of bacterial chromosomes mediated by DNA gyrase and quinolones. *Mol. Microbiol.* **61**: 810-825.

Mangiameli, S.M., C.N. Merrikh, P.A. Wiggins & H. Merrikh, (2017) Transcription leads to pervasive replisome instability in bacteria. *eLife* **6**: e19848.

Mani, R.-S. & A.M. Chinnaiyan, (2010) Triggers for genomic rearrangements: insights into genomic, cellular and environmental influences. *Nat. Rev. Genet.* **11**: 819-829.

Marianayagam, N.J., M. Sunde & J.M. Matthews, (2004) The power of two: protein dimerization in biology. *Trends Biochem. Sci.* **29**: 618-625.

Marians, K.J., (1987) DNA gyrase-catalyzed decatenation of multiply linked DNA dimers. *J. Biol. Chem.* **262**: 10362-10368.

Markham, N.R. & M. Zuker, (2005) DINAMelt web server for nucleic acid melting prediction. *Nucleic Acids Res.* **33**: W577-581.

Marshall, B., S. Darkin & R.K. Ralph, (1983) Evidence that mAMSA induces topoisomerase action. *FEBS Lett.* **161**: 75-78.

Martinez-Garcia, B., X. Fernandez, O. Diaz-Ingelmo, A. Rodriguez-Campos, C. Manichanh & J. Roca, (2014) Topoisomerase II minimizes DNA entanglements by proofreading DNA topology after DNA strand passage. *Nucleic Acids Res.* **42**: 1821-1830.

Martinez, J.L. & F. Baquero, (2000) Mutation Frequencies and Antibiotic Resistance. *Antimicrob. Agents Chemother.* **44**: 1771-1777.

Mathieu, A., S. Fleurier, A. Frénoy, J. Dairou, M.-F. Bredeche, P. Sanchez-Vizuete, X. Song & I. Matic, (2016) Discovery and Function of a General Core Hormetic Stress Response in *E. coli* Induced by Sublethal Concentrations of Antibiotics. *Cell Reports* **17**: 46-57.

Maxwell, A., (1997) DNA gyrase as a drug target. *Trends Microbiol.* **5**: 102-109.

Maxwell, A. & M. Gellert, (1984) The DNA dependence of the ATPase activity of DNA gyrase. *J. Biol. Chem.* **259**: 14472-14480.

Maxwell, A. & M. Gellert, (1986) Mechanistic Aspects of DNA Topoisomerases. *Adv. Protein Chem.* **38**: 69-107.

Maxwell, A. & A.J. Howells, (1999) Overexpression and Purification of Bacterial DNA Gyrase. In: Methods in Molecular Biology, Vol 94: Protocols in DNA Topology and Topoisomerases, Part 1: DNA and Enzymes. M. Bjornsti & N. Osheroff (eds). Totowa: Humana Press Inc., pp. 135-144.

Maxwell, A. & D.M. Lawson, (2003) The ATP-Binding Site of Type II Topoisomerases as a Target for Antibacterial Drugs. *Curr. Top. Med. Chem.* **3**: 283-303.

Mayer, C. & Y.L. Janin, (2014) Non-quinolone Inhibitors of Bacterial Type IIA Topoisomerases: A Feat of Bioisosterism. *Chemical Reviews* **114**: 2313-2342.

McDaniel, L.S., L.H. Rogers & W.E. Hill, (1978) Survival of recombination-deficient mutants of Escherichia coli during incubation with nalidixic acid. *J. Bacteriol.* **134**: 1195-1198.

McGann, P., P. Courvalin, E. Snesrud, R.J. Clifford, E.-J. Yoon, F. Onmus-Leone, A.C. Ong, Y.I. Kwak, C. Grillot-Courvalin, E. Lesho & P.E. Waterman, (2014) Amplification of Aminoglycoside Resistance Gene aphA1 in Acinetobacter baumannii Results in Tobramycin Therapy Failure. *mBio* **5**: e00915-00914.

McGlynn, P., N.J. Savery & M.S. Dillingham, (2012) The conflict between DNA replication and transcription. *Mol. Microbiol.* **85**: 12-20.

McPartland, A., L. Green & H. Echols, (1980) Control of recA gene RNA in E. coli: Regulatory and signal genes. *Cell* **20**: 731-737.

Meczes, E.L., K.L. Gilroy, K.L. West & C.A. Austin, (2008) The Impact of the Human DNA Topoisomerase II C-Terminal Domain on Activity. *PLoS ONE* **3**: e1754.

Mehta, P., S. Casjens & S. Krishnaswamy, (2004) Analysis of the lambdoid prophage element e14 in the E. coli K-12 genome. *BMC Microbiol.* **4**: 4.

Menzel, R. & M. Gellert, (1983) Regulation of the genes for E. coli DNA gyrase: homeostatic control of DNA supercoiling. *Cell* **34**: 105-113.

Meselson, M. & R. Yuan, (1968) DNA restriction enzyme from E. coli. *Nature* **217**: 1110-1114.

Michael, T.P., (2014) Plant genome size variation: bloating and purging DNA. *Brief. Funct. Genomics.* **13**: 308-317.

Michel, B., G. Grompone, M.-J. Florès & V. Bidnenko, (2004) Multiple pathways process stalled replication forks. *Proc. Natl. Acad. Sci. USA* **101**: 12783-12788.

Miki, T., Z.T. Chang & T. Horiuchi, (1984a) Control of cell division by sex factor F in Escherichia coli. II. Identification of genes for inhibitor protein and trigger protein on the 42.84-43.6 F segment. *J. Mol. Biol.* **174**: 627-646.

Miki, T., J.A. Park, K. Nagao, N. Murayama & T. Horiuchi, (1992) Control of segregation of chromosomal DNA by sex factor F in Escherichia coli. Mutants of DNA gyrase subunit A suppress letD (ccdB) product growth inhibition. *J. Mol. Biol.* **225**: 39-52.

Miki, T., K. Yoshioka & T. Horiuchi, (1984b) Control of cell division by sex factor F in Escherichia coli. I. The 42.84-43.6 F segment couples cell division of the host bacteria with replication of plasmid DNA. *J. Mol. Biol.* **174**: 605-625.

Miller, C., L.E. Thomsen, C. Gaggero, R. Mosseri, H. Ingmer & S.N. Cohen, (2004) SOS Response Induction by ß-Lactams and Bacterial Defense Against Antibiotic Lethality. *Science* **305**: 1629-1631.

Milne, I., G. Stephen, M. Bayer, P.J.A. Cock, L. Pritchard, L. Cardle, P.D. Shaw & D. Marshall, (2013) Using Tablet for visual exploration of second-generation sequencing data. *Brief. Bioinformatics* **14**: 193-202.

Mitelman, F., B. Johansson & F. Mertens, (2007) The impact of translocations and gene fusions on cancer causation. *Nat. Rev. Cancer* **7**: 233-245.

Miura-Masuda, A. & H. Ikeda, (1990) The DNA gyrase of *Escherichia coli* participates in the formation of a spontaneous deletion by recA-independent recombination *in vivo*. *Mol. Gen. Genet.* **220**: 345-352.

Mizushima, T., S. Natori & K. Sekimizu, (1993) Relaxation of supercoiled DNA associated with induction of heat shock proteins in Escherichia coli. *Mol. Gen. Genet.* **238**: 1-5.

Mizuuchi, K., L.M. Fisher, M.H. O'Dea & M. Gellert, (1980) DNA gyrase action involves the introduction of transient double-strand breaks into DNA. *Proc. Natl. Acad. Sci. USA* **77**: 1847-1851.

Mizuuchi, K., M. Gellert & H.A. Nash, (1978a) Involvement of supertwisted DNA in integrative recombination of bacteriophage lambda. *J. Mol. Biol.* **121**: 375-392.

Mizuuchi, K., M.H. O'Dea & M. Gellert, (1978b) DNA gyrase: subunit structure and ATPase activity of the purified enzyme. *Proc. Natl. Acad. Sci. USA* **75**: 5960-5963.

Mo, C.Y., S.A. Manning, M. Roggiani, M.J. Culyba, A.N. Samuels, P.D. Sniegowski, M. Goulian & R.M. Kohli, (2016) Systematically Altering Bacterial SOS Activity under Stress Reveals Therapeutic Strategies for Potentiating Antibiotics. *mSphere* **1**: e00163-00116.

Mogre, A., T. Sengupta, R.T. Veetil, P. Ravi & A.S.N. Seshasayee, (2014) Genomic Analysis Reveals Distinct Concentration-Dependent Evolutionary Trajectories for Antibiotic Resistance in Escherichia coli. *DNA Res.* **21**: 711-726.

Mogre, A. & A.S.N. Seshasayee, (2017) Modulation of global transcriptional regulatory networks as a strategy for increasing kanamycin resistance of EF-G mutants. *bioRxiv*.

Morais Cabral, J.H., A.P. Jackson, C.V. Smith, N. Shikotra, A. Maxwell & R.C. Liddington, (1997) Crystal structure of the breakage-reunion domain of DNA gyrase. *Nature* **388**: 903-906.

Morgulis, A., G. Coulouris, Y. Raytselis, T.L. Madden, R. Agarwala & A.A. Schäffer, (2008) Database indexing for production MegaBLAST searches. *Bioinformatics* **24**: 1757-1764.

Morrison, A. & N.R. Cozzarelli, (1981) Contacts between DNA gyrase and its binding site on DNA: features of symmetry and asymmetry revealed by protection from nucleases. *Proc. Natl. Acad. Sci. USA* **78**: 1416-1420.

Mustaev, A., M. Malik, X. Zhao, N. Kurepina, G. Luan, L.M. Oppegard, H. Hiasa, K.R. Marks, R.J. Kerns, J.M. Berger & K. Drlica, (2014) Fluoroquinolone-gyrase-DNA complexes: Two modes of drug binding. *J. Biol. Chem.*

Naito, A., S. Naito & H. Ikeda, (1984) Homology is not required for recombination mediated by DNA gyrase of Escherichia coli. *Mol. Gen. Genet.* **193**: 238-243.

Nash, H.A., (1990) Bending and supercoiling of DNA at the attachment site of bacteriophage λ. *Trends Biochem. Sci.* **15**: 222-227.

Negrini, M., C.A. Felix, C. Martin, B.J. Lange, T. Nakamura, E. Canaani & C.M. Croce, (1993) Potential topoisomerase II DNA-binding sites at the breakpoints of a t(9;11) chromosome translocation in acute myeloid leukemia. *Cancer Res.* **53**: 4489-4492.

Neuman, K.C., (2010) Single-molecule measurements of DNA topology and topoisomerases. *J. Biol. Chem.* **285**: 18967-18971.

Neuman, K.C., G. Charvin, D. Bensimon & V. Croquette, (2009) Mechanisms of chiral discrimination by topoisomerase IV. *Proc. Natl. Acad. Sci. USA* **106**: 6986-6991.

Nichols, M.D., K. DeAngelis, J.L. Keck & J.M. Berger, (1999) Structure and function of an archaeal topoisomerase VI subunit with homology to the meiotic recombination factor Spo11. *EMBO J.* **18**: 6177-6188.

Nicolas, E., A.L. Upton, S. Uphoff, O. Henry, A. Badrinarayanan & D. Sherratt, (2014) The SMC Complex MukBEF Recruits Topoisomerase IV to the Origin of Replication Region in Live Escherichia coli. *mBio* **5**: e01001-01013.

Nicoloff, H. & D.I. Andersson, (2013) Lon protease inactivation, or translocation of the lon gene, potentiate bacterial evolution to antibiotic resistance. *Mol. Microbiol.* **90**: 1233-1248.

Nicoloff, H., V. Perreten & S.B. Levy, (2007) Increased Genome Instability in Escherichia coli lon Mutants: Relation to Emergence of Multiple-Antibiotic-Resistant (Mar) Mutants Caused by Insertion Sequence Elements and Large Tandem Genomic Amplifications. *Antimicrob. Agents Chemother.* **51**: 1293-1303.

Nilsen, I.W., I. Bakke, A. Vader, O. Olsvik & M.R. El-Gewely, (1996) Isolation of cmr, a novel Escherichia coli chloramphenicol resistance gene encoding a putative efflux pump. *J. Bacteriol.* **178**: 3188-3193.

Nilsson, A.I., S. Koskiniemi, S. Eriksson, E. Kugelberg, J.C.D. Hinton & D.I. Andersson, (2005) Bacterial genome size reduction by experimental evolution. *Proc. Natl. Acad. Sci. USA* **102**: 12112-12116.

Nitiss, J.L., (2009a) DNA topoisomerase II and its growing repertoire of biological functions. *Nat. Rev. Cancer* **9**: 327-337.

Nitiss, J.L., (2009b) Targeting DNA topoisomerase II in cancer chemotherapy. *Nat. Rev. Cancer* **9**: 338-350.

Noble, C.G. & A. Maxwell, (2002) The Role of GyrB in the DNA Cleavage-religation Reaction of DNA Gyrase: A Proposed Two Metal-ion Mechanism. *J. Mol. Biol.* **318**: 361-371.

Nolivos, S., A.L. Upton, A. Badrinarayanan, J. Müller, K. Zawadzka, J. Wiktor, A. Gill, L. Arciszewska, E. Nicolas & D. Sherratt, (2016) MatP regulates the coordinated action of topoisomerase IV and MukBEF in chromosome segregation. *Nat. Commun.* **7**: 10466.

Nollmann, M., N.J. Crisona & P.B. Arimondo, (2007a) Thirty years of Escherichia coli DNA gyrase: From *in vivo* function to single-molecule mechanism. *Biochimie* **89**: 490-499.

Nollmann, M., M.D. Stone, Z. Bryant, J. Gore, N.J. Crisona, S.-C. Hong, S. Mitelheiser, A. Maxwell, C. Bustamante & N.R. Cozzarelli, (2007b) Multiple modes of Escherichia coli DNA gyrase activity revealed by force and torque. *Nat. Struct. Mol. Biol.* **14**: 264-271.

Normark, S., T. Edlund, T. Grundström, S. Bergström & H. Wolf-Watz, (1977) Escherichia coli K-12 Mutants Hyperproducing Chromosomal Beta-Lactamase by Gene Repetitions. *J. Bacteriol.* **132**: 912-922.

Norström, T., J. Lannergård & D. Hughes, (2007) Genetic and Phenotypic Identification of Fusidic Acid-Resistant Mutants with the Small-Colony-Variant Phenotype in Staphylococcus aureus. *Antimicrob. Agents Chemother.* **51**: 4438-4446.

O'Neill, J., (2016) Tackling drug-resistant infections globally: Final report and recommendations. In., pp. The Review on Antimicrobial Resistance. Final report.

O'Sullivan, D.M., J. Hinds, P.D. Butcher, S.H. Gillespie & T.D. McHugh, (2008) Mycobacterium tuberculosis DNA repair in response to subinhibitory concentrations of ciprofloxacin. *J. Antimicrob. Chemother.* **62**: 1199-1202.

Oakley, T.J. & I.D. Hickson, (2002) Defending genome integrity during S-phase: putative roles for RecQ helicases and topoisomerase III. *DNA Repair* **1**: 175-207.

Oliphant, C.M. & G.M. Green, (2002) Quinolones: a comprehensive review. *Am. Fam. Physician* **65**: 455-464.

Oram, M., A.A. Travers, A.J. Howells, A. Maxwell & M.L. Pato, (2006) Dissection of the Bacteriophage Mu Strong Gyrase Site (SGS): Significance of the SGS Right Arm in Mu Biology and DNA Gyrase Mechanism. *J. Bacteriol.* **188**: 619-632.

Orphanides, G. & A. Maxwell, (1994) Evidence for a conformational change in the DNA gyrase-DNA complex from hydroxyl radical footprinting. *Nucleic Acids Res.* **22**: 1567-1575.

Pang, Z., R. Chen, D. Manna & N.P. Higgins, (2005) A Gyrase Mutant with Low Activity Disrupts Supercoiling at the Replication Terminus. *J. Bacteriol.* **187**: 7773-7783.

Papillon, J., J.F. Menetret, C. Batisse, R. Helye, P. Schultz, N. Potier & V. Lamour, (2013) Structural insight into negative DNA supercoiling by DNA gyrase, a bacterial type 2A DNA topoisomerase. *Nucleic Acids Res.* **41**: 7815-7827.

Parks, W.M., (2004) The interaction between DNA gyrase and the peptide antibiotic microcin B17. In: Biological Chemistry Department, John Innes Centre. Norwich, UK: University of East Anglia, pp. 188.

Pato, M.L., (1994) Central location of the Mu strong gyrase binding site is obligatory for optimal rates of replicative transposition. *Proc. Natl. Acad. Sci. USA* **91**: 7056-7060.

Pendleton, M., R.H. Lindsey, C.A. Felix, D. Grimwade & N. Osheroff, (2014) Topoisomerase II and leukemia. *Ann. N. Y. Acad. Sci.*: 1-13.

Peng, H. & K.J. Marians, (1993) Escherichia coli topoisomerase IV. Purification, characterization, subunit structure, and subunit interactions. *J. Biol. Chem.* **268**: 24481-24490.

Peng, H. & K.J. Marians, (1995) The interaction of Escherichia coli topoisomerase IV with DNA. *J. Biol. Chem.* **270**: 25286-25290.

Pereira, R.V., J.D. Siler, J.C. Ng, M.A. Davis, Y.T. Grohn & L.D. Warnick, (2014) Effect of on-farm use of antimicrobial drugs on resistance in fecal Escherichia coli of preweaned dairy calves. *J. Dairy Sci.* **97**: 7644-7654.

Pérez-Capilla, T., M.-R. Baquero, J.-M. Gómez-Gómez, A. Ionel, S. Martín & J. Blázquez, (2005) SOS-Independent Induction of dinB Transcription by β-Lactam-Mediated Inhibition of Cell Wall Synthesis in Escherichia coli. *J. Bacteriol.* **187**: 1515-1518.

Perez-Cheeks, B.A., C. Lee, R. Hayama & K.J. Marians, (2012) A role for topoisomerase III in Escherichia coli chromosome segregation. *Mol. Microbiol.* **86**: 1007-1022.

Peter, B.J., J. Arsuaga, A.M. Breier, A.B. Khodursky, P.O. Brown & N.R. Cozzarelli, (2004) Genomic transcriptional response to loss of chromosomal supercoiling in Escherichia coli. *Genome Biol.* **5**: R87.

Peter, B.J., C. Ullsperger, H. Hiasa, K.J. Marians & N.R. Cozzarelli, (1998) The Structure of Supercoiled Intermediates in DNA Replication. *Cell* **94**: 819-827.

Pitiriga, V., G. Vrioni, G. Saroglou & A. Tsakris, (2017) The Impact of Antibiotic Stewardship Programs in Combating Quinolone Resistance: A Systematic Review and Recommendations for More Efficient Interventions. *Advances in Therapy* **34**: 854-865.

Piton, J., S. Petrella, M. Delarue, G. André-Leroux, V. Jarlier, A. Aubry & C. Mayer, (2010) Structural insights into the quinolone resistance mechanism of Mycobacterium tuberculosis DNA gyrase. *PLoS ONE* **5**: e12245.

Pletz, M.W.R., M. Rau, J. Bulitta, A. De Roux, O. Burkhardt, G. Kruse, M. Kurowski, C.E. Nord & H. Lode, (2004) Ertapenem Pharmacokinetics and Impact on Intestinal Microflora, in Comparison to Those of Ceftriaxone, after Multiple Dosing in Male and Female Volunteers. *Antimicrob. Agents Chemother.* **48**: 3765-3772.

Pogue-Geile, K.L., S. Dassarma, S.R. King & S.R. Jaskunas, (1980) Recombination between bacteriophage lambda and plasmid pBR322 in Escherichia coli. *J. Bacteriol.* **142**: 992-1003.

Pohlhaus, J.R. & K.N. Kreuzer, (2005) Norfloxacin-induced DNA gyrase cleavage complexes block Escherichia coli replication forks, causing double-stranded breaks *in vivo*. *Mol. Microbiol.* **56**: 1416-1429.

Pommier, Y., P. Pourquier, Y. Fan & D. Strumberg, (1998) Mechanism of action of eukaryotic DNA topoisomerase I and drugs targeted to the enzyme. *Biochim. Biophys. Acta* **1400**: 83-106.

Pope, C.F., D.M. O'Sullivan, T.D. McHugh & S.H. Gillespie, (2008) A Practical Guide to Measuring Mutation Rates in Antibiotic Resistance. *Antimicrob. Agents Chemother.* **52**: 1209-1214.

Postow, L., N.J. Crisona, B.J. Peter, C.D. Hardy & N.R. Cozzarelli, (2001) Topological challenges to DNA replication: conformations at the fork. *Proc. Natl. Acad. Sci. USA* **98**: 8219-8226.

Postow, L., C.D. Hardy, J. Arsuaga & N.R. Cozzarelli, (2004) Topological domain structure of the Escherichia coli chromosome. *Genes Dev.* **18**: 1766-1779.

Pruss, G.J., S.H. Manes & K. Drlica, (1982) Escherichia coli DNA topoisomerase I mutants: Increased supercoiling is corrected by mutations near gyrase genes. *Cell* **31**: 35-42.

Rajan, R., A. Osterman & A. Mondragón, (2016) Methanopyrus kandleri topoisomerase V contains three distinct AP lyase active sites in addition to the topoisomerase active site. *Nucleic Acids Res.* **44**: 3464-3474.

Rajan, R., B. Taneja & A. Mondragon, (2010) Structures of minimal catalytic fragments of topoisomerase V reveals conformational changes relevant for DNA binding. *Structure* **18**: 829-838.

Rau, D.C., M. Gellert, F. Thoma & A. Maxwell, (1987) Structure of the DNA gyrase-DNA complex as revealed by transient electric dichroism. *J. Mol. Biol.* **193**: 555-569.

Rau, M.H., R.L. Marvig, G.D. Ehrlich, S. Molin & L. Jelsbak, (2012) Deletion and acquisition of genomic content during early stage adaptation of Pseudomonas aeruginosa to a human host environment. *Environ. Microbiol.* **14**: 2200-2211.

Rawdon, E.J., J. Dorier, D. Racko, K.C. Millett & A. Stasiak, (2016) How topoisomerase IV can efficiently unknot and decatenate negatively supercoiled DNA molecules without causing their torsional relaxation. *Nucleic Acids Res.* **44**: 4528-4538.

Redgrave, L.S., S.B. Sutton, M.A. Webber & L.J. Piddock, (2014) Fluoroquinolone resistance: mechanisms, impact on bacteria, and role in evolutionary success. *Trends Microbiol.* **22**: 438-445.

Reece, R.J. & A. Maxwell, (1989) Tryptic fragments of the Escherichia coli DNA gyrase A protein. *J. Biol. Chem.* **264**: 19648-19653.

Reece, R.J. & A. Maxwell, (1991a) DNA gyrase: Structure and function. *Crit. Rev. Biochem. Mol. Biol.* **26**: 335-375.

Reece, R.J. & A. Maxwell, (1991b) Probing the limits of the DNA breakage-reunion domain of the Escherichia coli DNA gyrase A protein. *J. Biol. Chem.* **266**: 3540-3546.

Reisinger, V. & L.A. Eichacker, (2007) How to analyze protein complexes by 2D blue native SDS-PAGE. *Proteomics* **7 Suppl 1**: 6-16.

Reyes-Domínguez, Y., G. Contreras-Ferrat, J. Ramírez-Santos, J. Membrillo-Hernández & M.C. Gómez-Eichelmann, (2003) Plasmid DNA Supercoiling and Gyrase Activity in Escherichia coli Wild-Type and rpoS Stationary-Phase Cells. *J. Bacteriol.* **185**: 1097-1100.

Richardson, S.M., C.F. Higgins & D.M. Lilley, (1984) The genetic control of DNA supercoiling in Salmonella typhimurium. *EMBO J.* **3**: 1745-1752.

Rickenberg, H.V. & G. Lester, (1955) The preferential synthesis of beta-galactosidase in Escherichia coli. *Journal of General Microbiology* **13**: 279-284.

Robert, T., A. Nore, C. Brun, C. Maffre, B. Crimi, V. Guichard, H.-M. Bourbon & B. de Massy, (2016a) The TopoVIB-Like protein family is required for meiotic DNA double-strand break formation. *Science* **351**: 943-949.

Robert, T., N. Vrielynck, C. Mézard, B. de Massy & M. Grelon, (2016b) A new light on the meiotic DSB catalytic complex. *Semin. Cell Dev. Biol.* **54**: 165-176.

Roca, J., (2004) The path of the DNA along the dimer interface of topoisomerase II. *J. Biol. Chem.* **279**: 25783-25788.

Roca, J., J.M. Berger, S.C. Harrison & J.C. Wang, (1996) DNA transport by a type II topoisomerase: Direct evidence for a two-gate mechanism. *Proc. Natl. Acad. Sci. USA* **93**: 4057-4062.

Rocha, J.C., F.F. Busatto, T.N. Guecheva & J. Saffi, (2016) Role of nucleotide excision repair proteins in response to DNA damage induced by topoisomerase II inhibitors. *Mutat. Res. - Rev. Mut. Res.* **768**: 68-77.

Rodríguez, A.C., (2002) Studies of a positive supercoiling machine: Nucleotide hydrolysis and a multifunctional "latch" in the mechanism of reverse gyrase. *J. Biol. Chem.* **277**: 29865-29873.

Roerink, S.F., R. van Schendel & M. Tijsterman, (2014) Polymerase theta-mediated end joining of replication-associated DNA breaks in C. elegans. *Genome Res.* **24**: 954-962.

Rosenberg, S.M., C. Shee, R.L. Frisch & P.J. Hastings, (2012) Stress-induced mutation via DNA breaks in Escherichia coli: A molecular mechanism with implications for evolution and medicine. *Bioessays* **34**: 885-892.

Roth, J.R., E. Kugelberg, A.B. Reams, E. Kofoid & D.I. Andersson, (2006) Origin of Mutations Under Selection: The Adaptive Mutation Controversy. *Annu. Rev. Microbiol.* **60**: 477-501.

Rudolph, M.G., Y.d.T. Duany, S.P. Jungblut, A. Ganguly & D. Klostermeier, (2013) Crystal structures of Thermotoga maritima reverse gyrase: inferences for the mechanism of positive DNA supercoiling. *Nucleic Acids Res.* **41**: 1058-1070.

Rudolph, M.G. & D. Klostermeier, (2013) Mapping the spectrum of conformational states of the DNA- and C-gates in Bacillus subtilis gyrase. *J. Mol. Biol.* **425**: 2632-2640.

Rui, S. & Y.C. Tse-Dinh, (2003) Topoisomerase function during bacterial responses to environmental challenge. *Frontiers in Bioscience* **8**: d256-263.

Ruthenburg, A.J., D.M. Graybosch, J.C. Huetsch & G.L. Verdine, (2005) A superhelical spiral in the Escherichia coli DNA gyrase A C-terminal domain imparts unidirectional supercoiling bias. *J. Biol. Chem.* **280**: 26177-26184.

Rybenkov, V.V., C. Ullsperger, A.V. Vologodskii & N.R. Cozzarelli, (1997) Simplification of DNA topology below equilibrium values by type II topoisomerases. *Science* **277**: 690-693.

Sabourin, M., J.L. Nitiss, K.C. Nitiss, K. Tatebayashi, H. Ikeda & N. Osheroff, (2003) Yeast recombination pathways triggered by topoisomerase II-mediated DNA breaks. *Nucleic Acids Res.* **31**: 4373-4384.

Saing, K.M., H. Orii, Y. Tanaka, K. Yanagisawa, A. Miura & H. Ikeda, (1988) Formation of deletion in Escherichia coli between direct repeats located in the long inverted repeats of a cellular slime mold plasmid: participation of DNA gyrase. *Mol. Gen. Genet.* **214**: 1-5.

Sambrook, J., E.F. Fritsch & T. Maniatis, (1989) Bacteriophage Lambda Vectors. In: Molecular Cloning: A Laboratory Manual. N. Ford (ed). Cold Spring Harbour, New York: Cold Spring Harbour Laboratory, pp.

Sandegren, L. & D.I. Andersson, (2009) Bacterial gene amplification: implications for the evolution of antibiotic resistance. *Nat. Rev. Microbiol.* **7**: 578-588.

Sarkar, A., C.J. Coates, S. Whyard, U. Willhoeft, P.W. Atkinson & D.A. O'Brochta, (1997) The Hermes element from Musca domestica can transpose in four families of cyclorrhaphan flies. *Genetica* **99**: 15-29.

Savage, V.J., C. Charrier, A.-M. Salisbury, H. Box, N. Chaffer-Malam, A. Huxley, R. Kirk, G.M. Noonan, S. Mohmed, M.W. Craighead, A.J. Ratcliffe, S.A. Best & N.R. Stokes, (2016a) Efficacy of a Novel Tricyclic Topoisomerase Inhibitor in a Murine Model of Neisseria gonorrhoeae Infection. *Antimicrob. Agents Chemother.* **60**: 5592-5594.

Savage, V.J., C. Charrier, A.-M. Salisbury, E. Moyo, H. Forward, N. Chaffer-Malam, R. Metzger, A. Huxley, R. Kirk, M. Uosis-Martin, G. Noonan, S. Mohmed, S.A. Best, A.J. Ratcliffe & N.R. Stokes, (2016b) Biological profiling of novel tricyclic inhibitors of bacterial DNA gyrase and topoisomerase IV. *J. Antimicrob. Chemother.* **71**: 1905-1913.

Sawitzke, J.A. & S. Austin, (2000) Suppression of chromosome segregation defects of Escherichia coli muk mutants by mutations in topoisomerase I. *Proc. Natl. Acad. Sci. USA* **97**: 1671-1676.

Sawitzke, J.A., N. Costantino, X.-t. Li, L.C. Thomason, M. Bubunenko, C. Court & D.L. Court, (2011) Probing cellular processes with oligo-mediated recombination; using knowledge gained to optimize recombineering. *J. Mol. Biol.* **407**: 45-59.

Schagger, H., W.A. Cramer & G. Vonjagow, (1994) Analysis of Molecular Masses and Oligomeric States of Protein Complexes by Blue Native Electrophoresis and Isolation of Membrane

Protein Complexes by Two-Dimensional Native Electrophoresis. *Anal. Biochem.* **217**: 220-230.

Schedletzky, H., B. Wiedemann & P. Heisig, (1999) The effect of moxifloxacin on its target topoisomerases from Escherichia coli and Staphylococcus aureus. *J. Antimicrob. Chemother.* **43**: 31-37.

Schmidt, B.H., N. Osheroff & J.M. Berger, (2012) Structure of a topoisomerase II-DNA-nucleotide complex reveals a new control mechanism for ATPase activity. *Nat. Struct. Mol. Biol.* **19**: 1147-1154.

Schoeffler, A.J. & J.M. Berger, (2008) DNA topoisomerases: Harnessing and constraining energy to govern chromosome topology. *Q. Rev. Biophys.* **41**: 41-101.

Schoeffler, A.J., A.P. May & J.M. Berger, (2010) A domain insertion in Escherichia coli GyrB adopts a novel fold that plays a critical role in gyrase function. *Nucleic Acids Res.* **38**: 7830-7844.

Schröder, W., C. Goerke & C. Wolz, (2013) Opposing effects of aminocoumarins and fluoroquinolones on the SOS response and adaptability in Staphylococcus aureus. *J. Antimicrob. Chemother.* **68**: 529-538.

Schvartzman, J.B. & A. Stasiak, (2004) A topological view of the replicon. *EMBO Rep* **5**: 256-261.

Seol, Y. & K.C. Neuman, (2016) The dynamic interplay between DNA topoisomerases and DNA topology. *Biophys Rev* **8**: 101-111.

Sethi, S., P.W. Jones, M.S. Theron, M. Miravitlles, E. Rubinstein, J.A. Wedzicha & R. Wilson, (2010) Pulsed moxifloxacin for the prevention of exacerbations of chronic obstructive pulmonary disease: a randomized controlled trial. *Respiratory Research* **11**: 1-13.

Shanado, Y., J. Kato & H. Ikeda, (1998) Escherichia coli HU protein suppresses DNA-gyrase-mediated illegitimate recombination and SOS induction. *Genes Cells* **3**: 511-520.

Shaw, K.J., N. Miller, X. Liu, D. Lerner, J. Wan, A. Bittner & B.J. Morrow, (2003) Comparison of the changes in global gene expression of Escherichia coli induced by four bactericidal agents. *J. Mol. Microbiol. Biotechnol.* **5**: 105-122.

Shen, L.L., W.E. Kohlbrenner, D. Weigl & J. Baranowski, (1989) Mechanism of quinolone inhibition of DNA gyrase. Appearance of unique norfloxacin binding sites in enzyme-DNA complexes. *J. Biol. Chem.* **264**: 2973-2978.

Shen, X., R. Woodgate & M.F. Goodman, (2003) Escherichia coli DNA polymerase V subunit exchange: a post-SOS mechanism to curtail error-prone DNA synthesis. *J. Biol. Chem.* **278**: 52546-52550.

Sherratt, D.J., (2003) Bacterial Chromosome Dynamics. *Science* **301**: 780-785.

Shi, Y., M.J. Acerson, A. Abdolvahabi, R.A. Mowery & B.F. Shaw, (2016) Gibbs Energy of Superoxide Dismutase Heterodimerization Accounts for Variable Survival in Amyotrophic Lateral Sclerosis. *J. Am. Chem. Soc.* **138**: 5351-5362.

Shibata, T., S. Nakasu, K. Yasui & A. Kikuchi, (1987) Intrinsic DNA-dependent ATPase activity of reverse gyrase. *J. Biol. Chem.* **262**: 10419-10421.

Shimizu, H., H. Yamaguchi, Y. Ashizawa, Y. Kohno, M. Asami, J. Kato & H. Ikeda, (1997) Short-homology-independent illegitimate recombination in Escherichia coli: distinct mechanism from short-homology-dependent illegitimate recombination. *J. Mol. Biol.* **266**: 297-305.

Shimizu, H., H. Yamaguchi & H. Ikeda, (1995) Molecular analysis of lambda bio transducing phage produced by oxolinic acid-induced illegitimate recombination *in vivo*. *Genetics* **140**: 889-896.

Shuman, S., (1991) Recombination mediated by vaccinia virus DNA topoisomerase I in Escherichia coli is sequence specific. *Proc. Natl. Acad. Sci. USA* **88**: 10104-10108.

Shyamala, V., E. Schneider & G.F. Ames, (1990) Tandem chromosomal duplications: role of REP sequences in the recombination event at the join-point. *EMBO J.* **9**: 939-946.

Sissi, C. & M. Palumbo, (2010) In front of and behind the replication fork: bacterial type IIA topoisomerases. *Cell. Mol. Life Sci.* **67**: 2001-2024.

Slager, J., M. Kjos, L. Attaiech & J.-W. Veening, (2014) Antibiotic-Induced Replication Stress Triggers Bacterial Competence by Increasing Gene Dosage near the Origin. *Cell* **157**: 395-406.

Slesarev, A.I., K.O. Stetter, J.A. Lake, M. Gellert, R. Krah & S.A. Kozyavkin, (1993) DNA topoisomerase V is a relative of eukaryotic topoisomerase I from a hyperthermophilic prokaryote. *Nature* **364**: 735-737.

Smith, A.B. & A. Maxwell, (2006) A strand-passage conformation of DNA gyrase is required to allow the bacterial toxin, CcdB, to access its binding site. *Nucleic Acids Res.* **34**: 4667-4676.

Smoot, L.M., J.C. Smoot, M.R. Graham, G.A. Somerville, D.E. Sturdevant, C.A.L. Migliaccio, G.L. Sylva & J.M. Musser, (2001) Global differential gene expression in response to growth temperature alteration in group A Streptococcus. *Proc. Natl. Acad. Sci. USA* **98**: 10416-10421.

Snoep, J.L., C.C. van der Weijden, H.W. Andersen, H.V. Westerhoff & P.R. Jensen, (2002) DNA supercoiling in Escherichia coli is under tight and subtle homeostatic control, involving gene-expression and metabolic regulation of both topoisomerase I and DNA gyrase. *Eur. J. Biochem.* **269**: 1662-1669.

Snyder, M. & K. Drlica, (1979) DNA gyrase on the bacterial chromosome: DNA cleavage induced by oxolinic acid. *J. Mol. Biol.* **131**: 287-302.

Sobott, F., J.L. Benesch, E. Vierling & C.V. Robinson, (2002) Subunit exchange of multimeric protein complexes. Real-time monitoring of subunit exchange between small heat shock proteins by using electrospray mass spectrometry. *J. Biol. Chem.* **277**: 38921-38929.

Sogo, J.M., A. Stasiak, M.a.L. Martínez-Robles, D.B. Krimer, P. Hernández & J.B. Schvartzman, (1999) Formation of knots in partially replicated DNA molecules. *J. Mol. Biol.* **286**: 637-643.

Song, L.Y., M. Goff, C. Davidian, Z. Mao, M. London, K. Lam, M. Yung & J.H. Miller, (2016) Mutational consequences of ciprofloxacin in Escherichia coli. *Antimicrob. Agents Chemother.* **60**: 6165-6172.

Springer, A.L. & M.B. Schmid, (1993) Molecular characterization of the Salmonella typhimurium parE gene. *Nucleic Acids Res.* **21**: 1805-1809.

Stark, W.M., (2014) The Serine Recombinases. *Microbiol Spectr.* **2**.

Stewart, L., M.R. Redinbo, X. Qiu, W.G.J. Hol & J.J. Champoux, (1998) A Model for the Mechanism of Human Topoisomerase I. *Science* **279**: 1534-1541.

Stone, M.D., Z. Bryant, N.J. Crisona, S.B. Smith, A. Vologodskii, C. Bustamante & N.R. Cozzarelli, (2003) Chirality sensing by Escherichia coli topoisomerase IV and the mechanism of type II topoisomerases. *Proc. Natl. Acad. Sci. USA* **100**: 8654-8659.

Studier, F.W. & B.A. Moffatt, (1986) Use of bacteriophage T7 RNA polymerase to direct selective high-level expression of cloned genes. *J. Mol. Biol.* **189**: 113-130.

Stupina, V.A. & J.C. Wang, (2005) Viability of Escherichia coli topA Mutants Lacking DNA Topoisomerase I. *J. Biol. Chem.* **280**: 355-360.

Sugimoto-Shirasu, K., N.J. Stacey, J. Corsar, K. Roberts & M.C. McCann, (2002) DNA Topoisomerase VI Is Essential for Endoreduplication in Arabidopsis. *Curr. Biol.* **12**: 1782-1786.

Sugino, A. & N.R. Cozzarelli, (1980) The intrinsic ATPase of DNA gyrase. *J. Biol. Chem.* **255**: 6299-6306.

Sugino, A., N.P. Higgins, P.O. Brown, C.L. Peebles & N.R. Cozzarelli, (1978) Energy coupling in DNA gyrase and the mechanism of action of novobiocin. *Proc. Natl. Acad. Sci. USA* **75**: 4838-4842.

Sugino, A., N.P. Higgins & N.R. Cozzarelli, (1980) DNA gyrase subunit stoichiometry and the covalent attachment of subunit A to DNA during DNA cleavage. *Nucleic Acids Res.* **8**: 3865-3874.

Sugino, A., C.L. Peebles, K.N. Kreuzer & N.R. Cozzarelli, (1977) Mechanism of action of nalidixic acid: purification of Escherichia coli nalA gene product and its relationship to DNA gyrase and a novel nicking-closing enzyme. *Proc. Natl. Acad. Sci. USA* **74**: 4767-4771.

Sun, S., O.G. Berg, J.R. Roth & D.I. Andersson, (2009) Contribution of Gene Amplification to Evolution of Increased Antibiotic Resistance in Salmonella typhimurium. *Genetics* **182**: 1183-1195.

Sun, Y. & T.H. MacRae, (2005) The small heat shock proteins and their role in human disease. *FEBS J.* **272**: 2613-2627.

Suski, C. & K.J. Marians, (2008) Resolution of converging replication forks by RecQ and topoisomerase III. *Mol. Cell* **30**: 779-789.

Sutherland, J.H. & Y.-C. Tse-Dinh, (2010) Analysis of RuvABC and RecG Involvement in the Escherichia coli Response to the Covalent Topoisomerase-DNA Complex. *J. Bacteriol.* **192**: 4445-4451.

Swanberg, S.L. & J.C. Wang, (1987) Cloning and sequencing of the Escherichia coli gyrA gene coding for the A subunit of DNA gyrase. *J. Mol. Biol.* **197**: 729-736.

Swick, M.C., S.K. Morgan-Linnell, K.M. Carlson & L. Zechiedrich, (2011) Expression of Multidrug Efflux Pump Genes acrAB-tolC, mdfA, and norE in Escherichia coli Clinical Isolates as a Function of Fluoroquinolone and Multidrug Resistance. *Antimicrob. Agents Chemother.* **55**: 921-924.

Tamae, C., A. Liu, K. Kim, D. Sitz, J. Hong, E. Becket, A. Bui, P. Solaimani, K.P. Tran, H. Yang & J.H. Miller, (2008) Determination of antibiotic hypersensitivity among 4,000 single-gene-knockout mutants of Escherichia coli. *J. Bacteriol.* **190**: 5981-5988.

Tamura, J.K., A.D. Bates & M. Gellert, (1992) Slow interaction of 5'-adenylyl-beta,gamma-imidodiphosphate with Escherichia coli DNA gyrase. Evidence for cooperativity in nucleotide binding. *J. Biol. Chem.* **267**: 9214-9222.

Taneja, B., A. Patel, A. Slesarev & A. Mondragon, (2006) Structure of the N-terminal fragment of topoisomerase V reveals a new family of topoisomerases. *EMBO J.* **25**: 398-408.

Taneja, B., B. Schnurr, A. Slesarev, J.F. Marko & A. Mondragon, (2007) Topoisomerase V relaxes supercoiled DNA by a constrained swiveling mechanism. *Proc. Natl. Acad. Sci. USA* **104**: 14670-14675.

Tattevin, P., L. Basuino & H.F. Chambers, (2009) Subinhibitory fluoroquinolone exposure selects for reduced beta-lactam susceptibility in methicillin-resistant Staphylococcus aureus and alterations in the SOS-mediated response. *Res. Microbiol.* **160**: 187-192.

Taylor, R.G., D.C. Walker & R.R. McInnes, (1993) E. coli host strains significantly affect the quality of small scale plasmid DNA preparations used for sequencing. *Nucleic Acids Res.* **21**: 1677-1678.

Tennyson, R.B. & J.E. Lindsley, (1997) Type II DNA topoisomerase from Saccharomyces cerevisiae is a stable dimer. *Biochemistry* **36**: 6107-6114.

ter Kuile, B.H., N. Kraupner & S. Brul, (2016) The risk of low concentrations of antibiotics in agriculture for resistance in human health care. *FEMS Microbiol. Lett.* **363**: fnw210-fnw210.

Thi, T.D., E. López, A. Rodríguez-Rojas, J. Rodríguez-Beltrán, A. Couce, J.R. Guelfo, A. Castañeda-García & J. Blázquez, (2011) Effect of recA inactivation on mutagenesis of Escherichia coli exposed to sublethal concentrations of antimicrobials. *J. Antimicrob. Chemother.* **66**: 531-538.

Tomono, M., M. Shiozaki & H. Ikeda, (1989) Formation of λ transducing phage *in vitro*: Involvement of DNA gyrase. *Journal of Biochemistry* **105**: 423-428.

Torres-Barceló, C., M. Kojadinovic, R. Moxon & R.C. MacLean, (2015) The SOS response increases bacterial fitness, but not evolvability, under a sublethal dose of antibiotic. *Proc. R. Soc. Lond., Ser. B: Biol. Sci.* **282**: 20150885.

Tretter, E.M. & J.M. Berger, (2012a) Mechanisms for defining supercoiling set point of DNA gyrase orthologs I- a nonconserved acidic C-terminal tail modulates Escherichia coli gyrase activity. *J. Biol. Chem.* **287**: 18636-18644.

Tretter, E.M. & J.M. Berger, (2012b) Mechanisms for defining supercoiling set point of DNA gyrase orthologs II- the shape of the GyrA subunit C-terminal domain (CTD) is not a sole determinant for controlling supercoiling efficiency *J. Biol. Chem.* **287**: 18645-18654.

Trinh, T.Q. & R.R. Sinden, (1993) The Influence of Primary and Secondary DNA Structure in Deletion and Duplication between Direct Repeats in Escherichia Coli. *Genetics* **134**: 409-422.

Tse-Dinh, Y.C., (2009) Bacterial topoisomerase I as a target for discovery of antibacterial compounds. *Nucleic Acids Res.* **37**: 731-737.

Tse, Y. & J.C. Wang, (1980) E. coli and M. luteus DNA topoisomerase I can catalyze catenation of decatenation of double-stranded DNA rings. *Cell* **22**: 269-276.

Turley, H., M. Comley, S. Houlbrook, N. Nozaki, A. Kikuchi, I.D. Hickson, K. Gatter & A.L. Harris, (1997) The distribution and expression of the two isoforms of DNA topoisomerase II in normal and neoplastic human tissues. *Br. J. Cancer* **75**: 1340-1346.

Uemura, T., H. Ohkura, Y. Adachi, K. Morino, K. Shiozaki & M. Yanagida, (1987) DNA topoisomerase II is required for condensation and separation of mitotic chromosomes in S. pombe. *Cell* **50**: 917-925.

Ullsperger, C. & N.R. Cozzarelli, (1996) Contrasting enzymatic activities of topoisomerase IV and DNA gyrase from Escherichia coli. *J. Biol. Chem.* **271**: 31549-31555.

Valenti, A., M. De Felice, G. Perugino, A. Bizard, M. Nadal, M. Rossi & M. Ciaramella, (2012) Synergic and opposing activities of thermophilic RecQ-like helicase and topoisomerase 3 proteins in Holliday junction processing and replication fork stabilization. *J. Biol. Chem.* **287**: 30282-30295.

van Rijk, A. & H. Bloemendal, (2003) Molecular mechanisms of exon shuffling: illegitimate recombination. *Genetica* **118**: 245-249.

van Workum, M., S.J.M. van Dooren, N. Oldenburg, D. Molenaar, P.R. Jensen, J.L. Snoep & H.V. Westerhoff, (1996) DNA supercoiling depends on the phosphorylation potential in Escherichia coli. *Mol. Microbiol.* **20**: 351-360.

Vassetzky, Y.S., Q. Dang, P. Benedetti & S.M. Gasser, (1994) Topoisomerase II forms multimers *in vitro*: effects of metals, beta-glycerophosphate, and phosphorylation of its C-terminal domain. *Mol. Cell. Biol.* **14**: 6962-6974.

Vávrová, A. & T. Šimůnek, (2012) DNA topoisomerase IIβ: A player in regulation of gene expression and cell differentiation. *The International Journal of Biochemistry & Cell Biology* **44**: 834-837.

Vizan, J.L., C. Hernandez-Chico, I. del Castillo & F. Moreno, (1991) The peptide antibiotic microcin B17 induces double-strand cleavage of DNA mediated by E. coli DNA gyrase. *EMBO J.* **10**: 467-476.

Vos, S.M., E.M. Tretter, B.H. Schmidt & J.M. Berger, (2011) All tangled up: how cells direct, manage and exploit topoisomerase function. *Nature Reviews Molecular Cell Biology* **12**: 827-841.

Vrielynck, N., A. Chambon, D. Vezon, L. Pereira, L. Chelysheva, A. De Muyt, C. Mézard, C. Mayer & M. Grelon, (2016) A DNA topoisomerase VI–like complex initiates meiotic recombination. *Science* **351**: 939-943.

Wall, M.K., L.A. Mitchenall & A. Maxwell, (2004) Arabidopsis thaliana DNA gyrase is targeted to chloroplasts and mitochondria. *Proc. Natl. Acad. Sci. USA* **101**: 7821-7826.

Walsh, C., (2003) Where will new antibiotics come from? *Nat. Rev. Microbiol.* **1**: 65-70.

Walsh, C. & T.A. Wencewicz, (2016) *Antibiotics: Challenges, Mechanisms, Opportunities,* p. 477. ASM Press, Washington.

Walsh, C.T. & T.A. Wencewicz, (2014) Prospects for new antibiotics: a molecule-centered perspective. *J. Antibiot.* **67**: 7-22.

Wang, H.H. & G.M. Church, (2011) Multiplexed Genome Engineering and Genotyping Methods. *Methods Enzymol.* **498**: 409-426.

Wang, H.P. & C.E. Rogler, (1991) Topoisomerase I-mediated integration of hepadnavirus DNA *in vitro*. *J. Virol.* **65**: 2381-2392.

Wang, J.C., (1971) Interaction between DNA and an Escherichia coli protein ω. *J. Mol. Biol.* **55**: 523-IN516.

Wang, J.C., (2002) Cellular roles of DNA topoisomerases: a molecular perspective. *Nat. Rev. Mol. Cell Biol.* **3**: 430-440.

Wang, J.C., (2009) A journey in the world of DNA rings and beyond. In: Annu. Rev. Biochem., pp. 31-54.

Wang, X., Y. Kim, Q. Ma, S.H. Hong, K. Pokusaeva, J.M. Sturino & T.K. Wood, (2010) Cryptic prophages help bacteria cope with adverse environments. *Nat. Commun.* **1**: 147.

Warren, D.J., (2011) Preparation of highly efficient electrocompetent Escherichia coli using glycerol/mannitol density step centrifugation. *Anal. Biochem.* **413**: 206-207.

Watson, J.D. & F.H. Crick, (1953a) Genetical implications of the structure of deoxyribonucleic acid. *Nature* **171**: 964-967.

Watson, J.D. & F.H.C. Crick, (1953b) The Structure of DNA. *Cold Spring Harbor Symp. Quant. Biol.* **18**: 123-131.

Watt, P.M. & I.D. Hickson, (1994) Structure and function of type II DNA topoisomerases. *Biochem. J.* **303 (Pt 3)**: 681-695.

Webber, M.A., M.M.C. Buckner, L.S. Redgrave, G. Ifill, L.A. Mitchenall, C. Webb, R. Iddles, A. Maxwell & L.J.V. Piddock, (2017) Quinolone-resistant gyrase mutants demonstrate decreased susceptibility to triclosan. *J. Antimicrob. Chemother.* **72**: 2755-2763.

Webber, M.A., V. Ricci, R. Whitehead, M. Patel, M. Fookes, A. Ivens & L.J.V. Piddock, (2013) Clinically Relevant Mutant DNA Gyrase Alters Supercoiling, Changes the Transcriptome, and Confers Multidrug Resistance. *mBio* **4**.

Weisberg, R.A. & S. Adhya, (1977) Illegitimate recombination in bacteria and bacteriophage. *Annu. Rev. Genet.* **11**: 451-473.

Wentzell, L.M. & A. Maxwell, (2000) The Complex of DNA Gyrase and Quinolone Drugs on DNA Forms a Barrier to the T7 DNA Polymerase Replication Complex. *J. Mol. Biol.* **304**: 779-791.

White, R., T.A. Tran, C.A. Dankenbring, J. Deaton & R. Young, (2010) The N-terminal transmembrane domain of lambda S is required for holin but not antiholin function. *J. Bacteriol.* **192**: 725-733.

WHO, (2017) Critically important antimicrobials for human medicine - 5 rev. In. Geneva: World Health Organisation - WHO Advisory Group on Integrated Surveillance of Antimicrobial Resistance (AGISAR) pp. 48.

Wick, R.R., M.B. Schultz, J. Zobel & K.E. Holt, (2015) Bandage: interactive visualization of de novo genome assemblies. *Bioinformatics* **31**: 3350-3352.

Wicker, T., N. Yahiaoui & B. Keller, (2007) Illegitimate recombination is a major evolutionary mechanism for initiating size variation in plant resistance genes. *Plant J.* **51**: 631-641.

Wigley, D.B., G.J. Davies, E.J. Dodson, A. Maxwell & G. Dodson, (1991) Crystal structure of an N-terminal fragment of the DNA gyrase B protein. *Nature* **351**: 624-629.

Williams, N.L. & A. Maxwell, (1999a) Locking the DNA gate of DNA gyrase: investigating the effects on DNA cleavage and ATP hydrolysis. *Biochemistry* **38**: 14157-14164.

Williams, N.L. & A. Maxwell, (1999b) Probing the two-gate mechanism of DNA gyrase using cysteine cross-linking. *Biochemistry* **38**: 13502-13511.

Willmott, C.J.R., S.E. Critchlow, I.C. Eperon & A. Maxwell, (1994) The Complex of DNA Gyrase and Quinolone Drugs with DNA Forms a Barrier to Transcription by RNA Polymerase. *J. Mol. Biol.* **242**: 351-363.

Wilson, D.B., (1982) Effect of the lambda S gene product on properties of the Escherichia coli inner membrane. *J. Bacteriol.* **151**: 1403-1410.

Wittig, I., H.-P. Braun & H. Schagger, (2006) Blue native PAGE. *Nature Protocols* **1**: 418-428.

Wohlkonig, A., P.F. Chan, A.P. Fosberry, P. Homes, J. Huang, M. Kranz, V.R. Leydon, T.J. Miles, N.D. Pearson, R.L. Perera, A.J. Shillings, M.N. Gwynn & B.D. Bax, (2010) Structural basis of quinolone inhibition of type IIA topoisomerases and target-mediated resistance. *Nat. Struct. Mol. Biol.* **17**: 1152-1153.

Wullff, D.L. & S.M. Rosenberg, (1983) Establishment of Repressor Synthesis. In: Lambda II. R. Hendrix, J.W. Roberts, F.W. Stahl & R.A. Weisberg (eds). Cold Spring Harbor, USA: Cold Spring Harbor Laboratory, pp.

Xiao, B., M.M. McLean, X. Lei, J.F. Marko & R.C. Johnson, (2016) Controlled rotation mechanism of DNA strand exchange by the Hin serine recombinase. *Sci. Rep.* **6**: 23697.

Yang, X., W. Li, E.D. Prescott, S.J. Burden & J.C. Wang, (2000) DNA Topoisomerase IIβ and Neural Development. *Science* **287**: 131-134.

Yansich-Perron, C., J. Viera & J. Messing, (1985) Improved M13 phage cloning vectors and host strains: Nucleotide sequences of the M13mp18 and pUC19 vectors. *Gene* **33**: 103-119.

Yeeles, J.T.P. & M.S. Dillingham, (2010) The processing of double-stranded DNA breaks for recombinational repair by helicase–nuclease complexes. *DNA Repair* **9**: 276-285.

Yoshida, H., M. Bogaki, M. Nakamura & S. Nakamura, (1990) Quinolone resistance-determining region in the DNA gyrase gyrA gene of Escherichia coli. *Antimicrob. Agents Chemother.* **34**: 1271-1272.

Yoshida, H., M. Bogaki, M. Nakamura, L.M. Yamanaka & S. Nakamura, (1991) Quinolone resistance-determining region in the DNA gyrase gyrB gene of Escherichia coli. *Antimicrob. Agents Chemother.* **35**: 1647-1650.

Young, R.A. & R.W. Davis, (1983) Efficient isolation of genes by using antibody probes. *Proc. Natl. Acad. Sci. USA* **80**: 1194-1198.

Ysern, P., B. Clerch, M. Castańo, I. Gibert, J. Barbé & M. Llagostera, (1990) Induction of SOS genes in Escherichia coli and mutagenesis in Salmonella typhimurium by fluoroquinolones. *Mutagenesis* **5**: 63-66.

Zechiedrich, E.L. & N.R. Cozzarelli, (1995) Roles of topoisomerase IV and DNA gyrase in DNA unlinking during replication in Escherichia coli. *Genes Dev.* **9**: 2859-2869.

Zechiedrich, E.L., A.B. Khodursky & N.R. Cozzarelli, (1997) Topoisomerase IV, not gyrase, decatenates products of site-specific recombination in Escherichia coli. *Genes Dev.* **11**: 2580-2592.

Zhang, Z., S. Schwartz, L. Wagner & W. Miller, (2000) A Greedy Algorithm for Aligning DNA Sequences. *J. Comput. Biol.* **7**: 203-214.

Zhao, X. & K. Drlica, (2014) Reactive oxygen species and the bacterial response to lethal stress. *Curr. Opin. Microbiol.* **21**: 1-6.

Zhao, X., Y. Hong & K. Drlica, (2015) Moving forward with reactive oxygen species involvement in antimicrobial lethality. *J. Antimicrob. Chemother.* **70**: 639-642.

Zissler, J., E. Signer & F. Schaefer, (1971) The Role of Recombination in Growth of bacteriophage Lambda II. Inhibition of Growth by Prophage P2. In: The Bacteriophage lambda. A.D. Hershey (ed). Cold Spring Harbour: Cold Spring Harbour Laboratory, pp. 469-475.

Appendix I: Plasmid and DNA Substrate Maps

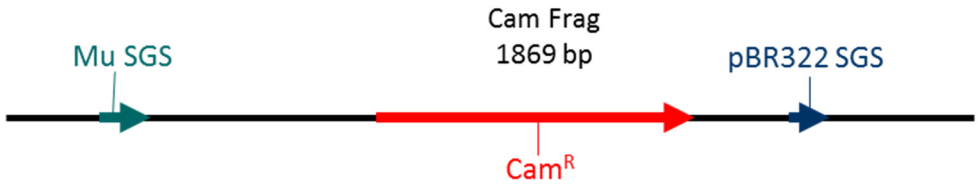

Figure XI: DNA map of Cam Frag. Linear DNA substrate of 1869 bp containing the chloramphenicol resistance cassette (Cam^R – in red) from pACYC184, the strong-gyrase binding site from pBR322 (pBR322 SGS – dark blue) and the Mu strong-gyrase binding site (Mu SGS – petrol blue).

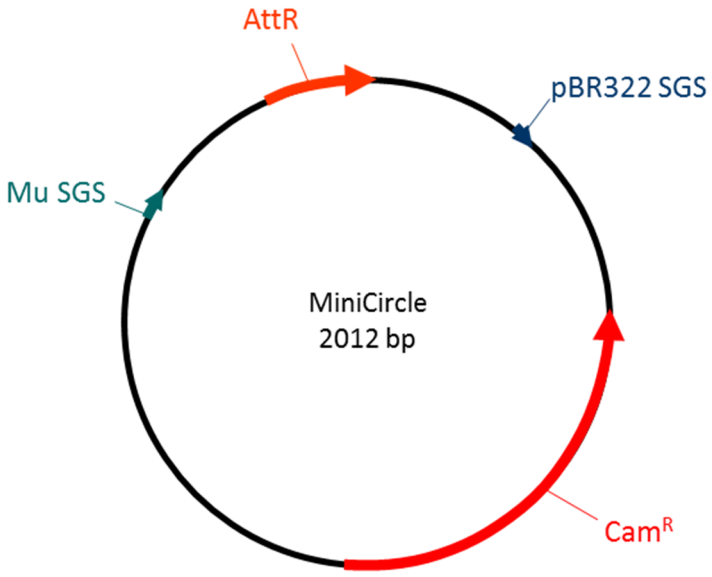

Figure XII: DNA map of the MiniCircle. Circular DNA substrate of 2012 bp containing the chloramphenicol resistance cassette (Cam^R – in red) from pACYC184, the strong-gyrase binding site from pBR322 (pBR322 SGS – dark blue) and the Mu strong-gyrase binding site (Mu SGS – petrol blue). It also contains the *E. coli* AttR site (orange) as a result of the manufacturing process.

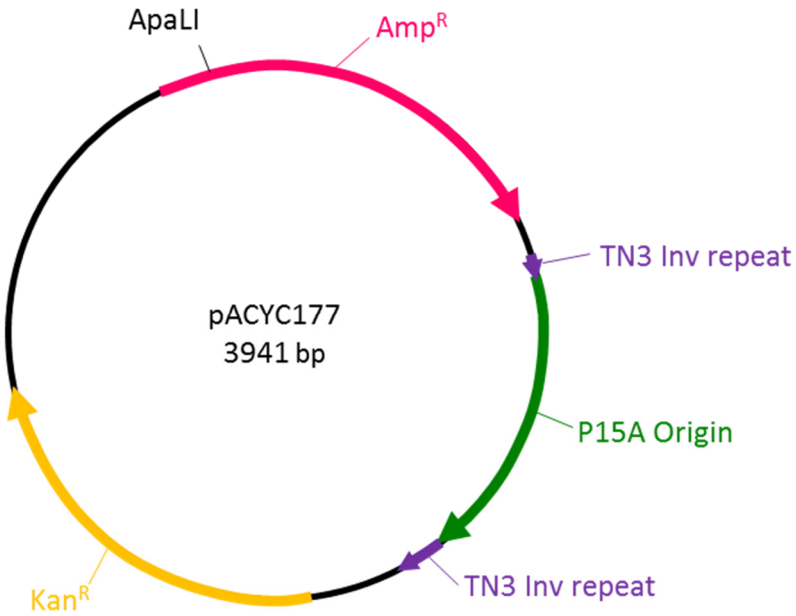

Figure XIII: Plasmid map of pACYC177. It has the P15A Origin (green) with an ampicillin (Amp^R – pink) and kanamycin (Kan^R – yellow) resistance cassettes. The purple indicates TN3 inverse repeats and the black line indicates the ApaLI restriction site.

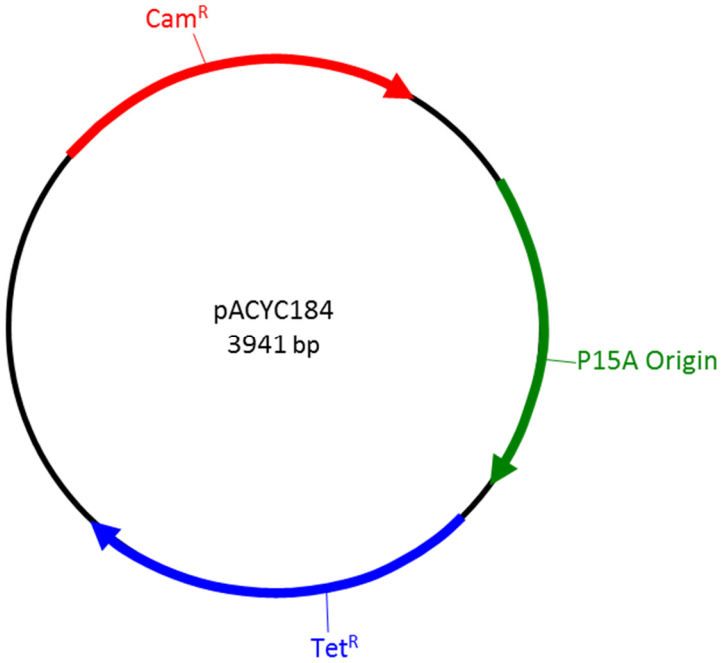

Figure XIV: Plasmid map of pACYC184. It has the P15A Origin (green) with a chloramphenicol (Cam^R – red) and tetracycline (Tet^R – royal blue) resistance cassettes.

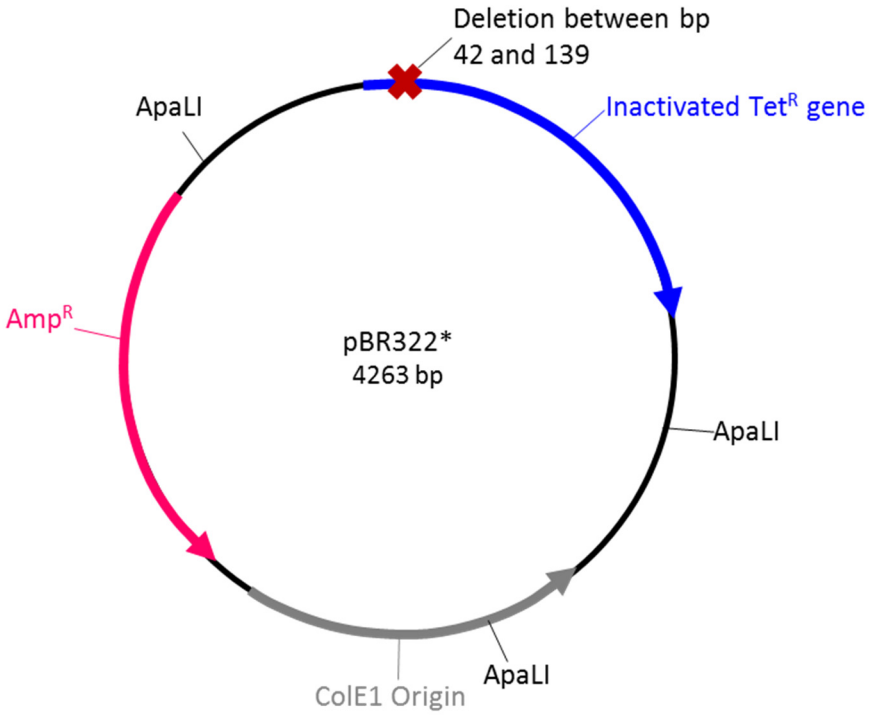

Figure XV: Plasmid map of pBR322*. It has the ColE1 Origin (grey) (with a single point mutation to increase copy number) with an ampicillin (Amp^R – pink) resistance cassette. The tetracycline (Tet^R – royal blue) resistance cassette has been inactivated by a deletion between bp 42 and 139 (indicated by the red cross). The black lines indicate the ApaLI restriction sites.

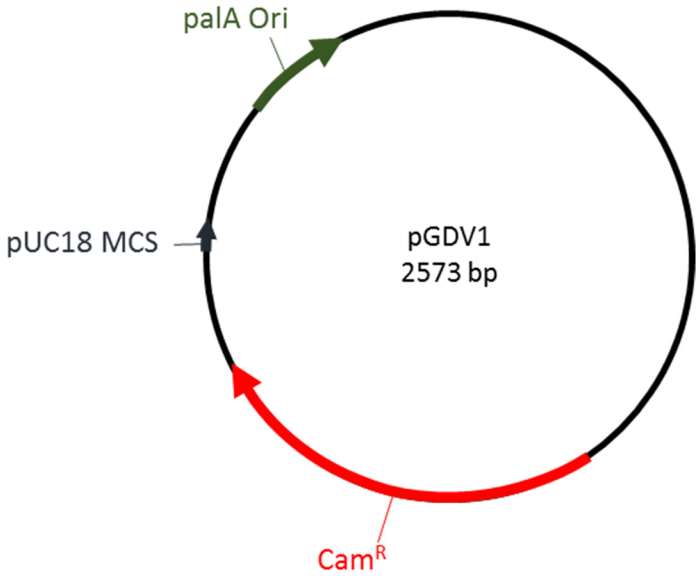

Figure XVI: Plasmid map of pGDV1. It has the palA Origin (green) with a chloramphenicol (Cam^R – red) resistance cassette and the pUC18 multiple cloning site (pUC18 MCS in dark blue).

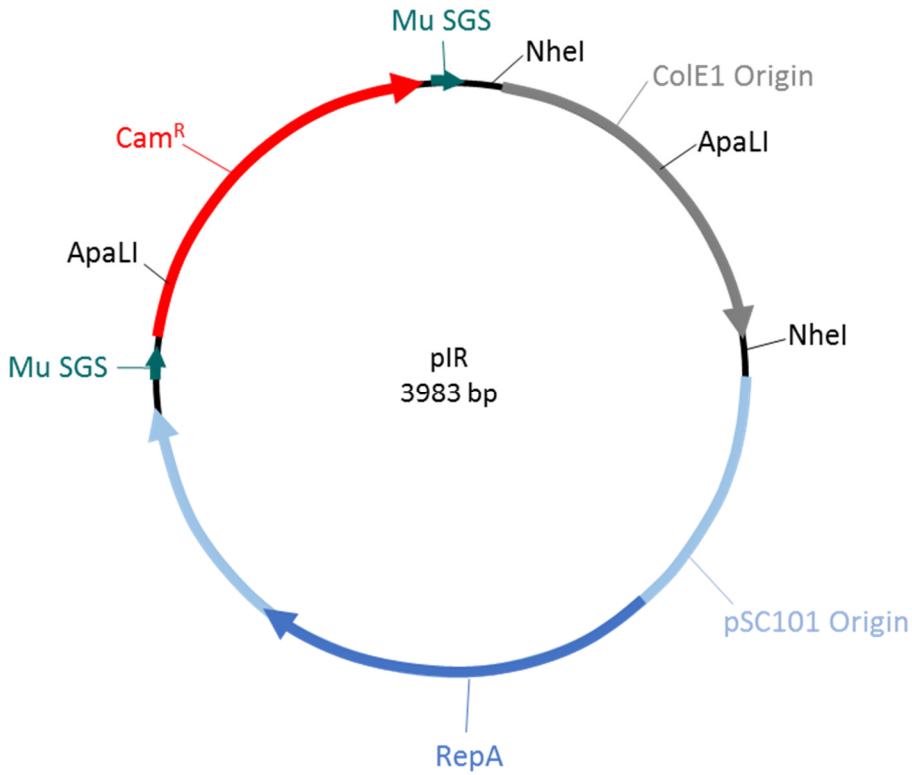

Figure XVII: Plasmid map of pIR. It has the ColE1 Origin (grey) (with a single point mutation to increase copy number) and the origin from pSC101 (light blue and RepA darker blue) with a chloramphenicol (Cam^R – red) resistance cassette from pACYC184. There are two the Mu strong-gyrase binding site (Mu SGS – petrol blue) around the Cam^R cassette. The black lines indicate the ApaLI and NheI restriction sites.

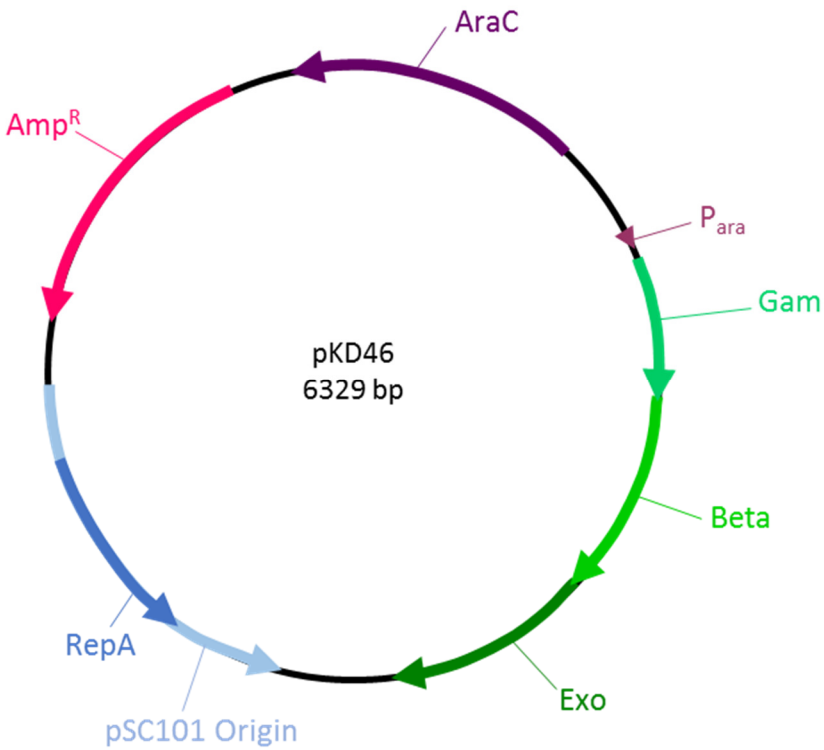

Figure XVIII: Plasmid map of pKD46. It has the origin from pSC101 (light blue and RepA darker blue) with an ampicillin (Amp^R – pink) resistance cassette. The AraC protein is indicated in purple. The Lambda Red proteins, Gam (light green), Beta (mid green) and Exo (dark green) proteins are under the inducible arabinose promoter (P_{ara} in mauve).

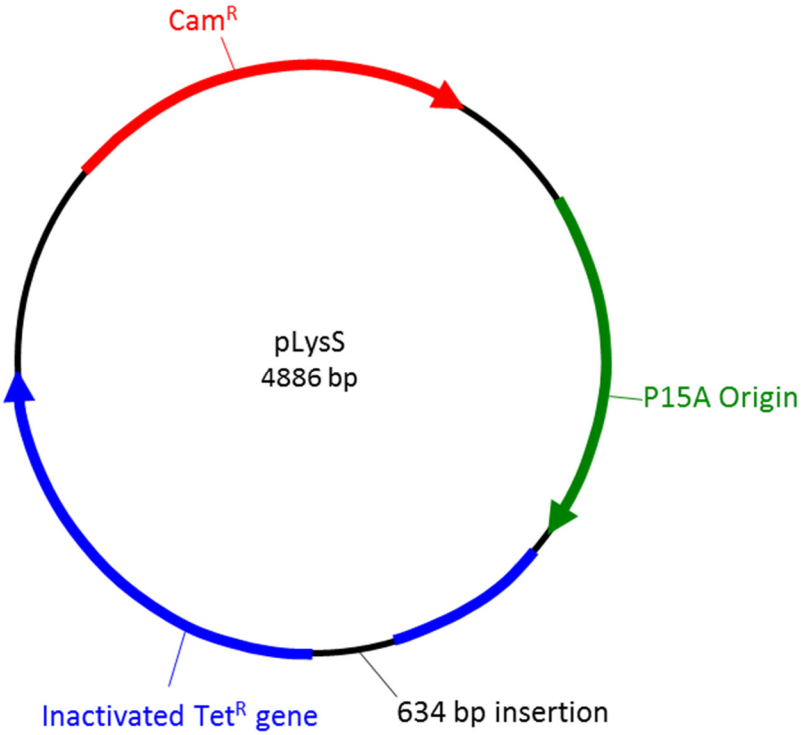

Figure XIX: Plasmid map of pLysS. It has the P15A Origin (green) with a chloramphenicol (Cam^R – red) resistance cassette. The tetracycline (Tet^R – royal blue) resistance cassette have been inactivated by a 634 bp insertion.

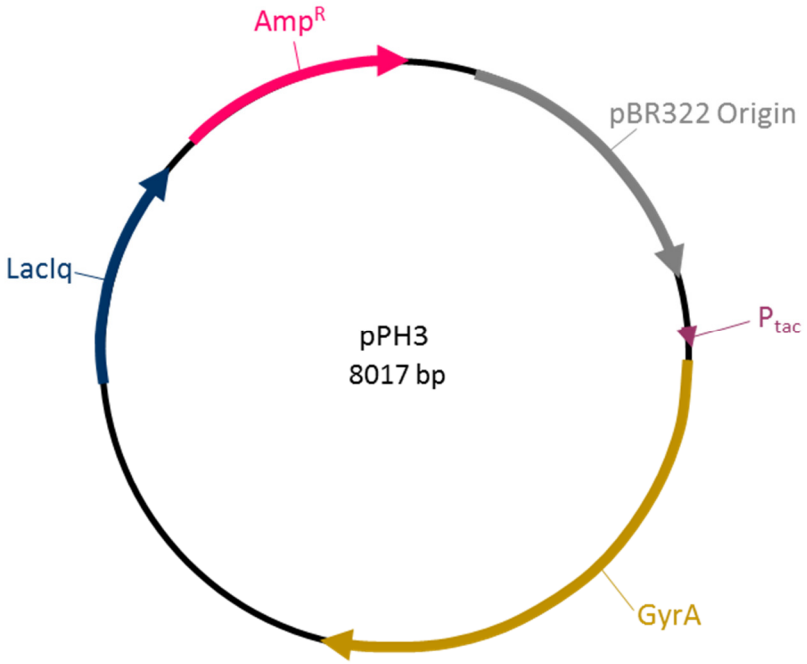

Figure XX: Plasmid map of pPH3. It has the pBR322 Origin (grey also known as the ColE1 origin) with an ampicillin (AmpR – pink) resistance cassette. The LacIq gene is indicated in dark

blue. The *gyrA* gene is indicated in mustard yellow (GyrA) under control of the inducible tac promoter (P_{tac} - mauve).

Appendix II: Relevant Publications

Bush, N.G., K. Evans-Roberts & A. Maxwell, (2015) DNA Topoisomerases. *EcoSal Plus* **6**.

Sipos, A., J. Pató, R. Székely, R.C. Hartkoorn, L. Kékesi, L. Őrfi, C. Szántai-Kis, K. Mikušová, Z. Svetlíková, J. Korduláková, V. Nagaraja, A.A. Godbole, N. Bush, F. Collin, A. Maxwell, S.T. Cole & G. Kéri, (2015) Lead selection and characterization of antitubercular compounds using the Nested Chemical Library. *Tuberculosis* **95**: S200-S206.

Djaout, K., V. Singh, Y. Boum, V. Katawera, H.F. Becker, N.G. Bush, S.J. Hearnshaw, J.E. Pritchard, P. Bourbon, P.B. Madrid, A. Maxwell, V. Mizrahi, H. Myllykallio & S. Ekins, (2016) Predictive modeling targets thymidylate synthase ThyX in Mycobacterium tuberculosis. *Scientific reports* **6**: 27792.

Maxwell, A., N.G. Bush, T. Germe & S.J. McKie, (Under Review) Non-quinolone topoisomerase inhibitors. In: Antimicrobial Resistance and Implications for the 21st Century. I.W. Fong, D. Shlaes & K. Drlica (eds).